



universität
wien

DISSERTATION

BIOADHESION OF COATED PARTICLES - THE
IMPACT OF FLOW PROBED WITH
ACOUSTICALLY-DRIVEN MICROFLUIDICS

angestrebter akademischer Grad

Doktor der Naturwissenschaften (Dr. rer. nat.)

Verfasser:	Mag. CHRISTIAN FILLAFER
Dissertationsgebiet:	A091 449
Betreuer:	Univ.-Prof. Mag. Dr. FRANZ GABOR

Wien, im Juni 2010

BIOADHESION OF COATED PARTICLES
- THE IMPACT OF FLOW PROBED WITH
ACOUSTICALLY-DRIVEN MICROFLUIDICS

CHRISTIAN FILLAFER

DOCTORATE THESIS

Department of Pharmaceutical Technology and
Biopharmaceutics

Faculty of Life Sciences

University of Vienna

June 2010

Christian Fillafer: *Bioadhesion of coated particles - The impact of flow probed with acoustically-driven microfluidics*, Doctorate Thesis, © June 2010
Typographic style by André Miede

ACKNOWLEDGMENTS

The thesis in its present form would not have been possible if I had not had the privilege of working with so many ingenious, diligent and dedicated people.

Foremost, I am indebted to my supervisors *Franz Gabor* and *Michael Wirth* for their constant support, time for discussions, inspiring ideas as well as advice on the academic and personal level.

In particular I thank *Silke Dissauer*, *Daniela Friedl*, *Adina Ilyes*, *Bettina Luser*, *Regina Nowotny*, *Clara Pichl*, *Manuela Prantl*, *Gerda Ratzinger*, and *Dietmar Pixner* who contributed to the data and concepts presented herein.

Collectively, I want to thank the recent and present members of our workgroup as well the whole staff of the Department of Pharmaceutical Technology and Biopharmaceutics for creating a productive, collaborative and humorous workplace.

I am deeply grateful for the stimulating interdisciplinary cooperations with *Jürgen Neumann* and *Matthias Schneider* (surface acoustic wave chips), *Renate Hofer-Warbinek* (endothelial cell culture), *Irene Lichtscheidl* (video microscopy) as well as *Claudia Meisslitzer-Ruppitsch* and *Adolf Ellinger* (electron microscopy).

Finally, I would like to thank my parents who supported me in all my pursuits and Gina for being there for me all along.

CONTENTS

I PREFIX	1
AUTHOR CONTRIBUTIONS	3
ABSTRACT	5
ZUSAMMENFASSUNG	7
II MAIN SECTION	9
INTRODUCTION	11
1 Protein and polyelectrolyte coatings to improve the bioadhesion of micro- and nanoparticles	13
1.1 Introductory works	13
1.1.1 Stabilizer-induced viscosity alteration biases nanoparticle sizing via dynamic light scattering	13
1.1.2 The role of surface functionalization in the design of PLGA micro- and nanoparticles	21
1.1.3 Cytoadhesion, internalisation and transcytosis of wheat germ agglutinin (WGA) investigated by electron microscopy	67
1.2 Specific Topics	75
1.2.1 Bionanoprobes to study particle-cell interactions	75
1.2.2 Fluorescent bionanoprobes to characterize cytoadhesion and cytoinvasion	87
1.2.3 Binding of positively and negatively charged micro- and nanoparticles to an epithelial and endothelial cell model	99
2 Surface acoustic wave (SAW) chips: Integrating flow into miniaturized biopharmaceutical test systems	111
2.1 Background	111
2.1.1 Relevance of flow to drug delivery with particles	111
2.1.2 Acoustically-driven microfluidics	115
2.2 Specific Topics	117
2.2.1 An acoustically-driven biochip – impact of flow on the cell-association of targeted drug carriers	117
2.2.2 A SAW-platform for parallelized microfluidic applications	133
2.2.3 Transport studies under flow: metal grids as growth supports for cell monolayers	137
CONCLUSIONS	143
III APPENDIX	147
BIBLIOGRAPHY	149
CURRICULUM VITAE	185

LIST OF FIGURES

- Figure 1 Polydispersity index (PDI) and mean particle size of PLGA nanoparticles determined by dynamic light scattering (—●—) as well as the respective content of Pluronic F-68 in the suspension (solid bars) in course of purification by diafiltration. 17
- Figure 2 TEM image of PLGA nanoparticles suspended in a 1.54% aqueous solution of Pluronic, negative stained with uranyl acetate. 18
- Figure 3 Mean particle size of PLGA nanoparticles dispersed in aqueous solutions of Pluronic F-68. Viscosity of water as dispersant property (open bars, DLS instrument's standard parameter). Results recalculated with the respectively determined dynamic viscosities (solid bars). 19
- Figure 4 Strategies for surface modification of PLGA particles. 24
- Figure 5 Caco-2 cell monolayer incubated with wheat germ agglutinin (WGA)-horseradish peroxidase (HRP) conjugate at 4°C. Nucleus (1), WGA-HRP (blackening) predominantly bound to apical membrane with microvilli (arrowheads). Filter (★) and no staining observed at the basolateral membrane (arrows). 69
- Figure 6 Caco-2 cell monolayer loaded with WGA-HRP at 4°C and post-incubated for 30 min at 37°C. Nucleus (1), early endosomes and multivesicular bodies (2), apical membrane with microvilli (arrowheads), and filter (★). Speckles of WGA-HRP (blackening) localized at the lateral and basolateral membrane (arrows). 70
- Figure 7 Caco-2 cell monolayer loaded with WGA-HRP at 4°C and post-incubated for 60 min at 37°C. Nucleus (1), early endosomes and multivesicular bodies (2), apical membrane with microvilli (arrowheads), and filter (★). Arrows indicate dense localization of WGA-HRP (blackening) at the lateral and basolateral membrane. 71
- Figure 8 Close-up view of apical part (top image) and basolateral side (bottom image) of Caco-2 monolayer loaded with WGA-HRP at 4°C and post-incubated for 60 min at 37°C. Nucleus (1), multivesicular bodies (2), lysosome (3). Note the blackenings at the apical (arrowheads) and basolateral membrane (arrows). 72
- Figure 9 Mean particle size (bar) and fluorescence intensity (line) of plain BOD-NP in selected dispersants at room temperature (closed) and after 90 min at 37°C (open). 82

- Figure 10 Release of BOD from nanoparticles in course of incubation at 4°C and 37°C. 84
- Figure 11 Mean cell associated fluorescence intensity of Caco-2 cells incubated with plain (-Δ-) and HSA-BOD-NP (-◆-) at 4°C. 84
- Figure 12 Caco-2 cells incubated with plain (A) and HSA-BOD-NP (B) for 60 min at 4°C. The centre of the cell is marked with an “x” for orientation. Scale bar represents 20 μm. 85
- Figure 13 Mean cell-associated fluorescence intensity of Caco-2 cells in course of time incubated with WGA-BOD-SMP, HSA-BOD-SMP, and plain BOD-SMP (25 ng mL⁻¹ corresponding concentration of BOD) at 4°C. 90
- Figure 14 Mean cell-associated fluorescence intensity of Caco-2 cells incubated with a diluted series of WGA-BOD-SMP, HSA-BOD-SMP, and plain BOD-SMP for 60 min at 4°C. 91
- Figure 15 Mean cell-associated fluorescence intensity of Caco-2 cells loaded with WGA-BOD-SMP for 60 min at 4°C in course of further incubation at 4°C and 37°C. 92
- Figure 16 Mean cell-associated fluorescence intensity (-Δ-) and percentage of inhibition (-■-) in course of competitive inhibition of WGA-BOD-SMP binding to Caco-2 cells by addition of increasing amounts of the complementary carbohydrate N,N',N''-triacetylchitotriose at 4°C. 93
- Figure 17 Fluorescence microscopy images of Caco-2 cells incubated with plain BOD-SMP (A), HSA-BOD-SMP (B), and WGA-BOD-SMP (C) for 60 min at 4°C. The center of the cell is marked with an “x” for orientation. Optical cross sections of Caco-2 cells incubated with WGA-BOD-SMP at 4°C taken at the top (D), center (E), and bottom (F) of the cell. Incubation for a further 30 min at 37°C and staining of the cell membrane with FM 4-64 (G). Scale bar represents 10 μm. 93
- Figure 18 Positively (closed symbols) and negatively charged particles (open symbols) associated with Caco-2 cell monolayers upon incubation in isoHEPES for 30 min at 37°C. Particle diameter 500 nm (Δ) and 2000 nm (o). Each data point consists of n= 27 measurements. 104
- Figure 19 Negatively (1) and positively charged (2) 500 nm particles (green) associated with Caco-2 cells after 30 min incubation. Concentration of particle suspension ~1 μg/100 μL (A) and ~8 μg/100 μL (B). Tight junction associated protein ZO-1 labelled in red. 105

- Figure 20 Positively (closed symbols) and negatively charged particles (open symbols) associated with Caco-2 cell monolayers upon incubation in PBS for 30 min at 37°C. Particle diameter 500 nm (Δ) and 2000 nm (o). Each data point consists of n=6 measurements. [106](#)
- Figure 21 Positively (closed symbols) and negatively charged particles (open symbols) associated with HUVEC cell monolayers upon incubation in PBS for 30 min at 37°C. Particle diameter 500 nm (Δ) and 2000 nm (o). Each data point consists of n=21 measurements. [107](#)
- Figure 22 Negatively (1) and positively charged (2) 2000 nm particles (green) associated with HUVECs after 30 min incubation. Concentration of particle suspension $\sim 1 \mu\text{g}/100 \mu\text{L}$ (A) and $\sim 8 \mu\text{g}/100 \mu\text{L}$ (B). Vascular endothelial cadherin (red). [108](#)
- Figure 23 Surface deformation associated with surface acoustic wave (SAW). Image by courtesy of T. Franke, University of Augsburg [115](#)
- Figure 24 Dye at the interface between a piezoelectric substrate and a fluid is ejected by pressure jets of a surface acoustic wave (SAW). Image by courtesy of T. Franke, University of Augsburg [115](#)
- Figure 25 Interdigital transducers (IDTs) on a piezoelectric substrate (PES) generating SAWs which lead to the streaming of fluid over a cell monolayer in a liquid-filled channel (A). SAW-pump consisting of the high frequency connector (HF-input) and the IDTs on a PES which are annulated in the bottom left corner of the 3D-microchannel. A PDMS-cast attached to a glass coverslip confines a channel structure for the cultivation of cells (B, for disassembled view see Figure 26, for close-up view of IDTs see Figure 27). Cross section of the flow velocity profile generated in the channel shown in (B) by acoustic streaming (C). Horizontal (D, solid line) and vertical cut (D, dashed line) through (C). [120](#)
- Figure 26 Acoustically-driven biochip and 3D-microchannel. Surface acoustic wave (SAW) pump consisting of the high frequency connector (HF-input) and piezoelectric substrate (PES) with interdigital transducers (IDTs). [121](#)
- Figure 27 Interdigital transducers (IDTs). Bar represents 100 μm . [121](#)
- Figure 28 Mean number of WGA- (squares) and BSA-MP (stars) associated with Caco-2 monolayers after loading for 30 min at stationary conditions, washing and chase-incubation under stationary or flow conditions. Each set of data points was obtained from independent experimental series. [123](#)

- Figure 29 Cell-associated microparticles (green) after stationary loading, washing and chase-incubation under stationary conditions (flow velocity_{max} = 0 μm s⁻¹; WGA-MP (A); BSA-MP (C)). Same loading procedure but chase-incubation under flow conditions (flow velocity_{max} = 1700 μm s⁻¹; WGA-MP (B); BSA-MP (D)). Tight junction associated protein ZO-1 (red). Bar represents 20 μm. [124](#)
- Figure 30 Mean number of WGA-MP (squares) and BSA-MP (stars) associated with Caco-2 monolayers upon incubation under stationary and flow conditions. Monolayers pre-loaded with microparticles for 30 min under stationary conditions (filled symbols). Direct incubation of microparticles with monolayers under stationary and flow conditions (open symbols). [126](#)
- Figure 31 Platform with four integrated SAW-pumps for flow studies in microchannels. [133](#)
- Figure 32 Flow velocities generated by four IDTs in microchannels on a SAW-platform for parallelized microfluidics. Channels 1-4 represent the respective microchannels arranged on top of the four IDTs of the chip (Figure 31). Flow velocities of n= 10 particles per channel were determined after 15 min (top graph) and 30 min of operation (bottom graph). [135](#)
- Figure 33 Flow velocities generated by one of the four IDTs of the SAW-platform in a microchannel on four different glass plates on consecutive days. Flow velocities of n= 10 particles were determined after 15 min of operation. [136](#)
- Figure 34 HUVEC monolayer grown in 3D-microchannels. VE-cadherin immunostained according to the procedure described in [1.2.3.2](#) (red). Note the border of the cell monolayer at the right as structured by the wall of the PDMS channel. [136](#)
- Figure 35 Transport of drug molecules from an apical compartment through a polarized cell monolayer grown on a filter membrane into a basolateral compartment. Insufficient filtration area due to low pore densities will result in the buildup of a concentration gradient inside the filter. [139](#)

Figure 36 Caco-2 layer grown on metal grid with mesh width of 25 μm . Tight-junction associated protein ZO-1 (green, top image) and cell nuclei stained with propidium iodide (red, bottom image). The steel wires appear as dark structures in the background. [141](#)

LIST OF TABLES

Table 1	Dynamic viscosities of aqueous solutions of Pluronic F-68 determined at 20 °C 19
Table 2	Currently approved drug formulations based on PLGA microparticles ¹ 23
Table 3	Comparison of some basic decisive parameters nanoparticle preparation ² 26
Table 4	Analytical methods for characterization of surface-modified PLGA particles 39
Table 5	Stability parameters of plain and modified BOD-NP stored in HEPES at 4°C or -80°C. 81
Table 6	Mean particle size, PDI, and zeta potential of plain BOD-SMP, HSA-BOD-SMP, and WGA-BOD-SMP. 89
Table 7	Zeta potential of 500 nm and 2000 nm polystyrene particles before and after surface modification with PEI. 103
Table 8	Diameter, flow velocity and total cross sectional area of blood vessels of the human body 112
Table 9	Comparison of commercially available filter materials for transport studies with metal grid 138

ACRONYMS AND ABBREVIATIONS

AAL	Aleura aurantia lectin
AFM	atomic force microscopy
APC	antigen-presenting cells
ATR	attenuated total reflectance
BCS	biopharmaceutics classification system
BOD	4,4-difluoro-1,3,5,7,8-pentamethyl-4-bora-3a,4a-diaza-s-indacene; BODIPY 493/503
BOD-NP	BODIPY-labelled nanoparticles

¹ US and EU; modified from [1]

² summarized from [2]

BOD-SMP	BODIPY-labelled submicroparticles
BSA	bovine serum albumin
BSA-MP	bovine serum albumin-modified microparticles
CPGS	cholecalciferol poly(ethylene glycol) succinate
CT	computerized axial tomography
CTAB	cetyltrimethylammonium bromide
DAB	3,3'-diaminobenzidine
DC	dendritic cell
DD	degree of deacetylation
DDAB	dimethyl dioctadecyl ammonium bromide
DDPC	1,2-didecanoylphosphatidylcholine
DPPC	1,2-dipalmitoylphosphatidylcholine
DSS	dioctyl sodium sulfosuccinate
DiI	1,1-dioctadecyl-3,3,3',3'-tetramethylindocarbocyanine perchlorate
DiO	3,3'-dioctadecyloxacarbocyanine perchlorate
DLS	dynamic light scattering
DMAB	didodecyl dimethyl ammonium bromide
DOTAP	1,2-dioleoyl-1,3-trimethylammonio propane
DPPC	1,2-dipalmitoylphosphatidylcholine
DSMZ	Deutsche Sammlung von Mikroorganismen und Zellkulturen
DSPE	distearoylphosphatidylethanolamine
EDAC	1-ethyl-3(3-dimethylaminopropyl) carbodiimide
EGF	epidermal growth factor
EPR	enhanced permeability and retention
F-BSA	fluorescent bovine serum albumin
F-WGA	fluorescent wheat germ agglutinin
FBS	fetal bovine serum
FDA	food and drug administration
FGF	fibroblast growth factor
FITC	fluorescein isothiocyanate
FTIR	Fourier transform infrared spectroscopy
GMBS	N-(α -maleimidobutyryloxy)succinimide ester
GM-CSF	granulocyte-macrophage colony-stimulating factor

HBEGF	heparin binding epidermal growth factor
HEPES	20 mM HEPES/NaOH buffer pH 7.4; 4-(2-hydroxyethyl)-1-piperazineethanesulfonic acid
HES	hydroxyethyl starch
HF	high frequency
HIC	hydrophobic interaction chromatography
HIV	human immunodeficiency virus
HRP	horseradish peroxidase
HSA	human serum albumin
HSA-BOD-NP	human serum albumin-modified BODIPY-labelled nanoparticles
HSA-BOD-SMP	human serum albumin-modified BODIPY-labelled sub-microparticles
HUVEC	human umbilical vein endothelial cells
ICAM-1	intercellular adhesion molecule-1
IDT	interdigital transducer
isoHEPES	isotonic HEPES/NaOH buffer pH 7.4
MP	microparticles
MRI	magnetic resonance imaging
MW	molecular weight
MWCO	molecular weight cut-off
NHS	N-hydroxysuccinimide
NP	nanoparticles
PAA	poly(acrylic acid)
PAMAM	polyamidoamine
PBS	phosphate-buffered saline pH 7.4
PC	polycarbonate
PCL	poly(ϵ -caprolactone)
PCS	photon correlation spectroscopy
PdI	polydispersity index
PDMS	poly(dimethylsiloxane)
pDNA	plasmid deoxyribonucleic acid
PE	polyester
PEG	poly(ethylene glycol)
PEI	poly(ethylene imine)

PEMA	poly(ethylene-alt-maleic acid)
PEO	poly(ethylene oxide)
PES	piezoelectric substrate
PET	poly(ethylene therephthalate); positron emission tomography
PLA	poly(D,L-lactic acid)
PLGA	poly(D,L-lactic-co-glycolic acid)
PLL	poly(L-lysine)
poly(I:C)	poly(inosine)-poly(cytidylic acid)
PPFC	parallel plate flow chamber
PPO	poly(propylene oxide)
PPG	poly(propylene glycol)
PS	polystyrene
PSMA	prostate-specific membrane antigen
PSS	poly(styrene-co-4-styrene-sulfonate)
PVA	poly(vinyl alcohol)
Re	Reynolds number
RES	reticuloendothelial system
RF	radio frequency
RFDA	radial flow detachment assay
RGD	arginine-glycine-aspartic acid
rhGH	recombinant human growth hormone
RPMI-1640	Roswell Park Memorial Institute 1640 cell culture medium
SAW	surface acoustic wave
SDS	sodium dodecyl sulfate
SEM	scanning electron microscopy
SIMS	secondary ion mass spectrometry
SLN	solid lipid nanoparticles
SMP	submicroparticles
SSIMS	static secondary ion mass spectrometry
tat	trans-activating transcriptor
TEER	transepithelial electrical resistance
TEM	transmission electron microscopy
TGF- β	transforming growth factor- β

TOF	time-of-flight
TPGS	D- α -tocopheryl polyethylene glycol 1000 succinate
UEA	Ulex europaeus agglutinin
VE	vascular endothelial
VEGF	vascular endothelial growth factor
WGA	wheat germ agglutinin
WGA-BOD-NP	wheat germ agglutinin-modified BODIPY-labelled nanoparticles
WGA-BOD-SMP	wheat germ agglutinin-modified BODIPY-labelled submicroparticles
WGA-MP	fluorescent wheat germ agglutinin-modified microparticles
XPS	X-ray photoelectron spectroscopy
ZO-1	zonula occludens-1

Part I

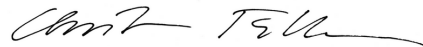
PREFIX

AUTHOR CONTRIBUTIONS

I hereby declare that I have significantly contributed to the realization of the studies included in the present thesis.

Concerning the publication “Stabilizer-induced viscosity alteration biases nanoparticle sizing via dynamic light scattering, *Langmuir* 23:8699-8702, 2007” [1.1.1] I designed and performed the experiments, analyzed and interpreted the data and wrote the paper. The review article “The role of surface functionalization in the design of PLGA nano- and microparticles, *Critical Reviews in Therapeutic Drug Carrier Systems* 27(1):1-83, 2010” [1.1.2] was written in collaboration with the other authors. Regarding the papers “Bionanoprobes to study particle-cell interactions, *Journal of Nanoscience and Nanotechnology* 9:3239-3245, 2009” [1.2.1] and “Fluorescent bionanoprobes to characterize cytoadhesion and cytoinvasion, *Small* 4(5):627-633, 2008” [1.2.2] I contributed to the study design, analyzed and interpreted the data and wrote the manuscripts. I conceived the experiments, analyzed the data and authored the manuscript for “Binding of positively and negatively charged particles to an epithelial and endothelial cell model” [1.2.3]. Concerning the publication “An acoustically-driven biochip - Impact of flow on the cell-association of targeted drug carriers, *Lab on a Chip* 9:2782-2788, 2009” [2.2.1] I participated in the design and elaboration of the chip setup. Moreover, I planned and was involved in the experiments, analyzed and interpreted the data and wrote the paper.

Vienna, June 2010



Christian Fillafer

ABSTRACT

The application of micro- and nanoparticles as drug carrier systems represents a highly promising approach to biopharmaceutically improve the administration of drugs. The interaction of particles with tissues of the human body will be determined by their size and most importantly surface characteristics. Consequently, modification of the particle surface with bioadhesive molecules could represent a potent means for controlling the residence time and localization of particles in the body.

In the present thesis it was investigated to what extent ionic and biorecognitive interactions can be employed for mediating the adhesion of particles to epithelial and endothelial cells. By adsorption of the cationic polyelectrolyte poly(ethylene imine) (PEI) the zeta potential of negatively charged polymer particles was inverted. As a consequence of this surface modification a 3-fold higher binding of microparticles and 5-fold higher binding of nanoparticles to artificial intestinal epithelium was observed. However, a general transfer of these results to other cell types does not seem possible since positively charged particles were not characterized by preferential binding to primary endothelial cells.

In order to enhance the specific bioadhesion of micro- and nanoparticles, covalent conjugation with wheat germ agglutinin (WGA) was employed. As a consequence of the interaction between the surface-bound lectin and carbohydrates in the glycocalyx, a 73-fold enhanced binding as compared to plain colloids was observed. This underlines that modification with lectins represents a promising concept for improving the bioadhesive properties of particulate drug carrier systems.

Usually, bioadhesion studies are performed under stationary conditions. However, upon peroral as well as parenteral administration hydrodynamic forces will act on the particles. This might substantially influence their interaction with the tissue. In order to facilitate studies on the effects of flow on bioadhesion, a miniaturized chip-based microfluidic system was developed. By controlled generation of surface acoustic waves (SAWs) fluids can be controllably actuated in this tissue-culture compatible device. Thereby, hydrodynamic conditions comparable with those in the gastrointestinal tract and in the circulatory system can be generated *in vitro*. This flow model was employed to investigate the influence of shear forces on the binding of WGA-modified and plain microparticles to epithelial monolayers. Clear discrepancies between the number of cell-associated particles under stationary and flow conditions were observed. These results illustrate that an integration of flow into preclinical biopharmaceutical test systems might enable an improved understanding of bioadhesion in a physiological environment.

The developed tissue-chip hybrid for flow studies as well as the techniques for surface modification and particle detection will represent versatile tools for future studies dealing with the biopharmaceutical optimization of drug administration.

ZUSAMMENFASSUNG

Der Einsatz von Nano- und Mikropartikeln als Trägersysteme stellt einen vielversprechenden Ansatz zur biopharmazeutisch verbesserten Applikation von hochpotenten etablierten und Biotech-Wirkstoffen dar. Die Interaktion der Partikel mit Geweben des menschlichen Körpers wird abgesehen von der Partikelgröße vorwiegend durch die chemische Struktur der Partikeloberfläche bestimmt. Folglich kann durch Modifikation der Oberfläche mit bioadhäsiven Molekülen die Lokalisation und Verweildauer der partikulären Arzneiform im Körper grundlegend beeinflusst werden.

Im Rahmen der vorliegenden Dissertation wurde untersucht, inwiefern elektrostatische oder biorekognitive Wechselwirkungen ausgenutzt werden können, um die Bindung von Nano- und Mikropartikeln an humane epitheliale und endotheliale Zellen zu erhöhen. Die negative Oberflächenladung von Polymerteilchen wurde durch Beschichtung mit dem kationischen Polyelektrolyt Polyethylenimin invertiert. Durch diese Ladungsumkehr konnte eine 3-fach erhöhte Bindung von Mikropartikeln und eine 5-fach erhöhte Bindung von Nanopartikeln an ein Gewebekulturmodell des humanen Dünndarms erzielt werden. Ein generelles Übertragen dieser Ergebnisse auf andere humane Zelltypen ist jedoch nicht uneingeschränkt möglich, da beispielsweise an primären humanen Endothelzellen keine bevorzugte Bindung von positiv geladenen Partikeln nachgewiesen werden konnte.

Zur Erhöhung der spezifischen Bioadhäsivität wurden Nano- und Mikropartikel kovalent mit Weizenkeimlektin derivatisiert. Die Wechselwirkung dieses zuckerbindenden Proteins mit Bestandteilen der zellulären Glykocalyx erhöhte die Bindungsraten an Caco-2 Einzelzellen 73-fach im Vergleich zu nicht modifizierten Partikeln. Dadurch konnte bestätigt werden, dass die Konjugation mit Lektinen ein vielversprechendes Konzept im Rahmen der Entwicklung bioadhäsiver Wirkstoffträger darstellt.

Standardgemäß werden Bioadhäsionsstudien unter stationären Bedingungen durchgeführt. Sowohl nach peroraler als auch nach parenteraler Applikation wirken jedoch Scherkräfte, die die Interaktion von Wirkstoffträgern mit dem Gewebe maßgeblich beeinflussen. Um eine Untersuchung der Bioadhäsivität von Partikeln unter annähernd physiologischen Bedingungen zu ermöglichen, wurde ein miniaturisiertes und dadurch potentiell parallelisierbares Flussmodell entwickelt. In diesem chipbasierten System werden mittels oberflächenakustischer Wellen hydrodynamische Kräfte erzeugt, die vergleichbar mit jenen im Darm und in den Blutgefäßen sind. Untersuchungen mit lektinmodifizierten Mikropartikeln zeigten, dass deutliche Diskrepanzen zwischen den zellgebundenen Partikelmengen unter stationären und dynamischen Bedingungen bestehen. Eine Integration von hydrodynamischen Parametern in präklinische biopharmazeutische Testmodelle erscheint demnach äußerst sinnvoll und könnte die Aussagekraft dieser Modelle deutlich erhöhen.

Die vorliegenden Ergebnisse zeigen, dass sowohl das entwickelte Chipmodell als auch die erarbeiteten Techniken zur Partikelmodifika-

tion und -detektion vielseitig anwendbares Potential für die biopharmazeutische Optimierung der Applikation von Wirkstoffen bieten.

Part II

MAIN SECTION

INTRODUCTION

Micro- and nanoparticles offer promising characteristics as drug delivery systems. Using suitable encapsulation techniques, hydrophilic and hydrophobic small molecules as well as proteins and peptides can be loaded into colloids.[1, 3] Hence, the active pharmaceutical ingredient is protected from premature degradation prior to and after administration to the patient. Most importantly, however, the surface of the drug carrier system can be chemically and structurally functionalized.[4] Thereby, the residence time of the formulation in the body can be prolonged and the biodistribution profile can be shifted towards specific cell types and tissues.

It is the aim of the present thesis to contribute to this thematic area by improving our current understanding of the interaction of surface modified particles with human cells. Since the size of particles is a decisive physical parameter that has to be known prior to any experimental studies, an introductory work will deal with the effects of excipients on the determination of nanoparticle size by dynamic light scattering techniques (1.1.1).

An array of approaches has been established for the surface modification of colloids. To provide an overview of the field, the underlying considerations and experimental realization of functionalization techniques will be discussed (1.1.2). The focus in this review of current literature is set on micro- and nanoparticles made of the intensely investigated polymer poly(D,L-lactide-co-glycolide) (PLGA). However, the involved strategies are certainly not limited to particles produced from this polymer but can be translated to a multitude of materials.

In the specific topics of the thesis, two particular surface modification approaches will be investigated regarding their effect on the bioadhesion of colloids.

Firstly, wheat germ agglutinin (WGA), a carbohydrate-binding protein will be employed to improve the cell-binding of micro- and nanoparticles by attachment to the cellular glycocalyx.[5] The fundamental interaction characteristics of WGA with a cell culture model of the human intestine will be elucidated in 1.1.3 on the basis of histological localization by transmission electron microscopy (TEM). In the subsequent section the elaboration of a technique for the fluorescence-labelling of lyophobic colloids will be described (1.2.1). By using these trackable particles as probes, the bioadhesive effects resulting from surface functionalization with molecules of interest can be investigated. This is exemplarily illustrated in a study which determines the cytoadhesion achieved by conjugation with WGA or human serum albumin (HSA) (1.2.2).

Secondly, negatively charged micro- and nanoparticles will be coated with the cationic polyelectrolyte poly(ethylene imine) (PEI) to investigate the role of particle surface charge on bioadhesion. Generally, the cell membrane of eukaryotic cells is negatively charged,[6] which suggests that positively charged carriers will preferentially bind due to ionic interactions. Whether modifications of particle surface charge are indeed a suitable means to improve bioadhesion will be investi-

gated with *in vitro* cell culture models of endothelium and intestinal epithelium (1.2.3).

Micro- and nanoparticles as drug carrier systems will behave differently from dissolved drug molecules upon administration to the human body. In order to allow for the development of efficient particulate formulations several fundamental parameters affecting the interaction of particles with the organism have to be investigated. Flow will disproportionately affect small molecules and particles.[7] How this can affect the performance of drug carrier systems will be discussed in an introductory section (2.1.1). Pertaining to bioadhesion, flow is expected to affect the binding of particles to tissues due to hydrodynamic forces. In order to estimate to which extent this factor will influence drug delivery with particles, reliable and versatile flow models have to be at hand. In the present thesis the development of a microfluidic system for this purpose will be reported. The device is operated by a state-of-the-art chip-based pumping technology which actuates fluids in a contact-free manner without the need for tubing. The underlying pumping principle relies on surface acoustic waves (SAW) which can be controlledly induced on a piezoelectric chip substrate (2.1.2).[8, 9] By using cell monolayers grown in microchannels in combination with the SAW-chip, a miniaturized *in vitro* tissue model is generated. This setup is used to investigate the effect of flow on the adhesion of WGA- and bovine serum albumin (BSA)-conjugated microparticles to artificial intestinal tissue (2.2.1).

As highlighted, SAW-devices have high potential for miniaturization. This will be exploited for the development of a parallelized *in vitro* flow model which in addition facilitates the use of microplate readers for detection of cell-associated absorbance, luminescence and fluorescence (2.2.2).

Finally, potential improvements of currently used systems for drug permeation studies across cell monolayers are discussed. At this, emphasis will be placed on the simulation of flow and a potential alternative to currently used filter membranes will be presented (2.2.3).

PROTEIN AND POLYELECTROLYTE COATINGS TO IMPROVE THE BIOADHESION OF MICRO- AND NANOPARTICLES

1.1 INTRODUCTORY WORKS

1.1.1 Stabilizer-induced viscosity alteration biases nanoparticle sizing via dynamic light scattering

Langmuir 2007, 23, 8699–8702

8699

Stabilizer-Induced Viscosity Alteration Biases Nanoparticle Sizing via Dynamic Light Scattering

Christian Fillafer, Michael Wirth, and Franz Gabor*

Department of Pharmaceutical Technology and Biopharmaceutics, Faculty of Life Sciences, University of Vienna, Vienna, Austria

Received February 23, 2007. In Final Form: June 14, 2007

The size dependent features of colloids at the nanometer scale have been issues of increasingly intensive research. In order to be able to correctly relate characteristics to certain size-populations, accurate and reliable particle sizing by dynamic light scattering (DLS) is a main prerequisite. So far, the complexity of the systems due to the presence of surfactants, proteins, and so forth in the nanoparticle suspensions has not been accounted for. In this work, practically relevant quantities of the frequently used PEO-PPO triblock copolymer surfactant Pluronic F-68 were studied for their effect on the size determination of nanoparticles by DLS. Induced changes in the tenside-content of the nanoparticle suspension were monitored using a photometric assay and were correlated to the respective variances in mean particle size. These measurements showed that alterations in the range from 0.005 to 2% of Pluronic content are associated with shifts in diameter of 200 nm-particles by as much as 65 nm. The considerable changes that were found have been attributed to the surfactant-concentration-dependent fluctuations in the viscosity of the nanoparticle suspension, which affect the dimensions of colloids calculated according to the Stokes–Einstein relation.

Introduction

The diversity of the exceptional features of nanoparticles is manifold, ranging from the photostability of semiconductor quantum dots^{1,2} to the passive accumulation of nanoparticulate drug delivery vehicles in tumor sites due to the enhanced permeability and retention (EPR) effect.^{3,4} These characteristics have in common that they cannot be generalized for submicrometer colloids but rather are dependent on the material properties and, very importantly, the actual size of the particles. In the case of quantum dots, this is strikingly illustrated by the precise interdependence between the particle's diameter and the wavelength at which fluorescence is emitted. However, not only the physical properties of nanoparticles but also their interaction with cells, subsequent intracellular trafficking, and therefore possible toxicity have been increasingly discussed issues.^{4–7} It is assumed that these characteristics are governed in a similarly grave manner by the dimensions of the colloids. The first evidence of such size dependence has been given by studies on the cellular and tissue uptake of nano- versus microparticles in the 1990s. It was shown that the uptake efficiency of 100 nm colloids is 15–250-fold higher as compared with that of 1–10 μm particles in a rat in-situ intestinal loop model.⁷ Similar tendencies toward the enhanced uptake of smaller particles were reported by Jani et al. using radiolabeled 50 nm–3 μm polystyrene microspheres in a rat in-vivo study.⁸

Although it has been known for several years that distinct size differences are inflicted with differential cellular uptake, account has been given lately that even very small alterations in size influence the cell association and intracellular processing of nanoparticles.^{9,10} Lai et al., for example, recently showed that small polymeric nanoparticles (<25 nm) but not larger ones (>42 nm) enter cells via a nondegradative pathway.¹⁰

Beyond the impact on the uptake of nanoparticles, the physical size also determines the biodistribution behavior of the colloids. In case of the EPR effect, this is illustrated by the accumulation of particles in the range from 70–200 nm because only such are suited to pass the fenestrated endothelium of tumor blood vessels.¹¹

These issues make clear that an accurate determination and knowledge of the physical dimensions of the particles are crucial prerequisites not only for toxicity studies but also for the rational design of nanoparticulate drug-delivery devices.

Currently, the method of choice for sizing nanoparticles in suspension is dynamic light scattering (DLS). If performed under standardized conditions, results obtained with this technique are rather comparable and reproducible. However, nanoparticle suspensions in practice represent complex and changing systems, which in most cases contain not only the dispersed colloids but also varying amounts of stabilizers, salts, proteins, and so forth. These substances not only physicochemically interact with the particles but also alter the properties of the dispersant. In the production process of single- or double-emulsion solvent evaporation techniques, for example, large amounts of surfactant serve the purpose of avoiding coalescence during the solidification of the nanodroplets. In the course of further treatments and modifications of the particles, however, the tenside content of the suspension and thus the viscosity vary considerably. Although such variations are expected to occur frequently and with a

* Corresponding author. E-mail: franz.gabor@univie.ac.at. Phone: (+43) 1 4277-55406. Fax: (+43) 4277-9554.

(1) Chen, F.; Gerion, D. *Nano Lett.* 2004, 4, 1827–1832.

(2) Guo, X.; Cui, Y.; Levenson, R. M.; Chung, J. W. K.; Nie, S. *Nat. Biotechnol.* 2004, 22, 969–976.

(3) Britanov-Peppas, L.; Blanchette, J. O. *Adv. Drug Delivery Rev.* 2004, 56, 1649–1659.

(4) Oberdorster, G.; Oberdorster, E.; Oberdorster, J. *Environ. Health Perspect.* 2005, 113, 823–839.

(5) Chithran, B. D.; Ghazani, A. A.; Chan, W. C. W. *Nano Lett.* 2006, 6, 662–668.

(6) Desai, M. P.; Labhasetwar, V.; Walter, E.; Levy, R. J.; Amidon, G. L. *Pharm. Res.* 1997, 14, 1568–1573.

(7) Desai, M. P.; Labhasetwar, V.; Amidon, G. L.; Levy, R. J. *Pharm. Res.* 1996, 13, 1838–1845.

(8) Jani, P.; Halbert, G. W.; Langridge, J.; Florence, A. T. *J. Pharm. Pharmacol.* 1996, 42, 821–826.

(9) Rejman, J.; Oberle, V.; Zahora, I. S.; Hockova, D. *Biochem. J.* 2004, 377, 159–169.

(10) Lai, S. K.; Hida, K.; Man, S. T.; Chen, C.; Machamer, C.; Schroer, T. A.; Hanes, J. *Biomaterials* 2007, 28, 2876–2884.

(11) Passirani, C.; Benoit, J. P. In *Biomaterials for Delivery and Targeting of Proteins and Nucleic Acids*; Mahato, R. I., Ed.; CRC Press: Boca Raton, FL, 2005; Chapter 6, p 204.

1.1.1.1 Abstract

The size dependent features of colloids at the nanometer scale have been issues of increasingly intensive research. In order to be able to correctly relate characteristics to certain size-populations, accurate and reliable particle sizing by dynamic light scattering (DLS) is a main prerequisite. So far, the complexity of the systems due to the presence of surfactants, proteins, and so forth in the nanoparticle suspensions has not been accounted for. In this work, practically relevant quantities of the frequently used poly(ethylene oxide)-poly(propylene oxide) (PEO-PPO) triblock copolymer surfactant Pluronic F-68 were studied for their effect on the size determination of nanoparticles by DLS. Induced changes in the tenside content of the nanosphere suspension were monitored using a photometric assay and were correlated to the respective variances in mean particle size. These measurements showed that alterations in the range from 0.005 to 2% of Pluronic content are associated with shifts in diameter of 200 nm-particles by as much as 65 nm. The considerable changes that were found have been attributed to the surfactant-concentration-dependent fluctuations in the viscosity of the nanoparticle suspension, which affect the dimensions of colloids calculated according to the Stokes-Einstein relation.

1.1.1.2 Introduction

The diversity of the exceptional features of nanoparticles is manifold, ranging from the photostability of semiconductor quantum dots,[10, 11] to the passive accumulation of nanoparticulate drug delivery vehicles in tumor sites due to the enhanced permeability and retention (EPR) effect.[11, 12] These characteristics have in common that they cannot be generalized for submicrometer colloids but rather are dependent on the material properties and, very importantly, the actual size of the particles. In the case of quantum dots, this is strikingly illustrated by the precise interdependence between the particle's diameter and the wavelength at which fluorescence is emitted. However, not only the physical properties of nanoparticles but also their interaction with cells, subsequent intracellular trafficking, and therefore possible toxicity have been increasingly discussed issues.[13, 14, 15, 16] It is assumed that these characteristics are governed in a similarly grave manner by the dimensions of the colloids. The first evidence of such size dependence has been given by studies on the cellular and tissue uptake of nano- versus microparticles in the 1990s. It was shown that the uptake efficiency of 100 nm colloids is 15-250-fold higher as compared with that of 1-10 μm particles in a rat in-situ intestinal loop model.[17] Similar tendencies toward the enhanced uptake of smaller particles were reported by Jani et al. using radiolabeled 50 nm-3 μm polystyrene microspheres in a rat *in vivo* study.[18] Although it has been known for several years that distinct size differences are inflicted with differential cellular uptake, account has been given lately that even very small alterations in size influence the cell association and intracellular processing of nanoparticles.[19, 20] Lai et al., for example, recently showed that small polymeric nanoparticles (<25 nm) but not larger ones (>42 nm) enter cells via a nondegradative pathway.[20] Beyond the impact on the uptake of nanoparticles, the physical size also determines the biodistribution behavior of the colloids. In case of the EPR effect, this is illustrated by the accumulation of particles in the range

from 70-200 nm because only such are suited to pass the fenestrated endothelium of tumor blood vessels.[21] These issues make clear that an accurate determination and knowledge of the physical dimensions of the particles are crucial prerequisites not only for toxicity studies but also for the rational design of nanoparticulate drug delivery devices. Currently, the method of choice for sizing nanoparticles in suspension is DLS. If performed under standardized conditions, results obtained with this technique are rather comparable and reproducible. However, nanoparticle suspensions in practice represent complex and changing systems, which in most cases contain not only the dispersed colloids but also varying amounts of stabilizers, salts, proteins, and so forth. These substances not only physicochemically interact with the particles but also alter the properties of the dispersant. In the production process of single- or double-emulsion solvent evaporation techniques, for example, large amounts of surfactant serve the purpose of avoiding coalescence during the solidification of the nanodroplets. In the course of further treatments and modifications of the particles, however, the tenside content of the suspension and thus the viscosity vary considerably. Although such variations are expected to occur frequently and with a practical impact, to the best of our knowledge, the importance of the factor viscosity on DLS measurements has not been accounted for.

In the present contribution, the existence and dimensions of such effects were investigated using the PEO-PPO triblock copolymer Pluronic F-68 and PLGA nanospheres as a model system. Pluronics, which are also referred to as poloxamers because of their surface activity and a wide range of tuneable hydrophilicity-lipophilicity balance, have been extensively used in the production and coating of colloids made from materials such as polystyrene,[22, 23, 24] poly(lactic acid) (PLA),[25, 26] poly(D,L-lactic-co-glycolic acid) (PLGA),[27, 28, 29, 30, 31] poly(β -malic acid-co-benzyl malate),[32] chitosan,[33] and solid lipid nanoparticles (SLN).[34]

1.1.1.3 Experimental Section

MATERIALS Resomer® RG503H (PLGA, 50:50 lactide/glycolide, inherent viscosity $0.32\text{-}0.44\text{ dL g}^{-1}$, acid number $>3\text{ mg of KOH g}^{-1}$) was purchased from Boehringer Ingelheim (Ingelheim, Germany). Pluronic® F-68, ammonium thiocyanate, and cobalt(II) nitrate hexahydrate were obtained from Sigma (Vienna, Austria). All other chemicals used were of analytical purity.

PREPARATION OF PLGA NANOSPHERES PLGA nanospheres were prepared by a water-in-oil-in-water solvent-evaporation technique.[35] Briefly, 400 μL of distilled water was emulsified with a solution containing 400 mg of PLGA in 2 g of ethyl acetate by sonication for 60 s (sonifier, Bandelin electronic UW70/HD 70; tip, MS 72/D, Berlin, Germany). Following the addition of 6 mL of a 10% aqueous solution of Pluronic F-68, the emulsion was sonicated again for 50 s, yielding the (w/o)/w emulsion that was poured into 100 mL of a 1% aqueous solution of Pluronic F-68. After mechanical stirring (600 rpm) for 1 h at room temperature, the residual ethyl acetate was removed under reduced pressure. The resulting nanosphere suspension was filtered (1 μm pore size) to eliminate aggregates.

PARTICLE SIZE ANALYSIS AND PROCESSING OF THE NANOSPHERES The mean particle size and distribution were determined by DLS (Zetasizer Nano ZS, Malvern Instruments Ltd, U.K.). All measurements were carried out in triplicate at 20°C after 5 min of equilibration time.

The removal of Pluronic was practically achieved by diafiltration. For this, 20 mL of a PLGA nanosphere suspension was repeatedly washed with 40 mL of distilled water on a tangential flow filtration system based on an ultrafiltration membrane (Vivaflow 50; 100,000 molecular weight cut-off (MWCO) poly(ether sulfonate), Sartorius Vivascience GmbH) which was operated by a peristaltic pump (MV-CA 8, Ismatec, Glattbrugg) at a system pressure of 2.5 bar.

QUANTIFICATION OF THE PEO-PPO BLOCK COPOLYMER Pluronic F-68 was quantified using a photometric assay relying on the complexation of a purple cobalt thiocyanate reagent with the copolymer.[36] The cobalt thiocyanate reagent used for the photometric quantification was prepared by dissolving 20 g of ammonium thiocyanate and 3 g of cobalt(II) nitrate-6H₂O in 100 mL of distilled water. Ethanol (80 µL, 96%), ethyl acetate (200 µL), cobalt thiocyanate reagent (100 µL), and the sample (50, 150, or 250 µL, depending on the concentration range) were mixed in a 2 mL Eppendorf cup. Following centrifugation of the precipitated complex at 10,400 rpm for 1 min (Centrifuge 5804R, Eppendorf), the supernatant was removed. After the tube walls and pellet were washed with ethyl acetate, the precipitate was dissolved in 2 or 0.5 mL of acetone, and the absorbance at 328 nm was determined using a U-3000 UV/vis spectrophotometer (Hitachi).

VISCOSITY MEASUREMENTS The dynamic viscosities of aqueous solutions of Pluronic were determined according to run-time measurements on a microviscometer (AMVn, Anton Paar GmbH, Graz) at 20°C using calibrated capillary/ball sets at an angle of inclination of 60°. The densities of the samples that are required to calculate the viscosities were determined with an oscillating U-tube densitometer (Anton Paar GmbH, Graz). All measurements were performed in triplicate with water as a reference, and the dynamic viscosity η was calculated according to (1.1) with K as the calibration constant, t as the run time of the ball, ρ_B as the density of the ball, and ρ_S as the density of the sample.

$$\eta = K t (\rho_B - \rho_S) \quad (1.1)$$

1.1.1.4 Results and Discussion

To investigate concentration-dependent effects of Pluronic on the particle sizing of nanospheres, a method for the quantification of the tenside is required. This was provided by a cobalt thiocyanate assay described in the literature.[36] Modifications of the sample size as well as the acetone volume for dissolution of the reagent/Pluronic complex lowered the detection limit of the assay and thereby allowed the direct determination of the tenside in aqueous solutions in the range from 2.5 to 0.005%.

When the Pluronic content of a PLGA nanoparticle suspension was analyzed in the course of diafiltration with distilled water, a rapid

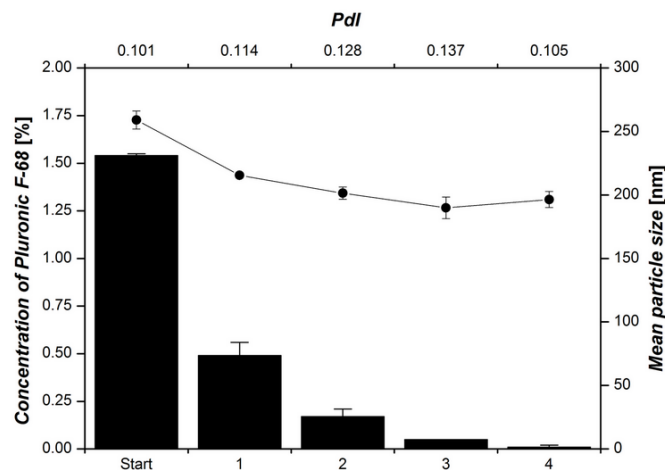


Figure 1: Polydispersity index (Pdl) and mean particle size of PLGA nanoparticles determined by dynamic light scattering (—●—) as well as the respective content of Pluronic F-68 in the suspension (solid bars) in course of purification by diafiltration.

decrease in the concentration was observed, reaching the detection limit of the photometric assay after four washing steps (Figure 1).

Starting with a PLGA nanosphere suspension containing 1.54% Pluronic, $96.7 \pm 0.35\%$ was removed during the first three washings, and 99.74% of the tenside was removed after one more purification step. Thus, a considerable amount of Pluronic contained in nanoparticle suspensions prepared according to the double-emulsion solvent-evaporation technique described above can be removed in a controllable manner by diafiltration with distilled water. In parallel, possible shifts in the particle size distribution were monitored by sizing the colloids via dynamic light scattering after each washing step. Commonly used purification methods such as (ultra)centrifugation impede the complete redispersibility of the pellet into single nanospheres as a result of the high rotation rates necessary for sufficient sedimentation. In contrast, tangential flow filtration allows to study the implication of washed-out surfactant in an unaffected manner.

These particle size measurements showed, concurrent with the previously discussed decrease in Pluronic content, that the sizes were notably lowered from 259 ± 7 to 196 ± 6 nm within the first four purification steps (Figure 1). During the next three washings, the suspension remained rather stable as controlled by DLS, and the mean particle size was not reduced below a threshold of about 195 nm.

These monitored size differences might partially be due to the desorption of surfactant molecules from the particle surface in the later stages of the washing procedure. However, according to Baker and Berg, size alterations in the hydrodynamic diameter of the colloids due to the adlayer of Pluronic F-68 solely amount to 6 nm.[37]

Furthermore, the seeming drop in particle size by 63 ± 6 nm can not be attributed to a gradual degradation of the nanospheres because otherwise the decrease would have progressed in the course of further washing steps. It is also known from molecular weight loss studies of microparticles made from PLGA with the same lactide/glycolide ratio

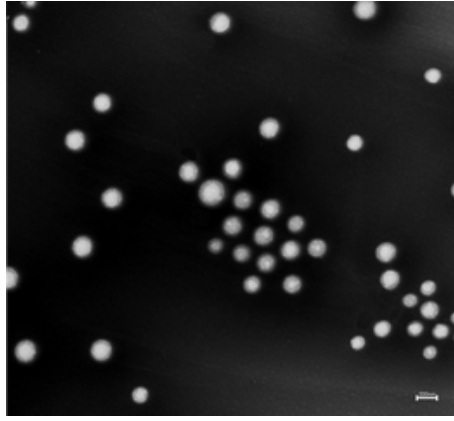


Figure 2: TEM image of PLGA nanoparticles suspended in a 1.54% aqueous solution of Pluronic, negative stained with uranyl acetate.

of 50:50 that the polymer decomposes rather slowly as illustrated by a half-life (50% molecular weight loss) of 15 days.[38]

Thus, the apparent decrease in the mean particle size during the first four washing steps might be attributed to the lowering of the Pluronic concentration (Figure 1). To narrow the observed effect down to an interference of varied Pluronic levels with DLS, the physical dimensions of the particles suspended in a 1.54% aqueous solution of Pluronic were analyzed by an independent imaging method (Figure 2). Indeed, as assessed by TEM (Zeiss EM 902) measurements, the mean particle size of the colloids is only about 200 nm compared with 259 ± 7 nm determined via the light scattering technique. To determine if the apparent decrease in size during diafiltration is reversible, 0.5, 1, 1.5, and 2% tenside were added to 1 mL aliquots of a purified nanoparticle suspension with a Pluronic content of <0.005%. As illustrated in Figure 3 (open bars), this results in a stepwise increase in the determined mean particle size with rising Pluronic content. The cause of these reversibly controllable size shifts was considered to be linked to particle size calculation by the DLS instrument. Using this technique, the random movement of colloids is monitored according to fluctuations in the intensity of the scattered light. From this, a decaying exponential correlation function is derived, and it contains the translational diffusion coefficient D . According to the Stokes-Einstein relation (1.2), D is inversely proportional to the dynamic viscosity η and the radius of an idealized sphere r with k as the Boltzmann constant and T as the absolute temperature. Thus, if the temperature is held constant, the diffusion coefficient for a sphere with the given radius r will be solely dependent on the dynamic viscosity of the suspension.

$$D = \frac{kT}{6\pi\eta r} \quad (1.2)$$

Experimentally, the influence of Pluronic on this variable was confirmed by a determination of the dynamic viscosities of 0.5, 1, 1.5, and 2% aqueous solutions of tenside. While viscosity measurements implicate shear stress of the sample, dynamic light scattering experiments are performed under static conditions. If the fluid exhibits Newtonian behavior, however, the viscosity can be extrapolated to that of a system under no shear stress and thus can be applied for this purpose.

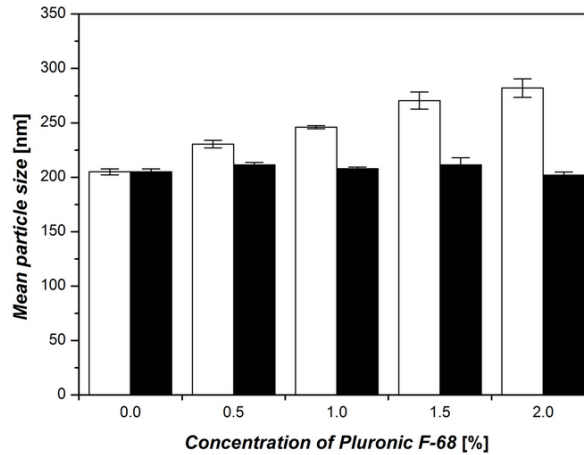


Figure 3: Mean particle size of PLGA nanoparticles dispersed in aqueous solutions of Pluronic F-68. Viscosity of water as dispersant property (open bars, DLS instrument's standard parameter). Results recalculated with the respectively determined dynamic viscosities (solid bars).

Table 1: Dynamic viscosities of aqueous solutions of Pluronic F-68 determined at 20 °C

dispersant	dynamic viscosity at 20°C [mPas]
water (reference)	1.0100±0.002
0.5% aqueous solution of Pluronic F-68	1.0765±0.021
1% aqueous solution of Pluronic F-68	1.1595±0.009
1.5% aqueous solution of Pluronic F-68	1.2578±0.0001
2% aqueous solution of Pluronic F-68	1.3772±0.003

Because of the low polymer content used in the experiments, it can be assumed that the determined viscosity of the fluid is rather shear-independent. Measurements illustrated in Table 1 show that increasing concentrations of the surfactant lead to incremental increases in the dynamic viscosity of the solution. The effect of this increased viscosity on the size calculation by the DLS instrument, as compared to that of the standard dispersant water, was assessed by a re-evaluation of the previous results from suspensions with different Pluronic content using the respectively adjusted viscosities. Consequently, the sizes of all samples were determined to be approximately 205 nm (Figure 3, solid bars), which corresponds to that of the control sample with less than 0.005% Pluronic as a reference.

Furthermore, preliminary results from viscosity measurements of poly(vinyl alcohol) (PVA), another frequently used stabilizing agent for the production of polymeric nanoparticles,[29, 39, 40] imply a similar effect on nanoparticle sizing as observed for Pluronic. The viscosities of 1 and 2% aqueous solutions of practically used PVA (MW~67,000) were determined to be 1.735±0.002 and 2.922±0.012 mPas, respectively. When extrapolating these viscosities to sizing results of nanospheres

with a mean diameter of 200 nm, apparent increases to 425 nm (1% PVA) and 687 nm (2% PVA) can be expected.

1.1.1.5 *Summary*

In the present work, it has been demonstrated that the results obtained from nanoparticle sizing by dynamic light scattering are prone to influences by tensides contained in the suspension. Practically relevant concentration variances between 0.005 and 2% PEO-PPO surfactants in a PLGA nanoparticle suspension are associated with significant alterations of the determined mean particle size. This effect has been attributed to the Pluronic concentration- dependent fluctuations in the dynamic viscosity of the nanoparticle suspension, which directly affect particle sizing by the dynamic light scattering technique. Because of the general cause of this implication, it can be deduced that the presence of any substance that might alter the suspension's properties needs to be considered.

To receive reliable results, the respective dynamic viscosities of the samples that can be determined either directly by viscometry or indirectly by quantification of the Pluronic concentration have to be supplied for the size calculation process. This will provide more accurate information on the actual size of the colloids, which is of special importance for studies on size-dependent properties of nanoparticles.

Acknowledgements

We thank M. Thiem and B. Berger (Anton Paar GmbH, Graz, Austria) for dynamic viscosity measurements and D. Gruber (Department of Ultrastructural Research, University of Vienna, Vienna, Austria) for performing the TEM analyses. Parts of this work were supported by the CellPROM project, funded by the European Community as contract no. NMP4-CT-2004-500039 under the 6th Framework Programme for Research and Technological Development in the thematic area of "Nanotechnologies and nanosciences, knowledge-based multifunctional materials and new production processes and devices". The contribution reflects the author's views, and the community is not liable for any use that may be made of the information contained therein.

1.1.2 The role of surface functionalization in the design of PLGA micro- and nanoparticles

Critical Reviews™ in Therapeutic Drug Carrier Systems, XX(X), xxx-xxx (2010)

The Role of Surface Functionalization in the Design of PLGA Micro- and Nanoparticles

Gerda Ratzinger, Christian Fillafer, Vera Kerleta, Michael Wirth, & Franz Gabor

Department of Pharmaceutical Technology and Biopharmaceutics, Faculty of Life Sciences, University of Vienna, Vienna, Austria

*Address all correspondence to XXXXX

ABSTRACT: Nano- and microcarriers prepared from the biocompatible and biodegradable polymer poly(D,L-lactide-co-glycolide) (PLGA) are being extensively studied for drug-delivery purposes. Apart from size, their fate in the body is mainly determined by surface characteristics that govern the interaction of the particles with their environment. The present review provides an overview of the currently established concepts for the surface functionalization of particles made from PLGA. In the first part, a concise description of the material-borne surface features and the related functionalization strategies are given, followed by current methods for the physical and chemical characterization of the particle surface. The second part highlights the aims of functionalization, which include improved drug delivery, vaccination, and imaging. Targeting approaches for site-specific delivery of drug-loaded particles to certain tissues or even to intracellular targets are presented, as well as stealth coatings for a prolonged blood circulation, labeling methods for imaging purposes, and strategies for the immobilization of macromolecular drugs on the particle surface. Finally, present limitations and future challenges will be discussed, with a focus on the surface-modification procedure and essential demands on functional particulate systems posed by the dynamic and complex in vivo environment.

ABBREVIATIONS

AFM	atomic force microscopy	APC	antigen-presenting cell
ATR	attenuated total reflectance	BSA	bovine serum albumin
CPGS	cholecalciferol polyethylene glycol succinate	CTAB	cetyltrimethylammonium bromide
DC	dendritic cell	DD	degree of deacetylation
DDAB	dimethyl dioctadecyl ammonium bromide	DDPC	1,2-didodecanoylphosphatidylcholine
DDS	dioctyl sodium sulfosuccinate	DiI	1,1'-dioctadecyl-3,3',3'-tetramethylindocarbocyanine perchlorate

0743-4863/10 \$35.00

© 2010 by Begell House, Inc. www.begellhouse.com

1

Gerda Ratzinger, Christian Fillafer, Vera Kerleta, Michael Wirth, Franz Gabor. The role of surface functionalization in the design of PLGA micro- and nanoparticles. *Critical Reviews in Therapeutic Drug Carrier Systems*, 27(1):1-83, 2010.

1.1.2.1 Abstract

Nano- and microcarriers prepared from the biocompatible and biodegradable polymer PLGA are being extensively studied for drug-delivery purposes. Apart from size, their fate in the body is mainly determined by surface characteristics that govern the interaction of the particles with their environment. The present review provides an overview of the currently established concepts for the surface functionalization of particles made from PLGA. In the first part, a concise description of the material-borne surface features and the related functionalization strategies are given, followed by current methods for the physical and chemical characterization of the particle surface. The second part highlights the aims of functionalization, which include improved drug delivery, vaccination, and imaging. Targeting approaches for site-specific delivery of drug-loaded particles to certain tissues or even to intracellular targets are presented, as well as stealth coatings for a prolonged blood circulation, labeling methods for imaging purposes, and strategies for the immobilization of macromolecular drugs on the particle surface. Finally, present limitations and future challenges will be discussed, with a focus on the surface-modification procedure and essential demands on functional particulate systems posed by the dynamic and complex *in vivo* environment.

1.1.2.2 Introduction

As indicated by 3869 published research papers, 3351 issued patents, and 393 disclosed theses by the end of July 2009, PLGA is one of the most extensively investigated polymers for drug delivery and tissue engineering.[41, 42] Although only a few pharmaceuticals are available on the market to date (Table 2), the high number of patents compared with research papers points to a powerful and promising excipient and much commercial interest. PLGA offers unique properties for drug-delivery purposes, such as worldwide approval for medical use, biodegradability, biocompatibility, and controlled release. However, some issues are not manageable by a single polymer, such as targeting the diseased tissue, cellular uptake and preprogrammed intracellular trafficking, and escaping the reticuloendothelial system (RES). Because contact with the body and the consequences thereof are mediated via the surface of the device, surface modification of sub-millimeter PLGA particles by grafting with selected biomimetic ligands can meet some of these ambitious challenges to pave the way toward a more efficacious medication with reduced side effects and improved patient compliance.

At present, GMP-grade PLGA is marketed as Lactel® (Polymers International, Pelham, AL), Medisorb® (Alkermes, Cambridge, MA), Purasorb® (Purac resp. CSM, Amsterdam), and Resomer® (Boehringer Ingelheim, Germany). Usually, the polymer is prepared by ring-opening polymerization of the cyclic dimeric anhydrides, D,L-lactide and glycolide in presence of Sn(II)-2-ethyl-hexanoate, Zn, or Zn-lactate as a catalyst.[43] Due to toxicological concerns regarding Sn and esterification of the hydroxyl group at one end of the polymer chain, which yields a more hydrophobic polymer, the latter two catalysts are preferred. In general, increasing the amount of catalyst generates more polymerization nuclei so that the molecular weight (MW) of the polymer decreases. Moreover, the higher reactivity of glycolide facilitates formation of glycolide microblocks rather than lactide ones.[44]

Table 2: Currently approved drug formulations based on PLGA microparticles ^a

ACTIVE PHARMACEUTICAL INGREDIENT	PRODUCT	LICENSE HOLDER
Peptides and Proteins		
buserelin acetate	Suprecur Depot® ^b	Hoechst
lanreotide acetate	Somatuline Depot® ^c	Beaufour Ipsen
	Somatuline LA® ^b , Somatuline retard® ^b	Ipsen
leuprolide acetate	Lupron Depot®, -3, -4, -PED ^c	Abbott Labs
	Prostap SR® ^b , Enantone® ^b	Takeda
octreotide acetate	Sandostatin LAR® ^{b, c}	Novartis
somatropin recombinant	Nutropin Depot® ^{c, d}	Genentech
triptorelin acetate	Gonapeptyl Depot® ^b	Ferring
triptorelin embonate	Decapeptyl SR® ^b	Ipsen
triptorelin pamoate	Pamorelin® ^b , Pamorelin LA® ^b	Debioclinic, Ipsen
	Trelstar Depot® ^c , Trelstar LA® ^c	Watson Lab
Small Molecules		
minocycline hydrochloride	Arestin® ^{b, c}	OraPharma
naltrexone	Vivitrol® ^c	Alkermes
risperidone	Risperdal Consta® ^{b, c}	Ortho McNeil Janssen, Janssen Cilag

^a US and EU; modified from [1]

^b approved in ≥ 1 countries of the EU (according to <http://www.hma.eu/mr1.html> (Mutual Recognition Index); <http://emc.medicines.org.uk/default.aspx> (Great Britain); http://pharmaweb.ages.at/pharma_web/index.jsf (Austria)); actual name of the marketed products may differ between countries

^c approved by FDA (according to <http://www.accessdata.fda.gov/scripts/cder/drugsatfda>)

^d commercialization discontinued in 2004

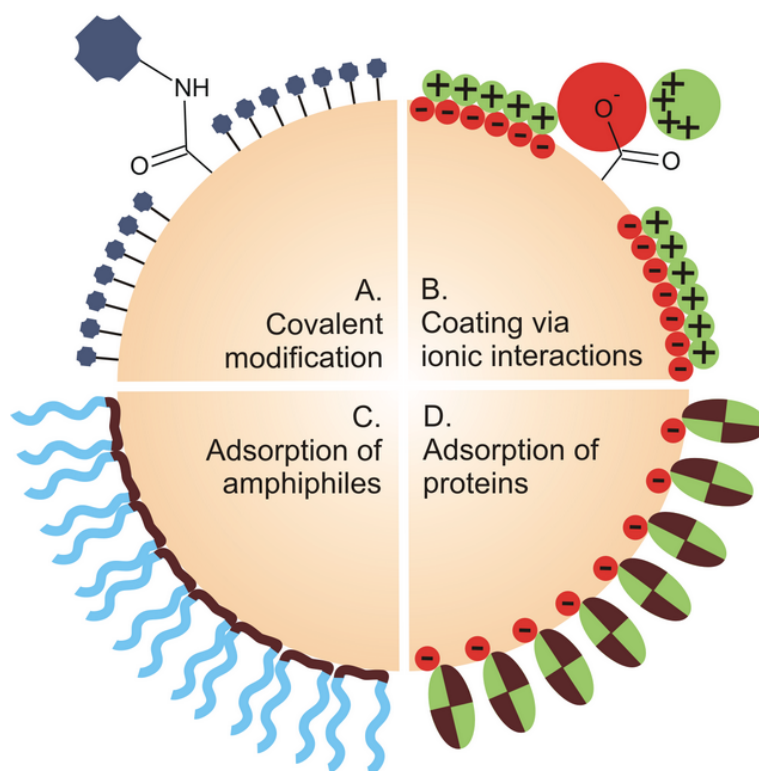


Figure 4: Strategies for surface modification of PLGA particles.

Most important for selection of the underlying mechanism of surface modification is the choice of the chain-length controller. Employing lactic acid to stop polymerization yields a polymer with a free carboxylic end group (uncapped), whereas lactic acid ethyl ester yields end-capped PLGA. Particles made from the carboxylate polymers, or so-called “H-type” products, open two basic pathways for stable surface modification: the covalent binding of bioactive moieties, preferably via carbodiimide, and grafting via ionic interactions due to the negative surface charge of particles (Figure 4). The third approach to surface modification relies on the overall hydrophobicity of both “H-type” and “non-H-type” PLGA, which allows adsorptive coating; however, this carries the risk of rapid desorption of the coat in biological fluids due to swelling and erosion of the particles.[23, 45, 46]

Generally, PLGA particles are prepared by so-called top-down processes starting with the polymer. For preparation of microparticles from PLGA, various techniques are available at the laboratory level, which basically rely on solvent extraction/evaporation, phase separation, and spray drying. According to the type of emulsion applied, several modifications of solvent extraction/evaporation are distinguished. The o/w technique relies on an emulsion prepared from a solution containing PLGA and the hydrophobic drug in a volatile organic solvent and an aqueous stabilizer solution. The organic solvent is removed by evaporation or extraction into the continuous cohesive phase causing hardening of the droplets. In the s/o/w method, instead of a solution, solid small-sized drug material is processed as before. The incorporation of a hydrophilic drug by the w/o/w method comprises emulsification of a small volume of an aqueous drug solution in a PLGA-rich organic

phase, followed by dispersion in a second aqueous phase containing a stabilizer. Diffusion of the organic solvent through the second aqueous phase and evaporation yields solid particles. In the o/o technique, the first oily solution, usually acetonitrile, contains PLGA and a hydrophobic drug with a certain water solubility. The first oily solvent is then extracted by the second oily solvent (e.g., cottonseed oil), leading to hardening of the droplets.[47]

The second basic technique is phase separation or coacervation, comprising dispersion of a solid or emulsified drug in the solution of PLGA, followed by the addition of a nonsolvent so that a co-acervate is formed at the interface. In the case of PLGA, salting out is a modification of this process in that the polymer is precipitated by the addition of water to an emulsion of PLGA dissolved in organic, water-miscible solvent and viscous PVA/salt solution.[48]

Finally, spray-drying is particularly suited for hydrophobic drugs but problematic for hydrophilic drugs, especially proteins and small batches.[49, 50] Alkermes, Inc. and Genentech, Inc. reported about a cryogenic spray technique, also known as Alkermes' ProLease® technology, at the developmental scale for the preparation of Zn-recombinant human growth hormone (Zn-rhGH)-loaded PLGA microspheres. Homogenized Zn-rhGH lyophilisate was dispersed in PLGA/dichloromethane and sprayed into liquid nitrogen. The organic solvent was extracted from the frozen droplets step-wise with liquid ethanol, first at -105°C and then at -40°C .[51]

The basic mechanisms for the formation of PLGA-nanoparticles are similar to those for microparticles but require smaller droplet diameters to enter the nanoscale. In the case of solvent extraction/ evaporation higher energy input is usually provided by sonication, high-pressure homogenization, or vigorous mechanical stirring.[52, 53] The nanoprecipitation technique relies on the interfacial deposition of PLGA by a nonsolvent following the displacement of a semipolar solvent miscible with water from a lipophilic solution, and yields nano- particles in the range of 100 to 300 nm with narrow size distribution in a one-step procedure.[54, 55, 56] Table 3 presents some basic parameters for nanoparticle preparation (for more detailed information, the reader is referred to some excellent reviews covering preparation of PLGA micro- and nanoparticles).[3, 57, 2, 58, 1]

As confirmed by the long and successful history of the absorbable sutures called Vicryl® (Polyglactin®910 by Ethicon, Inc., now subsidiary of Johnson & Johnson; 8% L-lactic acid and 92% glycolic acid), PLGA matrices are biodegradable.[59] In the aqueous biological environment, the polymer is first hydrated by adsorption of water and swelling of the matrix, a process lasting for days to months. Both hydrophilicity and crystallinity are key issues in this initial process. Among the different types of PLGA, the polymer composed of equal amounts of lactic and glycolic acid exhibits highest hydrophilicity and lowest crystallinity, leading to the fastest degradation. Because free carboxylate groups are more easily hydrated than ester moieties, the uncapped PLGA degrades faster than the end-capped polymer. This water uptake mediates random hydrolytic scission of ester bonds, yielding water-insoluble oligomers. Consequently, the mean MW of the polymer decreases but the mass of the particle remains constant. Because the PLGA-oligomers contain a free carboxylate on one end and ester hydrolysis is acid-catalyzed, carboxylated oligomers promote further degradation and

Table 3: Comparison of some basic decisive parameters nanoparticle preparation ^a

	EMULSION EVAPORATION	EMULSION DIFFUSION	SALTING OUT	SOLVENT DIFFUSION OR DISPLACEMENT NANOPRECIPIATION
solvent	not highly toxic	not highly toxic	not highly toxic but explosive	not highly toxic
drug	hydrophilic (double emulsion), hydrophobic (single emulsion)	hydrophobic	hydrophobic	poorly water soluble, highly soluble in polar solvent
energy consumption	high (emulsification and evaporation)	low except for high-speed homogenization	low	low
time requirement	moderate	high	low, but additional purification step required	high

^a summarized from [2]

a decrease in pH. This so-called “acidic microclimate” is observed in microparticles and in turn catalyzes scission of the polymer backbone. As soon as the MW of the oligomers drops below about 5.2 kDa, the oligomers become water-soluble, diffuse out of the matrix, and erosion of the particle is indicated by mass loss.[60] As opposed to surface erosion, homogeneous or bulk erosion is the mechanism generally accepted for degradation of PLGA particles less than 300 μm in diameter.[61] According to the degradation mechanism, a triphasic release profile is most commonly observed in PLGA microparticles: The so-called first burst effect, mainly due to release of surface-associated drug but also to pore formation upon water-entry,[62] is followed by a lag phase with diffusion-controlled slow release until erosion accelerates the release again.[53, 63] As opposed to the situation *in vitro*, *in vivo* biodegradation of PLGA was shown to be faster because of the plasticizing effect of lipids, the release of radicals due to a local immune response, autocatalytic cleavage of the polymer due to particle-aggregation, or contribution of enzymes to degradation.[1, 64] Due to bulk erosion upon biodegradation, it is expected that surface-modified PLGA particles retain their biorecognitive coating and thus their functionality even during release of the active pharmaceutical ingredient (API), as opposed to particles made from surface-eroding polymers.

Regarding *in vivo* administration, biocompatibility is another issue for drug-delivery purposes. The tissue response after subcutaneous injection of PLGA microparticles occurs in three phases:[38] Within the first 2 weeks, a minimal acute or finally chronic inflammatory response is observed at the site of administration associated predominantly with monocytes. The second phase comprises the foreign body reaction, which is associated with macrophages in the case of smaller microspheres or foreign body giant cells in the case of large microspheres, and the development of a fibrous capsule and granulation tissue. Upon erosion, the particles of microspheres are phagocytosed within weeks by either macrophages or foreign-body giant cells according to their size. In addition, some long-term studies have reported inflammatory responses, sometimes causing tissue necrosis but diminishing with time. This was observed in 15- μm PLGA particles and has also been attributed to degraded oligomers.[65, 66] After intraperitoneal administration of PLGA particles, a similar response comprising chronic inflammation and phagocytosis was reported in microparticles. However, nanoparticles caused minimal phagocytic activity, most likely due to clearance from the peritoneum within 2 d.[67] Because the open diameter of the smallest capillaries is 5 to 6 μm , particles smaller than 3 μm can be administered intravenously. Hemocompatibility studies with alendronate-loaded PLGA nanoparticles revealed no significant effect on hemolysis, leukocyte number, platelet activation, activated partial thromboplastin time, and complement consumption, and no cytotoxic effects on endothelial cells of blood vessels.[68] With the use of simulated blood fluid, however, the formation of 750-nm aggregates from 100-nm particles was observed and attributed to decreased electrostatic repulsion due to adsorption of cations.[69] Finally, the end-products of hydrolytic degradation of PLGA contribute to the biocompatibility of PLGA. Lactate is converted to pyruvate, which enters the Krebs cycle via acetylation of coenzyme A, and carbon dioxide, which is mainly eliminated by respiration. Part of the glycolate is excreted directly via the urine, another part is oxidized to glyoxylate, which is converted to

glycine, serine, and pyruvate. Pyruvate again enters the Krebs cycle to yield finally carbon dioxide and water.[60, 70]

As to the biocompatibility of PLGA, the utility of micro- and nanospheres as adjuvants for vaccination seems to be contradictory at the first sight. The immune response, however, is modified by design: particles less than 5 μm are taken up by antigen-presenting cells such as macrophages or dendritic cells. Additionally, the large surface area presents multiple copies of the adsorbed antigen. Finally, the matrix traps and retains the antigen in local lymph nodes and protects it from degradation, resulting in prolonged stimulation of the immune system.[71] Considering these issues, nanoparticles seem to be best suited for vaccination because they offer an increased surface area for antigen adsorption, possibly enhanced immunogenicity due to higher uptake rates, and are sterilizable by simple filtration.[72]

While the size of the PLGA particles is the key issue for successful vaccination, the application of these powerful potential carriers for certain therapeutic indications requires some further modifications to meet given specific demands. Considering the physicochemical characteristics of a preformed PLGA particle, the surface carboxylate groups of uncapped PLGA allow for covalent and electrostatic conjugation of ligands, whereas the hydrophobicity of the PLGA matrix can be exploited for adsorption of hydrophobic or even amphiphilic ligands. This review is intended to give an overview about the current knowledge of surface modification techniques, followed by a short description of the methods available for characterization. Further chapters deal with the different aims of functionalization, including nonspecific and specific bioadhesion, improved internalization, preprogrammed intracellular trafficking, imaging, prolonged circulation time, and stabilization of biomacromolecules. After discussing future challenges (1.1.2.5) the "Outlook" section (1.1.2.6) attempts to give a vision of this emerging field of research.

1.1.2.3 *Surface characteristics and related functionalization strategies*

CARBOXYLATE GROUPS: COVALENT MODIFICATION As outlined above, PLGA is available in two forms: uncapped, i.e. containing terminal carboxylate groups, and end-capped, i.e. terminated by an alkyl ester. The terminal carboxylates are often used for covalent conjugation of ligands either to the dissolved polymer prior to particle formation or to surface-exposed carboxylic groups of preformed particles. Owing to the high stability of covalent linkages, these approaches are generally preferable to other immobilization strategies in order to guarantee efficient functionalization. Many chemically sensitive ligands, such as proteins or peptides, should not be coupled to PLGA prior to particle preparation because they are prone to denaturation by organic solvents or shear stress during the emulsification process. Moreover, for a number of applications, the immobilized ligands have to be displayed at the particle surface. To meet these requirements, covalent coupling to the surface of preformed PLGA particles may be advantageous.

There are only few chemical groups that specifically react with carboxylates. Because carboxylic acids are rather weak nucleophiles in aqueous solutions, they do not easily couple via nucleophilic addition.[73] The most important chemical reaction for the covalent modification of PLGA carboxylates is the carbodiimide-mediated cross-linking with

amine-containing molecules. In this process, the carboxylic group reacts with a carbodiimide to yield an O-acylisourea intermediate, which is highly reactive and forms amide bonds with amine nucleophiles. Most importantly, the reaction works in aqueous buffers under mild conditions, including neutral pH, which makes it applicable to proteins, peptides, and other easily degradable molecules. At this, the water-soluble derivative 1-ethyl-3-(3-dimethylaminopropyl) carbodiimide (EDAC) can either be used alone or together with N-hydroxysuccinimide (NHS) or sulfo-NHS. While the O-acylisourea intermediate is prone to rapid hydrolysis, sulfo-NHS, and NHS give more stable active ester intermediates, which finally react with the amine. The increased stability may result in a higher coupling efficiency. Moreover, the application of the succinimide enables a two-step procedure for conjugation, which may be advantageous for ligands that bear not only amine but also carboxylic groups in order to avoid cross-linking. To saturate unreacted binding sites, an excess of small amine-containing ligands such as glycine or ethanolamine may be used. Until now, the carbodiimide method has been successfully used for conjugating a broad range of different amine-containing molecules, especially targeters such as peptides, lectins, and antibody fragments, but also polycations.[74, 75, 76, 77]

To enable the coupling of ligands that cannot directly react with carboxylate groups, various spacers such as diamines, polyamines, or dihydrazides may be applied.[78] Depending on their length and flexibility, spacers may enable or enhance the conjugation of certain ligands with barely accessible reactive groups. Moreover, they can influence the orientation of coupled ligands, which might have an impact on their bioactivity.

Although the number of carboxylic groups available for coupling to the particle surface has been criticized for being limited, it has proven sufficient to obtain a targeting effect, as already confirmed by enhanced particle-cell interactions.[75] However, for efficient coupling to PLGA carboxylates, the presence of steric stabilizers such as PVA or poloxamer should be considered, because the adsorbed stabilizer may compromise the reaction via steric hindrance.[79, 80]

SURFACE CHARGE: COATING VIA IONIC INTERACTIONS Nano- and microparticles made from uncapped PLGA are characterized by a negative surface charge at physiological pH. Primarily, this charge is due to carboxyl groups that arrange at the liquid/particle interface in the course of the preparation procedure. Because the pKas of the carboxyl groups of lactic and glycolic acid are 3.86 and 3.83, respectively, these groups increasingly exist in their dissociated form with increasing the suspension's pH above 4. Making use of these ionized groups, the particle surface can be coated with cationic polyelectrolytes via ionic interactions. The adsorption of polyelectrolytes onto the surface of particles in suspension is complex and influenced by several parameters. The packing and structure of the adsorbed layer is widely determined by the particle surface charge density, polyelectrolyte charge density, as well as by the pH and ionic strength of the suspension. The degree of dissociation of ionizable groups on particle surface and polymer can be varied by adjusting the pH, thus regulating the affinity between the surface and the polyelectrolyte.

In addition to pH, ionic strength is also decisive for the structure of adsorbed polymer.[81] Generally, in aqueous solutions of low ionic strength, polyelectrolytes have an expanded and rather rigid conformation due to intrachain repulsive forces. The adsorption of such stretched polymer molecules onto particles can lead to compensation of the surface charge, but does not necessarily introduce a surplus of cationic groups.[82] However, for most applications, an inversion of the negative surface charge by the cationic polyelectrolytes is desired. This can be achieved by adsorption from solutions containing appropriate amounts of salt. Increasing the solution's ionic strength leads to screening of repulsive intra- and interchain interactions, and consequently the polymer can adopt coiled and more flexible conformations. Due to this structural flexibility and reduced interpolymer repulsion, the adsorption of coiled polyelectrolytes can lead to higher deposition densities. Because not all of the ionized groups participate in binding to the particle, an overcompensation of surface charge, and thus inversion of the ζ -potential, occurs.[83] However, if the ionic strength of the adsorption medium exceeds a specific threshold, the charges on the polymer and on the particle surface might be screened to such an extent that adsorption is drastically reduced.[81]

Coating of negatively charged particles has been found to be advantageous for several applications. The positive charges imparted at the particle surface, for example, efficiently complex anionic macromolecules such as plasmid DNA (pDNA), and this has received considerable interest for the formulation of vaccines. Moreover, decoration with polycations is considered to be a rather unspecific but simple approach to enhance the adhesion of particles to mucus[84, 85] and cells.[86, 87, 88, 89] The mechanisms involved and possible influences of coating with cationic polyelectrolytes on internalization[86] and endosomal processing[90] will be discussed later. To make use of these potential benefits, natural, processed natural, and synthetic polyelectrolytes have been employed for the coating of negatively charged PLGA nano- and microparticles. These include protamine,[89] chitosan,[84, 88, 91, 92, 93, 94, 95, 96, 97, 98, 99] gelatine,[100] diethylaminoethyl dextran,[101] Eudragit® RL/RS,[85] PEI,[102, 103, 104, 105, 106] and poly(L-lysine) (PLL).[46, 87, 103, 107, 108, 109]

Protamine sulfate is an arginine-rich protein (approximately 4 kDa) that shares structural similarities with the human immunodeficiency virus (HIV) tat peptide and is characterized by membrane-translocating and nuclear-localizing activity.[110] Possibly due to these membrane-penetrating properties, microparticles coated with cationic protamine possessed transfection activity in HEK cells and increased immunogenicity compared with plain particles.[89]

A considerable number of studies have addressed the usability of chitosan for the surface modification of nano- and microparticles made from PLGA. Chitosan, which is a partially deacetylated derivative of the polysaccharide chitin, is commercially available in a variety of MWs and degrees of deacetylation (DD). The considerable variety of these materials is reflected in the studies dealing with coating, which report use of chitosans with MWs of approximately 48 kDa (DD: 75%–80%),[98, 99] 50 kDa (DD: 80%),[93] over 50 kDa (DD: 85%),[84] 88 kDa (DD: 85%),[96] as well as MWs of 150 and 150 to 400 kDa.[95] Primarily, surface modification of PLGA particles has been achieved by using chitosan/PVA blends as stabilizers in course of the parti-

cle preparation procedure.[84, 91, 92, 94, 96, 97] The incorporation of chitosan in the particle surface can be confirmed qualitatively by derivatization of the introduced amino groups with NHS-poly(ethylene glycol)-biotin, subsequent addition of Oregon Green®-streptavidin, and flow-cytometric analysis of the particle-associated fluorescence intensity.[94] Similarly, an assay using fluorescamine can be used to gain information on the qualitative and quantitative degree of polyamine adsorption.[83, 94, 96, 105] This assay is based on the reaction of the nonfluorescent compound fluorescamine with primary amino groups, yielding fluorescent pyrrolinones (excitation/emission: 390/475–490 nm).

As an alternative for the quantification of chitosan, complexation of the anionic dye Orange II with ammonium groups in acidic solution has been reported.[83] According to a systematic study by Guo et al., the amount of adsorbed chitosan increases with the polyelectrolyte concentration employed. As illustrated by fitting experimental data to adsorption isotherm models, the coating mechanism involved complies with a multilayer adsorption behavior on a heterogeneous surface.[96] Although adsorption in course of the preparation procedure is a facile and supposedly effective approach, it only offers limited control over the conformation and quantity of adsorbed polyelectrolyte. In this regard, the adsorption of chitosan onto preformed PLGA particles from solution seems preferable and has been achieved.[88, 93, 99, 98] Chitosan adsorption from solution is a spontaneous process governed by the electrostatic interactions of the polyamine with the negatively charged particle surface. However, additional anchoring of adsorbed polymer molecules can occur via hydrophobic interactions.[83] In a detailed study, the coating of PLA nanoparticles, which are expected to bear similar surface characteristics to PLGA particles, with various chitosans has been investigated. It was found that the amount of adsorbed polymer increased with rising MW with a deposition maximum for chitosan of approximately 150 kDa. Adsorption was also increased for chitosans with lower DD. Supposedly, less-deacetylated polymer chains exhibit reduced interactions with the aqueous solvent and consequently tend to adopt condensed conformations. In conjunction with decreased interpolymer repulsion at the surface, this leads to higher mass deposition rates.[83]

In contrast to chitosan, which bears a rather rigid carbohydrate backbone, synthetic polyamines such as PEI and PLL are characterized by enhanced polymer flexibility and higher charge densities. In the case of PEI, which is commercially available in linear and branched forms ranging from MW <1 kDa to 1.3×10^3 kDa, every third atom is a nitrogen atom that can be ionized by protonation. While linear PEIs mainly consist of secondary amino groups, branched PEIs are characterized by a theoretical primary to secondary to tertiary amine ratio of 1:2:1. These polymers have found widespread use for gene delivery *in vitro* and *in vivo* owing to an enhanced interaction with the negative cell membrane, the “proton sponge” effect, and the high potential for complexing anionic macromolecules (plasmid deoxyribonucleic acid (pDNA), antisense oligonucleotides).[111, 112, 113] To confer these features on PLGA nano- and microparticles, coating with PEI in course of the preparation procedure,[102, 103, 104, 114, 115] or onto preformed particles[105, 106] has been investigated. Yang et al. also showed that a layer-by-layer approach is feasible by using dextran sulfate as an anionic

counter-polyelectrolyte.[106] While in most studies, PEIs with a MW of 25 to 70 kDa have been used, high-MW compounds (600–1000 kDa) have also been employed. From a toxicological point of view, the latter seems questionable because the systemic administration of 800-kDa PEI has caused considerable toxicity, possibly due to a high potential for erythrocyte agglomeration.[112] Coating with branched PEI (MW approximately 25 kDa) has been shown to generate PLGA particles with a distinctly increased surface binding capacity for pDNA.[104, 105] Furthermore, successful polyamine adsorption was indicated by a clear increase of the buffering capacity towards HCl compared with plain particles.[105] Trimaille et al. studied the coating of PLA nanoparticles with branched PEI (MW approximately 10 and 25 kDa), and found that the optimum pH for ionization of surface carboxyl groups and polyelectrolyte amino groups was 5.8. The amount of nonadsorbed PEI was determined by a Coomassie blue assay. Moreover, visual proof of surface-deposited polymer was given by scanning electron microscopy (SEM). Consistent with theory, coating from solutions with low ionic strength resulted in the adsorption of flat molecules and a ζ -potential of approximately 1 mV, while coating in the presence of higher salt concentrations led to the deposition of coiled polymers and charge inversion.[82]

The synthetic polycation PLL has also been used for coating of negatively charged PLGA particles via ionic interactions in several studies. As with PEI, low MW polymers should be applied to avoid toxic side effects.[116] According to Cui et al., ionization of the ϵ -amino groups of PLL (MW approximately 150–300 kDa) by titration can be used to regulate the hydrophile-lipophile balance and secondary structure of the polyamine.[107] By using a reaction assay for the quantification of PLL via o-phthalaldehyde, it was found that a dissociation degree of $\geq 68\%$ and an α -helix content of $\geq 50\%$ is needed for sufficient surface entrapment of the polymer and stable microparticle formation. An alternative and quite promising approach has relied on the coating of preformed PLGA particles with multifunctional PLL-g-PEG polymers.[46, 108, 109] Two syntheses of PLL-g-PEG have been described in the literature. Spencer et al. conjugated a PLL backbone (MW approximately 20 kDa) with N-hydroxysuccinimidyl esters of methoxypoly(ethylene glycol) propionic acid (MW approximately 2 kDa) and attained a grafting ratio of lysine units to PEG chain of 3.5:1.[46, 108, 45] Thereby, sufficient ϵ -amino groups were still available for electrostatic interactions with surface carboxyl groups of the particles.[46, 108] By using PLL backbones grafted with methoxy-capped PEGs, protein-repellent coatings can be introduced to PLGA microparticles.[108] Moreover, it has been shown that PLL can be conjugated with arginine-glycine-aspartic acid (RGD)-capped PEGs and that subsequent adsorption of the PLL-g-PEG-RGD onto preformed microparticles yields target specific carriers.[46] An alternative approach to the synthesis of PLL-g-PEG has been reported by Kim et al.[109] The terminal primary amino group of a PLL backbone (MW approximately 2 kDa) with carbobenzoxy-protected ϵ -amino groups (ϵ -CBZ-PLL) was conjugated to carbodiimide-activated COOH-PEG-folate (MW approximately 3.4 kDa). Upon removal of CBZ with hydrogen bromide in acetic acid and coating of PLGA nanoparticles with polycationic PLL-g-PEG-folate, an enhanced binding of the colloids to folate receptor overexpressing cells was observed.[109] The direct electrostatic immobilization of a proteinaceous targeting agent

at the particle surface has been achieved by Kou et al., who expressed a single-chain antibody with a polylysine tag in *Escherichia coli* and characterized its adsorption onto PLGA nanospheres.[117]

As reported, the coating of nano- and microparticles made from PLGA by adsorption of polycations can be realized by two techniques. The hydrophile-lipophile balance and concentration of polyamine govern the incorporation of polyelectrolyte chains into the particle surface and matrix in course of the preparation procedure. In contrast, adsorption of polycations onto preformed particles is dominated by electrostatic interactions with negatively charged surface groups. However, the advantages and limits for pharmaceutical applications of either of the coating approaches have rarely been discussed. In general, systematic studies dealing with the effects of polyelectrolyte MW and charge density, solution pH, and ionic strength on the adsorption process are scarce for PLGA particles. Moreover, most reports in the literature lack a clear description of the adsorption protocol and specifications regarding the pH and ionic strength of the medium used for ζ -potential measurements. Without these parameters, the contribution of free carboxyl groups to the measured ζ -potential cannot be estimated correctly. The necessity of a critical interpretation of the ζ -potential is further illustrated by the fact that even particles prepared from end-capped PLGA exhibit a negative ζ -potential,[31] probably due to the adsorption of anions to the particle surface. In this context, the impact of stabilizers or surfactants on the surface carboxyl density of PLGA particles has not been addressed sufficiently. Although the formation of a nonremovable corona on the particle surface has been reported with PVA,[114, 29, 118] it is not clear to what extent the coating via ionic interactions is affected. Finally, since the anchoring stability of an adsorbed polyelectrolyte layer can be drastically compromised by electrolytes, tensides, and proteins,[119] investigations carried out in physiological media are needed to identify potential limits of polyelectrolyte coatings for pharmaceutical applications.

HYDROPHOBICITY: ADSORPTION OF AMPHIPHILES Due to the rather hydrophobic nature of PLGA, hydrophobic or amphiphilic molecules, polymers, and other substances may be adsorbed via hydrophobic interactions. Adsorption is defined as the accumulation or concentration of materials of one phase at the interfacial surface of the other phase.[120] The extent of adsorption increases with a decreasing solubility of an adsorbate in a solvent. The strong attraction between hydrophobic molecules and surfaces in water is a mainly entropic phenomenon.[121] In this section, adsorption that is predominantly based on hydrophobic interactions is described. Because protein adsorption is also strongly determined by electrostatic interactions, it is discussed separately.

During particle preparation via the solvent evaporation technique or similar procedures, an organic solution of PLGA is emulsified in an aqueous medium. In order to avoid coalescence, the dispersed organic-phase droplets must be prevented from contacting each other. This can be achieved by adding amphiphilic substances such as surfactants, polymers, or proteins that arrange themselves at the polar-apolar interface forming mono- or multibilayers.[122] Stabilizing polymers adsorb at the interface and may extend into both phases, preferably into the continuous phase. The polymer fractions located at the outside of the

droplets repel each other and therefore stabilize the emulsion. After solvent removal and particle solidification, amphiphiles are still necessary to complement the electrostatic stabilization of the suspension. While some stabilizers are adsorbed at the particle surface in a reversible manner, others may be physically entrapped in the particle matrix and build a residual layer at the surface that resists washing. Therefore, the choice of a certain stabilizer governs the surface characteristics of PLGA particles and can be exploited for designing carriers with tailored features. Moreover, even preformed particles may be exposed to hydrophobic molecules in order to achieve a surface-modification via adsorption.

PVA is one of the most frequently used emulsifiers for the preparation of micro- and nanoparticles from PLGA and related polymers. PVA is prepared by partial hydrolysis of poly(vinyl acetate) and therefore consists of rather hydrophobic vinyl acetate moieties and rather hydrophilic vinyl alcohol moieties. Upon particle preparation via a solvent evaporation technique, PVA and PLGA form an interconnected network at the interface with PVA anchored via its hydrophobic vinyl acetate moieties.[118] While PVA has been suspected to be carcinogenic,[123, 124, 125] the International Agency for Research on Cancer regards it as “not classifiable as to carcinogenicity to humans.”[126] Another commonly used group of emulsifiers are the poloxamers (Pluronics®), which are amphiphilic ABA triblock copolymers consisting of a hydrophobic poly(propylene glycol) (PPG) middle block and two hydrophilic PEG outer blocks. They are approved by the FDA for topical, oral, and parenteral application,[127] and are listed in the European Pharmacopoeia. Concerning the thickness of the adsorption layer, which depends on the hydrophobicity of the particle surface and the HLB of the respective Pluronic® type, the values in the literature range from 3 nm to even 20 nm.[30, 128] At high concentrations, Pluronic® hemimicelles are adsorbed. Further emulsifiers include semisynthetic derivatives of cellulose, such as methylcellulose and hydroxypropylmethyl cellulose, and polysorbates (Tween®).[1] However, for Tween 20, a strong toxicity was observed by a dramatically increased paracellular transport of [¹⁴C]sucrose in a blood-brain barrier endothelial cell culture.[129] In addition to nonionic stabilizers, ionic surfactants have also been assessed. Cationic emulsifiers such as cetyltrimethylammonium bromide (CTAB), dimethyl dioctadecyl ammonium bromide (DDAB), and 1,2-dioleoyl-1,3-trimethylammonio propane (DOTAP) were used during particle preparation to stabilize the emulsion owing to their amphiphilic properties. At the same time they furnish the resulting particles with a positive surface charge that allows the adsorption of DNA.[130, 131] Accordingly, anionic emulsifiers like sodium dodecyl sulfate (SDS) and dioctyl sodium sulfosuccinate (DSS) were employed for the preparation of PLGA particles with negative surface charge in order to enable the adsorption of antigens for immunization purposes.[132, 133] Nevertheless, for toxicity reasons the repertory of possible surfactants for parenteral administration is limited and some of the mentioned emulsifiers such as SDS will not be applicable.

Recently, there have been some approaches to substitute traditional nonbiodegradable surfactants by fully degradable alternatives. Phospholipids, especially those with saturated chains such as 1,2-didecanoylphosphatidylcholine (DDPC) or 1,2-dipalmitoylphosphatidylcholine (DPPC), were proposed as efficient emulsifiers for the preparation

of PLGA nanospheres.[134] Compared with PVA, a higher emulsifying efficiency was observed for DPPC, which was attributed to a more complete surface coating. In another approach, PLGA nanoparticles were coated with a pegylated-lipid envelope composed of PEG-distearoylphosphatidyl-ethanolamine (PEG-DSPE), phosphatidylcholine, and cholesterol, resulting in the formation of a so-called nanocell.[135] Upon encapsulation of a drug within the PLGA matrix and incorporation of a second lipophilic agent within the envelope, a temporal release of the two drugs was reported. Hydroxyethyl starch (HES) is a well-established plasma volume expander that could be an interesting alternative to the nonbiodegradable PEG.[136] HES can be hydrophobically modified by the formation of fatty acid esters. Using HES laurate for stabilization, PLGA nanoparticles with a narrow size distribution and a mean particle size of 110 nm were prepared and further characterized in protein adsorption assays using HSA and fibrinogen.[128] Therefore, HES laurate provided a stealth character comparable to Pluronic® F127 and even superior to Pluronic® F68, which was also confirmed by *in vitro* phagocytosis assays with murine macrophages. Another promising approach is the use of alkylpolyglucosides, which are nonionic surfactants consisting of glucose units and a fatty alcohol.[125]

The adsorption characteristics of amphiphiles also play an important role in the covalent surface modification of PLGA particles. In the presence of PVA, the conjugation of polyclonal antibodies to PLGA nanoparticles was reduced by 48%.[79] In the presence of high concentrations of Pluronic® F68, ligand coupling decreased by up to 65%.[80] Thus, easily removable emulsifiers may be preferred in order to enable access to the PLGA carboxylate groups. However, there are an increasing number of studies that exploit the irreversible adsorption of amphiphilic molecules for the functionalization of PLGA particles. This might be achieved either by using high-affinity emulsifiers that remain stably associated with the particle surface and confer an inherent additional functionality to the particles in order to alter their interaction with cells, or by covalent coupling of targeters and other substances to surface-anchored emulsifiers.

Currently, there are attempts to prepare particles with a specific surface functionality in a one-step procedure by enhancing the surface activity of functional molecules. The vitamin-PEG conjugate D- α -tocopheryl polyethylene glycol 1000 succinate (TPGS) is an amphiphilic and water-soluble derivative formed by conjugation of vitamin E succinate with PEG.[137] TPGS inhibits P-glycoprotein-mediated drug transport and might thus improve the bioavailability of P-gp substrates.[138] A similar approach was assessed for vitamin D using cholecalciferol polyethylene glycol succinate (CPGS).[139] Amphiphilic derivatives of hyaluronic acid were used as surfactants for the preparation of PLA nanoparticles.[140] The resulting particles bound preferentially to chondrocytes owing to hyaluronate-targeting of the CD44 receptor. As a versatile modification platform, avidin-fatty acid conjugates were prepared and added to the PVA solution upon microparticle preparation via solvent evaporation.[141] This process should allow for a quick immobilization of various biotinylated ligands to surface-exposed avidin, which resulted in a maximum of 2.5 μ g biotin-phycoerythrin (240 kDa) per milligram of polymer. For a new approach in vaccination, lipopolysaccharides have been added to the stabilizer solution during

particle preparation to act as inflammasome-activating adjuvants.[142] By contrast, aiming at an enhanced blood and tissue compatibility, certain salts or amino acid complexes of heparin have been used for the preparation of microparticles.[143] Nevertheless, it has to be considered that a major fraction of surface-associated heparin and TPGS can be removed from the particle surface by repeated washing.[144] In general, the adsorption of amphiphilic molecules for a specific surface modification is a rapid and convenient method, provided that the interaction is strong enough to resist premature desorption.

Several biorecognitive molecules are not amphiphilic and cannot be physically entrapped during particle preparation; therefore, these molecules need to be immobilized to preformed particles. The classic approach to couple ligands to terminal PLGA carboxylate groups exposed at the particle surface may often not be feasible due to steric hindrance or inappropriate coupling chemistry. As an alternative, covalent conjugation to certain functional groups that are present at the particle surface due to physically entrapped stabilizers has been reported. Glutaraldehyde was used to couple lectins to PVA- or BSA-stabilized PLA microspheres.[145] When two adjacent hydroxyl groups of PVA formed an acetal with glutaraldehyde, the remaining aldehyde group could then either react with the lectin or with another PVA molecule resulting in PVA cross-linking.

Alternatively, a multifunctional epoxy linker that reacts with PVA hydroxyl groups and with amine groups of a ligand was used for the conjugation of transferrin and the tat peptide to surface-anchored PVA.[146, 147] However, it should be considered that PVA is not biodegradable and only low-MW PVA is quickly eliminated from the body. In animal studies, medium- and high-MW PVA have been found deposited in various organs.[124] Thus, cross-linked PVA might not be eliminated from the body and may accumulate in certain organs, causing inflammatory reactions. For another approach, antibodies were coupled to surface-anchored PVA via cyanogen bromide, which creates a link between PVA hydroxyl groups and primary amines.[148] Although the reagent is well established for the preparation of matrices for affinity chromatography, its applicability in drug-delivery systems might be limited due to its acute toxicity. To overcome the PVA-shielding effect, PVA was replaced by poly(ethylene-alt-maleic acid) (PEMA), which contains carboxylic acid side chains and thus allows for carbodiimide-mediated coupling of amine-containing ligands to the surface-anchored stabilizer.[149] Similarly, when the hydroxyl groups of Pluronic® F127 were succinylated, the resulting carboxylated poloxamer could be used as an emulsifier for the preparation of PLGA nanoparticles followed by covalent coupling of a peptide via a modified carbodiimide method.[150] In addition to neutral or carboxylated stabilizers, cationic amphiphiles were used to introduce reactive groups. Polylysine that is usually immobilized at negatively charged surfaces via electrostatic interactions is unable to stabilize emulsions at neutral pH due to its high charge density. Upon the addition of sodium hydroxide, however, the polypeptide becomes amphiphilic and the secondary structure is shifted from random-coil to α -helix. Under these conditions, the polypeptide was applied as a surfactant for the preparation of PLGA microparticles by a solvent evaporation technique.[107] The surface-anchored polylysine was then coupled via its ϵ -amino groups

to thiol groups of a synthetic peptide using the bifunctional crosslinker sulfo-N-(γ -maleimidobutyryloxy)succinimide (GMBS).[151]

To conclude, surface adsorption of different substances via hydrophobic interactions has an impact on the stability of the suspension, the access to PLGA carboxylate groups for covalent surface modification, and can even be exploited for imposing certain characteristics to the surface itself. The main prerequisite for the latter approach is a strong hydrophobic interaction, which resists desorption during repeated washings. For the future, only biocompatible stabilizers should be applied, and should either be biodegradable or at least easily eliminated via urinary or biliary excretion.

PROTEIN ADSORPTION The adsorption of proteins to the surface of PLGA particles is discussed separately, because it relies on a combination of hydrophobic and electrostatic interactions. On the one hand, protein adsorption is being exploited for the preparation of carriers for therapeutic proteins or protein vaccines as well as for targeting purposes. On the other hand, the adsorption of blood proteins upon parenteral administration is most often unwanted because it leads to a rapid clearance of administered colloids via the RES. Protein adsorption to the particle-liquid interface also has an impact on the stability of a suspension. Moreover, adsorption phenomena may even affect the release of encapsulated protein drugs.

To elucidate the mechanisms that govern protein adsorption, model proteins containing different amounts of charged amino acids were used. Amphoteric molecules often have their maximum adsorption capacity at the isoelectric point, where the net charge of the adsorbate becomes zero.[120] Nevertheless, a strong dependence on electrostatic interactions has also been described. An examination of the surface affinity of proteins with different isoelectric points from 4.6 to 10.7 under varying pH conditions revealed that protein adsorption was significantly enhanced by attractive electrostatic interactions, while a certain extent of binding even took place under electrostatically repulsive conditions via non-Coulomb forces.[152] In another study, the positively charged model protein lysozyme was adsorbed onto negatively charged nanoparticles prepared from either PLGA alone or from blends with the strongly negative poly(styrene-co-4-styrene sulfonate) (PSS). Increasing lysozyme loading was observed with enhanced negative surface charge.[153] When the negative charge of PLGA particles was increased with anionic surfactants such as SDS or DSS for particle preparation, recombinant p55 gag protein from HIV-1 or antigens from *Neisseria meningitidis* type B could be adsorbed to the charged particles. A potent immune response was elicited upon immunization of mice, and was superior to that achieved by co-administration of antigen and PVA-stabilized PLGA microparticles.[132, 133]

Upon adsorption of positively charged protein, the initially negative ζ -potential of the particle surface shifts towards zero and the particles start to aggregate.[153] Because electrostatic repulsion is probably the most important factor for maintaining stable suspensions, the impact of protein adsorption must not be neglected.

Another interesting aspect is the influence of nonspecific protein adsorption on the release of encapsulated protein drugs.[154, 155] When the inner surface of the particles expands in the course of polymer

degradation, increasing amounts of the therapeutic protein may be adsorbed, which results in a slower release. Generally, the type of interaction with the surface seems to affect the release kinetics of the adsorbed protein. A stronger contribution of electrostatic interactions was associated with a quicker release compared with predominantly hydrophobic interactions.[153] In contrast to hydrophobic interactions, electrostatic forces are affected by changes in pH or salt concentration.

Sensitive proteins that would be degraded during encapsulation due to shear forces or organic solvents or during covalent coupling might thus be immobilized via simple adsorption to the particle surface. The functionality of adsorbed proteins was assessed for different applications. For targeting purposes, transferrin-coated PLGA nanoparticles were prepared by incubation of blank nanoparticles with the protein.[129] The uptake of the transferrin-grafted particles into blood-brain barrier cells was increased 20-fold compared with blank nanoparticles and 2-fold compared with BSA-coated particles. This effect could be inhibited by an excess of free transferrin, which points to selective endocytosis. Upon comparing covalently immobilized and surface-adsorbed monoclonal antibodies, it was reported that only the nanoparticles with adsorbed antibody were specifically taken up into MCF-10A neo-T cells.[156] This observation was attributed to an inactivation of the antibody during the carbodiimide-mediated coupling procedure.

To conclude, the adsorption of various proteins to PLGA particle surfaces has been described as a rapid and simple alternative for the delivery of sensitive proteins and for the immobilization of targeters. The main problems, however, have not been addressed adequately so far. The stability of the adsorptive protein-particle interaction under physiological conditions remains questionable because adsorbed molecules may be displaced by competitive adsorption of other substances, for example, by plasma proteins. Moreover, pH and ionic strength influence the affinity of the adsorbed protein to the surface. Finally, particles that easily adsorb proteins at their surface are expected to be rapidly opsonized and eliminated by the RES, which might limit their applicability *in vivo*. Thus, the most important aspect concerning protein adsorption is generally not how to enforce it, but how to reduce it. Strategies to reduce opsonization via the so-called stealth effect are discussed in one of the following sections.

METHODS FOR SURFACE CHARACTERIZATION Several sensitive and sophisticated techniques are available for the physicochemical characterization of PLGA-particles, including their surface properties. It is obvious that a single method cannot cover the whole spectrum of analytical questions, and thus the available techniques listed in Table 4 need to be combined to fully elucidate the surface modification of particles.

Size and polydispersity represent key parameters not only for biodistribution and clearance but they are also useful as a rough estimate of the particle surface available for coupling. Laser diffractometry, dynamic light scattering (also known as photon correlation spectroscopy), and, less frequently, multi-angle laser light scattering after asymmetric flow-field flow-fractionation represent light scattering techniques for particle size determination. Due to multiple pitfalls associated with these techniques, it is highly recommended to confirm particle size by

Table 4: Analytical methods for characterization of surface-modified PLGA particles

TECHNIQUE	ABBREVIATION	PARAMETER INVESTIGATED	REFERENCE
dynamic light scattering	DLS	hydrodynamic diameter (5 - 5000 nm)	[157, 158]
photon correlation spectroscopy	PCS		
quasi elastic light scattering	QELS		
laser diffractometry	LD	volume-based particle size distribution (50 nm - 1000 μm)	[158]
asymmetric flow field-flow fractionation with multi-angle light scattering (MALS)	AFFFF (AF ₄)	hydrodynamic size; radius of gyration up to 500 nm	[159, 160, 161]
scanning electron microscopy	SEM	number-based particle size distribution (50 nm - 100 μm); particle morphology	[162, 163, 164]
transmission electron microscopy	TEM	number-based particle size distribution (50 nm - 100 μm); particle morphology	[165, 166]
cryogenic transmission electron microscopy	cryo-TEM	number-based particle size distribution (50 nm - 100 μm); particle morphology	[167]

Table 4 continued

TECHNIQUE	ABBREVIATION	PARAMETER INVESTIGATED	REFERENCE
atomic force microscopy, scanning probe microscopy	AFM SPM	number-based particle size distribution; particle morphology; binding forces	[168]
small angle X-ray scattering	SAXS	radius of gyration; shape; surface structure	[159, 169]
electrophoretic techniques	-	electrophoretic mobility; ζ -potential	[170, 171, 172, 173]
hydrophobic interaction chromatography	HIC	hydrophobicity/hydrophilicity	[174]
contact angle measurement	-	hydrophobicity/hydrophilicity	[175]
underwater contact angle measurement	-	hydrophobicity/hydrophilicity	[176]
Rose Bengal adsorption assay	RB	hydrophobicity/hydrophilicity	[165, 177]
resonant mirror system	RMS	ligand-ligand interaction	[178]
two-dimensional gel electrophoresis	SD-PAGE	protein adsorption	[175, 179]

Table 4 continued

TECHNIQUE	ABBREVIATION	PARAMETER INVESTIGATED	REFERENCE
X-ray photoelectron spectroscopy	XPS	surface chemistry	[114, 29, 166, 176]
electron spectroscopy for chemical analysis	ESCA	(penetration depth: 2-10 nm)	
secondary ion mass spectrometry	SIMS	surface chemistry (penetration depth: 1 nm)	[180]
time-of-flight secondary ion mass spectrum	TOF-SIMS	surface chemistry	[181]
static secondary ion mass spectrometry	SSIMS	surface chemistry (thermally labile compounds)	[29]
Fourier transform infrared spectroscopy-attenuated total reflection	FTIR-ATR	chemical composition	[92]
flow cytometry	FCM	mean fluorescence per particle	[80]
MicroRaman spectroscopy	-	molecular composition; crystal localization (penetration depth in μm -range)	[164]
Brunnauer-Emmett-Teller method	BET	specific surface area	[182, 183]

an imaging technique.[163] These microscopic methods, including SEM, TEM, cryo-TEM, and, recently, atomic force microscopy (AFM) provide additional information about particle morphology (see 1.1.2.5).

For determination of the specific surface area, the Brunauer-Emmett-Teller method, which relies on adsorption-desorption isotherms of N₂ and Kr gases at the particle surface, is applied. Although this method is preferably used to characterize porous microparticles and the associated initial burst release,[182, 183] it might also be a versatile tool for the determination of the surface area available for coupling of ligands considering porosity, size, and polymer composition of PLGA micro- and nanoparticles.

In addition to the surface morphology and size, two additional parameters describing the characteristics of particles are their surface charge and hydrophobicity. The surface charge strongly influences the stability of aqueous nanosuspensions and particle-cell interactions.[172, 173] Usually, the surface charge is assessed via the mobility of the particles in an electrical field, and is expressed as electrophoretic mobility (μ) or converted to zeta (ζ) potential, which represents the potential at the hydrodynamic shear plane of the particle. For the theoretical background and calculation of mobility and ζ -potential the reader is referred to Agnihotri et al.[170] The surface charge is dependent on the degree of ionization of particle surface groups and on ion adsorption. In practice, ζ -potential measurements are highly sensitive to the conductivity of the dispersant medium and its pH. Generally, values above 30 mV indicate physically stable PLGA-particle suspensions that are widely stabilized via electrostatic repulsion.[171]

Surface hydrophobicity can influence the adsorption of excipients and proteins. Whereas the contact angle measurements of water, octane drops, and air bubbles are only applicable to PLGA films,[175] the hydrophilicity and conversely the hydrophobicity of particles can be determined by a Rose Bengal adsorption assay.[165, 177] Nanoparticles are incubated with an aqueous solution of the hydrophilic dye, spun down, and the dye content in the supernatant is determined by spectrometry at 564 nm. From the difference between blank and sample, the amount of dye adsorbed by the nanoparticles is calculated considering the density and diameter of the particles. In addition, hydrophobic interaction chromatography (HIC) proved useful to monitor changes in particle surface hydrophobicity upon modification with hydrophilic ligands.[174]

X-ray photoelectron spectroscopy (XPS), also called electron spectroscopy for chemical analysis, is routinely applied for particle surface analysis. The samples are prepared on substrates such as glass slides or aluminum foil by drop casting of aqueous particle suspensions followed by drying. X-ray irradiation causes emission of photoelectrons with specific binding energies according to the electron core level at the site of ejection. The peak intensity is proportional to the atomic concentration within the sample. XPS provides qualitative information about the surface chemistry and quantitative information about the element composition and functional groups at the particle surface with high sensitivity, usually 1 atom in 1000.[29] Unfortunately, interpretation of the spectra is complex because varying ligand coverage of the particle surface and/or the penetration depth in the range of 2 to 10 nm might lead to interference between strong signals from the underlying PLGA matrix and only weak signals from the modified

surface. In addition, precise quantification of data may be difficult.[176] Nevertheless, XPS analysis at a penetration depth of 10 nm revealed that rhodamine was not present at the surface of PLGA nanoparticles but rather was embedded in the core.[114] Additionally, XPS has proven to be a powerful tool to detect the presence of a chitosan or PVA shell on PLGA nanoparticles.[166, 176]

A surface analytical technique complementary to XPS is secondary ion mass spectrometry (SIMS). At this, secondary ions emitted from the particles under high vacuum are analyzed according to their mass/charge (m/z) ratio. Compared with XPS, SIMS offers the advantage of detecting all elements including their isotopic distribution, has low detection limits and a low penetration depth of only 1 nm of the particle surface,[180] but the drawback of sample damage. Time-of-flight (TOF)-SIMS is preferentially applied for mass analysis of high-MW samples, and static SIMS (SSIMS) is used to collect the mass spectra of thermally labile organic compounds. Both complementary surface analytical techniques, XPS and SSIMS, have been employed to determine residual surfactant at the surface of PLGA nanoparticles after purification by centrifugation or gel-permeation chromatography.[29] Moreover, XPS and TOF-SIMS have been applied for the surface characterization of PLGA microparticles after vaccine antigen adsorption. Although some amino acid residues known to be specific for certain proteins were identified by TOF-SIMS, the spectra were too complex to provide specific information about protein identity and quantity. However, the combination of the two techniques allowed for the identification and quantification of both the protein and the surfactant adsorbed at the outermost surface and revealed that the antigen concentration decreased with increasing surfactant concentration.[181]

Whereas the chemical composition of polymers can be elucidated by Fourier transform infrared (FTIR) spectroscopy, the attenuated total reflectance (ATR) mode is applied for surface characterization. After spreading the nanoparticle suspension onto the ATR crystal and drying with nitrogen, it was possible to detect the presence of positively charged chitosan and surfactant at the surface of PLGA nanoparticles.[92]

In addition, the adhesive capacity of surface modified particles and their binding specificity were assessed by the resonant mirror system, an optical biosensor based on the phase shift of an incident beam that occurs in reflected light, which passes through a prism underlying the resonant mirror. This label-free technique allows monitoring of the interaction between a dissolved molecule or a dispersed nanoparticle of interest (ligate) and its biospecific partner (ligand) immobilized at the waveguide sensing surface. Depending on the extent of binding, a change in the resonance angle is observed. Using this technique, the interaction between biotinylated nanoparticles and Neutr-Avidin-coated surfaces was assessed. Strong and specific binding was observed, but no equilibrium, presumably due to the rearrangement of nanoparticles.[178]

Among the fluorometric methods, fluorescence microscopy and flow cytometry allow for the detection and quantification of fluorescence-labeled ligands coupled onto the particle surface. Flow cytometry, relying on forward versus side scatter analysis of a few thousand single microparticles in a sheath flow one by one, offers a multiparametric

analysis in terms of size, granularity, and fluorescence intensity after surface modification with fluorescence-labeled ligands.[80]

MicroRaman spectroscopy allows for studying molecule vibrations in micron-sized materials due to their interaction with photons. Accomplishing a penetration depth in the micrometer range, this technique comprises the surface and the core of particles. Applying this technique, the distribution of drug crystals in PLGA microparticles was found to be close to the surface in high-MW PLGA matrices but was located in the core of low-MW PLGA.[164]

Perhaps the most important aspect of surface characterization is the interaction of the functionalized nano- and microparticles with the biological environment, which requires either *ex vivo* studies with human cell culture models or *in vivo* studies in animals.

1.1.2.4 Aims of functionalization

MODIFIED BIOADHESION AND POTENTIAL INTERNALIZATION

Nonspecific mechanisms A rather nonspecific approach to enhancing the binding of polymer particles to human cells makes use of the net negative charge of the extracellular face of the plasma membrane. Although the quantitative and qualitative compositions of the charged groups contributing to the overall negative ζ -potential on different cell types have not been fully resolved yet, it seems clear that negative charges generally prevail.[6] Theoretically, these charges bear a considerable potential for attractive electrostatic interactions with positively charged drug carriers, and consequently might be exploited to increase the cell-binding[184, 86] and transfection efficiency of particulate carrier systems.[185] Nano- and microparticles prepared from uncapped PLGA and stabilized by PVA or poloxamers, however, are usually negatively charged due to free surface carboxyl groups. To induce a positive ζ -potential on these particles, several coating techniques with cationic excipients have been developed. As expected, PLGA nanoparticles coated with didodecyl dimethyl ammonium bromide (DMAB) preferentially associated with the negative endothelial layer in a femoral artery *ex vivo* model.[186] This led to a 7- to 10-fold enhanced delivery of an antiproliferative agent compared with plain particles.

Interestingly, the density of negative charges in the vasculature was found to be further increased in malignantly transformed tissue.[187] Supposedly, this is due to an induced exposure of anionic phospholipids, most likely phosphatidylserine, on the cell membrane. This surplus of negative charges compared with the normal vasculature, in combination with the reportedly low pH in tumors, could be exploited for the accumulation of cationic drug carriers or imaging agents.[98] In addition to increasing cytoadhesion, coating with cationic excipients also affects the internalization rate and intracellular processing of particles. While negatively charged polystyrene beads were only taken up to a low extent by macrophages and dendritic cells (DC), positively charged beads were readily internalized and induced maturation of DCs.[86] These positively charged particles were characterized by a similarly high cell-binding affinity to antigen-presenting cells (APC) as immunoglobulin G-modified beads. This led to phagocytosis and subsequent engulfment in tightly apposed phagosomes, which

do not undergo maturation. In contrast, albumin-modified particles were taken up in loosely apposed phagosomes, which rapidly fuse with lysosomes.[90] Thus, coating of drug and vaccine carriers with cationic polyelectrolytes could not only result in enhanced uptake into APCs, but also in intraphagosomal protection of the payload to be delivered. However, in addition to these promising reports with *in vitro* and *ex vivo* setups, studies performed under physiological conditions are rare. In particular, it is not clear to what extent the adsorption of serum proteins alters the cationic charge density of the particle surface, and consequently effectiveness of the electrostatic bioadhesion approach. This issue deserves attention, especially since a recent report indicated that the adsorption of serum onto PLL-coated polystyrene (PS) microspheres leads to reduced uptake into DCs compared with untreated cationic beads.[184] The probably limited influence of particle surface charge in the presence of serum was also indicated by Roser et al., who observed no differences in the blood circulation times and biodistribution of cationic, anionic, and neutral albumin nanospheres in rats.[188]

If not administered via the parenteral or topical route, drug-carrier systems will encounter the sticky, viscous, and elastic mucus layer that lines all mucosal tissues.[189, 190] Due to its constant secretion, transport, and excretion, mucus functions as a dynamic protective barrier that efficiently removes foreign materials from the body. This severely limits the residence time and thus efficiency of sustained-release drug-carrier systems. Therefore, mucoadhesion and mucopenetration have been investigated as approaches to counteract premature removal[190, 191] and to enhance transport of particulate drug carriers through the mucin mesh to underlying tissues.[189]

Polymers utilized to formulate mucoadhesive drug-delivery systems have comprised polyanions, polycations, and thiolated polymers. Polyanions such as poly(acrylic acid) (PAA) and sodium carboxymethylcellulose and their derivatives supposedly bind to mucus via hydrogen bonding. In contrast, polycations such as chitosan are anchored by a combination of hydrogen bonds and electrostatic interactions with sulfonic- or sialic acid groups of glycosylated moieties of mucus.[190] To transfer mucoaffinity to PLGA nano- and microparticles, coating with mucoadhesive polymers such as PAA,[192, 39] chitosan and thiolated derivatives,[84, 93, 97, 192, 193] PEI,[114] and Eudragit® RL/RS[85] has been investigated. As opposed to particles prepared in the presence of poloxamer 188 and PVA, PLGA nanoparticles produced with PAA as a stabilizer were indeed characterized by mucoadhesive properties.[39]

According to Yamamoto et al., surface modification of particles with chitosan led to higher retention rates in the lungs of guinea pigs after administration by nebulization compared with plain colloids.[93] The prolonged pharmacological action of calcitonin co-administered in these particles was attributed to the mucoadhesive properties and probably an opening of tight junctions. Furthermore, it was shown that chitosan-coated PLGA nanoparticles exhibit higher binding to a rat everted intestinal sac model than PAA- and alginate-modified controls.[192] These proof-of-principle studies illustrate that mucoadhesive properties can be integrated into a priori non-mucoadhesive particles made from PLGA by surface coating. Whether PLGA is suitable as a sustained-release polymer for mucoadhesive systems, however, is questionable. Even if mucoadhesion is established, the particles are expected to be

removed from the body at a rate similar to that of mucus turnover. However, these turnover rates range from about 20 min in the nasal tract to 10 to 20 min for the luminal layer in the respiratory tract and 4 to 6 h in the gastrointestinal tract,[189] and thus lie well below the degradation half-life of PLGA.

Very recently, it has been found that mucopenetrating nanoparticles can be engineered with potential advantages over traditional mucoadhesive formulations. While mucoadhesive particles adhere to the outer luminal mucus layer, which is rapidly cleared, mucopenetrating nanoparticles are supposed to diffuse into low-viscosity aqueous pores of the mucin mesh and to thereby reach deeper adherent mucus layers.[189, 194] The surface functionalization rationales that are used to generate mucopenetrating properties have been deduced from studying nature. Using fluorescence recovery after photobleaching and multiple image photography, Olmsted et al. investigated the diffusion of viruses and polystyrene particles (59–1000 nm) in human cervical mucus.[195] While viruses with a net neutral surface charge such as human papilloma virus (approximately 55 nm) and Norwalk virus (approximately 38 nm) diffused as rapidly in mucus as in saline, negatively charged polystyrene particles were trapped and adhered to mucin via hydrophobic interactions. From these and similar findings, it was proposed that sufficiently small particles with a neutral surface charge would exhibit minimal interactions with mucus and thus be able to diffuse relatively unhindered.[189, 194]

A well-established strategy to render the particle surface inert and neutral is based on the modification with PEG. Upon conjugation of polystyrene nanoparticles with high surface densities of low-MW PEGs of 2 and 5 kDa, particles with enhanced diffusivity in mucus were generated.[196] In contrast, conjugation with higher-MW PEG (>10 kDa) might induce mucoadhesive properties due to the increased penetration of longer polymer chains into the mucin network. After surface modification with PEG, nanoparticles with mean diameters of 200 and 500 nm, which are clearly larger than the reported mucin mesh pore size (10–200 nm), diffused in mucus at rates only 4- to 6-fold slower than in water.[197] Consequently, surface modification with PEGs of appropriate MW might drastically improve the transport of particles toward the underlying epithelium.

Making use of the same principle, but via a different approach to surface modification, PLGA nanoparticles have been rendered mucopenetrating.[198] Avidin-decorated particles (170 ± 57 nm) were prepared by using palmitate-avidin/PVA blends as stabilizer in course of the preparation procedure. By adding different amounts of biotinylated PEG to these particles, varying degrees of grafting were achieved. By increasing the surface grafting density of PEG, an increase in the diffusivity of the PLGA nanoparticles in human cervical mucus was observed.[198] Increased diffusion coefficients in mucus upon alteration of the surface charge of particles have also been monitored without PEGylation.[199] By modification of PLGA nanoparticles with DDAB and subsequent loading with plasmid DNA, 10-fold higher diffusion rates were achieved compared with negatively charged polystyrene nanoparticles of similar size. These reports seem promising for the delivery of drugs, genes, or antigens through the mucus barrier to the underlying epithelium. However, the therapeutic advantages of mucopenetrating particles over mucoadhesive systems have yet to be

proven *in vivo*. Furthermore, PEG-decorated nanoparticles will be expected to have a low uptake rate into epithelial cells due to the hydrophilic surface coating. In this regard, grafting of mucopenetrating nanoparticles with low-MW targeting moieties, which enhance uptake into epithelial cells, might be advantageous.

Biorecognitive mechanisms Bioadhesion can be enhanced by a biorecognitive interaction between particle surface-immobilized active targeters and tissue-characteristic structures at the cell surface. These targets comprise a broad range of receptors, including cell-adhesion molecules, carriers, and other membrane proteins or glycoproteins. The fundamental problem is the identification of appropriate tissue-specific targets. However, few of them are uniquely present in only one single tissue and it is thus important to consider the relative selectivity of the targeted moiety in relation to the potency of the delivered drug. Moreover, these tissue markers have to be accessible to allow for an interaction with the targeted particles. The route of administration is also crucial for successful targeting. If a drug-delivery system attaches to the target cells via noninternalizing epitopes, high local drug concentrations at the outer surface of the target cell may result in a higher therapeutic efficacy than free drug released in the circulation. However, even upon localized release, only part of the drug will enter the target cells. Therefore, most strategies focus on internalizing epitopes. As ligands for active targeting, proteins such as antibodies or lectins, as well as peptides and peptide-analogs, aptamers, vitamins, and other natural-derived, semisynthetic, or synthetic molecules that bind to certain target structures with high affinity and specificity are applicable.

The application of antibodies for clinically applied immunoconjugates is a well-established strategy in cancer treatment. Similarly, drug-delivery devices might be guided to their target cells via surface-immobilized immunoglobulins. Antibodies against the human epidermal growth factor receptor (EGFR; HER) for targeted breast cancer therapy,[200, 201] against the siglec-7 (CD33-like) receptor that is expressed on most acute myeloid leukemias,[202] and against the Fas (CD95/Apo-1) death receptor[79] mediated enhanced PLGA nanoparticle internalization. Antibodies against VEGFR-2 (vascular endothelial growth factor receptor-2) for systemic targeting to angiogenic sites in prostate tumors resulted in enhanced cytoadhesion of microparticles.-[148] To mimic leukocyte adhesion to inflamed endothelium, PLGA microspheres were decorated with two different ligands, an antibody against ICAM-1 (intercellular adhesion molecule-1) and the selectin ligand sialyl LewisX for glycotargeting.[203]

Glycotargeting is another extensively studied strategy that relies on the specific interaction between nonenzymatic sugar-binding proteins, so-called lectins, and certain carbohydrate moieties.[204] Either endogenous lectins or, inversely, endogenous sugars serve as targets. A prominent group of mammalian lectins are the selectins, a family of adhesion receptors, which can be addressed by the above-mentioned sialyl LewisX. Another example is the galactose-specific asialoglycoprotein receptor, which is expressed at the surface of hepatocytes and overexpressed in hepatocarcinoma. Recently, pDNA-loaded cationic nanoparticles were prepared from a blend of PLGA and DOTAP followed by adsorption of the asialoglycoprotein receptor ligand asialofe-

tuin for targeted delivery to liver tumor cells.[205] In a mouse xenograft tumor model, complete tumor regression was reported for 75% of mice treated with these targeted gene carriers.

For targeting cartilage, PLA nanoparticles were coated with the glycosaminoglycan hyaluronate, which has a high affinity to the CD44 receptor that is present at the surface of chondrocytes and other articular cells.[140] Nevertheless, the majority of glycotargeting approaches relies on lectin-mediated targeting to specific carbohydrates. Each mammalian cell bears a sugar coat, the so-called glycocalyx, which is composed of the oligosaccharide moieties of membrane-anchored proteoglycans, glycolipids, and glycoproteins. The glycosylation pattern is not only tissue-specific, but may also change upon malignant transformation.[206] Screenings of the binding pattern of a range of plant lectins with different carbohydrate binding specificities to different cell types pave the way for lectin-mediated targeting.[207, 208, 209, 210, 211] Moreover, sugars are also present in the mucus and the extracellular matrix. WGA, the lectin derived from *Triticum vulgare*, specifically interacts with N-acetyl-D-glucosamine and sialic acid residues. These sugars form part of the intestinal mucus and the glycocalyx of human intestinal epithelium.[212] Moreover, they are present in the glycosylated extracellular domain of the EGF (epidermal growth factor) receptor.[213] WGA and WGA-decorated PLGA particles are not only cytoadhesive, but may even be taken up into enterocytes via receptor-mediated endocytosis,[5] which might open the way to improved peroral drug delivery.

Not only enterocytes may be targeted in the intestine, but also M cells being addressed in peroral immunization. Thus, allergen-loaded PLGA microparticles were functionalized with the α -L-fucose-specific *Aleura aurantia* lectin (AAL) for binding to the glycocalyx of murine M cells.[214] In mice, peroral gavage of the targeted formulation resulted in a favorable shift from a Th2-type allergic to a Th1-type immune response. Similar results were obtained with the α -L-fucose-specific UEA-1 (Ulex europaeus agglutinin-1).[215] However, the glycosylation pattern of M cells exhibits species-related variations, and for human M cells targets other than α -L-fucose will be necessary.[215] In addition to peroral application, there are also possible targets in other tissues demanding other routes of application. For example, human macrophage-like THP-1 cells preferably internalized WGA-modified PLGA nanoparticles,[211] which might enable a new approach for the treatment of infectious diseases provoked by intracellular pathogens. Furthermore, lectin binding to bladder cancer cells might be exploited for designing targeted drug carriers with a prolonged residence time in the bladder upon instillation.[210]

Another strategy is targeting of the transferrin receptor, which plays an essential role in the iron metabolism of cells and is overexpressed in certain tissues such as the liver, epidermis, intestinal epithelium, vascular endothelium of the brain capillary, certain blood cells, and malignant tissues. Functionalization of paclitaxel-loaded PLGA nanoparticles with transferrin enhanced the antiproliferative activity of the encapsulated drug in MCF-7 and drug-resistant MCF-7/Adr breast cancer cells, which was attributed to a sustained intracellular drug retention.[146] Transferrin has also been proposed for brain delivery of nanoparticles. In an attempt to study the endocytosis of targeted particulates by blood-brain barrier cells, an *in vitro* model of the blood-brain barrier made of co-cultured endothelial cells and astrocytes was incubated

with transferrin-coated PLGA nanoparticles.[129] The interaction was found to be specific and caveolae-mediated endocytosis was proposed.

Other approaches are aimed at mimicking the interaction of different bacteria with their hosts. Various bacteria such as *Yersinia*, *Shigella*, *Salmonella*, and *Listeria species* enter the body through the intestine aided by enteroinvasive proteins. The *Yersinia* adhesin invasin binds to a subset of β_1 integrin receptors at the apical membrane of M cells, leading to host cell invasion.[216] Although β_1 integrin expression is generally limited to the basolateral membranes of polarized epithelia, there is evidence that they also occur at the apical side of M-cells.[217] A large fusion protein containing the carboxyl terminal 479 amino acids of invasin (MBP-Inv479) was covalently coupled to the surface of PLGA nanoparticles.[218] For these modified particles, an enhanced interaction with invasin-binding cells was reported that could be inhibited by free MBP-Inv479 or the competing ligand RGD, which points to a specific interaction with integrins. Another approach is based on the neuronal transport of tetanus toxin. The nontoxic C fragment of tetanus toxin binds with high affinity to the neuronal ganglioside GT1b, which leads to efficient endocytosis and retrograde transport from the distal axonal terminus to the neuronal cell body, thus allowing it to bypass the blood-brain barrier and enter the central nervous system. This transport mechanism seems promising for new treatment opportunities in neurodegenerative diseases. To study a possible strategy for targeted drug delivery to neurons, PLGA nanoparticles were surface-modified with tetanus toxin.[219] Flow-cytometric studies with neuroblastoma, liver, and endothelial cells revealed selective targeting to the neuroblastoma cells.

Proteinaceous targeters also bear some possible disadvantages: they may elicit undesirable immune responses; they are degraded by proteolytic enzymes; they change their conformation under unfavorable conditions, which may impair their binding properties; their biotechnological production is often subject to a significant batch-to-batch variability; it is often difficult to immobilize these large molecules in an adequate orientation being favorable for cell interactions; due to their size they provide a large area for possible nonspecific binding and may thus counteract a stealth effect regardless of an existing PEG coat; and they are generally rather expensive. Most of these problems might be avoided by using peptides or peptidomimetics instead.

Respective binding peptides may be identified by affinity selection such as phage display, yeast surface display, messenger RNA display, or peptide-on-bead display.[220] The most prominent peptide for targeting purposes is the cell-binding motif RGD, which efficiently triggers integrin-stimulated cell adhesion.[221] The affinity of RGD-containing peptides to different integrins is influenced by the conformation of the RGD-containing loop and by the neighboring amino acids. Cells differ as to their typical integrin pattern, which may be exploited with an appropriate RGD-containing peptide. Surface-grafted RGD was employed as a model ligand to demonstrate the specific uptake of targeted stealth PLGA microparticles by phagocytes *in vitro*.[46] In another example, enhanced delivery of drug to integrin-overexpressing cancer cells upon RGD functionalization was reported.[222] Upon oral immunization in a mouse model, RGD grafting was reported to provoke a slightly enhanced immune response, which was attributed to M-cell targeting.[223] The targeting effect observed in the *in vitro* co-culture

model was, however, more pronounced than the *in vivo* results. Thus, a partial degradation of the RGD peptide in the gastrointestinal tract was suspected and alternative peptide analogues were tested.[224] Peroral immunization of mice with PLGA nanoparticles that were grafted either with an RGD peptidomimetic or a leucine-aspartic acid-valine tripeptide derivative revealed increased immunoglobulin G production. However, there were differences observed depending on the relative affinity of the targeters to M cells and APCs, which probably induced different induction pathways.

For delivery to the pulmonary epithelium, the above-mentioned ICAM-1 has been proposed, which is expressed on inflammatory and immune effector cells, fibroblasts, and endothelial and epithelial cells, and is up-regulated in some types of carcinomas (e.g., lung carcinoma).[150] ICAM-1 may not only be targeted by antibodies, but also by the cyclic peptide cyclo-(1,12)-PenITDGEATDSCG (cLABL). Conjugated to PLGA nanoparticles, cLABL enhanced the endocytosis into human umbilical cord vascular endothelial cells with up-regulated ICAM-1 and into A549 lung epithelial cells.[150, 225] In an attempt to enable PLGA nanoparticles to cross the blood-brain barrier, PLGA was derivatized with different short peptides that were similar to synthetic opioid peptides.[226] Functionalized fluorescent-labeled particles were tested in an *in vivo* experiment with rats. In contrast to plain PLGA particles, confocal microscopic analyses of tissue cuts revealed some penetration into the cerebral tissue with some of the modified particle preparations. Recently, PLGA was conjugated with the glycosylated heptapeptide H₂N-Gly-L-Phe-D-Thr-Gly-L-Phe-L-Leu-L-Ser(O-β-D-Glucose)-CONH₂ (g7) and loperamide-loaded nanoparticles were prepared.[227] *In vivo* nociceptive testing in rats using the hot plate test revealed an extraordinary analgesic effect of these functionalized drug-loaded carriers, which was attributed to a successful transport of loperamide across the blood-brain barrier.

Aptamers are DNA or RNA oligonucleotides with unique tertiary conformations, which allow for antigen binding with high affinity and specificity. They are nonimmunogenic and highly stable in a wide range of pH and temperatures and in the presence of organic solvents. Docetaxel-loaded PLGA nanoparticles were surface modified with the A10 2'-fluoropyrimidine RNA aptamer, which binds to PSMA (prostate-specific membrane antigen) that is overexpressed in prostate cancer.[228] In a mouse xenograft tumor model, the targeted particles gave promising results, inducing complete tumor regression in five of seven mice at a 109-day survivability of 100%.

Interestingly, vitamins can also be exploited for targeting purposes. The most prominent representative of this group of targeters is folate (vitamin B₉), a small, innocuous, and nonimmunogenic molecule, which is accessible for conjugation via its γ-carboxylate group without losing its binding properties. Moreover, it is highly stable in the presence of organic solvents and under different pH and temperature conditions. Folate is taken up into cells either by the ubiquitous low-affinity folate carriers or by high-affinity folate receptors, which occur only in a limited range of tissues such as certain tumor cells and activated macrophages.[229] In contrast to the carrier, the folate receptor is also able to endocytose folate-linked cargo, which makes it an interesting target in cancer and inflammation therapy. Folate-decorated doxorubicin-loaded PLGA particles were not only taken up into folate

receptor-overexpressing KB cells to a higher extent than nontargeted carriers in an *in vitro* experiment, but they also reduced tumor growth *in vivo* in a xenograft mouse model.[230] An enhanced particle uptake into KB cells was also observed with PLL-PEG-folate coated PLGA nanoparticles.[109] Doxorubicin-loaded nanoparticles prepared with vitamin E TPGS-folate exhibited significantly higher cytotoxicity toward C6 glioma cells than free drug or the nontargeted formulation.[231] In addition to folate, other vitamins such as thiamine (vitamin B₁) or cobalamine (vitamin B₁₂) might also provide interesting targeting opportunities.[232, 233] Furthermore, low-MW synthetic molecules may be applied for active targeting. In an approach to selectively deliver drug carriers to bone, PLGA was modified with the bisphosphonate alendronate, which has a high affinity to hydroxyapatite, the major inorganic component of bone and teeth.[234]

However, even the highest affinity and selectivity of a ligand-target interaction will sometimes not suffice for successful nanoparticle delivery because various barriers may limit the access of a particulate carrier. Upon peroral administration, particles need to overcome the mucus barrier in order to interact with the underlying cells.[215] In solid tumors, the diffusion of targeted nanoparticles is impaired, and in dense, avascular tissues such as cartilage, the extracellular matrix limits the entry of drug carriers.[220] Moreover, functionalized carriers are only efficient if they are not prematurely eliminated. Thus, systemically administered particulates require a combination of optimum targeting and optimum stealth characteristics.

DIRECTED INTRACELLULAR TRAFFICKING For some applications, it may be sufficient to deliver a drug to a certain tissue, while others must be delivered to a specific intracellular target. These targets can be located in the cytoplasm or, for proteins or siRNA, in the nucleus; for DNA, antisense oligonucleotides or DNA intercalators in mitochondria; and for antiapoptotic drugs, in other compartments.[235, 236] For successful gene delivery, directed intracellular delivery remains the main challenge. First of all, the mechanism of particle uptake into the cell seems to affect their intracellular sorting and thus the extent of possible exocytosis.[146] The fraction that remains inside the cell has to evade lysosomal degradation. Subsequently, the carrier or its respective payload has to migrate through the cytoplasm to the specific target. In the case of gene delivery, the vehicle or its respective payload finally has to enter the nucleus.

One possible mechanism for endosomal escape of polymeric vectors via an intrinsic endosomolytic activity is described by the proton sponge hypothesis.[237] Due to their high buffer capacity, branched polyamines such as PEI or polyamidoamine (PAMAM) dendrimers that contain numerous secondary and tertiary amines counteract the acidification during endocytic trafficking.[238] Moreover, the resulting influx of ions leads to osmotic swelling, and finally to the rupture of the endosomes and the release of their content into the cytoplasm. This mechanism has been exploited with PEI-PLGA nanoparticles with surface-immobilized DNA for gene delivery to pulmonary epithelium.[102] Upon incubation of Calu-3 human airway submucosal epithelial cells with DNA-loaded nanocarriers, a rhodamine-labeled plasmid DNA that drives the expression of a green fluorescent protein was primarily found in lysosomes.

However, a low amount of green fluorescent protein was also detected, which pointed to endosomal escape and nuclear delivery of a certain percentage of the administered DNA.

Recently, PEI-PLGA nanoparticles have been loaded with a DNA vaccine encoding a Mycobacterium tuberculosis latency antigen.[239] The particles stimulated human monocyte-derived dendritic cells and induced their maturation, which was concluded from an increase in the expression of surface markers and the secretion of cytokines that was comparable to the positive control. In mice, pulmonary application resulted in more efficient immunization than intramuscular application, which was attributed to a more efficient uptake. In another study, PEI-PLGA particles were prepared either by PEI adsorption or by covalent coupling via the carbodiimide chemistry.[105] The ζ -potential of the PEI-conjugated PLGA particles amounted to approximately +35 mV, which was significantly higher than for PEI adsorption (+10 to 24 mV). Uptake studies in RAW murine macrophages and subsequent determination of the gene and protein expression revealed a high amount of PEI-modified particles in the cytoplasm and a successful transfection, whereas unmodified particles were accumulated in phagolysosomes. For PEI and other polycations, cytotoxicity issues should be considered.[113] Surface-conjugated PEI seems to exhibit a lower cytotoxicity than free PEI.[105] In addition to the proton sponge hypothesis for polycations, a mechanism for endosomal escape has been proposed also for PVA-stabilized PLGA nanoparticles.[240] Upon uptake into human arterial smooth muscle cells, their intracellular localization pointed to an endosomal escape of the particles, which was attributed to a cationization of the particle surface in acidic pH followed by a localized destabilization of the endo-lysosomal membrane.

A recent approach for direct delivery to the cytoplasm relies on conjugation with "cell-penetrating peptides" or "protein-transduction domains" that mediate membrane transport.[236, 241, 242] One prominent representative of this group is the viral protein tat, which might be responsible for cell penetration by lipid raft-dependent macropinocytosis[243] and for the delivery of genetic material to the nucleus.[241] Fluorescence-labeled tat-PLGA nanoparticles were incubated with human keratinocytes HaCaT, which resulted in higher fluorescence intensities at the cell membrane and in the cytoplasm upon confocal laser scanning microscopic imaging than was observed for nontargeted particles.[244] Another example of a cell-penetrating peptide is the arginine peptide (RRRRRRRCK-fluorescein isothiocyanate [FITC]).[245]

Another barrier for intracellularly migrating drug-delivery systems is the cytoplasm itself. The cytoplasm is crowded with proteins, cytoskeletal filaments, and other organelles. Thus, particles greater than 500 kDa or 20 nm are largely immobile unless there is some kind of assisted transport.[246] Among others, intracellular transport of organelles relies on active transport mechanisms that are mediated by cytoskeleton-dependent motor proteins such as myosin, kinesin, and dynein. Particle-tracking experiments revealed that some PEI/ DNA complexes are actively transported by motor proteins along microtubules similar to endogenous organelles or invading pathogens.[247] An interesting approach for the active intracellular transport of PLGA particles relies on a mechanism that is used by several bacteria such as *Listeria monocytogenes*. [248] The protein ActA, which is expressed at the bacterial surface, initiates actin polymerization by interacting

with host cell proteins and thus promotes actin-based motility. PLGA particles with surface-adsorbed ActA also were found to polymerize actin, which resulted in comet-tail propulsion. Interestingly, this effect was only observed for anionic carriers, whereas cationic PLGA-PEI particles did not form comet tails. Although the direction of this kind of transport was random, it enabled the particles to overcome restricted diffusion, and thus the carriers were able to reach the perinuclear region. Interestingly, actin-based motility was about 100-fold faster than passive diffusion and larger particles moved quicker than smaller ones.

Last but not least, therapeutic genes have to be delivered to the nucleus. All types of transport, active as well as passive, into and out of the nucleus have to pass through nuclear pore complexes.[246] While small molecules of up to 40 kDa or 10 nm may overcome this barrier by passive diffusion, molecules over 45 kDa must contain a nuclear localization signal to be recognized by importins, which mediate the nuclear transport. The upper size limit for active transport through the nuclear pore complexes is reported to be about 40 to 60 nm. However, it may not always be necessary to deliver the whole carrier into the nucleus. Instead, the payload may be released in the perinuclear region, facilitating transport through the nuclear pore complexes. Recently, the delivery of nuclear localization signal peptide-functionalized PLGA nanoparticles to the nucleus was reported.[249] Briefly, FITC-loaded PLGA nanoparticles were prepared and covalently grafted with amino-PEG-coated quantum dots. The remaining quantum dot-amine groups were coupled with thiol-terminated nuclear localization signal peptides. Upon modification, the diameter of the particles increased from 72 to 168 nm. The modified particles were tested for their uptake into HeLa (human cervical cancer) cells and their intracellular localization was analyzed by confocal laser scanning microscopy, revealing that targeted nanocarriers not only attained the cytoplasm, but also the nucleus. However, the modified carriers widely surpassed the reported size limit of the nuclear pore complexes. Therefore, the authors hypothesized that the carriers were able to pass due to size losses upon degradation, but PLGA is usually not degraded that quickly (see 1.1.2.2) and, more importantly, it is generally difficult to distinguish between labeled carriers and released marker. Encapsulated fluorescent dye is quickly released from the hydrophobic PLGA matrix, and some of the quantum dots might be cleaved from the PLGA surface. Thus, the observed fluorescence might not necessarily represent the localization of the PLGA carriers. This was highlighted by a comparison between PLGA nanoparticles that physically encapsulated Nile red and PLGA nanoparticles prepared from fluoresceinamine-coupled polymer.[250] Xu et al. reported that the increase in intracellular fluorescence intensity observed with physically entrapped markers was a result of dye transfer rather than particle uptake.

To sum up, there are still several crucial open questions about the fate of endocytosed PLGA particles and potential intracellular targeting strategies. Targeting to organelles other than the nucleus (such as mitochondria) is still in its beginnings.[236] For further elucidation, labeling procedures should be applied that guarantee a stable association of the marker with the carrier throughout the whole study. Despite the mentioned challenges, the increasing knowledge about the mechanisms of intracellular pathogen trafficking might enable new strategies for organelle-specific delivery in the future.[251, 252]

PROLONGED CIRCULATION TIME When “foreign” nano- or microparticles are injected into the bloodstream, these materials are rapidly cleared from systemic circulation. This removal is the consequence of a coordinated interplay between the adsorption of serum proteins at the particle surface and a subsequent uptake of the colloids by cells of the RES. Phagocytosis of particles is predominantly achieved by Kupffer cells in the liver, but also by macrophages in the spleen and, to a lesser extent, by macrophages in the bone marrow. It has been known since 1903 that specific serum proteins are involved in the labeling of particles as “foreign.”[253] These opsonins can be categorized into immune opsonins, which interact with receptors on macrophages to stimulate endocytosis (immunoglobulin G and complement proteins C₃ and C_{3b}) and nonimmune opsonins (fibronectin, C-reactive protein, tuftsin, mannose-binding protein, and lipopolysaccharide-binding protein), which alter the particle’s surface characteristics and thus render it more adhesive to phagocytes.[254] In contrast to opsonins, dysopsonins such as IgA and α 1-acid glycoprotein have been suggested to function as adsorptive serum components that play a regulatory role in inhibiting phagocytosis.[254, 255, 256] For a more detailed discussion of the mechanisms underlying the sequestration of particles from the bloodstream, the reader is directed to excellent reviews from recent years.[254, 256, 257, 258, 259, 260, 261]

As a consequence of the efficient removal by cells of the RES, it arises that if the spleen or liver are not the primary targets of nanoparticulate delivery systems, the particles will have to be disguised in order to evade the body’s defense mechanisms and to avoid inflammatory responses. Appropriate engineering of stealth particles will consequently be necessary for the successful application of nano- and microparticles as circulating drug reservoirs with controlled release properties, as artificial oxygen carriers, as vasculature imaging agents, and as passive and active targeting devices.[262] In order to reduce the interaction of particles with macrophages and to limit protein adsorption, adaption of the particle size and surface coating techniques have been proposed. Generally, keeping the size of the particles under 100 nm seems to be advantageous for prolonging blood half-life. Supposedly, this is due to the low surface area per particle, in combination with the high curvature that does not promote adsorption of the proteins needed for complement activation in a proper geometric configuration.[262, 256, 261] The complement system consists of more than 20 plasmatic proteins with enzymatic or binding capabilities and some receptors on cells. Adsorption of serum complement proteins and subsequent activation of the complement cascade can be determined with the complement activation assay,[261, 263, 264] and should always be validated by using zymosan particles as a positive control.[259] In addition to particle size, high charge density, and hydrophobicity of the surface have been identified as characteristics that promote serum protein adsorption.[256, 261] This is in agreement with theoretical predictions indicating that ionic and hydrophobic interactions, along with an entropy gain caused by changes in protein conformation, represent the driving forces for protein adsorption.[265] Consequently, in order to render biodegradable PLGA nanoparticles long-circulating, the hydrophobic and negatively charged particle surface has to be shielded.

This is expected not only to decrease opsonization but also to minimize interactions with macrophages.

To hydrophilize colloids, coating techniques with hydrophilic macromolecules have been investigated. While polysaccharides such as dextran and heparin have been employed for this purpose and might be advantageous due to their biodegradability,[266] most studies have used PEG and its co-polymers for surface modification. Because PEG contains a high number of ether groups that can bind water molecules via hydrogen bonding, their anchoring at the particle surface introduces a highly hydrated hydrophilic coating layer. This flexible layer sterically stabilizes the particles, screens underlying surface charges, and reduces the interfacial free energy, thus minimizing attractive forces for protein adsorption.[261] In practice, the introduction of a PEG layer is accompanied by a decrease of the particle's ζ -potential due to a shift of the shear plane away from the particle surface.[263, 174] The efficiency of protein repulsion is dependent on the MW of the PEG, the distance between the surface grafting points, and the conformational flexibility of the PEG chains.[261] For a detailed review on the interconnections between these parameters see Vonarbourg et al.[261]

According to a theoretical model,[267] the optimal distance between two terminally attached PEG chains should be in the range of 1 nm to repulse small proteins (approximately 2 nm) and around 1.5 nm to repulse large proteins (6–8 nm).[268] These theoretical predictions imply that the particle surface has to be entirely covered by the PEG coating to achieve sufficient repellence, and have been confirmed in studies with PLA nanoparticles.[269, 179] Due to the wide variety of particle matrix materials and grafting techniques described in the literature, it is difficult to identify an optimal PEG chain length. However, coating with PEGs in the MW size range between 1.5 to 3.5 kDa at appropriate grafting densities seems to generate a high degree of protein repulsion in most systems.[261] Generally, techniques for the PEGylation of PLGA nanospheres have comprised the production of particles from blends of PLGA/PEG-PLGA,[270, 271, 272, 273, 274, 275] the use of PEG-co-polymers as surfactants in course of the particle preparation procedure,[31, 174, 276] as well as the adsorptive coating of preformed particles with PEG-co-polymers.[46, 277, 108, 109, 31, 278]

By introducing hydrophilic PEG-blocks to the hydrophobic PLGA backbone, polymers with amphiphile characteristics can be prepared.[279] Despite higher water uptake into the particle matrix, particles prepared from PEG-PLGA oligomers are expected to be characterized by similar degradation characteristics as particles prepared from PLGA.[280] Upon cleavage of the ester bonds, the PEG molecules will be liberated from the carrier and excreted mainly via the kidneys if the MW is in the range of 1 to 20 kDa.[279] The preparation of nano- and microparticles from PEG-PLGA can be achieved with or without additional stabilizer by emulsification solvent evaporation procedures, solvent displacement, salting out,[281] and hydrodynamic flow focusing,[282] respectively. The surface density of PEG chains can be controlled by varying the ratio of the PLGA/PEG-PLGA blends used for particle preparation. In combination with the MW of the PEG, surface density determines whether the coating layer will mainly exist in a brush- or mushroom-like conformation.[279, 261]

As illustrated by studies with PLA/PEG-PLA blends, the majority of PEG chains orient themselves towards the outer aqueous phase in

the course of particle formation.[179] When incubated with serum and subsequently analyzed regarding the particles' protein adsorption pattern by 2D-PAGE, protein-repellent properties were already observed at blending ratios of 0.5:99.5 (PEG-PLA:PLA). However, the highest protein repellence compared with nanoparticles prepared from plain PLA was observed with blending ratios of at least 5:95 and a conjugate of PLA (MW approximately 45 kDa) with a PEG chain of at least 5 kDa MW.[179] The calculated distance between two terminally attached PEGs in this system corresponded to about 1.4 nm, which is in the theoretically predicted range for optimal protein repulsion.[268] In relation to these findings, a recent study has indicated that nanoparticles made from PEG-PLGA might be characterized by an even higher resistance to protein adsorption.[272] When comparing the protein adsorption capacity of particles made from co-polymers of PEG with the polyesters poly(ϵ -caprolactone) (PCL), PLA, and PLGA, the highest degree of polymer core protection from opsonization was observed for PLGA-PEG. Similarly prepared PEGylated PLGA nanoparticles have not only exhibited low protein adsorption, but also altered biodistribution.[271, 273, 274] In order to be able to track the nanoparticles *in vivo* and to determine their uptake into different tissues, ^{125}I -cholesterylaniline was encapsulated as radiolabel. Upon intravenous injection in rats, a clearly prolonged blood circulation half-life was observed for the PEGylated nanoparticles (approximately 7 h) compared with colloids produced from plain PLGA (approximately 15–35 s). Furthermore, uptake of the particles into spleen and liver was drastically reduced.[271] These results were confirmed by the same authors in mice; however, it should be highlighted that the nanoparticles used in all three studies exhibited a broad size distribution, as indicated by polydispersity indices of ≥ 0.3 .²⁴⁸ Using a similar approach to radiolabeling, Li et al. encapsulated ^{125}I -BSA as a model protein drug into nanoparticles made from PLGA or PEG-PLGA.[270] After encapsulation into PEGylated particles, the plasma half-life of BSA was increased from 13.6 min for plain PLGA carriers to about 4.5 h. Moreover, the biodistribution profile of PEG-PLGA particles was altered, indicating increased localization of BSA-loaded particles in the spleen and lung instead of the liver.[270]

In addition to the production of colloids from PEG-PLGA, PEGylation of preformed PLGA nano- and microparticles has been achieved by surface modification with a variety of PEG-copolymers via hydrophobic or electrostatic interactions. Because a large body of research has been generated on the successful coating of PS nanoparticles with poloxamers and poloxamines in the 1980s and 1990s,[259, 262] surface modification of PLGA with these block co-polymers of PEG and PPG suggested itself. Indeed, addition of poloxamer 407 or poloxamine 904 or 908 during the preparation procedure or adsorption onto preformed PLGA nanospheres generated long-circulating colloids with altered biodistribution in rats and rabbits.[31] However, while 39% and 28% of the administered dose of poloxamer 407- and poloxamine 908-coated particles, respectively, were detected 3 h post injection, only about 5% of plain and poloxamine 904-modified particles remained circulating in the bloodstream. The rather high sequestration of poloxamine 904-modified nanospheres was attributed to the comparably short PEG blocks (4 \times MW approximately 0.6 kDa) compared with poloxamer 407 (2 \times MW approximately 4 kDa) and poloxamine 908 (4 \times MW ap-

proximately 5 kDa). Interestingly, coating in course of the preparation procedure or onto preformed particles led to similar alterations of the biodistribution profiles.[31] This is remarkable, because it has been shown that poloxamer 407 and poloxamine 908 adsorbed onto preformed PLGA nanoparticles are displaced by serum proteins.[277] To monitor the displacement rate, the two surfactants were radiolabeled with ^{125}I Bolton-Hunter reagent and adsorbed onto particles made from PLGA and PS. Upon incubation in phosphate-buffered saline (PBS) for 24 hours, a removal of ~5% of surfactant was monitored. However, upon incubation in serum ~20% of surfactant was removed from PS nanospheres. In the case of PLGA nanoparticles, displacement was even more pronounced as illustrated by 71% removal of poloxamer 407 and 78% of poloxamine 908.[277] Although the studied PEG-copolymers are obviously rather weakly linked to the PLGA matrix, these carriers were characterized by prolonged plasma half-lives and a biodistribution shifted away from the liver.[278] When PEG-PLA was used as the coating polymer, varying biodistribution profiles were observed.[174] By coating PS and PLGA nanoparticles with PEG-PLA copolymers or poloxamine 908, hydrophilic colloids were generated (as monitored by HIC). However, while all coated PLGA nanospheres were characterized by prolonged plasma half-lives upon injection in rats, only PS particles coated with poloxamine 908 exhibited stealth properties 3 h post-injection. Although the PS nanospheres coated with PLA-PEG were characterized by an altered biodistribution shortly after administration, no differences were observed after 3 h compared with plain particles. This was attributed to potential differences in the affinity of the PLA-block to PS and PLGA as particle matrix materials.[174]

The modification of preformed PLGA nano- and microparticles has also been achieved using an electrostatic coating approach with PLL-PEG.[46, 108, 109] The PEG segments are anchored to the particle surface via ionic interactions between the polycationic PLL-backbone and carboxyl groups at the particle interface. In addition, coating of PLGA nanoparticles with protein-repellent carbohydrate derivatives has been investigated.[128] HES, which is fully biodegradable, was conjugated to lauric acid, and the resulting amphiphilic HES-laurates were used as a stabilizer in course of the production procedure. These PLGA nanoparticles adsorbed similarly low levels of BSA and fibrinogen as poloxamer 407-coated colloids. Moreover, reduced phagocytosis of the HES-laurate-modified particles by a monocyte macrophage cell line was observed.[128]

In conclusion, the coating of hydrophobic and negatively charged PLGA nanoparticles with PEG or polysaccharide derivatives results in hydrophilization of the particle surface. Even with theoretically optimal PEG surface densities, no complete inhibition, only a reduction of serum protein adsorption, was observed.[179] Nevertheless, several reports have described a drastically increased plasma half-life and altered biodistribution upon coating of PLGA nanoparticles with PEG, indicating success of this approach for engineering long-circulating nanoparticles. However, it remains to be addressed whether PEGylated PLGA nanoparticles retain their long-circulating properties upon repeated administrations. In the case of poloxamer- and poloxamine-modified PS nanospheres, it has been shown that PEGylated particles administered in a second injection 3 to 13 d after the first injection are rapidly removed by the RES.[283] This was attributed to an ac-

quired ability of liver and spleen macrophages to recognize the injected colloids. Furthermore, it is not clear whether the coating techniques generate homogenous PEG layers at the particle surface. Using HIC, a study has indicated that heterogeneities in surface coating might be responsible for the premature removal of fractions of PEGylated carriers.[263] Finally, the introduction of cell-specific homing moieties at the protein-repellent surface layer has been achieved recently and represents a crucial step forward to fully exploring the potential of long-circulating PLGA nanoparticles as targeted drug-carrier devices.[46, 109, 228]

TRACKING Sensitive analytical detectability is a crucial prerequisite for *in vivo* and *in vitro* studies dealing not only with biodistribution and elimination kinetics, but also with cytoadhesion, cytoinvasion, and intracellular trafficking of nano- and microparticles made from PLGA. The most commonly employed labeling techniques are based on the tagging of particles with fluorophores or radioisotopes.

Fluorescence labeling Fluorescence-based labeling techniques have been the methods of choice to render polymer particles trackable for *in vitro* cell interaction studies. The most frequently used concept is based on the encapsulation of a fluorescent dye in the polymer matrix in course of the preparation procedure of the particles. PLGA nano- and microparticles have mainly been labeled with hydrophobic fluorophores such as 1,1'-dioctadecyl-3,3',3'-tetramethylindocarbocyanine perchlorate (DiI),[128, 284] 3,3'-dioctadecyloxacarbocyanine perchlorate (DiO),[165] BODIPY® 493/503,[285] BODIPY® FL,[286] coumarin 6,[46, 88, 198, 240] pyren,[93] or Nile red.[250] However, hydrophilic dye molecules such as rhodamine 123,[227] rhodamine 6G,[287, 114] rhodamine B,[288] dextran-rhodamine,[105] indocyanine green,[289] as well as quantum dots,[290] have also been employed. Additionally, Panyam et al. developed a dual labeling technique with coumarin 6 and osmium tetroxide, yielding colloids that can be detected by fluorescence and electron microscopy.[291] Dye-labeled PLGA conjugates primarily have been synthesized by carbodiimide-mediated activation of the uncapped polymer backbone and subsequent reaction either directly with the fluorescein derivatives fluoresceinamine[250, 292] or fluorescein cadaverine[75] or via a diamine spacer with carboxyfluorescein[293] or FITC.[109] Moreover, Tosi et al. have described a method for synthesizing a versatilely applicable, biotin-capped derivative of PLGA. Particles made from this polymer were tracked in tissue sections by electron microscopy after reaction with a streptavidin-peroxidase conjugate and subsequent incubation with diaminobenzidine.[293] Speaking from experience in our laboratory, the binding of avidin to biotin-modified nanoparticles, however, can be clearly limited in the presence of proteins. This is probably due to protein adsorption at the particle surface, which leads to steric obscuration of the small biotin binding site (unpublished results). Considering this, a versatile two-step approach for the decoration of particles with biotin as reported by Müller et al. seems more promising.[108] A cationic PLL-g-PEG-biotin conjugate, which adsorbs to the negatively charged PLGA surface via the PLL-block, was used to introduce sterically flexible biotin for subsequent labeling with Oregon Green®-streptavidin.

Furthermore, the covalent fluorescence labeling of preformed particles has been investigated. Following activation of surface carboxyl groups and amination with ethylene diamine, the introduced amino groups on PLGA microspheres were subsequently conjugated with FITC.[294] In addition to this rather complicated two-step procedure, direct surface modification of PLGA nano- and microparticles with fluorescent entities also has been reported. The well-established carbodiimide chemistry was used to covalently immobilize fluorescein-tagged proteins[295, 296] or amine-functionalized quantum dots.[249]

Radioactive labeling The techniques for the modification of PLGA particles with radioactive isotopes rely on similar rationales as fluorescence labeling. Primarily, radioactive labeled particles have been used analytically to investigate the effect of surface modifications with PEG or PEG-containing surfactants on the biodistribution of PLGA particles in rodents.[270, 297, 298, 299, 300] In addition, the possibility of using radioactive particles for the delivery of a radiation dose to tumor tissue was discussed.[301] Several studies report the labeling of PLGA particles by encapsulation of small molecules or proteins conjugated to radioactive isotopes. These include ^{188}Re -dimercaptosuccinic acid,[301] ^{111}In -oxine,[31, 174, 297] ^3H -paclitaxel,[302] ^{125}I -cholesterylaniline,[271] ^{125}I -tetanus toxoid,[84] and ^{125}I -tagged BSA.[270] Direct labeling of PLGA has been achieved by reaction of ^{14}C -acetic acid anhydride with terminal hydroxyl groups of the polymer chains.[303] Furthermore, the widely used approach for the labeling of proteins and proteinaceous colloids with metastable $^{99\text{m}}\text{Tc}$ by stannous reduction has been applied to pre-formed PLGA particles.[298, 299, 300] While the reaction mechanism underlying the conjugation of $^{99\text{m}}\text{Tc}$ to proteins is clear,[304] detailed information about the labeling of polymeric particles is scarce. A lowering of the valency state of $^{99\text{m}}\text{Tc}$ by the reducing agent stannous chloride and subsequent complexation with amine groups has been proposed as the labeling mechanism for chitosan nanoparticles.[305] The adsorption of $^{99\text{m}}\text{Tc}$ onto PLGA particles is probably driven by the high affinity of multivalent cations for negatively charged interfaces.

Radiolabeling of PLGA nanoparticles has also been achieved by coating of plain colloids with radioactively tagged poloxamers and poloxamines.[277, 299] The hydroxyl end group of the PEG-containing surfactants is aminated and subsequently conjugated with ^{125}I -hydroxyphenylpropionic acid. The interested reader is directed to Neal et al.[277] for a comprehensive discussion of reaction schemes and for alternative approaches to the radioactive labeling of PEGs.

In conclusion, it has to be highlighted that adequate labeling of particles made from PLGA, especially using fluorescent dyes, is not trivial. Although the degradation half-life of PLGA lies well beyond the time scale of most *in vitro* cell-interaction studies, marker is already expected to be released from the particles in the course of short experiments.[306, 250] As a rule of thumb, small hydrophilic dye molecules cannot be efficiently loaded and are poorly retained in the particle matrix. However, low-MW hydrophobic compounds also suffer from premature release. As illustrated by recent reports, the extent of this leakage probably has been underestimated so far due to the use of protein- and lipid-free buffer systems for the liberation tests.[250, 307] The consequences of this have not necessarily

hampered the interpretation of studies using microparticles because their relation to free label in physical size is unambiguous. However, in the case of nanoparticles optical microscopy hits on its resolution limits and discrimination between free marker molecules and particles becomes a tremendous challenge. The resulting susceptibility of nanoparticle-cell interaction studies to misinterpretation has been discussed recently.[250, 307] Considering this, it becomes clear that results solely based on fluorescence detection should be interpreted with particular care. To improve the value of studies in this field, limitations of existing protocols have to be addressed and the development of more effective labeling approaches is strongly needed. From the current perspective, covalent modification of PLGA seems promising due to the stable linkage between marker molecules and the polymer. The encapsulation of hydrophobic, high-MW species such as quantum dots might prove to be a valuable alternative, because their diffusion coefficients in the particle matrix are expected to be clearly lower than those of low-MW compounds. In the long run, however, an integration of ultrastructure-resolving techniques will be needed to fully resolve the cytoadhesive and cytoinvasive properties as well as the subcellular trafficking of polymer nanoparticles.

STABILIZATION OF BIOMACROMOLECULES Because it was shown in the early 1990s that biomacromolecules can be encapsulated into PLGA microspheres and might thereby be protected from degradation,[308] numerous studies have investigated the delivery of peptides, proteins, oligonucleotides, and DNA using carriers made from PLGA.[58, 309, 310] However, several difficulties have been found to be associated with this concept. First, although the encapsulation of hydrophilic molecules is feasible using water-in-oil-in-water solvent evaporation techniques, the loading efficiency is often limited. Second, the dispersion steps involved in particle preparation are associated with contact with organic solvents and shear stress due to sonication or homogenization. These processes might result in denaturation of the biomacromolecules during encapsulation.[311, 312] In addition, molecules incorporated in a PLGA matrix are increasingly exposed to an acidic microclimate by time. This has been visualized recently by confocal laser scanning microscopy and is a consequence of polymer hydrolysis and the accumulation of degradation products in aqueous pores.[313, 314] While the stability of drug released during the “first-burst” phase is not necessarily compromised, pronounced degradation might occur over the course of later stages of release.[315] Several strategies have been proposed for the stabilization of labile biomacromolecules under these circumstances, including complexation of proteins with zinc, the addition of PEG, and co-encapsulation of antacid excipients.[312, 316] An alternative approach to circumvent these limitations is based on the adsorption of the biomacromolecules to be delivered onto the surface of preformed nano- and microparticles made from PLGA.[104, 317]

Because the coating is applied to preformed particles, exposure of the biomacromolecules to potentially deleterious solvent and shear conditions is avoided. Furthermore, the release of the payload from the carrier proceeds relatively quickly and is not strictly dependent on the slow bulk erosion release kinetics of PLGA.[105] This might prove especially advantageous in the case of vaccination, as a typical

phagocytic cell only has a lifespan of several days.[185] Because it has been reported by several groups that loading of biomacromolecules onto the particle surface can provide sufficient protection against enzymatic degradation,[104, 130] the delivery of proteins,[103, 132, 133, 152, 294, 318, 319] plasma membrane preparations,[320] tumor cell lysates,[320] oligonucleotides,[95, 321] and pDNA[74, 92, 102, 104, 105, 115, 130, 322, 323, 324, 325, 326] has been investigated. While direct coating of plain PLGA particles has been achieved,[318, 327] precedent surface functionalization with excipients has proven advantageous for enhancing the efficiency of the subsequent coating. Heparin, for example, is characterized by a high binding affinity to growth factors such as FGF (fibroblast growth factor), VEGF (vascular endothelial growth factor), HBEGF (heparin-binding epidermal growth factor), and TGF- β (transforming growth factor- β). Making use of this affinity, Chung et al. showed that conjugation of heparin to the surface of highly porous uncapped PLGA particles via carbodiimide chemistry generates microspheres with 4-fold higher FGF-loading capacity compared with plain particles.[294]

Coating of PLGA particles with cationic polyelectrolytes or amphiphilic molecules can also enhance the binding capacity for biomacromolecules. PLGA nano- and microparticles have been regarded as promising biodegradable antigen carriers and adjuvants for the formulation of vaccines.[185, 328, 329, 330] Because vaccines made from purified preparations from pathogenic organisms or recombinant proteins are often not sufficiently immunogenic, site-specific delivery systems are needed to optimally present the antigen to the innate and adaptive immune systems.[330] Nanoparticles might prove beneficial for this purpose because they diffusively spread upon injection and can reach lymph nodes.[185] To date, however, microparticles have been studied more extensively. Due to their relatively large size, microparticles are minimally taken up by nonphagocytic cells but can be internalized by APCs such as macrophages or DCs. This passive targeting effect supposedly leads to preferential delivery to APCs and has been reported to be most pronounced for particles in the size range of 1 to 3 μm .[330]

Microparticles produced from PLGA have been investigated as potential carriers for protein antigens. One approach is based on the formation of particles from blends of end-capped PLGA and the anionic amphiphile dioctyl sulfosuccinate. The resulting microparticles are characterized by a negative ζ -potential and have been shown to adsorb proteins such as ovalbumin, carbonic anhydrase, lysozyme, lactic acid dehydrogenase, BSA,[152] the recombinant proteins MB1/MB2 from *N. meningitides*,[152, 133] recombinant p55 gag from HIV-1,[132] and the recombinant HIV envelope glycoprotein gp120dV2.[152, 319] In the latter, adsorptive coating of the particles retained the antigenic structure of the glycoprotein, while encapsulation into PLGA microparticles did not. According to protein quantification by size-exclusion chromatography and the bicinchoninic acid assay, the highest loading rate with gp120dV2 (isoelectric point approximately 8.5) was achieved at pH 5. This indicates a preferential adsorption of positively charged protein molecules onto the negatively charged carriers via ionic interactions.[319] The importance of the isoelectric point in protein adsorption was confirmed in MB1/MB2, in which the highest loading rates on negatively charged PLGA microparticles were observed for the positively and noncharged form of the protein, respectively.[133] In addition, positively charged

microparticles have been investigated as protein carriers. Mandal et al. used PEI- and PLL-coated PLGA microparticles for the delivery of granulocyte-macrophage colony-stimulating factor (GM-CSF), which is a differentiation factor for hematopoietic progenitor cells and may act as an adjuvant.[103] Similar amounts of GM-CSF adsorption were monitored on plain and polyamine-modified particles, hinting at a dominant role of the hydrophobic PLGA matrix for this protein.

In recent years, gene-based vaccination has evolved as an alternative to traditional vaccine strategies.[185, 310] The transfection of cells with pDNA results in sustained intracellular antigen production, which in turn can lead to a coordinated activation of humoral and cell-mediated immune responses. Because delivery of naked pDNA is severely limited due to premature enzymatic degradation,[331] alternative approaches have been investigated using polymeric particles as carriers.[185, 330] For example, particles were prepared containing encapsulated naked or polyamine-complexed pDNA.[310, 332] Because naked pDNA is prone to degradation in course of the particle preparation process,[311] approaches based on the encapsulation of pDNA complexed with PLL [331] or PEI [333, 334] have proven to be more promising. The polyamines form stable complexes with pDNA due to electrostatic interactions between amine and phosphate groups. This has been shown to stabilize pDNA during particle formation and limits its susceptibility to enzymatic degradation by DNase I.[331] Furthermore, free amino groups of the polyelectrolyte are expected to buffer the intraparticle pH drop during polymer erosion, which will also contribute to the stability of the formulation.[333]

As an alternative approach, pDNA has been loaded onto the surface of PLGA particles modified with cationic surfactants or polyelectrolytes. Several studies, especially those by Singh et al., have dealt with the applicability of the cationic amphiphiles CTAB, DDAB, and DOTAP for the introduction of positive charges at the surface of end-capped PLGA microparticles during particle preparation.[130, 199, 322, 323, 325, 335] Positively charged carriers, primarily modified with CTAB, have been loaded with plasmids encoding antigens from *M. tuberculosis*,[336] avian metapneumovirus,[337] foot and mouth disease virus,[338] hepatitis B virus,[339] hepatitis C virus,[335] HIV,[130, 322, 323, 325] and measles virus.[340] By varying the amount of CTAB used for particle coating, the loading efficiency and release rate of pDNA can be regulated.[323, 325] The amount of pDNA associated with the microparticles was determined by agarose gel electrophoresis or after ultracentrifugation of the loaded particles into an OptiPrep® density gradient, complexation with ethidium bromide, and fluorometric analysis of the gradient fractions. Compared with naked pDNA, CTAB-modified particles loaded with pDNA were found to elicit higher immune responses, possibly due to an adjuvant effect of the cationic particles.[130, 322, 323] The sequential loading of two plasmids encoding the antigens p55 gag and gp-140 of HIV-1 has also been reported.[325] While only low loading levels were achieved for unmodified particles, the plasmids were efficiently adsorbed to cationic PLGA particles. Furthermore, protection of surface-adsorbed pDNA from degradation by DNase I was observed *in vitro*. [325] In contrast to these observations, Oster et al. have reported that coating of negatively charged particles with CTAB does not provide protection of pDNA against degradation by DNase I.[104] However, surface modification with branched PEI (MW approximately

25 kDa) led to highly positive carriers that protect surface-adsorbed plasmids from enzymatic cleavage. While naked pDNA was degraded by DNase I within 5 min, pDNA adsorbed onto PEI-coated particles was stable for about 12 h. PEI/PLGA blends also have been frequently used for the preparation of nanoparticulate transfection vectors that bear a positive surface charge and have been successfully loaded with plasmids.[102, 115] Moreover, covalent conjugation of PEI onto the particle surface has been investigated.[74, 105, 324] Polyamine anchoring at the surface of preformed microparticles is probably a result of a combination of electrostatic interactions and the formation of covalent bonds via active esters. According to Pai Kasturi et al., covalently modified PEI-PLGA particles are characterized by 5-fold enhanced pDNA adsorption efficiency compared with plain particles.[341] Furthermore, it was observed that surface modification with linear PEI (MW approximately 25 kDa) led to a quicker release of plasmid and decreased buffering capacity toward acid titration compared with branched PEI (MW approximately 70 kDa).

Whether these observations were due to varying degrees of complexation of pDNA by linear and branched PEI could be investigated with an ethidium bromide replacement assay.[82] By mixing plasmids with ethidium bromide, pDNA with intercalated fluorophores was obtained. Upon adsorption of pDNA prepared in such a manner onto PLA particles coated with branched PEI, different amounts of free “squeezed out” ethidium bromide were detected. Coating with “coiled” PEI resulted in particles with a high potency for DNA condensation and thus high replacement of ethidium bromide. In comparison, particles coated with PEI that had been adsorbed in a “stretched” conformation were characterized by less free surface charges and a consequently decreased potency for complexation.[82] Chitosan has also been used for the preparation of positively charged PLGA nanoparticles that were subsequently coated with plasmids [92] or antisense oligonucleotides.[95] According to AFM studies, pDNA-chitosan complexes appeared to form clusters at the particle surface.[92] Another interesting approach for the introduction of a surplus of positive charges on uncapped PLGA particles is the conjugation with PAMAM dendrimers.[326] Microparticles were conjugated with third- to sixth-generation PAMAM dendrimers by carbodiimide coupling chemistry. As determined by UV-spectrophotometric analysis (absorption, 260nm) of the coating solution’s residual pDNA content, 5-fold higher pDNA loading efficiencies were obtained on PAMAM-modified compared with plain particles. While the ζ -potential and buffering capacity toward acid titration increased with increasing dendrimer generation, the transfection efficiency was constantly higher than that of pDNA-loaded plain particles but was not influenced by dendrimer generation.[326]

The development of particle-based vaccination strategies has also included the loading of microparticles with immunostimulatory substances. Nonmethylated nucleotide sequences containing cytosine linked to guanine by a phosphodiester (CpG DNA) belong to this group of molecules. Sequences containing the CpG motif are frequently found in prokaryotic DNA, but in vertebrate DNA they do not occur as abundantly in their nonmethylated form.[321] Because CpG DNA induces the conversion of immature DCs to mature APCs, they are considered to be a promising class of vaccine adjuvants. By adsorbing phosphorothioate oligonucleotides containing CpG on cationic PLGA micropar-

ticles, a potent immunostimulatory effect was observed in mice compared with free CpG.[321] Similarly, poly(inosine)-poly(cytidylic acid) (poly(I:C)), which is a synthetic analog of viral double-stranded RNA characterized by affinity for toll-like receptor 3, also serves as a maturation signal for DCs.[342] Poly(I:C) electrostatically adsorbed onto PLGA microparticles coated with cationic diethylaminoethyl dextran was observed to be a more potent inductor of DC maturation compared with the free soluble substance.[101]

As illustrated, the rationale of adsorbing plasmids, proteins, or antisense oligonucleotides onto the surface of preformed particles represents a promising approach for gene- and antisense-delivery as well as vaccination. Moreover, surface-based techniques offer the possibility to co-deliver substances encapsulated in the particles. The feasibility of this approach has been shown by adsorption of a plasmid encoding luciferase onto the surface of PLGA microspheres with encapsulated FITC-BSA.[105] These first proofs of principle could stimulate the development of bifunctional vaccine formulations with pDNA/protein antigen at the particle surface for a “first burst” and encapsulated pDNA/protein for sustained delivery to enhance the immune response.[309] Moreover, biodegradable delivery systems carrying the antigen and immunomodulatory substances could be prepared and decorated with targeting moieties. However, for these approaches to be successful, the surface adsorption protocols yielding high loading efficiencies and protection of the biomacromolecules from degradation have to be identified. It also remains to be addressed whether adsorptive coating techniques generate sufficiently stable linkages, because relatively quick displacement of proteins from the carrier system can occur due to competitive adsorption of serum proteins.[103]

1.1.2.5 *Future challenges*

Despite the mentioned large number of successful proof-of-concept studies, several challenges still have to be overcome on the way to successful clinical application of surface-modified PLGA-based carriers. Until now, most of the reported methods for the preparation and surface modification of PLGA particles involved rather small batches. A scale-up to large production volumes will certainly introduce additional challenges. Moreover, reasonable production costs will remain an important prerequisite for successful application.

In order to prevent unwanted effects that might be caused by residual reagents, efficient purification methods are needed. The removal of reagents applied for surface modification has rather been neglected so far. Currently, particle suspensions are most often purified by methods that exploit the difference in size between the particles and the employed reagents, such as centrifugation,[76, 77, 80, 343] ultracentrifugation,[201, 205] diafiltration,[344] size-exclusion chromatography,[218, 226] or dialysis.[234, 146] However, these methods are generally intricate and time-consuming and they do not allow for a quantitative elimination of unwanted reagents. Future functionalization strategies will have to consider these limitations.

As a basis for further advancements, a more detailed understanding of PLGA particle morphology is also required. Although electron microscopy enables a very high magnification, the resolution that may be achieved upon imaging of PLGA particles is strictly limited. Due to the low glass transition temperature of PLGA of about 40°C, the par-

ticles quickly start to “melt” upon irradiation with the electron beam, which may result in artifacts. So far, SEM has enabled valuable insights concerning the size and porosity of PLGA microparticles.[345] With cryo-TEM or via freeze-fracture replica, even PLGA particles in the submicron range have been visualized.[159] However, the only reliable information obtained was about the size and the overall shape of the PLGA nanoparticles. Electron microscopy is a valuable complement for other frequently used sizing techniques such as photon correlation spectrometry, which can only determine the hydrodynamic diameter of suspended particles and is influenced by numerous parameters.[344] Because the molecules typically used for surface modification of PLGA particles have a diameter of only a few nanometers at the largest, their presence and conformation cannot be evaluated by currently available electron microscopic techniques; at best, it is possible to distinguish between smooth, rough, and porous surfaces.[114]

Alternatively, AFM (also known as scanning probe microscopy)[346] has been explored to characterize the morphology of PLGA particles. In AFM, the sample surface is scanned with a mechanical probe to generate a topographic map of the sample. Additionally, this technique can be used to gain information about the rigidity of the sample or even about the affinity of ligand-receptor interactions. In contrast to SEM, not only dry but also liquid samples can be imaged, and it is not necessary to work under vacuum. Nevertheless, AFM is most useful for the characterization of rather flat surfaces, and it is not possible to examine steep walls or overhangs. Moreover, the particles need to be immobilized prior to imaging, which is often a tedious task. Concerning PLGA particles, the method is still in its infancy. So far, it is possible to reliably determine only the particle size and shape and to distinguish between smoother or rougher surfaces.[92]

Aside from the characterization of the nano- and microparticles themselves, their distribution in a complex organism and their interaction with specific cells need to be investigated using appropriate models. Typically, *in vitro* experiments are performed in stationary setups with particles dispersed in buffer. However, the stability of plain and surface-modified particles might be compromised substantially in physiological media with high protein content.[99] It has been observed that charged particles preferentially accumulate in certain tissues,[347, 348] but it is not clear whether this is due to ionic interactions between particles and endothelial cells or whether plasma protein adsorption or microaggregate formation also play a decisive role. To accurately study the interaction of particles with tissues that are exposed to flow *in vivo* (endothelium, urinary tract epithelium, gastrointestinal tract), alternatives to currently used stationary assays have to be developed.[349, 296] Using a microfluidic flow chip, it has been shown recently that plain PLGA microparticles are characterized by negligible bioadhesion in the presence of hydrodynamic drag.[296] Consequently, in order to engineer drug carriers that efficiently adhere to a target tissue in the presence of shear forces, sophisticated surface functionalization strategies might have to be developed.

1.1.2.6 Outlook

In 2004, Nutropin Depot, the first and only marketed protein-loaded PLGA microparticle formulation, was withdrawn from the market because of high costs. This fact does not encourage further research

in this area, but only at the first sight. Apart from profit and demand, PLGA micro- and nanoparticles including covalently functionalized ones will gain ground in three fields of application in future.

In the broad and sometimes sophisticated area of targeted therapy, covalent conjugation of targeting ligands offers the advantage of stable attachment compared with possible detachment or even loss of the ligand in the case of adsorptive immobilization. Additionally, the biorecognitive ligand is antennary exposed toward the biological environment, allowing optimal biointeraction compared with electrostatic or adsorptive coating. The latter approaches sometimes suffer from unknown folding of amphiphilic ligands, probably shielding the target moiety, especially when cross-linking is required to stabilize the coat. Nevertheless, two issues must be addressed: First, the biocompatibility and biodegradability of surfactants used for the preparation of PLGA particles has rarely been considered. Second, the covalent surface modification requires processing of the drug-loaded particle, which remains time-consuming in spite of optimization. On the one hand, there is the risk of premature drug loss due to the first burst effect; on the other hand, this drawback might turn to an advantage when the release rate is supposed to be controlled by diffusion and/ or erosion alone.

Targeted diagnostics will be another field of application for surface-modified PLGA-nanoparticles. In particular, multi-labeling by simultaneous covalent immobilization at the surface of targeted particles with contrast labels for magnetic resonance imaging (MRI), positron emission tomography (PET), computerized axial tomography (CT), and ultrasound[350] is a promising approach and beneficial for the patient. In clinical practice, however, some combinations might be pointless. Whereas fluorescent imaging is very useful in research, its utility in humans is highly questionable. With respect to patient comfort, imaging should be feasible in one step, for example, by a combination of PET and MRI. Finally, the most frequently stressed combination of therapy and diagnosis (theranostics) by one particulate formulation might hit a snag. Apart from the high costs for the health care system, the benefit for a patient with an unknown disease remains questionable because the particle will release the drug irrespective of sickness or health.

All in all, the increasing knowledge in surface modification of PLGA particles will considerably contribute to realize Paul Ehrlich's dream of magic bullets for targeted therapy, although the bullets will be invisible owing to their small size in the micro- or nanometer range.

1.1.3 Cytoadhesion, internalisation and transcytosis of wheat germ agglutinin (WGA) investigated by electron microscopy

1.1.3.1 Introduction

Associated with the external face of the plasma membrane of eukaryotic cells is the glycocalyx which consists of sugar moieties of glycosylated membrane lipids and proteins. Mainly, these contain galactose and galactosamine, glucose and glucoseamine, sialic acid, mannose as well as fucose. At maximum, carbohydrate side chains carry fifteen saccharide residues. The composition of this carbohydrate coat differs between cell types and is subject to variations upon malignant transformation of a cell.[351] The glycocalyx thus represents a structure which can be addressed to enhance the cytoadhesion of drug carriers to normal cells and cancer cells in a potentially targeted way. In order to make use of this rationale for drug delivery, lectins can be employed.

Lectins represent a group of proteins which specifically bind to carbohydrates.[352] By screening a library of lectins, suitable candidates are identified which mediate cytoadhesion to specific cell types. WGA from *triticum vulgare* has been shown to exhibit high binding to bladder cancer cells,[210] chondrocytes,[209] brain microvascular endothelial cells,[353] as well as enterocyte-like cell lines such as Caco-2 cells.[354] Moreover, the quantity of WGA-binding is increased upon malignant transformation. WGA is a dimeric protein with MW ~36 kDa which possesses two high and two low affinity binding sites for N-acetyl-D-glucosamine and N-acetylneuraminic acid. Due to its binding to enterocytes it has been discussed as a promising agent to enhance the cytoadhesion and to thereby prolong the residence time of prodrugs and drug carrier systems upon peroral administration.[5] Aside from improving cytoadhesion, conjugation with WGA has been shown to induce uptake of proteins [355] and possibly nanoparticles [285] into cells. Moreover, evidence exists that WGA could serve as a shuttle to mediate transcytosis across cell monolayers.[5]

To further understand these properties, the aim of the presented study will be to investigate the cytoadhesion, internalisation and potential transcytosis of WGA through Caco-2 cell monolayers. Caco-2 cells morphologically and functionally resemble human enterocytes and are an accepted cell model for permeability studies according to the biopharmaceutics classification system (BCS). Thus, they have been used extensively as an *in vitro* model for studies relating to intestinal absorption.[356] Transmission electron microscopy will be employed to resolve the temporal evolution of the ultrastructural localization of the lectin.

1.1.3.2 Experimental setup

CELL CULTURE The Caco-2 cell line was purchased from the Deutsche Sammlung von Mikroorganismen und Zellkulturen (DSMZ; Braunschweig, Germany) and was used for the experiments between passage 35 and 54. Tissue culture reagents were obtained from Sigma (St. Louis, USA) and Gibco Life Technologies Ltd. (Invitrogen Corp., Carlsbad, CA, USA). Cells were cultivated in RPMI 1640 cell culture medium containing 10% fetal bovine serum, 4 mM L-glutamine and 150 mg mL⁻¹ gentamycine in a humidified 5% CO₂/95% air atmosphere at

37°C and were subcultured by trypsination. Differentiated Caco-2 cell monolayers were obtained by seeding of 120 µL of cell suspension (1.05×10^5 cells mL⁻¹) in ThinCert™ tissue culture inserts (0.4 µm pore size, translucent; Greiner Bio One, Kremsmünster, Austria) and cultivation for 21 days.

PULSE-CHASE INCUBATION OF CELL MONOLAYERS WITH WGA-HORSERADISH PEROXIDASE (HRP) The cell culture medium was removed from the monolayers and replaced with isotonic HEPES/NaOH buffer pH 7.4 (isoHEPES) that had been cooled to 4°C. Upon incubation of the cell layers for 15 min at 4°C, the buffer was replaced with 120 µL of a precooled solution of WGA-HRP (20 µg mL⁻¹) in isoHEPES followed by incubation for 15 min at 4°C. Subsequently, the Caco-2 monolayers were washed with isoHEPES twice. For chase-incubation, 120 µL of isoHEPES warmed to 37°C was added and the cells were incubated for 30 min or 60 min at 37°C. After one washing step with isoHEPES, pulse- and chase-incubated cells were fixed by addition of 120 µL of a 2 % (v/v) solution of glutaraldehyde in PBS for 60 min at 4°C.

PREPARATION FOR ELECTRON MICROSCOPY The filters with attached Caco-2 monolayers were excised from the insert and left to react with a solution of 3,3'-diaminobenzidine (DAB; 0.5 mg mL⁻¹) in TRIS/HCl buffer pH 7.6 for 15 min under protection from light. The DAB was removed and upon addition of a 1 % (v/v) solution of H₂O₂ and reaction for 30 min the sample was washed thrice with distilled water. Subsequently the sample was postfixed for 15 min with a 1:1 mixture of aqueous solutions of potassium ferrocyanide (3%) and osmium tetroxide (2%). After incubation with a 1 % solution of osmium tetroxide in veronalacetate buffer for 30 min at 4°C the cells were dehydrated in a graded series of ethanol (70 % overnight at 4°C, 70 % for 10 min, 80 % for 10 min, 96 % for 10 min, 2 x 100 % for 10 min). The dehydrated samples were embedded in Epon 812 epoxy resin (Serva, Heidelberg, Germany) which was hardened for 2 days at 40°C followed by 2 days at 60°C. Sections (80-100 nm) were cut with an UltraCut-UCT ultramicrotome (Leica Inc., Vienna, Austria) and transferred to copper grids.

ELECTRON MICROSCOPY The cell samples were inspected in a Tecnai-20 transmission electron microscope (Tecnai-20 LaB6, FEI Company, Eindhoven, The Netherlands). Digital images were recorded with a slow-scan CCD camera (MSC 794, 1k x 1k pixel, Gatan Inc., Pleasanton, USA).

1.1.3.3 *Results and Discussion*

WGA EXTENSIVELY BINDS TO THE APICAL MEMBRANE OF ENTEROCYTE-LIKE CACO-2 CELLS To be able to analyze the association of WGA with Caco-2 cell monolayers, a conjugate of WGA with HRP was used. HRP catalyzes the oxidation of the chromogenic substrate DAB and thus enables indirect histological localization of WGA.

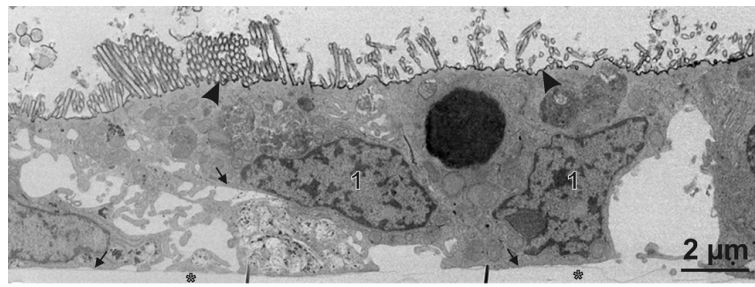


Figure 5: Caco-2 cell monolayer incubated with wheat germ agglutinin (WGA)-horseradish peroxidase (HRP) conjugate at 4°C. Nucleus (1), WGA-HRP (blackening) predominantly bound to apical membrane with microvilli (arrowheads). Filter (*) and no staining observed at the basolateral membrane (arrows) .

The 21-day old Caco-2 monolayers were cooled to 4°C in order to reduce the cellular metabolism and the fluidity of the plasma membrane. At this temperature cytoadhesive agents are expected to bind to the cellular membrane but no internalization will occur. As illustrated by the blackening in Figure 5 (arrowheads), WGA was densely associated with the apical side of the polarized cell monolayer upon loading for 15 min at 4°C. The homogenous staining of the apical plasma membrane including the microvilli indicates a rather uniform distribution of carbohydrate binding sites within the glycocalyx. At the intracellular region proximal to the apical plasma membrane no blackening of endosomes, multivesicular bodies or lysosomes was observed. This indicates no or only minimal uptake of WGA-HRP into the cell in course of loading at 4°C. The lack of staining of the lateral and basolateral plasma membrane (Figure 5, arrows) underlines the functional integrity of tight junctions and their barrier function for macromolecules dissolved in the fluid phase or associated with the membrane. Interestingly, when equimolar quantities of HRP were used in the same experimental setup, no blackening of the apical membrane of the Caco-2 monolayer was observed. This underlines the cytoadhesive properties of WGA which can be transferred onto HRP by chemical conjugation with the lectin.

Regarding the predictive value of the employed cell model it has to be highlighted that Caco-2 cells do not produce mucus and thus do not entirely reflect the intestinal epithelial barrier *in vivo*. Binding of lectin to mucus will at least partially result in its removal from the gastrointestinal tract by mucus shed. However, WGA binding to mucus is reversible and competitive with the binding to cell surface carbohydrates.[357] Consequently, although mucus might initially capture WGA or WGA-conjugated carrier systems, a reallocation to enterocytes is expected to occur.

MEMBRANE-BOUND WGA IS INTERNALIZED VIA ENDOSOMES Upon removing of non-bound WGA-HRP and increasing the incubation temperature to 37°C for 30 min, the apical part of the cell membrane was still occupied with a dense layer of WGA-HRP (Figure 6, arrowheads). However, endosomes were already positive for WGA and fusion of endosomes to multivesicular bodies had occurred. This underlines that membrane-bound WGA is indeed taken up by Caco-2 cells. The time

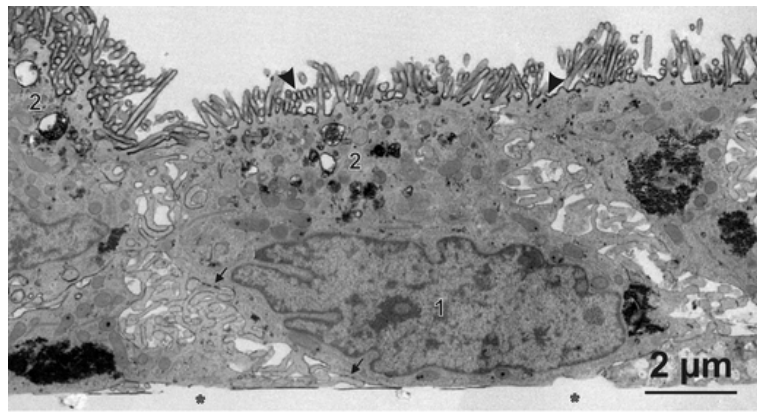


Figure 6: Caco-2 cell monolayer loaded with WGA-HRP at 4°C and post-incubated for 30 min at 37°C. Nucleus (1), early endosomes and multivesicular bodies (2), apical membrane with microvilli (arrowheads), and filter (*). Speckles of WGA-HRP (blackening) localized at the lateral and basolateral membrane (arrows).

scales for internalization to occur are probably even shorter than 30 min. This is illustrated by the fact that WGA-positive endosomes were already found after incubation for 15 min at 37°C (data not shown). While no localization of WGA-HRP was observed at the lateral and basolateral membrane after 15 min, isolated patches were detected after 30 min (Figure 6, arrows). Consequently, while most of the internalized WGA was localized in singular and multivesicular endosomes, a small fraction had already been transported to the (baso-)lateral plasma membrane within 30 min.

TRANSCYTOSIS OF WGA The localization of WGA in Caco-2 monolayers chase-incubated for 60 min at 37°C was similar to that observed after 30 min. However, the quantities of WGA-HRP associated with the different compartments had shifted. When comparing the blackening of the apical plasma membrane (Figure 7 and Figure 8 (top image), arrowheads) with that after loading at 4°C (Figure 5, arrowheads), a slight decrease in intensity is monitored. This indicates that the high concentration of apically bound WGA-HRP is decreased by internalization into the cytoplasm. At the apical side of the cytoplasm a considerable number of WGA positive endosomes, multivesicular bodies and also some lysosomes (Figure 8 (bottom image), 3) was observed. Moreover, a pronounced accumulation of WGA-HRP was detected at the basolateral side of the Caco-2 monolayer. This is exemplified by the intense and continuous blackening of the basolateral plasma membrane in Figure 7 (arrows) and 8 (bottom image, arrows). Importantly, neither equimolar nor fluid phase marker quantities of HRP ($500 \mu\text{g mL}^{-1}$) led to any contrasting of the basolateral membrane. This underlines that WGA can mediate transcytosis of a protein which otherwise would not reach the basolateral side of a polarized epithelial cell monolayer. A quantification of the amount of WGA localized in lysosomes and transported to the basolateral side is difficult. Due to the enzymatic conversion of DAB and variations in contrasting during sample preparation, only semi-quantitative estimates are possible. As reported by Wirth et al. the

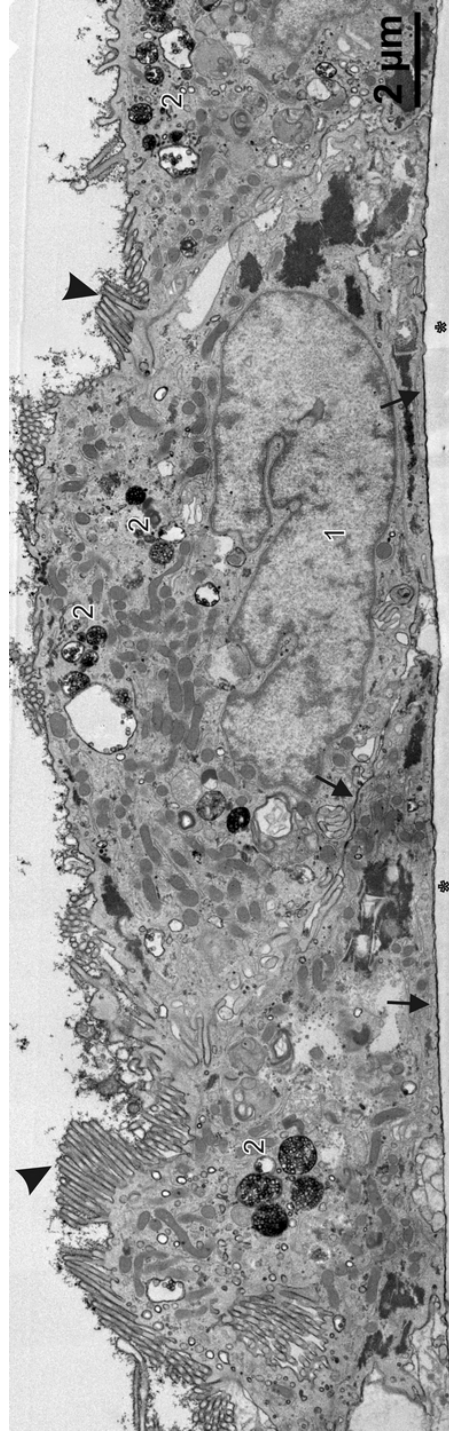


Figure 7: Caco-2 cell monolayer loaded with WGA-HRP at 4°C and post-incubated for 60 min at 37°C. Nucleus (1), early endosomes and multivesicular bodies (2), apical membrane with microvilli (arrowheads), and filter (*). Arrows indicate dense localization of WGA-HRP (blackening) at the lateral and basolateral membrane.

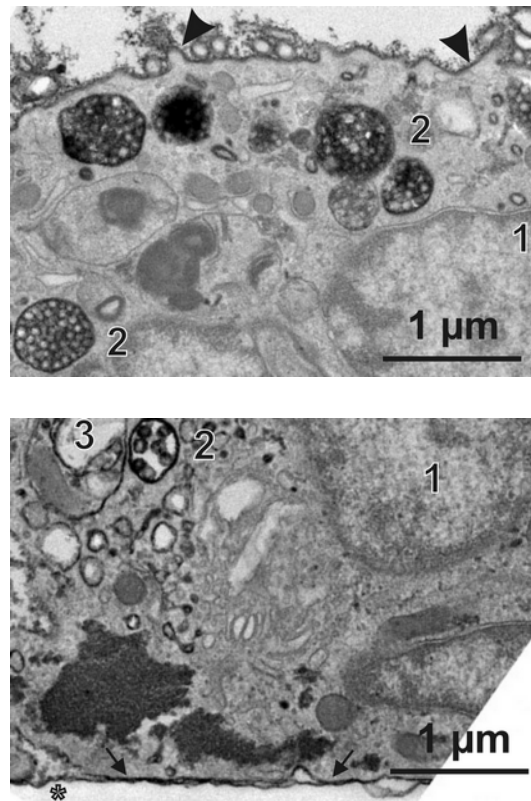


Figure 8: Close-up view of apical part (top image) and basolateral side (bottom image) of Caco-2 monolayer loaded with WGA-HRP at 4°C and post-incubated for 60 min at 37°C. Nucleus (1), multivesicular bodies (2), lysosome (3). Note the blackenings at the apical (arrowheads) and basolateral membrane (arrows).

fraction of WGA in lysosomes after 60 min amounts to about 50 % of the internalized lectin.[358]

It remains to be answered in future studies whether the basolaterally localized WGA-HRP remains membrane-bound or is released into the intercellular space. Regardless of the latter, it is illustrated by the present study that WGA can serve as a shuttle that mediates transcytosis of proteins across a model of human intestinal epithelium. The HRP type VI conjugated to WGA has a MW of ~44 kDa and thus well in the size range of therapeutically relevant proteins like insulin (MW ~5.8 kDa), granulocyte colony-stimulating factor (G-CSF, MW ~19.6 kDa) or erythropoietin (MW ~34 kDa). However, it remains to be resolved if these proteins can similarly endure the intracellular transport pathway as HRP.

1.1.3.4 Conclusions

As illustrated by the presented results, WGA extensively binds to Caco-2 monolayers which are an accepted in vitro model for human intestinal epithelium. This underlines that conjugation with WGA could be used to improve the cell-binding properties of particles and macromolecules which *per se* are not bioadhesive. Moreover, as indicated by the rapid internalization of membrane-bound WGA within ~15 - 30 min, increased uptake of drug conjugates into enterocytes could be achieved. These results corroborate the fluorescence-based studies by Wirth et al. who

observed similar time scales and pathways for the uptake of WGA by Caco-2 cells.[358] Finally, the use of WGA as a mediator of transcytosis bears promising potential for increasing the absorption of poorly bioavailable drugs. While HRP conjugated to WGA retained its activity during passage through the Caco-2 cell in the present study, it remains to be shown if more sensitive biomacromolecules bound to WGA can pass the cytoplasm similarly unaffected.

1.2 SPECIFIC TOPICS

1.2.1 Bionanoprobes to study particle-cell interactions



Copyright © 2009 American Scientific Publishers
All rights reserved
Printed in the United States of America

Journal of
Nanoscience and Nanotechnology
Vol. 9, 3239–3245, 2009

Bionanoprobes to Study Particle-Cell Interactions

Christian Fillafer, Daniela S. Friedl, Adina K. Ilyes,
Michael Wirth, and Franz Gabor*

Department of Pharmaceutical Technology and Biopharmaceutics, Faculty of Life Sciences,
University of Vienna, Althanstraße 14, A-1090 Vienna, Austria

A variety of research reports have provided evidence that the interplay between nanoparticles and biological systems is strongly dependent on the composition as well as on the size of the particles. However, irrespective of that a fine tuning of the interaction characteristics can be attained by functionalisation of the particle surface. In order to be able to monitor such interactions, an analytically accessible model system for potentially target-specific therapeutically relevant nanoparticles (NP) was generated by encapsulation of the highly hydrophobic fluorophore BODIPY® 493/503 into poly(D,L-lactide-co-glycolide) (PLGA) nanodroplets. Analyses of the mean particle size and zeta potential revealed that plain and human serum albumin (HSA) conjugated NP can be stored without agglomeration for at least 28 days at 4 °C as well as –80 °C. Although transfer of the particles into commonly used buffers and cell culture medium did not affect the system's stability, protein-containing dispersants should not be used for experiments demanding high sensitivity as distinct quenching effects were observed. Concerning liberation of the fluorescent marker, no release occurred when incubating the suspension for 7 days at 4 °C, while an onset of release was expectedly detected after 3 h at 37 °C. These experimental limitations were taken into account for the particle-cell interaction studies which, as a consequence of the more hydrophilic particle surface, showed an enhanced adhesion of HSA-conjugated colloids to Caco-2 cells by means of flow cytometry and fluorescence microscopy.

Keywords: Nanoparticle, BODIPY, Albumin, Stability, Fluorescence.

1. INTRODUCTION

The interaction characteristics between particles in the nanometer range and biological systems have been increasingly investigated issues of interest.^{1,2} Intensive research in this field partly results from the possible toxicological consequences inflicted with nanoscaled materials,³ but mainly has been driven forward in order to exploit the promising features of submicron particles for diagnostic and drug delivery purposes.⁴ At this, the suitability of a specific nanoparticulate system for therapeutic applications of the colloids, most important the actual size, core and surface composition. While the core material is rather limited to a range of biocompatible and biodegradable substances, a high number of potential bioactive targeting moieties can be introduced to the particle surface in order to alter the biodistribution profile of the nanomedicine.⁵ Consequently, analytical platforms for the study of targeted nanoparticle interactions with biological systems

need to be highly sensitive probes and have to consist of pharmaceutically approved materials which offer the possibility of surface functionalisation. In the process of tracking the association and distribution of colloids at the cellular and tissue level, efficient analytical access poses another crucial parameter. At this, fluorescent marking has been widely preferred due to the comparably simple handling of the substances and the qualitative as well as quantitative information obtained from these experiments.⁶ Generally, the marker substance is either covalently conjugated with the polymer forming the particle matrix or physicochemically encapsulated into the colloids by appropriate preparation techniques. Ongoing from the latter approach and considering the previously discussed prerequisites, the aim of this study was to design a highly sensitive analytical bionanoprobe. This was practically attained by incorporation of a 4,4-difluoro-1,3,5,7,8-pentamethyl-4-bora-3a,4a-diaza-s-indacene (BOD; BODIPY® 493/503) in biocompatible as well as biodegradable poly(D,L-lactide-co-glycolide) (PLGA) nanoparticles via an oil-in-water (o/w) solvent evaporation procedure.

*Author to whom correspondence should be addressed.

Christian Fillafer, Daniela S. Friedl, Adina K. Ilyes, Michael Wirth, Franz Gabor. Bionanoprobes to study particle-cell interactions. *Journal of Nanoscience and Nanotechnology*, 9:3239-3245, 2009.

1.2.1.1 *Abstract*

A variety of research reports have provided evidence that the interplay between nanoparticles and biological systems is strongly dependent on the composition as well as on the size of the particles. However, irrespective of that a fine tuning of the interaction characteristics can be attained by functionalisation of the particle surface. In order to be able to monitor such interactions, an analytically accessible model system for potentially target-specific therapeutically relevant nanoparticles (NP) was generated by encapsulation of the highly hydrophobic fluorophore BODIPY® 493/503 (BOD) into PLGA nanodroplets. Analyses of the mean particle size and zeta potential revealed that plain and HSA conjugated NP can be stored without agglomeration for at least 28 days at 4°C as well as -80°C. Although transfer of the particles into commonly used buffers and cell culture medium did not affect the system's stability, protein-containing dispersants should not be used for experiments demanding high sensitivity as distinct quenching effects were observed. Concerning liberation of the fluorescent marker, no release occurred when incubating the suspension for 7 days at 4°C, while an onset of release was expectedly detected after 3 h at 37°C. These experimental limitations were taken into account for the particle-cell interaction studies which, as a consequence of the more hydrophilic particle surface, showed an enhanced adhesion of HSA-conjugated colloids to Caco-2 cells by means of flow cytometry and fluorescence microscopy.

1.2.1.2 *Introduction*

The interaction characteristics between particles in the nanometer range and biological systems have been increasingly investigated issues of interest.[359, 19] Intensive research in this field partly results from the possible toxicological consequences inflicted with nanoscaled materials,[13] but mainly has been driven forward in order to exploit the promising features of submicron particles for diagnostic and drug delivery purposes.[360] At this, the suitability of a specific nanoparticulate system for therapeutic applications is highly influenced by several key characteristics of the colloids, most important the actual size, core and surface composition. While the core material is rather limited to a range of biocompatible and biodegradable substances, a high number of potential bioactive targeting moieties can be introduced to the particle surface in order to alter the biodistribution profile of the nanomedicine.[361] Consequently, analytical platforms for the study of targeted nanoparticle interactions with biological systems need to be highly sensitive probes and have to consist of pharmaceutically approved materials which offer the possibility of surface functionalisation. In the process of tracking the association and distribution of colloids at the cellular and tissue level, efficient analytical access poses another crucial parameter. At this, fluorescent marking has been widely preferred due to the comparably simple handling of the substances and the qualitative as well as quantitative information obtained from these experiments.[362] Generally, the marker substance is either covalently conjugated with the polymer forming the particle matrix or physico-chemically encapsulated into the colloids by appropriate preparation techniques. Ongoing from the latter approach and considering the previously discussed prerequisites, the aim of this study was to design a

highly sensitive analytical bionanoprobe. This was practically attained by incorporation of a 4,4-difluoro-1,3,5,7,8-pentamethyl-4-bora-3a,4a-diaza-s-indacene (BOD; BODIPY® 493/503) in biocompatible as well as biodegradable PLGA nanoparticles via an oil-in-water (o/w) solvent evaporation procedure. The main objectives for the experimental part of the present study encompassed a detailed characterisation of the colloids' stability in various media under commonly used storage conditions as well as leakage of fluorescent marker from the nanoparticles in order to evaluate the suitability of the system for routine analytical purposes. To exemplarily investigate the potential of BOD-nanoparticles (BOD-NP) as a tool to study the nanoparticle-cell interaction, HSA-conjugated colloids were prepared and compared to plain BOD-NP regarding cytoadhesivity to Caco-2 cells. This epithelial cell line is highly relevant as a point of application for targeted nanomedicines, since it represents an accepted model which can be used to investigate drug delivery via the human intestinal barrier.[356]

1.2.1.3 *Materials and Methods*

MATERIALS 4,4-difluoro-1,3,5,7,8-pentamethyl-4-bora-3a,4a-diaza-s-indacene was obtained from Molecular Probes (Invitrogen Corp., Carlsbad, California, USA). Resomer® RG503H (PLGA; lactide/glycolide ratio 50:50, inherent viscosity 0.32-0.44 dL g⁻¹, acid number >3 mg KOH g⁻¹) was bought from Boehringer Ingelheim (Ingelheim, Germany). HSA, EDAC, NHS and Pluronic® F-68 were purchased from Sigma Aldrich (Vienna, Austria). All other chemicals used were of analytical purity.

PREPARATION OF BOD-LOADED PLGA-NANOPARTICLES (BOD-NP) The fluorescence-labelled PLGA-nanoparticles were produced by an o/w solvent evaporation procedure. Briefly, 1 mg BOD and 400 mg PLGA were dissolved in 2 g ethyl acetate. This solution was emulsified with a 10% aqueous solution of Pluronic by sonication for 50 s yielding the o/w emulsion (sonifier: Bandelin electronic UW 70/HD 70, tip: MS 72/D, Berlin, Germany), which was poured into a 1% aqueous solution of Pluronic. After mechanical stirring (600 rpm) for 1 h at room temperature, the residual ethyl acetate was removed under reduced pressure resulting in the hardening of nanodroplets. The final particle suspension was filtered (1 µm pore size) in order to eliminate aggregates.

PARTICLE SIZE AND ZETA POTENTIAL ANALYSIS Prior to all measurements the nanoparticle suspensions were diluted 1:20 with double distilled water. The mean particle size and size distribution were determined by DLS on a Zetasizer Nano ZS (Malvern Instruments Ltd., United Kingdom). Zeta potential analyses were carried out at 25°C in disposable folded capillary cells and were performed in triplicate.

MODIFICATION OF THE PARTICLE SURFACE The model protein HSA was conjugated to the nanoparticle surface by a commonly used carbodiimide-mediated coupling procedure.[363] 20 mL of the nanoparticle sus-

pension were purified with 40 mL of 20 mM HEPES/NaOH buffer pH 7.4 (HEPES) on a tangential flow filtration system (Vivaflow 50; 100,000 MWCO PES, Sartorius Vivascience GmbH, Goettingen, Germany) to adjust the pH and to eliminate PLGA monomers as well as non-encapsulated BOD. Subsequently, 240 mg EDAC and 10 mg NHS, each dissolved in 1 mL of the same buffer, were added to the suspension and incubated end-over-end for 2 h at room temperature. To remove excess cross-linking agent, the suspension was washed twice with 40 mL HEPES followed by addition of 1.22 mg HSA in 1 mL HEPES. After end-over-end incubation at room temperature overnight, unreacted coupling sites were saturated by addition of 300 mg glycine in 1 mL HEPES and further incubation at room temperature for 1 h. Finally, the surface modified nanoparticles were washed five times with 20 mL HEPES to remove excess coupling agents and the suspension was concentrated to 15 mL during the last purification step.

STORAGE STABILITY OF NANOPARTICLES In order to assess the storage stability, plain BOD-NP and HSA-BOD-NP suspended in HEPES were incubated for up to 28 days at 4°C and -80°C. After one, seven, fourteen, twenty one and twenty eight days aliquots were drawn from the suspensions stored at 4°C and subjected to mean particle size-, polydispersity index- and zeta potential analysis. The suspensions stored frozen at -80°C were thawed after twenty eight days, sonified for 30 s and analysed accordingly.

STABILITY OF NANOPARTICLES IN WATER, BUFFERS, AND CELL CULTURE MEDIUM In order to identify suitable dispersants for the particle-cell interaction studies, BOD-NP were transferred to commonly used buffers and cell culture medium. After diluting the BOD-NP suspension 1:20 with isoHEPES, aliquots were taken and mixed 1:1 with double distilled water, isoHEPES, PBS, RPMI 1640 cell culture medium (+10% fetal bovine serum) (RPMI+FBS) and a 0.1% as well as 1% solution of HSA in HEPES. The mean particle size and fluorescence intensity of the suspension were determined immediately and after incubation for 90 min at 37°C.

RELEASE OF FLUOROPHORE The BOD-NP suspension was diluted 1:20 with PBS and divided into 1 mL aliquots, which were incubated end-over-end at 4°C and 37°C respectively. After 1, 3, 5, 24, 48, 72 and 168 h, 900 µL were transferred into centrifuge tubes and spun down on an ultracentrifuge (100,000 rpm/30 min/9°C; Optima™ MAX Ultracentrifuge, Beckmann Coulter Inc., Fullerton, USA). To quantify the amount of label which leaked from the particles the fluorescence intensity of the supernatant after centrifugation was determined on a microplate reader (ex/em: 480/525 nm; Infinite™ 200, Tecan Group Ltd., Grödig, Austria). Each sample was analysed in triplicate.

CELL CULTURE The Caco-2 cell line was purchased from the American Type Culture Collection (Rockville, MD, USA) and used between passage 28 and 39. Tissue culture reagents were obtained from Sigma (St.

Louis, USA) and Gibco Life Technologies Ltd. (Invitrogen Corp., Carlsbad, California, USA). Cells were cultivated in RPMI 1640 cell culture medium containing 10% fetal bovine serum, 4 mM L-glutamine and 150 g mL⁻¹ gentamycine in a humidified 5% CO₂/95% air atmosphere at 37°C and subcultured by trypsination.

FLOW CYTOMETRY The association of plain and HSA-BOD-NP with Caco-2 single cells was investigated using flow cytometry. To grant comparability between the nanoparticle suspensions, dilutions exhibiting the same relative fluorescence intensity were used. These were prepared with isoHEPES prior to all experiments and controlled on a microplate reader. For the binding studies 50 µL trypsinated cell-suspension (5×10⁶ cells mL⁻¹) were mixed with 50 µL of the respective nanoparticle suspension and incubated for 30, 60 and 120 min at 4°C. Following incubation, unbound and loosely associated particles were removed by centrifugation and washing with 500 µL HEPES (Centrifuge 5804R, Eppendorf; 1000rpm/5 min /4°C). The cell pellet was resuspended in 1000 µL PBS-buffer and analysed on an EPICS XL-MCL analytical flow cytometer (Coulter, Miami, USA) using a forward versus side scatter gate for inclusion of the single cell population and exclusion of debris and cell aggregates. Fluorescence was detected at 525 nm (10 nm bandwidth) and the mean channel number of the logarithmic intensities of individual peaks was used for further calculations. Amplification of the fluorescence signals was adjusted to put the autofluorescence signal of unlabelled cells in the first decade of the 4-decade log range. Data of 3000 cells were collected for each measurement.

FLUORESCENCE MICROSCOPY In order to visually identify the binding characteristics of plain and surface modified BOD-NP to Caco-2 cells, fluorescence microscopy was performed. Following incubation of 50 µL trypsinated cell suspension (5×10⁶ cells mL⁻¹) with 50 µL of plain or HSA-BOD-NP for 60 min at 4°C and washing with HEPES, the Caco-2 single cells were analysed on a Nikon Eclipse 50i microscope (Nikon Corp., Japan) equipped with an EXFO X-Cite 120 fluorescence illumination system. The focus was set to the middle of the cell and the pictures taken were subjected to deconvolution processing by the Image Analyser software.

1.2.1.4 Results and Discussion

CHARACTERISATION OF PLAIN BOD-NP AND HSA-BOD-NP The labelling of polymeric nanoparticles with fluorescent marker molecules has frequently been employed as a strategy to render colloids trackable and to consecutively enable an investigation of their fate in biological systems.[364] Hereby, mainly two approaches are being pursued. Firstly, a labelled conjugate, which is subsequently used for the production of nanoparticles, can be synthesised by introduction of a fluorescent head group to a polymer backbone.[363, 364, 292, 227] This technique offers the advantage of covalent linkage of the dye molecule, which ensures enhanced attachment of the label, but often involves elaborate synthesis, laborious purification and analytically challenging charac-

terisation of the conjugate. Secondly, the fluorophore can be physico-chemically entrapped in the polymeric matrix via suitable preparation techniques.[227] At this, the hydrophobicity of the marker molecule has to be selected according to that of the polymer core, since the resulting interactive forces determine stability of the labelling. Exploiting the latter principle, a simple and effective approach for the preparation of fluorescence-marked biodegradable and biocompatible nanoparticles has been developed. The highly hydrophobic compound BOD, which exhibits fluorescein-like spectral properties as well as high photostability and quantum efficiency, was embedded into PLGA cores by a o/w solvent evaporation procedure. This method yielded colloids with a mean particle size of 120 ± 1 nm and a narrow size distribution represented by a PDI of 0.087 (Table 1). As illustrated by zeta potential measurements, plain BOD-NP exhibited a negative surface charge of -39.2 ± 0.2 mV due to free carboxyl groups of the H-type PLGA present at the particle-dispersant interface. These carboxylate moieties provide potential grafting points for covalent ligand-attachment on the particle surface, which was exemplified by immobilization of the model protein HSA via a carbodiimide-mediated active ester method. As a consequence of the successful conjugation with proteinaceous ligand, an increase in mean particle size by about 4 nm was observed concurrent with a decrease of the zeta potential to -30.7 ± 0.8 mV. This reduction of surface potential can be attributed to direct amidation of carboxyl groups as well as shielding of remaining charges by the protein layer. Importantly, despite the surface modification and the slightly lowered zeta potential, the size distribution of HSA-BOD-NP remained narrow throughout the coupling process as indicated by a PDI of 0.092.

STORAGE STABILITY OF BOD-NP In order to grant that a series of particle-cell interaction studies can be performed with the same batch of nanoparticle suspension, sufficient short-term storage has to be granted. Consequently, plain and HSA-BOD-NP were continually analysed regarding their mean particle size, PDI and zeta potential as stability parameters, in course of storage over a period of 28 days at 4°C and -80°C . As illustrated in Table 5, these parameters remained constant for plain and modified nanoparticles incubated at 4°C . Obviously, despite bearing a layer of immobilised protein molecules and thus slightly lower zeta potential of about -30 mV, the HSA-BOD-NP had not agglomerated after 28 days which is underlined by the low PDI of 0.087. This might be due to a combination of the possibly sufficient electrostatic repulsive forces with steric stabilisation by residual Pluronic from the preparation process.[24] Although storage for four weeks at -80°C involved freezing and thawing of the colloids, the suspensions exhibited similar stability as compared to incubation at 4°C . This is illustrated by consistently constant mean particle sizes of 123 ± 1 nm and 126 ± 1 nm for plain- and HSA-BOD-NP respectively, which underline that plain and surface modified suspensions stored at 4°C or -80°C can serve as stable reservoirs for comparable long-term studies.

STABILITY OF BOD-NP IN WATER, BUFFERS, AND CELL CULTURE MEDIUM Generally, the dispersant's properties like ionic strength, pH-value, and presence of charged macromolecules have to be optimized for the

Table 5: Stability parameters of plain and modified BOD-NP stored in HEPES at 4°C or -80°C.

Storage conditions					
Temperature [°C]	Time	Mean particle size [nm]	Polydispersity index	Zeta potential [mV]	
4	After preparation	120.0±1.0	0.087	-39.2±0.2	PLAIN BOD-NP
	7 days	121.3±0.6	0.091	-37.2±0.2	
	14 days	120.7±0.6	0.081	-37.3±0.8	
	21 days	122.0±1.0	0.096	-36.6±0.9	
	28 days	122.0±1.0	0.079	-36.5±0.3	
	28 days	123.0±0.0	0.104	-37.4±0.4	
-80	After preparation	124.0±1.2	0.092	-30.7±0.8	HSA-BOD-NP
	7 days	125.7±1.2	0.099	-31.4±0.5	
	14 days	124.7±1.2	0.106	-30.7±0.8	
	21 days	125.5±0.8	0.095	-29.9±0.5	
	28 days	126.0±1.0	0.087	-30.5±0.8	
	28 days	126.0±1.0	0.118	-31.5±0.3	

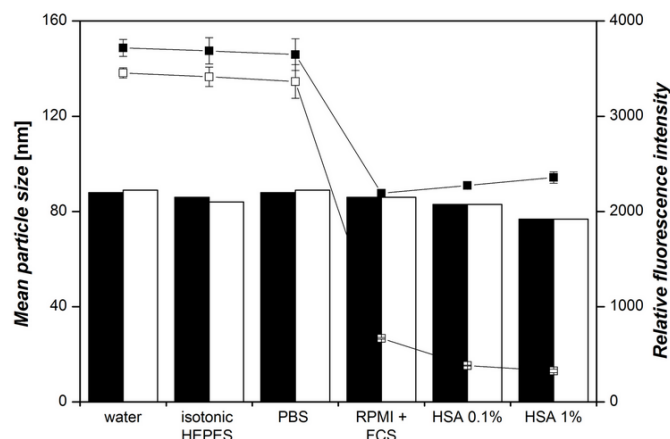


Figure 9: Mean particle size (bar) and fluorescence intensity (line) of plain BOD-NP in selected dispersants at room temperature (closed) and after 90 min at 37°C (open).

preparation procedure and further storage in order to efficiently prevent the formation of aggregates.[365] However, these suspension media in most cases lack physiological pH conditions as well as isotonicity and therefore do not comply with cells or tissues. Thus, transfer into a cell-friendly dispersant for the studied system is often deemed to be necessary. To meet this issue, destabilising tendencies and possible effects on the fluorescence intensity of BOD-NP were assessed after dilution of a stock suspension in selected, commonly used media for cell and tissue culture studies.

As illustrated in Figure 9, the mean particle size of BOD-NP remained rather constant, immediately upon mixing and after further incubation for 90 min at 37°C, with all buffers and media used. Interestingly, the higher concentration of HSA in the dispersant medium led to a slight reduction of the mean particle size as determined by DLS. This effect is very likely due to the presence of large amounts of protein in the medium bearing relatively high diffusion coefficients. Since the DLS-system calculates the mean particle size via the average diffusion coefficient determined in course of the measurement, the size of the BOD-NP is only apparently reduced by the presence of rapidly diffusing proteins, but actually expected to be the same as in water. Regarding the fluorescence intensity of the nanoparticle suspension, rather drastic effects were observed in dispersants containing proteins. While diluting the particles with isotonic HEPES and PBS did not lead to an alteration of the suspension's mean fluorescence intensity as compared to water, the presence of proteins obviously resulted in highly reduced quantum yields. This is explicated by an average reduction of the mean fluorescence intensity by 36% immediately after mixing, which is even increased to 81% after incubation for 90 min at 37°C. Since similar quenching effects have been reported for BOD dyes covalently conjugated to proteins,[366] the clear drop in fluorescence intensity is expected to be due to physical contact between fluorophore and protein. From this it is inferred, that immediate adsorption of HSA molecules or serum proteins to the nanoparticle surface results in a

rapid drop of the suspension's mean fluorescence intensity, which is further enhanced by additional adsorption in course of incubation at 37°C. While posing a distinct disadvantage for studies to be performed in cell culture medium supplemented with serum, this effect has in contrast been shown to be beneficial for the interpretation of cellular uptake studies.[285] Since cytoinvasion via vesicular internalisation is associated with membrane proteins densely enwrapping the colloid, a reduction of the mean cell associated fluorescence can serve as an indicator to discriminate between sole membrane binding and intracellular uptake.

RELEASE OF FLUORESCENT MARKER FROM BOD-NP Undesired release of the fluorescent marker from particles due to insufficient attachment and due to the high surface area available for dissolution has posed a main challenge for the characterisation of a colloid's interaction with biological systems.[307] Especially in the case of particle-cell interaction studies the interpretation of the results is hampered by the presence of freely diffusing marker and possibly generated artefacts thereof. Thus, as a highly important preliminary step, the liberation of fluorescent marker has to be determined under experimental conditions and accordingly, limits for further studies have to be set in order to minimise misinterpretations.

The release of BOD from unmodified BOD-NP was determined in course of incubation for seven days at 4°C and 37°C. In order to solely detect released fluorophore and to exclude particle-associated fluorescence, aliquots of the suspension were subjected to ultracentrifugation at each time point of the analysis. According to fluorescence measurements of the supernatant after centrifugation, 4.1 ng mL⁻¹ of free BOD were detectable at the start point of the incubation, which represents the quantity of fluorophore not encapsulated in course of the solvent evaporation procedure. When stored at 4°C, this amount remained constant over the whole incubation period pointing at no release of BOD from the PLGA-nanospheres (Figure 10). Upon incubation at 37°C, similarly low quantities of free marker were detected during the first three hours. Following this time lag, a steady increase of non-encapsulated fluorescence was determined which seemed to reach a plateau after 72 h. This markedly higher liberation of fluorophore from the nanoparticles at 37°C is supposed to be due to increased swelling of the polymer matrix and thus increased solubility and diffusion of BOD to the dispersant phase. Consequently, these results imply that quantitative as well as qualitative measurements using BOD-NP can be performed for at least seven days at 4°C and about three hours at 37°C without major artefacts due to released fluorescent label.

INTERACTION OF PLAIN- AND HSA-BOD-NP WITH CACO-2 CELLS In order to investigate the applicability of plain and surface-conjugated BOD-NP as a model system for a detailed analysis of the nanoparticle-cell interaction, binding studies for 30 to 120 min at 4°C were performed with Caco-2 single cells using plain and HSA-modified colloids. As the cellular metabolism and fluidity of the membrane is reduced to a minimum at 4°C, nanoparticles can only associate with the cell surface, but are not actively taken up into the cytosol.⁸ Following the incubation

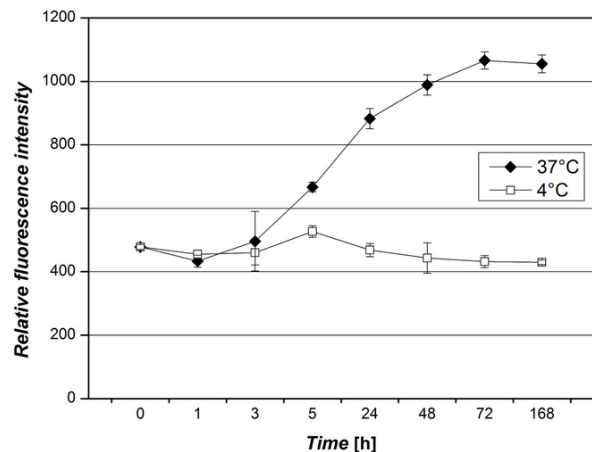


Figure 10: Release of BOD from nanoparticles in course of incubation at 4°C and 37°C.

and washing of the cells, flow cytometry was used to determine the mean cell associated fluorescence intensity. As illustrated in Figure 11, the binding of plain nanoparticles remained constantly low over the

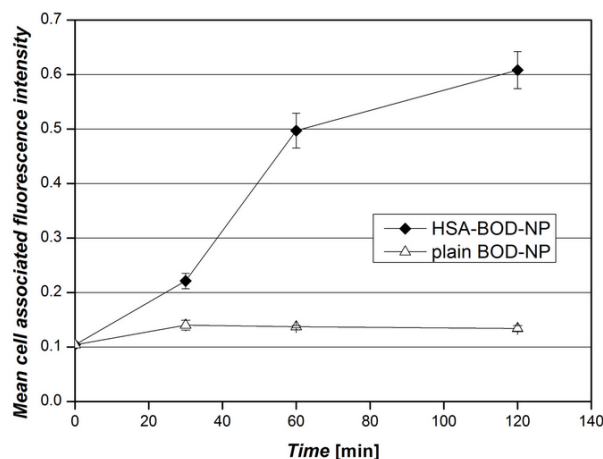


Figure 11: Mean cell associated fluorescence intensity of Caco-2 cells incubated with plain (Δ -) and HSA-BOD-NP (\blacklozenge -) at 4°C.

whole incubation period and ranged just slightly above the cellular autofluorescence. In contrast, when incubated with HSA-BOD-NP, a distinctly increasing amount of mean cell associated fluorescence intensity was monitored over time. As compared to plain BOD-NP, this difference was reflected by a 58% higher association rate after 30 min. Upon incubation for 120 min, binding of HSA-BOD-NP to Caco-2 cells is even 3.5 times higher, which might be explained by non-specific protein-protein interactions between the HSA-conjugated colloids and the cell membrane, while the low binding in the case of plain BOD-NP is supposed to be a consequence of the poorly cytoadhesive characteristics of the

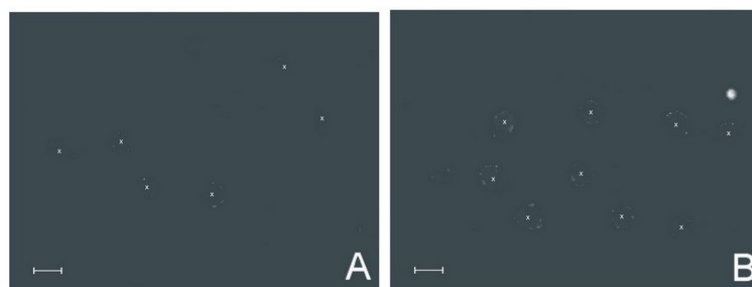


Figure 12: Caco-2 cells incubated with plain (A) and HSA-BOD-NP (B) for 60 min at 4°C. The centre of the cell is marked with an “x” for orientation. Scale bar represents 20 μm .

PLGA-polymer. The amount of cell associated plain- and HSA-BOD-NP after incubation for 60 min at 4°C was also investigated by fluorescence microscopy. As is clearly illustrated by the green fluorescent dot-like structures in Figure 12 A, only few unmodified nanoparticles had associated with the cell membrane. In contrast, a denser corona was visualised for HSA-BOD-NP under the same experimental conditions (Figure 12 B) which confirmed the higher cell-binding potential of albumin modified particles as detected in the flow cytometric experiments. These results are especially interesting since HSA is generally known as a model protein mediating only low, non-specific interactions which thus further underlines the potential of BOD-NP as probes to detect slight alterations of the interactive forces between particle and target cell.

1.2.1.5 Conclusions

In this work, a novel method to label biodegradable and biocompatible nanoparticles via encapsulation of the compound 4,4-difluoro-1,3,5,7,8-pentamethyl-4-bora-3a,4a-diaza-s-indacene in PLGA-nanoparticles is presented. The colloids prepared by a o/w solvent evaporation procedure can readily be conjugated with proteins and were shown to be stable for at least 28 days upon storage at 4°C and -80°C. Interestingly, transfer of the BOD-NP into protein-containing media leads to drastic quenching of the suspensions' mean fluorescence intensity and thus should be avoided if high analytical sensitivity is desired. Regarding the release of fluorescent label over time it has to be highlighted, that BOD-NP are to be considered stably-labelled when used at 4°C and that liberation of the fluorophore is negligible for 3 hours at 37°C. Most importantly and as revealed by binding studies with Caco-2 cells, BOD-NP can serve as highly sensitive probes to analyse alterations in the cell-binding characteristics of nanoparticles as a result of surface conjugation with targeting molecules. At this, it was exemplarily shown that plain BOD-NP exhibit clearly lower membrane binding than colloids surface-modified with HSA.

In conclusion it can be denoted, that the stability of BOD-NP, combined with the ease of covalent surface immobilisation of bioactive molecules, suggests broad applicability of the system to investigate ligand-dominated nanoparticle-cell interactions. Accordingly, BOD-labelled colloids are expected to represent an effective and analytically

sensitive tool to study potential biotargeting moieties for site-specific diagnostics and nanoparticulate drug delivery.

Acknowledgements

Parts of this work were supported by the CellPROM project, funded by the European Community as contract No. NMP4-CT-2004-500039 under the 6th Framework Programme for Research and Technological Development in the thematic area of "Nanotechnologies and nanosciences, knowledge-based multifunctional materials and new production processes and devices". The contribution reflects the author's views and the community is not liable for any use that may be made of the information contained therein.

1.2.2 *Fluorescent bionanoprobes to characterize cytoadhesion and cytoinvasion*

small

Fluorescent bionanoprobes

DOI: 10.1002/smll.200701086

Fluorescent Bionanoprobes to Characterize Cytoadhesion and Cytoinvasion**

Christian Fillafer, Daniela S. Friedl, Michael Wirth, and Franz Gabor*

To overcome current limitations in diagnostic imaging and targeted drug delivery, a highly versatile tool is presented that can be used to representatively investigate the effects of submicroparticles intended for the use in biological systems. An effective approach to render colloids trackable is developed by stable attachment of the fluorescent probe BODIPY 493/503 (BOD: 4,4-difluoro-1,3,5,7,8-pentamethyl-4-bora-3a,4a-diaza-s-indacene) to a biodegradable and biocompatible particle core matrix. BOD submicroparticles are shown to be stable, can be surface modified, and exhibit high fluorescence emission. Upon conjugation with human serum albumin (nonspecific) and wheat germ agglutinin (biorecognitive) as model ligands explicit differences are found in the cytoadhesive and cytoinvasive characteristics of the submicroparticles using Caco-2 cells. These results demonstrate the potency of BOD-labeled colloids as a versatile analytical platform for a multifaceted investigation of cell-particle interactions in biological systems.

Keywords:

- cytoadhesion
- cytoinvasion
- labelling
- nanoparticles

1. Introduction

The intensive research in all fields of micro- and nanoscale science has generated a variety of approaches for the engineering of submicroparticles with tailored properties. These efforts are driven forward in order to elucidate and to

gain control over the interaction characteristics of such devices with biological systems. The immobilisation of appropriate bioactive ligands such as antibodies^[1], peptides^[2] or aptamers^[3] to the submicroparticles' surface is expected to overcome existing limitations in a number of fields such as cancer therapy, drug targeting, or diagnostic imaging. When bearing future medical applications in mind however, the matrix of the particles has to meet certain requirements in order to minimise side effects and to avoid possibly toxic accumulation in the body. Consequently, the use of several inorganic components or nondegradable polymers such as polystyrene is limited for these applications. Considering this it seems rather preferable to revert to materials that have been intended to be used in organisms due to their biodegradable and biocompatible nature.^[4] Poly(D,L-lactic-co-glycolic)acid (PLGA) is a representative of this class of polymers that has been shown to comply with the food and drug administration (FDA). FDA regulations and thus is permitted to be used for medical applications in humans.^[5] Nano- and microparticles can be produced from PLGA in various sizes by solvent-evaporation techniques and have mainly been investigated for drug-delivery purposes.^[6]

In order to address these requirements and to engineer an analytically versatile particulate system for biological

[*] C. Fillafer, D. S. Friedl, Prof. M. Wirth, Prof. F. Gabor
Department of Pharmaceutical Technology and Biopharmaceutics
Faculty of Life Sciences
University of Vienna
Althanstr. 14, A-1090 Vienna (Austria)
Fax: (+43) 142-779-554
E-mail: franz.gabor@univie.ac.at

[**] Parts of this work were supported by the CellPROM project, funded by the European Community as contract No. NMP4-CT-2004-500039 under the 6th Framework Programme for Research and Technological Development in the thematic area of "nanotechnologies and nanosciences, knowledge-based multifunctional materials, and new production processes and devices". The contribution reflects the authors' views and the community is not liable for any use that may be made of the information contained therein.

Supporting Information is available on the WWW under <http://www.small-journal.com> or from the author.

Christian Fillafer, Daniela S. Friedl, Michael Wirth, Franz Gabor. *Small*, 4(5):627-633, 2008.

1.2.2.1 *Abstract*

To overcome current limitations in diagnostic imaging and targeted drug delivery, a highly versatile tool is presented that can be used to representatively investigate the effects of submicroparticles intended for the use in biological systems. An effective approach to render colloids trackable is developed by stable attachment of the fluorescent probe BOD to a biodegradable and biocompatible particle core matrix. BOD submicroparticles are shown to be stable, can be surface modified, and exhibit high fluorescence emission. Upon conjugation with human serum albumin (nonspecific) and wheat germ agglutinin (biorecognitive) as model ligands explicit differences are found in the cytoadhesive and cytoinvasive characteristics of the submicroparticles using Caco-2 cells. These results demonstrate the potency of BOD-labeled colloids as a versatile analytical platform for a multifaceted investigation of cell-particle interactions in biological systems.

1.2.2.2 *Introduction*

The intensive research in all fields of micro- and nanoscale science has generated a variety of approaches for the engineering of submicroparticles with tailored properties. These efforts are driven forward in order to elucidate and to gain control over the interaction characteristics of such devices with biological systems. The immobilisation of appropriate bioactive ligands such as antibodies,[367] peptides,[368] or aptamers[369] to the submicroparticles' surface is expected to overcome existing limitations in a number of fields such as cancer therapy, drug targeting, or diagnostic imaging. When bearing future medical applications in mind however, the matrix of the particles has to meet certain requirements in order to minimise side effects and to avoid possibly toxic accumulation in the body. Consequently, the use of several inorganic components or nondegradable polymers such as polystyrene is limited for these applications. Considering this it seems rather preferable to revert to materials that have been intended to be used in organisms due to their biodegradable and biocompatible nature.[370] PLGA is a representative of this class of polymers that has been shown to comply with the food and drug administration (FDA) regulations and thus is permitted to be used for medical applications in humans.[371] Nano- and microparticles can be produced from PLGA in various sizes by solvent-evaporation techniques and have mainly been investigated for drug delivery purposes.[372]

In order to address these requirements and to engineer an analytically versatile particulate system for biological applications, a methodology has been elaborated to generate fluorescence-labelled and surface-modified colloids that can subsequently be used to investigate cell-submicroparticle interactions. While PLGA was used as a core material in order to ensure biocompatibility and biodegradability of the particles, a novel approach for detectability was developed via encapsulation of the hydrophobic fluorophore BOD. These stably labelled and therefore trackable colloids were investigated as a tool to monitor different stages of the cell-submicroparticle interaction. The particles were conjugated with HSA as a model protein for nonspecific protein-protein interactions and WGA as a model ligand for specific protein-carbohydrate interactions.[373, 208, 209] Following the characterization of the protein-immobilisation step, the analytical applicability of BOD-labeled sub-

Table 6: Mean particle size, PdI, and zeta potential of plain BOD-SMP, HSA-BOD-SMP, and WGA-BOD-SMP.

	Mean particle size [nm]	Polydispersity index	Zeta potential [mV]
plain BOD-SMP	120±1.0	0.087	-39.2±0.23
HSA-BOD-SMP	124±1.2	0.092	-30.7±0.75
WGA-BOD-SMP	159±1.2	0.153	-33.9±1.03

microparticles (BOD-SMP) for discrimination of the cytoadhesive and cytotoxic properties of plain and surface-modified colloids was investigated using a combination of flow cytometry and fluorescence microscopy.

1.2.2.3 Results

CHARACTERIZATION OF BOD-SMP The mean particle size, PdI, and zeta potential of the BOD-SMP were determined prior to and after the surface modification. As represented by a PdI of 0.087 the submicroparticles produced by the solvent-evaporation procedure were nearly monodisperse with a mean particle size of 120±1.0 nm (Table 6). The activation of the submicroparticles' surface carboxyl groups, conjugation with HSA or WGA, and saturation of unreacted NHS intermediates with glycine resulted in slightly increased mean particle sizes. A narrow size distribution was retained throughout the coupling as illustrated by PdIs of 0.092 for HSA-BOD-SMP and 0.153 for WGA-BOD-SMP. In order to confirm successful immobilisation of HSA and WGA, the zeta potential of the colloids was monitored. In the case of plain BOD-SMP the high density of surface carboxyl groups led to a strongly negative potential of -39.2±0.23 mV. As a consequence of the modification step the surface charge was lowered by derivatization as well as inherent shielding of the carboxyl groups of PLGA by covalently attached proteins. This is reflected by a decrease in zeta potential to -30.7±0.75 mV and -33.9±1.03 mV, respectively. Despite these lowered values due to the successful immobilisation of HSA and WGA to the submicroparticle surface, the still clearly negative zeta potentials are expected to enhance stability of the suspension by electrostatic repulsion between the colloids.[374]

INTERACTION OF PLAIN AND MODIFIED BOD-SMP WITH CACO-2 CELLS

Time dependency In order to assess time dependency of the binding of plain and surface-modified BOD-SMP to Caco-2 single cells, incubation with the particles was performed for up to 300 min at 4°C. As indicated by the mean cell-associated fluorescence intensities in Figure 13, the quantity of cell-bound plain BOD-SMP remained consistently low over the entire incubation period and ranged just slightly above the cellular autofluorescence. A similarly low binding was observed for HSA-BOD-SMP. As compared to the unmodified colloids only a

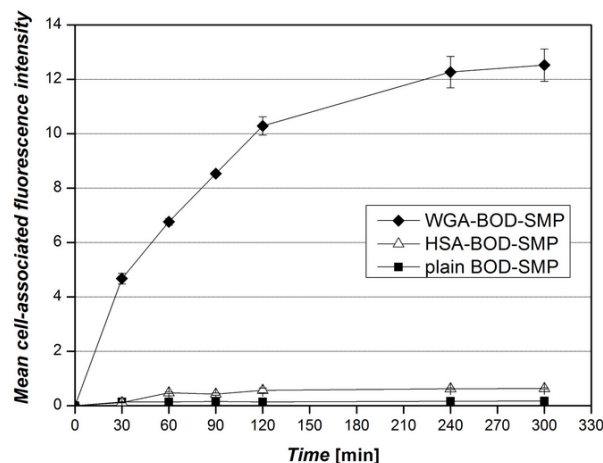


Figure 13: Mean cell-associated fluorescence intensity of Caco-2 cells in course of time incubated with WGA-BOD-SMP, HSA-BOD-SMP, and plain BOD-SMP (25 ng mL^{-1} corresponding concentration of BOD) at 4°C .

marginally increased mean cell-associated fluorescence intensity of 0.48 was detected after 60 min, which remained rather constant at this level over the course of further incubation for 240 min. In contrast, the quantity of WGA-BOD-SMP associated with Caco-2 cells strongly increased over time. As illustrated by the steep onset of the slope in Figure 13, rapid binding of the surface-modified submicroparticles had occurred within 30 min. After incubation for 60 min the mean cell-associated fluorescence intensity corresponded to about 54% of the total number of particles bound at the end of the assay. Over the course of prolonged incubation the binding seemed to reach a plateau, probably indicating saturation. As compared to HSA-BOD-SMP and plain BOD-SMP the cell-association of WGA-BOD-SMP with Caco-2 cells was determined to be 14.2 times (60 min) to 19.8 times (300 min) higher than HSA-BOD-SMP and 49.3 times (60 min) to 73.2 times (300 min) higher than plain BOD-SMP. These differences in the time-dependent association rates indicate that the cell binding of plain and HSA-BOD-SMP might mainly be based on nonspecific interactions, while a specific mechanism underlies the WGA-BOD-SMP binding to the Caco-2 cell surface.

Concentration dependency Dilution series of plain, HSA- and WGA-BOD-SMP were used to investigate concentration-dependent interaction profiles with Caco-2 single cells. As determined by flow cytometry, the mean cell-associated fluorescence intensity concurrently increased with higher concentrations of the submicroparticle suspensions (Figure 14). This effect was on a distinctly lower level for plain and HSA-BOD-SMP, starting at minimal mean cell-associated fluorescence intensities of 0.1 and 0.11, respectively, for the lowest concentration used. With eightfold higher quantity, a maximum of only 0.92 and 1.04, respectively, was reached. As opposed to this, the interaction of WGA-BOD-SMP with Caco-2 cells is characterized by high association rates already at the lowest concentration used. This is illustrated by a mean cell-associated

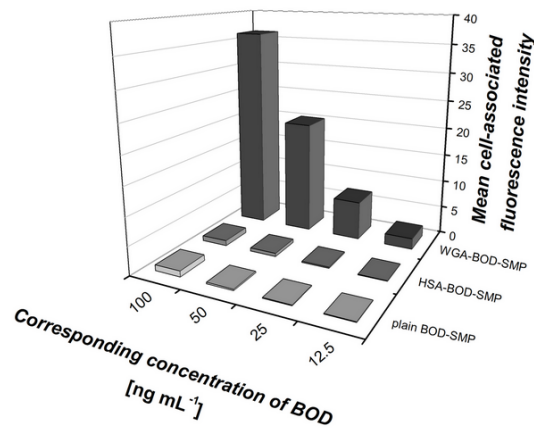


Figure 14: Mean cell-associated fluorescence intensity of Caco-2 cells incubated with a diluted series of WGA-BOD-SMP, HSA-BOD-SMP, and plain BOD-SMP for 60 min at 4°C.

fluorescence intensity of 1.9, which concurrently increased up to 20.2 and 36.3, respectively, for the two highest concentrations. As compared with plain BOD-SMP and HSA-BOD-SMP the interaction of WGA-BOD-SMP with Caco-2 cells was 18.6 times and 17.2 times higher, respectively, at the lowest concentration. This difference increased up to 35.1 and 39.5 times, respectively, at the highest quantities used. Interestingly, no signs of saturation of the cell binding were observed with increasing amounts of WGA-BOD-SMP, which points to the presence of a rather high number of accessible binding sites for lectin-carbohydrate interactions on the cell surface.

INTERNALIZATION OF WGA-BOD-SMP A pulse-chase incubation was performed in order to investigate whether bound WGA-BOD-SMP are internalised into Caco-2 cells. At 4°C the fluidity of the membrane and the cellular metabolism are reduced to a minimum. As a consequence, only binding takes place. Under these conditions single cells were loaded with submicroparticles at 4°C for 60 min resulting in a mean cell-associated fluorescence intensity of 8.1 (0 min, Figure 15). When further incubated at 4°C, the mean cell-associated fluorescence intensity did not noticeably vary over 240 min. This indicates that WGA-BOD-SMP initially associated with the cells did not detach upon successive incubation at 4°C. By raising the temperature to 37°C energy-consuming transport processes are enabled and thus uptake of membrane-bound materials can proceed. During this chase incubation for 240 min at 37°C, the mean cell-associated fluorescence intensity rapidly decreased by 36.8% within 10 min. However, possible release of WGA-BOD-SMP from their binding sites on the cell membrane was excluded as only minor amounts of fluorescence were detected in the supernatants of the cell suspension during washing. After incubation for 60 min the initially detected mean cell-associated fluorescence intensity had decreased by 60.5% to 3.08 and remained at this plateau for the last 180 min of the experiment. These results indicate that WGA-BOD-SMP

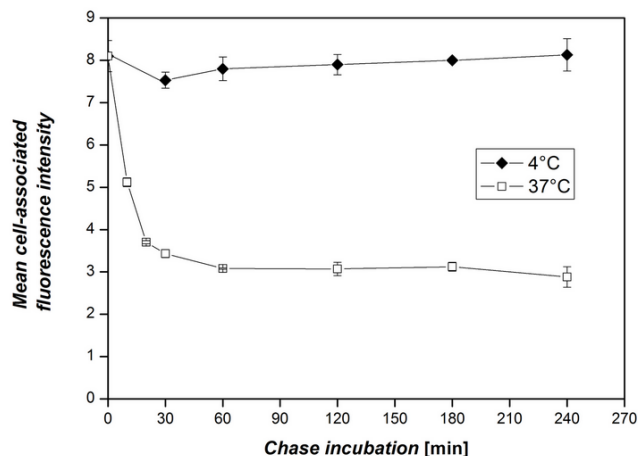


Figure 15: Mean cell-associated fluorescence intensity of Caco-2 cells loaded with WGA-BOD-SMP for 60 min at 4°C in course of further incubation at 4°C and 37°C.

were internalized by Caco-2 single cells by energy-consuming transport processes at 37°C while no internalization took place at 4°C due to the minimized cellular metabolism.

BINDING SPECIFICITY OF WGA-BOD-SMP In order to estimate the extent to which the binding of WGA-BOD-SMP to Caco-2 cells is mediated by the specific interaction of the immobilized lectin with carbohydrate moieties of the cells' glycocalyx, an inhibition assay was performed. Since WGA specifically binds to N-acetyl-neuraminic acid and N-acetyl-D-glucosamine, N,N',N''-triacylchitotriose was used as a complementary carbohydrate.[375] As illustrated in Figure 16, addition of increasing amounts of the inhibitor led to a corresponding decrease of the mean cell-associated fluorescence intensity. In the presence of high amounts of complementary carbohydrate, the binding of WGA-BOD-SMP to Caco-2 cells was inhibited by $89.48 \pm 0.58\%$, suggesting that at the most 10.5% of the submicroparticles were bound via nonspecific interactions. Consequently, the bulk of WGA-BOD-SMP attached via specific lectin-carbohydrate binding mediated by the WGA immobilized on the particle surface.

FLUORESCENCE MICROSCOPY OF CACO-2 CELLS INCUBATED WITH PLAIN AND MODIFIED BOD-SMP Complementary information on the association and uptake characteristics of plain and modified BOD-SMP by Caco-2 cells was collected via fluorescence microscopy. Single cells were incubated with plain, HSA-, and WGA-BOD-SMP for 60 min at 4°C. As illustrated in Figure 17, only low amounts of plain (Figure 17 A) and HSA-BOD-SMP (Figure 17 B) were associated with the cell membrane after incubation at 4°C, while a high density of bound WGA-BOD-SMP was detected as dotlike structures (Figure 17 C-F). By raising the incubation temperature to 37°C, however, active transport processes were

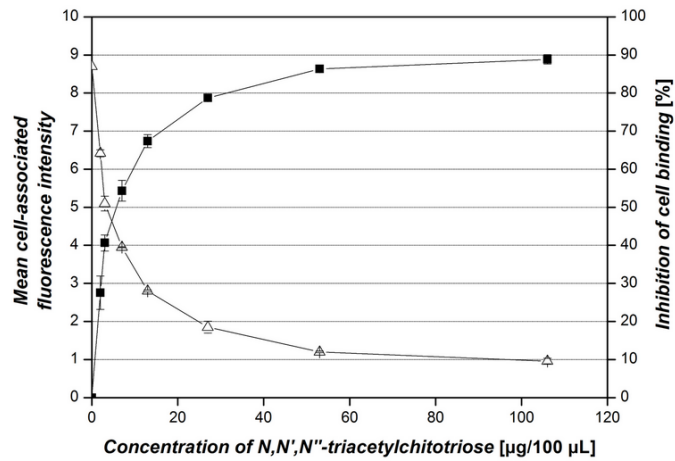


Figure 16: Mean cell-associated fluorescence intensity (- Δ -) and percentage of inhibition (- \blacksquare -) in course of competitive inhibition of WGA-BOD-SMP binding to Caco-2 cells by addition of increasing amounts of the complementary carbohydrate N,N',N'' -triacetylchitotriose at 4°C.

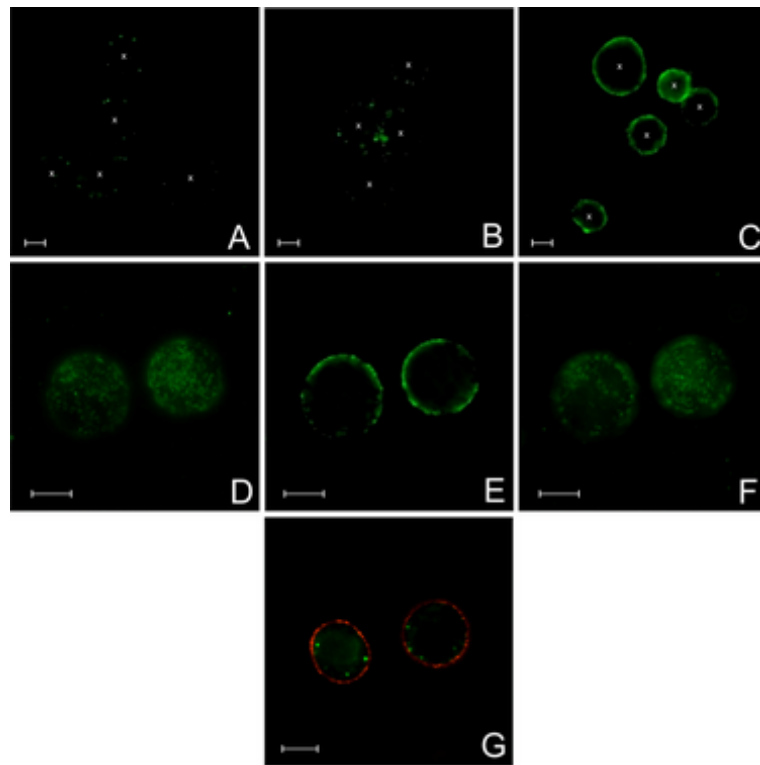


Figure 17: Fluorescence microscopy images of Caco-2 cells incubated with plain BOD-SMP (A), HSA-BOD-SMP (B), and WGA-BOD-SMP (C) for 60 min at 4°C. The center of the cell is marked with an "x" for orientation. Optical cross sections of Caco-2 cells incubated with WGA-BOD-SMP at 4°C taken at the top (D), center (E), and bottom (F) of the cell. Incubation for a further 30 min at 37°C and staining of the cell membrane with FM 4-64 (G). Scale bar represents 10 μm .

enabled, resulting in the uptake of WGA-BOD-SMP into intracellular compartments, which appear as vesicles in the cytosol (Figure 17 G).

1.2.2.4 Discussion

For a comprehensive investigation of the cytoadhesive and cytoinvasive characteristics of plain and ligand-conjugated submicroparticles, a stable and versatile fluorescence-labelled colloid is required. In this regard, as most analytical methods in cell and tissue research are based on fluorescence detection, labeling of the submicroparticle with a fluorophore is preferable.[362] In the present approach the hydrophobic photochemical probe BODIPY 493/503 was encapsulated in a hydrophobic PLGA matrix in order to produce colloids labeled by strong hydrophobic interactions between dye and polymer. The utilized member of the BODIPY series was chosen due to its highly nonpolar structure and is characterized by a fluorescein-like emission spectrum and exceptional photostability. As illustrated by the polydispersity index in Table 6, the solvent-evaporation procedure yielded stable submicroparticles with a mean diameter of 120 nm and high fluorescence emission with no leakage of the dye during the course of the experiments. Particularly for drug delivery purposes it has to be considered that particle sizes around 100 nm are required to achieve sufficient load of active agent for a therapeutic response. Although particles with similar size are commercially available, the constituents of these, such as polystyrene or inorganic materials, are of limited usability for the screening of effects in biological systems. For such purposes, consequences owing to the submicroparticle itself or possibly toxic accumulations have to be excluded, which suggested the use of the biodegradable and biocompatible polyester polymer PLGA.[371] This generated a highly useful model for studying the cell-particle interaction of colloids intended for medical and pharmaceutical applications. Furthermore, the consequences owing to covalently conjugated bioeffective molecules on the preformed submicroparticles were investigated.

In this study the two model proteins HSA and WGA were coupled to free carboxyl groups at the surface of the fluorescent BOD-SMP followed by an analysis of the cytoadhesive and cytoinvasive properties of the colloids using Caco-2 cells. While HSA was chosen due to its widely nonspecific protein-protein interactions, WGA was selected as a specific ligand that binds to membrane-associated glycoproteins.[373, 208, 209] Furthermore, plain BOD-SMP were used as a negative control allowing discrimination between the association of submicroparticles alone and the proteinaceous component of the interaction.

When Caco-2 cells were incubated with plain and modified BOD-SMP, distinctly different association rates were observed. Generally, plain BOD-SMP were shown to exhibit very low binding (Figure 17 A), which is in concordance with previous reports on the poor cytoadhesive characteristics of hydrophobic, unmodified PLGA.[363] Interestingly, although supposedly bearing altered—more hydrophilic—surface features due to the immobilized protein molecules, similar results were observed for HSA-BOD-SMP (Figure 17 B). In contrast, studies with WGA-BOD-SMP revealed high and fast association rates for the submicroparticles as evidenced by flow cytometry and fluorescence microscopy. An inhibition assay with N,N',N''-triacylchitotriose showed that 89.48% of the binding of WGA-BOD-SMP to Caco-2 cells was due to specific lectin-carbohydrate interactions (Figure 16), which sug-

gests that the bioactive conformation of wheat germ agglutinin was retained over the course of the covalent coupling to the submicroparticles' surface. Upon incubation at 4°C this highly specific attachment was illustrated by a dense occupation of the cell membrane with dot-like fluorescent particles (Figure 17D–F). A quantitative relation to the visually explicit differences was provided via flow cytometric detection of the mean cell-associated fluorescence intensity. Results from these analyses underline the cytoadhesive potency of the WGA-BOD-SMP as compared to plain and HSA-BOD-SMP. This is explicated by 49 and 14 times higher binding rates, respectively, after 60 min incubation at 4°C and was confirmed upon alteration of the submicroparticle concentration (Figures 13 and 14). Besides the increase in mean cell-associated fluorescence intensity, the strong cytoadhesivity of WGA-BOD-SMP was also exemplified by distinctly higher granularity of the cells (see Figure S1 of the Supporting Information). This parameter was monitored by the side-scattering signal from flow cytometry and provides fluorescence-independent information on the cell binding of particles.

These sub-items contribute to a comprehensive characterization of the cytoadhesive properties of stably fluorescence-labeled and surface-engineered submicroparticles. Beyond the binding process of modified colloids to cells or tissues, possible cytoinvasion, its mechanisms and the subsequent intracellular fate are also considered to be paramount questions.[20] In this regard it was shown that BOD-SMP can furthermore serve as a valuable analytical tool for the investigation of these processes. However, it has to be highlighted that a sufficient number of submicroparticles need to be membrane bound in order to be able to qualitatively and quantitatively analyze cytoinvasion. Considering the mean cell-associated fluorescence intensities in Figure 13, the critical threshold would correspond to a relative fluorescence intensity of about 2. Although this poses a slightly limiting factor for the assay, this requirement needs to be fulfilled for a reliable detection of internalization via flow cytometry and fluorescence microscopy. Since that was not granted for plain and HSA-BOD-SMP due to their low cell association, an analysis and judgment of their cytoinvasive properties would be rather speculative from the data obtained.

After loading Caco-2 cells with WGA-BOD-SMP at 4°C, where the fluidity of the membrane and cellular metabolism are reduced, raising the temperature to 37°C was found to result in uptake of the membrane-bound submicroparticles (Figure 17 G). This was not only visualized but also supported by data from flow cytometric analyses, which show a decrease of the mean cell-associated fluorescence intensity upon incubation at higher temperature. Considered in conjunction with evidence from fluorescence microscopy studies, it appears that the particles' intracellular constriction to vesicular compartments might be accountable for this observation due to quenching effects between the fluorophores and shielding by the membrane as well as other intracellular structures.

1.2.2.5 Conclusions

The entrapment of the fluorophore BOD into PLGA submicroparticles yields stably labeled and highly fluorescent colloids whose surface can readily be conjugated with bioactive ligands. These particles with biocompatible and biodegradable core material were shown to be suitable tools for an investigation of submicroparticle-cell interactions. By combination of fluorescence microscopy and flow cytometry it was

possible to analyze the cytoadhesive characteristics of plain and surface modified BOD-SMP as well as the cytoinvasion of WGA-BOD-labeled submicroparticles. Hydrophobic plain BOD-SMP exhibited only very low binding to the Caco-2 cells, similar to HSA-BOD-SMP which were presumed to possess altered surface hydrophobicity due to the attached protein molecules. In contrast, immobilization of WGA onto BOD-SMP resulted in highly cytoadhesive as well as cytoinvasive submicroparticles due to specific binding of the lectin to carbohydrate moieties of the cells' glycocalyx. Currently, efforts are put forth in order to extend the presented analysis beyond the limits of uptake towards a comprehensive investigation of the consecutive subcellular localization of the submicroparticles. In addition, further studies with various cytoinvasive molecules attached to the "centerpiece", BOD-SMP, are expected to shed light on the intracellular fate of colloidal substances as a consequence of surface functionality. Based on these results it can be concluded, that BOD-labeled submicroparticles will provide a versatile and valuable platform for biocompatible screening of novel ligands with broad applicability in labeling, drug delivery, and targeted contrast agents.

1.2.2.6 Experimental section

MATERIALS BOD was obtained from Molecular Probes (Invitrogen Corp., Carlsbad, CA, USA). Resomer® RG503H (PLGA; lactide/glycolide ratio 50:50, inherent viscosity $0.32\text{--}0.44\text{ dL g}^{-1}$, acid number $>3\text{mg KOH g}^{-1}$) was bought from Boehringer Ingelheim (Ingelheim, Germany). Wheat germ agglutinin from *Triticum vulgare* was obtained from Vector laboratories (Burlingame, USA). HSA, EDAC, NHS, Pluronic® F-68, and N,N',N''-triacetylchitotriose were purchased from Sigma Aldrich (Vienna, Austria). All other chemicals used were of analytical purity.

PREPARATION OF BOD-SMP The BOD-SMP were prepared by an oil-in-water (o/w) solvent-evaporation technique under protection from light to prevent photobleaching of the fluorophore. Briefly, BODIPY (1 mg) and PLGA (400 mg) were dissolved in ethyl acetate (2 g). This solution was emulsified with a 10% aqueous solution of Pluronic (6 mL) by sonication for 50 s yielding the o/w emulsion (sonifier: Bandelin electronic UW 70/HD 70, tip: MS 72/D, Berlin, Germany), which was poured into a 1% aqueous solution of Pluronic (100 mL). After mechanical stirring (600 rpm) for 1 h at room temperature, the residual ethyl acetate was removed under reduced pressure. The resulting submicroparticle suspension was filtered (1- μm pore size) in order to eliminate aggregates.

PARTICLE SIZE AND ZETA-POTENTIAL ANALYSIS Prior to all measurements the submicroparticle suspensions were diluted 1:20 with double-distilled water. The mean particle size and size distribution were determined by dynamic light scattering on a Zetasizer Nano ZS (Malvern Instruments Ltd., UK). Zeta-potential analyses were carried out at 25°C in disposable folded capillary cells using the same instrument. All measurements were performed in triplicate.

MODIFICATION OF THE PARTICLE SURFACE 40 mL of the submicroparticle suspension was purified with HEPES (80 mL) on a tangential flow filtration system (Vivaflow 50; 100,000 MWCO PES, Sartorius Vivascience GmbH, Goettingen, Germany) to adjust the pH value and to eliminate PLGA monomers as well as non-encapsulated BOD. Subsequently, EDAC (480 mg) and NHS (20 mg), each dissolved in the same buffer (1 mL), were added to the suspension and incubated end-over-end for 2 h at room temperature. To remove excess cross-linking agent, the suspension was washed twice with HEPES (80 mL). After division into two parts (20 mL), solutions of WGA (0.67 mg) in HEPES (1 mL) and HSA (1.22 mg) in HEPES (1 mL) were added, respectively. Following end-over-end incubation at room temperature overnight, unreacted coupling sites were saturated by addition of glycine (300 mg) in HEPES (1 mL) and further incubation at room temperature for 1 h. The surface-modified submicroparticle suspensions were washed five times with HEPES (20 mL) to remove excess coupling agents and concentrated to 15 mL during the last purification step.

CELL CULTURE The Caco-2 cell line was purchased from the American Type Culture Collection (Rockville, MD, USA) and used between passage 28 and 39. Tissue culture reagents were obtained from Sigma (St. Louis, USA) and Gibco Life Technologies Ltd. (Invitrogen Corp., Carlsbad, CA, USA). Cells were cultivated in RPMI 1640 cell culture medium containing 10% fetal bovine serum, 4 mM L-glutamine and 150 mg mL⁻¹ gentamycine in a humidified 5% CO₂/95% air atmosphere at 37°C and subcultured by trypsination.

FLOW CYTOMETRY The association of plain and surface-modified BOD-SMP with Caco-2 single cells was investigated using flow cytometry. Briefly, 50 µL cell suspension (5x10⁶ cells mL⁻¹) were mixed with 50 µL of the respective submicroparticle suspension and incubated under varied conditions. To grant comparability between plain, HSA-, and WGA-BOD-SMP, dilutions to standardized relative fluorescence intensities were used. These were prepared with isoHEPES prior to all experiments and controlled on a microplate reader (e/e: 480/525 nm; Infinite 200i, Tecan Group Ltd., Grödig, Austria). Following incubation, unbound and loosely associated particles were removed by centrifugation and washing with 500 µL HEPES (Centrifuge 5804R, Eppendorf; 5 min/1000 rpm/4°C). The cells were resuspended in PBS (1000 µL) and analyzed on an EPICS XL-MCL analytical flow cytometer (Coulter, Miami, USA) using a forward-versus-side scatter gate for inclusion of the single-cell population and exclusion of debris and cell aggregates. Fluorescence was detected at 525 nm (10 nm bandwidth) and the mean channel number of the logarithmic intensities of individual peaks was used for further calculations. Amplification of the fluorescence signals was adjusted to put the auto fluorescence signal of unlabeled cells in the first decade of the four decade log range. Data of 3000 cells were collected for each measurement.

BINDING SPECIFICITY OF WGA-BOD-SMP Binding specificity of the

carbohydrate-lectin interaction between WGA-BOD-SMP and the Caco-2 cell surface was assessed by a competitive assay with N,N',N''-triacylchitotriose. Caco-2 cell suspension (50 μL), WGA-BOD-SMP suspension (50 μL), and 100 μL solution of N,N',N''-triacylchitotriose (100, 50, 25, 12.5, 6.25, 3.125, 1.57 $\mu\text{g}/100 \mu\text{L}$) in isoHEPES were mixed and incubated for 60 min at 4°C. After washing with isoHEPES, the mean cell associated fluorescence intensity was determined by flow cytometry. Each concentration was analysed in triplicate with isoHEPES (100 μL) as a negative control.

INTERNALIZATION OF WGA-BOD-SMP A pulse-chase incubation at different temperature levels was performed in order to investigate uptake of bound WGA-BOD-SMP into Caco-2 cells. The single cells were loaded with WGA-BOD-SMP for 60 min at 4°C and washed once with HEPES. The mean cell-associated fluorescence intensity at this point in time represents the start of the chase incubation. Following this, the loaded Caco-2 cells were incubated at 4°C/37°C and analysed regarding the mean cell associated fluorescence intensity in course of an incubation time up to 240 min.

FLUORESCENCE MICROSCOPY In order to visually investigate binding and uptake of plain and modified BOD-SMP into Caco-2 cells, a 50 μL cell suspension (5×10^6 cells mL^{-1}) was incubated with 50 μL of a suspension of plain BOD-SMP, HSA-BOD-SMP, and WGA-BOD-SMP in isoHEPES for 60 min at 4°C. For the internalization experiments the cells were washed twice with HEPES (500 μL) and incubated for 30 min at 37°C followed by staining of the cell membrane with a solution of FM® 4-64 in HEPES. Imaging of the BOD-SMP with live cells was performed on a Nikon Eclipse 50i microscope (Nikon Corp., Japan) equipped with an EXFO X-Cite 120 fluorescence illumination system. Except for the stack, the focus was set to the middle of the cell and the pictures taken were subjected to deconvolution processing by the Image Analyser software.

1.2.3 *Binding of positively and negatively charged micro- and nanoparticles to an epithelial and endothelial cell model*

Christian Fillafer, Bettina Luser, Manuela Prantl, Winfried Neuhaus, Renate Hofer-Warbinek, Michael Wirth, Franz Gabor. *to be submitted.*

1.2.3.1 *Introduction*

The most prominent biological barriers encountered by particulate drug carriers upon administration to the human body are represented by epithelial and endothelial cells. Hence, a strong interaction with these tissues is essential to prolong the residence time of particles in the body or to achieve their absorption. Aside from surface modification with biorecognitive ligands,[4] coating of colloids with cationic polyelectrolytes has been discussed as a potential strategy to enhance the interaction with epithelial and endothelial cells.[4, 186] This rationale is based on the observation that all cell types of multicellular organisms are characterized by negatively charged cell surfaces.[6] The charges in the cell membrane largely derive from sialic acid carboxy groups and phosphates of phospholipid head groups. Aside from negative groups, cationic charges also exist which probably can be attributed to ϵ -amino groups of lysine side chains of membrane proteins.[6] It is not clear whether these charged moieties in the plasma membrane are evenly distributed or clustered, but generally negative groups seem to prevail.

As indicated by several studies, ionic interactions between the particle surface and the cell might indeed mediate improved bioadhesion. Thiele et al. showed that clearly higher quantities of PLL-coated PS microspheres were associated with and internalized into APCs *in vitro* as compared with negatively charged beads.[86] Moreover, positively charged particles were phagocytosed in endosomes which showed considerable interactions between the particle surface and the vesicle membrane.[90]

That positively charged carriers are also characterized by an altered biodistribution as compared to their negatively charged counterparts has been shown in *in vivo* studies. Polystyrene latices sized 1.3 μm , which had been surface modified with polylysyl gelatine, were preferentially located in the lung 15 min after injection.[347] However, it was not clear if this altered biodistribution was essentially due to altered bioadhesion of positively charged colloids. Rather than that the authors argued that positively charged particles might be more prone to the formation of aggregates in whole blood. These aggregates might subsequently be trapped in the extensive capillary bed of the lung. More concrete evidence of enhanced bioadhesion of positively charged particles to the endothelium was provided by Labhassetwar et al.[186] PLGA nanoparticles sized ~ 100 nm that had been coated with the cationic excipient DDAB delivered 7-10 fold higher drug levels to isolated artery segments *ex vivo* than negatively charged colloids. Even more interesting in regards to potential targeting via charge, Thurston et al. reported that cationic liposomes preferentially bind to and are taken up by angiogenic endothelial cells in mouse tumor models and in a mouse model of chronic inflammation.[348] Thus, modifying the surface charge of particles might not only lead to increased bioadhesion, but might also represent an approach for targeting to specific cell populations.

From most studies in the literature it is difficult to deduce whether bioadhesion of charged particles is mediated by the charge itself, by proteins specifically adsorbed from serum or by other factors such as aggregate formation in whole blood. In this study, plain carboxylated PS nano- and microspheres and the same particles coated with the cationic polyelectrolyte PEI will serve as model colloids, since they resemble micro- and nanoparticulate drug carriers in size and charge. Caco-2 and human umbilical vein endothelial cell (HUVEC) monolayers will be employed as epithelial and endothelial cell models respectively which are highly relevant for drug delivery. Using these particle and cell types in a controllable *in vitro* setting, it will be investigated if positively charged carriers are indeed characterized by higher bioadhesion than their negative counterparts.

1.2.3.2 Materials and methods

MATERIALS Yellow-green fluorescent carboxylated polystyrene particles with diameters of 500 nm and 2000 nm as well as PEI (branched, MW~ 10 kDa) were obtained from Polysciences Europe GmbH (Eppelheim, Germany). All other chemicals used were of analytical purity.

CELL CULTURE The Caco-2 cell line was purchased from DSMZ (Braunschweig, Germany) and was used for the experiments between passage 41 and 57. Tissue culture reagents were obtained from Sigma (St. Louis, USA) and Gibco Life Technologies Ltd. (Invitrogen Corp., Carlsbad, CA, USA). Cells were cultivated in RPMI 1640 cell culture medium containing 10% fetal bovine serum, 4 mM L-glutamine and 150 mg mL^{-1} gentamycine in a humidified 5% CO_2 /95% air atmosphere at 37°C and were subcultured by trypsination. Confluent Caco-2 cell monolayers in 96-well polystyrene microplates were obtained by seeding of 1.7×10^4 cells/160 μL /well and cultivation for 5-6 days.

HUVECs were isolated from human umbilical cords by treatment with collagenase Type I and were used for the experiments between passage 2 and 4. The tissue culture flasks and microplates used for HUVEC cultivation were coated with a 1% (w/v) aqueous solution of gelatin for 30 min at 37°C prior to seeding of the cells in endothelial growth medium-2 (EGM-2, Lonza, Basel, Switzerland). Confluent monolayers in 96-well polystyrene microplates were obtained by seeding of 1.7×10^4 cells/160 μL /well and cultivation for 3 days.

Caco-2 and HUVEC cell monolayers for fluorescence microscopy were grown on glass cover slips in 24-well microplates. For cultivation of endothelial cells the glass slips were coated with a $100 \mu\text{g mL}^{-1}$ solution of fibronectin (from BD Biosciences Europe) in PBS for 30 min at 37°C prior to seeding of the cells.

COATING OF CARBOXYLATED NANO- AND MICROPARTICLES WITH PEI
Coating of carboxylated polystyrene particles with diameters of 500 nm (PS₅₀₀) and 2000 nm (PS₂₀₀₀) was achieved by a technique modified from [82]. 100 μL of a 5 mg mL^{-1} suspension of PS₅₀₀ or 100 μL of a 20 mg mL^{-1} suspension of PS₂₀₀₀ were added dropwise to a 5 mg mL^{-1} solution of PEI in 100 mM phosphate buffer pH 5.8 in a tube placed in an ultrasonic bath. In principle, the coating protocol can be

adapted to various particle sizes as long as the ratio of total particle surface area (A_{total}): PEI concentration is held constant. The surface area A [m^2] of a sphere with radius r [m] is calculated according to 1.3

$$A = 4r^2\pi \quad (1.3)$$

If the total particle mass M [kg] is known, the total number of particles N can be obtained from 1.4

$$N = \frac{M}{m} \quad (1.4)$$

where m [kg] is the mass of a single particle as given by 1.5

$$m = \rho_p V \quad (1.5)$$

with ρ_p [kg m^{-3}] as the density of the particle material and V [m^3] as the volume of a single particle 1.6.

$$V = \frac{4r^3\pi}{3} \quad (1.6)$$

Accordingly, A_{total} [m^2] can be calculated from 1.7

$$A_{\text{total}} = NA \quad (1.7)$$

and by substituting, the simplified expression 1.8 is obtained.

$$A_{\text{total}} = \frac{3c}{r\rho_p} \quad (1.8)$$

Upon reaction of PEI with the particles under sonication for 10 min, 1300 μL of 100 mM phosphate buffer pH 5.8 were added and the particles were spun down on a centrifuge (Eppendorf 5804R).

As a rough guide, the centrifugation parameters for particle washing can be calculated according to 1.9

$$t_{\text{max}} = \frac{9}{2} \frac{\eta}{(\rho_p - \rho_s)r^2\omega^2} \ln \frac{R_e}{R_a} \quad (1.9)$$

where t_{max} [s] is the time needed to spin down all particles, η [$\text{kg m}^{-1} \text{s}^{-1}$] is the viscosity of the suspension¹, ρ_p [kg m^{-3}] and ρ_s [kg m^{-3}] are the densities of the particles² and suspension medium³ respectively, r [m] is the particle radius, ω [s^{-1}] is the angular frequency and R_a [m] is the distance from the rotor axis to the upper level of the suspension and R_e [m] to the bottom level of the suspension respectively⁴.^[377]

The angular frequency ω can be obtained from 1.10

$$\omega = 2\pi v_{\text{rot}} \quad (1.10)$$

with v_{rot} [s^{-1}] as the rotation velocity. For PS₅₀₀ and PS₂₀₀₀ this results in centrifugation times of 3 min and 1 min respectively at 14000 rpm.

The pellet was washed with 100 mM phosphate buffer pH 5.8 and was finally resuspended in 1 mL HEPES under sonication for 15 s (sonifier, Bandelin electronic UW70/HD 70; tip, MS 72/D, Berlin, Germany).

1 water at 10°C: 0.0013 $\text{kg m}^{-1} \text{s}^{-1}$, water at 20°C: 0.001 $\text{kg m}^{-1} \text{s}^{-1}$, water at 25°C: 0.0009 $\text{kg m}^{-1} \text{s}^{-1}$, water at 30°C: 0.0008 $\text{kg m}^{-1} \text{s}^{-1}$, glycerine: 1.16 $\text{kg m}^{-1} \text{s}^{-1}$

2 polystyrene: 1050 kg m^{-3} , PLGA: ~1280 kg m^{-3} [376]

3 water at 25°C: 997 kg m^{-3} , 1% aqueous solution of Poloxamer 188: 1000 kg m^{-3} , glycerine: 1260 kg m^{-3}

4 for Eppendorf 5804R with rotor F45-30-11: $r_a = 0.07$ m, $r_e = 0.095$ m

Control particles were treated as described above, but without PEI in the coating solution. The zeta potential of PEI-coated and control particles was determined upon dilution in HEPES (conductivity $\sim 0.69 \text{ mS cm}^{-1}$) by laser Doppler electrophoresis with a ZetaSizer Nano ZS (Malvern Instruments Ltd., U.K.). Prior to the binding studies on Caco-2 and HUVEC cell monolayers a small sample of all particle suspensions was drawn and checked for agglomerates under a fluorescence microscope.

BINDING STUDIES ON CELL MONOLAYERS The stock suspensions of negatively and positively charged PS₅₀₀ and PS₂₀₀₀ in HEPES were diluted with isoHEPES + 0.1 % of Poloxamer 188 or PBS + 0.1 % of Poloxamer 188 to yield the working concentrations. All binding studies were performed with suspensions containing 16 $\mu\text{g}/100 \mu\text{L}$, 8 $\mu\text{g}/100 \mu\text{L}$, 4 $\mu\text{g}/100 \mu\text{L}$, 2 $\mu\text{g}/100 \mu\text{L}$, 1 $\mu\text{g}/100 \mu\text{L}$, and 0.5 $\mu\text{g}/100 \mu\text{L}$ PS particles. Upon removal of the cell culture medium each well was filled with 100 μL of particle suspension or plain buffer as control. The homogeneity of loading between wells was checked via fluorimetry with a microplate reader (ex/em: 440/485 nm; Infinite 200i, Tecan Group Ltd., Grödig, Austria). Following incubation for 30 min at 37°C the particle suspension was removed and the cell monolayer was washed twice with 100 μL of buffer. Finally, the fluorescence of the cell monolayer which corresponds to the amount of cell-associated particles was determined by fluorimetry.

FLUORESCENCE MICROSCOPY HUVEC and Caco-2 cell monolayers grown on glass cover slips were used for fluorescence microscopy. Upon incubation with positively or negatively charged polystyrene particles for 30 min at 37°C the cell layers were washed twice with PBS. Subsequently, the cells were fixed with ice cold methanol (-20°C) for 10 min at -20°C. After rehydration in PBS for 20 min at room temperature the cells were washed with PBS containing 1% BSA. Then, 100 μL of a 1:200 dilution of the primary antibody were added followed by incubation for 1 h at 37°C. In case of Caco-2 cells, purified mouse-anti-human ZO-1 antibody (250 $\mu\text{g mL}^{-1}$, BD Transduction Laboratories) was used to label tight junction associated protein ZO-1 while in case of HUVECs a polyclonal goat-anti-human VE-cadherin (C-19) antibody (200 $\mu\text{g mL}^{-1}$, Santa Cruz Biotechnology) was used to label vascular endothelial cadherin. After washing with PBS + 1% BSA, 100 μL of a 1:200 dilution of R-phycoerythrin (RPE)-labelled goat-anti-mouse antibody (1 mg mL^{-1} , Dako) in case of ZO-1 staining and 100 μL of a 1:200 dilution of rhodamine-labelled rabbit-anti-goat antibody (1 mg mL^{-1} , Abcam) in case of VE-cadherin staining were added to the cells and left to react for 30 min at 37°C. Finally, the cell layers were washed twice with PBS + 1% BSA and embedded in a drop of FluorSave. All images were taken on a Nikon Eclipse 50i or a Zeiss Observer.Z1 microscope.

1.2.3.3 Results and Discussion

ADSORPTION OF PEI LEADS TO POSITIVELY CHARGED PARTICLES The PS particles which were used in this study are not biodegradable and consequently not suitable for administration as drug carriers. However, they can be prepared in precise size classes and with custom surface

chemistry which makes them an advantageous model for systematic particle studies.

Many polymers used as matrix materials for the preparation of biocompatible and biodegradable drug delivery systems are characterized by carboxyl end groups which impose a negative charge on the produced particle. Similarly, carboxylated PS particles carry negatively charged groups on the particle surface. As illustrated in Table 7, this

Table 7: Zeta potential of 500 nm and 2000 nm polystyrene particles before and after surface modification with PEI.

	Surface chemistry	Zeta potential [mV]
500 nm	carboxyl groups	-82.5±2.0
	PEI	54.0±2.8
2000 nm	carboxyl groups	-82.7±4.0
	PEI	60.5±4.9

results in clearly negative zeta potentials of > -80 mV at pH 7.4. The negative charges on the particle surface can be used to drive the adsorption of cationic polyelectrolytes. For this purpose, a series of natural, processed natural, and synthetic polyelectrolytes can be employed. These include protamine,[89] chitosan,[84, 88, 91, 92, 93, 94, 95, 96, 97, 98, 99] gelatine,[100] diethylaminoethyl dextran,[101] Eudragit® RL/RS,[85] PEI,[102, 103, 104, 105, 106] and PLL.[46, 87, 103, 107, 108, 109] In this study, low molecular weight branched PEI was used due to its high density of amino groups.[111] In slightly acidic buffer the amino groups exist in their protonated and thus charged form. These cationic groups are expected to interact with negatively charged carboxyls on the particle surface by ionic interactions. At this, the composition of the adsorption buffer is expected to influence the polyelectrolyte configuration as well as adsorption efficiency. While PEI will exist as a rather stretched molecule in water or low ionic strength buffers, it will adapt a coiled configuration if the adsorption buffer's ionic strength is sufficiently high. Adsorption of coiled polyelectrolytes will not only result in direct charge compensation and neutralization of a particle's surface potential. Moreover, surplus positive charges will be introduced and the zeta potential will be inverted.[82] However, if the ionic strength of the adsorption buffer is increased further, the charges of the polyelectrolyte will be screened and electrostatic interactions with dissociated groups on the particle surface will be reduced. 100 mM phosphate buffer has proven to represent a suitable compromise in terms of ionic strength and was successfully used for coating of colloids with PEI.[82] In the present study, adsorption of PEI from 100 mM phosphate buffer onto PS nano- and microparticles was achieved. This was confirmed by a clear shift of the zeta potentials of PS particles to positive values as illustrated in Table 7. However, it has to be highlighted that the protocol by Trimaille et al. [82] had to be modified to generate satisfactory results with PS particles. While in the original study a PEI concentration of less than $30 \mu\text{g mL}^{-1}$ was sufficient for introduction of a positive

zeta potential, an about 50 fold higher PEI concentration had to be employed in the present study. The increase in PEI concentration was necessary since irreversible agglomeration of the particles occurred at lower concentrations. A possible reason for this might lie in the different quantities of carboxyl groups on the surface of PS and PLA particles. PS particles might be characterized by a clearly higher surface carboxyl group density. This could explain why a PEI concentration in the range of $30 \mu\text{g mL}^{-1}$ led to aggregation of the particles. Due to insufficient charge compensation on the particle surface colloids with partially negative and partially positive surface sites might be created. This would inherently reduce electrostatic stabilization of the dispersion and consequently favour the formation of aggregates. With higher PEI concentrations, the particle surface charge is rapidly reversed and thus the potential for aggregation is low. Generally, as observed by fluorescence microscopy negatively charged particles used in this study were free from agglomerates. Positively charged particles tended to agglomerate upon dilution and prolonged storage in isotonic buffer. At this, the suspension was sonified until the majority of colloids were redispersed and ready to use for studies with cell monolayers.

POSITIVELY CHARGED PARTICLES EXHIBIT HIGHER BINDING TO CACO-2 CELL MONOLAYERS The usability of micro- and nanoparticles for drug delivery purposes depends on their delivery efficiency. To be able to compare the cell binding efficiency of differently sized particles, the mass deposition data will be presented in this study.

Upon incubation of negatively and positively charged colloids with Caco-2 cell monolayers for 30 min at 37°C in isoHEPES, clear differences in the amount of cell-binding were observed. As illustrated in Figure 18, negatively charged PS₅₀₀ were only detected when at least $6 \mu\text{g}$ had

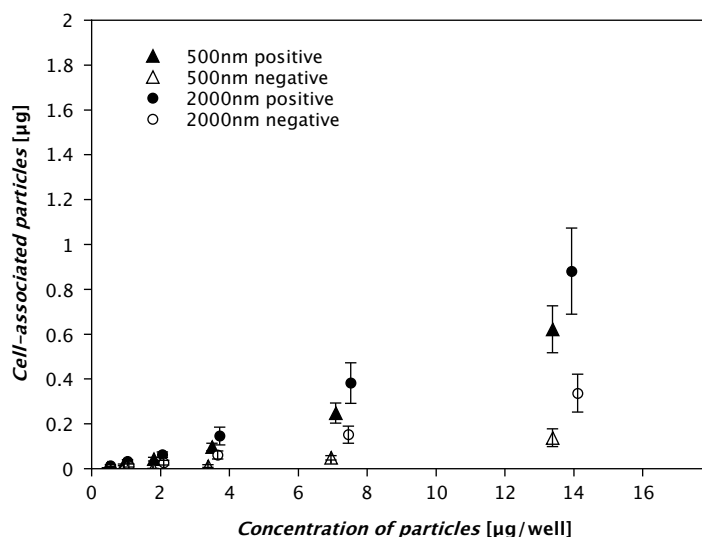


Figure 18: Positively (closed symbols) and negatively charged particles (open symbols) associated with Caco-2 cell monolayers upon incubation in isoHEPES for 30 min at 37°C . Particle diameter 500 nm (Δ) and 2000 nm (o). Each data point consists of $n=27$ measurements.

been added to the cell layer which resulted in $0.05 \pm 0.1 \mu\text{g}$ of cell-associated particles. In contrast, positively charged PS₅₀₀ were already unambiguously detected upon addition of $\sim 1 \mu\text{g}$ which resulted in $0.017 \pm 0.004 \mu\text{g}$ of cell-associated particles. At concentrations of $\geq 6 \mu\text{g}$ of particles added per well, the amount of cell-bound PS₅₀₀ particles was constantly 4-5 fold higher in the case of positively charged colloids as compared to their negative counterparts. This was also confirmed by fluorescence microscopy as illustrated in Figure 19. Consistent with

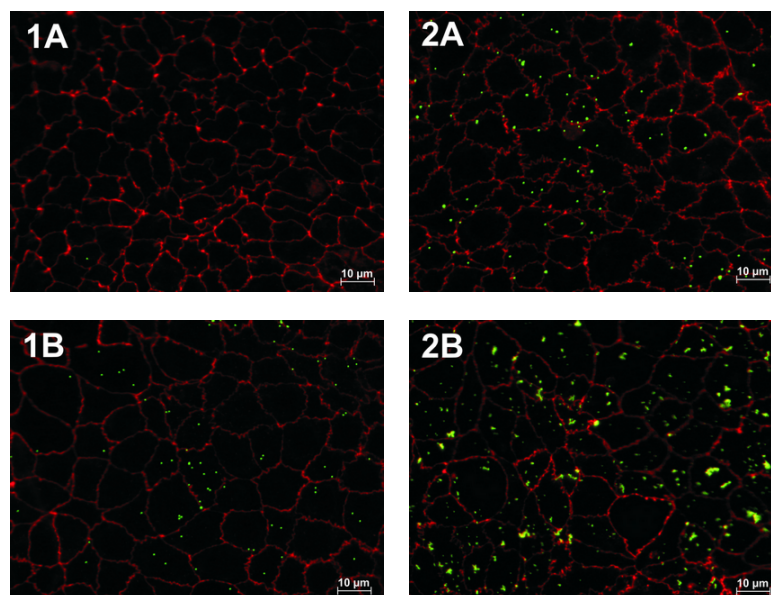


Figure 19: Negatively (1) and positively charged (2) 500 nm particles (green) associated with Caco-2 cells after 30 min incubation. Concentration of particle suspension $\sim 1 \mu\text{g}/100 \mu\text{L}$ (A) and $\sim 8 \mu\text{g}/100 \mu\text{L}$ (B). Tight junction associated protein ZO-1 labelled in red.

the quantitative results obtained by fluorimetry, almost no negatively charged PS₅₀₀ were observed on the Caco-2 cell monolayer upon incubation with a suspension containing $1 \mu\text{g}/100 \mu\text{L}$. (Figure 19 1A). At the same concentration, positively charged PS₅₀₀ were already clearly visualized as regularly distributed green dots (Figure 19 2A). The quantitative data plotted in Figure 18 were still reflected in the visually observed densities of bound particles when the concentration had been increased 8-fold (Figure 19 B).

Similar observations as with PS₅₀₀ were made in the case of PS₂₀₀₀. Starting at a concentration of $\sim 1 \mu\text{g}$ per well, cell-associated particles were unambiguously detected. Over the whole concentration range tested, the positively charged colloids were characterized by a 2.5 fold higher cell binding than the negatively charged PS₂₀₀₀.

Particle binding studies with Caco-2 cells can be performed in isoHEPES without notable morphological alterations of the cells or disintegration of the monolayer. However, HUVEC monolayers proved to be highly sensitive to the composition and type of the incubation buffer. Thus, binding studies had to be performed in PBS. In order to be able to compare the quantities of cell-associated particles between the endothelial and epithelial cell model, particle binding studies with Caco-2 cell monolayers were also performed in PBS. When comparing the binding rates in isoHEPES (Figure 18) with those in PBS (Figure 20)

it becomes obvious that in the latter case the amount of cell-associated

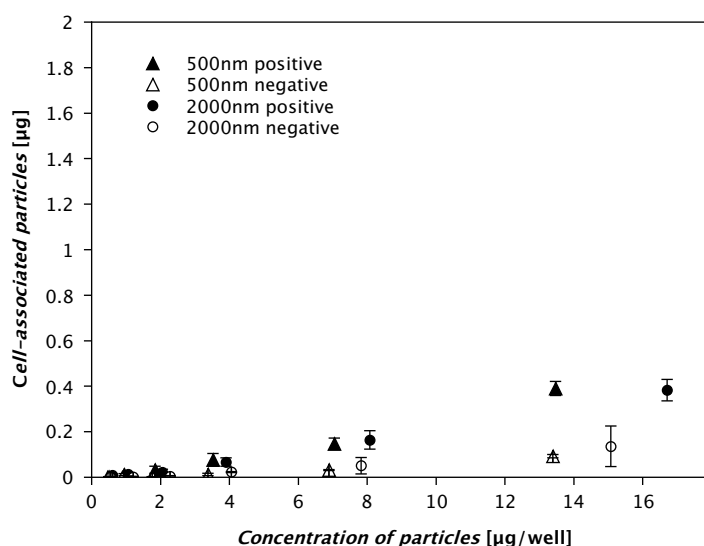


Figure 20: Positively (closed symbols) and negatively charged particles (open symbols) associated with Caco-2 cell monolayers upon incubation in PBS for 30 min at 37°C. Particle diameter 500 nm (Δ) and 2000 nm (o). Each data point consists of n=6 measurements.

particles was clearly reduced in all cases. Interestingly, the effect of PBS on cell-binding was more pronounced in case of PS₂₀₀₀. This was exemplified by a consistent reduction of the the amount of cell-bound positively and negatively charged particles by about 60%. In case of PS₅₀₀ the reduction was not as distinct as in the case of PS₂₀₀₀ but nevertheless amounted to about 30 %. For both sizes, the effect was neither dependent on the concentration nor on the surface charge of the particles. This indicates involvement of a nonspecific mechanism that probably either affects the particles' detection via fluorimetry or their ionic interaction with the cell monolayer. However, neither of these reasons can be conclusively argued to be involved in this case. Since the pH as well as osmolarity of PBS and isoHEPES were identical according to measurements, buffer-induced fluorescence intensity alterations are unlikely. The interaction between two oppositely charged species is known to depend on the concentration and type of ions in the medium. Consequently, the buffer composition determines the surface potential of dispersed colloids and charged groups in the cell membrane and might alter the interaction between oppositely charged species. Although PBS contains multivalent ions, the main component contributing to its osmolarity and thus ionic strength is sodium chloride. Calculations confirm that a similar ionic strength as for isoHEPES can be expected. This probably precludes effects of multivalent ions on the interface and thus interaction potential of colloids as well as cells.

Regardless of the different quantities of cell-bound particles in PBS and isoHEPES, the results clearly demonstrate a particle size independent preferential binding of cationic particles to Caco-2 cell monolayers. Very likely, this can be attributed to ionic interactions between the polycation-coated colloids and negative charges of the Caco-2 cell membrane. Thus, with the epithelial cell model the hypotheses and reports

in the literature according to which positively charged particles are more bioadhesive than their negative counterparts were confirmed.

It should be borne in mind, however, that Caco-2 cells were originally isolated from a colon carcinoma. Tumor or regenerating cells are characterized by higher electrophoretic mobilities and thus higher cell surface charge than their normal counterparts.[378, 379] As a consequence it might be possible that the clearly preferential binding of positively charged particles onto Caco-2 cells does not exactly reflect the binding to normal intestinal epithelium. Studies with primary intestinal epithelial cells might help to clarify this issue.

NEGATIVE AND POSITIVE PARTICLES EQUALLY BIND TO ENDOTHELIAL CELLS
In contrast to the results obtained with Caco-2 cell monolayers, no preferential attachment of positively charged particles was observed on HUVEC monolayers. As illustrated in Figure 21, the adhesion data

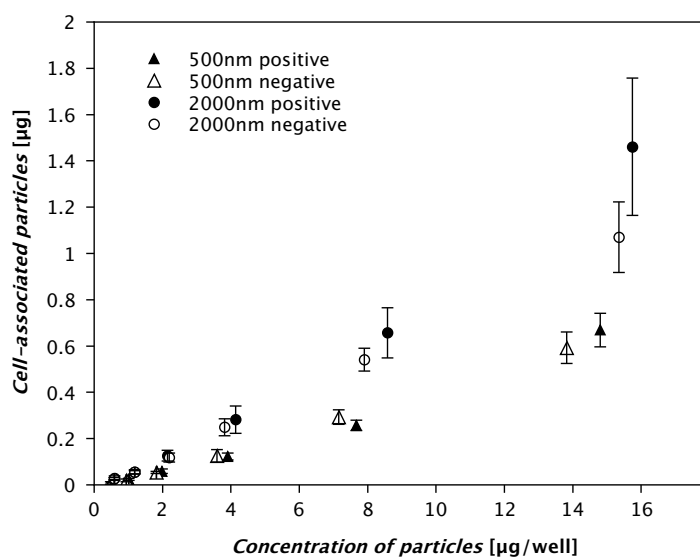


Figure 21: Positively (closed symbols) and negatively charged particles (open symbols) associated with HUVEC cell monolayers upon incubation in PBS for 30 min at 37°C. Particle diameter 500 nm (Δ) and 2000 nm (o). Each data point consists of n=21 measurements.

for positively and negatively charged PS₅₀₀ are clearly similar. When both data sets are collectively fitted with a linear function, a coefficient of determination (R^2) of 0.99 is obtained. Similarly, no pronounced differences between positively and negatively charged PS₂₀₀₀ were observed. This was confirmed by fluorescence microscopy as illustrated in Figure 22. These results indicate that HUVEC monolayers, unlike Caco-2 cell monolayers, bear equal binding capacity for negatively and positively charged particles. Related observations were reported by Osaka et al., who investigated the uptake of positively and negatively charged magnetite nanoparticles into MCF-7 breast cancer cells and HUVECs.[380] While a preferential uptake of positively charged nanoparticles into MCF-7 cells was detected, the data for HUVECs revealed no difference between positively and negatively charged colloids. In connection with the presented results, this indicates that higher

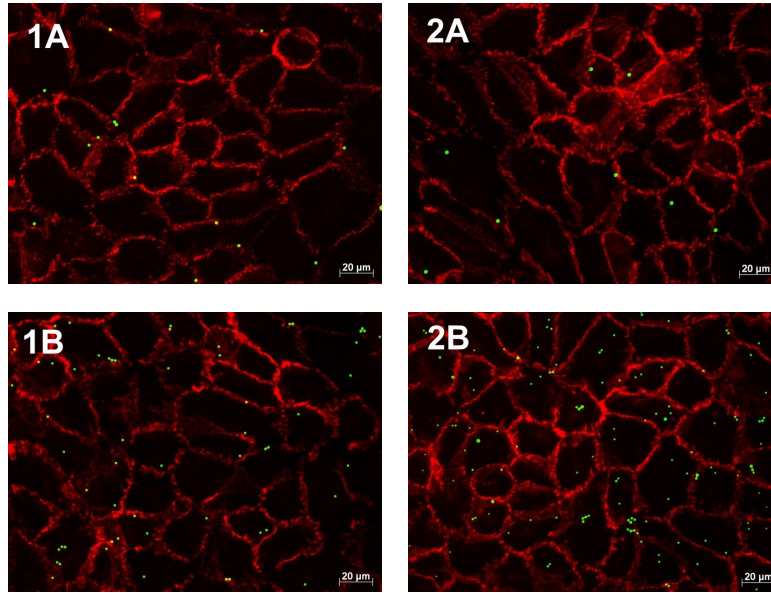


Figure 22: Negatively (1) and positively charged (2) 2000 nm particles (green) associated with HUVECs after 30 min incubation. Concentration of particle suspension $\sim 1 \mu\text{g}/100 \mu\text{L}$ (A) and $\sim 8 \mu\text{g}/100 \mu\text{L}$ (B). Vascular endothelial cadherin (red).

bioadhesion of positively charged particles obviously can not be presumed for all cell types.

HUVEC MONOLAYERS BIND MORE PARTICLES THAN CACO-2 MONOLAYERS In terms of the quantities of cell-associated particles, HUVECs obviously represent a comparatively affine cell substrate for particle binding. Over the concentration range investigated, HUVEC monolayers exhibit a 2-fold and 4-5 fold higher binding capacity than Caco-2 cell monolayers for positively charged PS₅₀₀ and PS₂₀₀₀ respectively. In the case of negatively charged colloids, this was even more pronounced as illustrated by 6-8 fold and 10-fold higher binding of PS₅₀₀ and PS₂₀₀₀ respectively. This could be specific for endothelial cells. However, it is also possible that primary intestinal epithelial cells differ from Caco-2 cells in terms of their binding capacity for positively and negatively charged particles. This point and possible differences between primary cells and cell lines should be clarified in future studies.

HIGHER BINDING EFFICIENCY OF NANOPARTICLES As illustrated by the fluorescence microscopic images in Figure 19 and Figure 22, PS₅₀₀ are more uniformly distributed on the cell monolayer. In regards to drug delivery this implies that the incorporated drug will be released more homogenously to the cells if delivered in smaller carriers.

To be able to estimate the binding efficiency the theoretical particle deposition rates during the experiment can be calculated. Deposition rates for particles in the sedimentation controlled regime depend on the sedimentation velocity v_{sed} of the particles according to 1.11

$$v_{sed} = \frac{2}{9} \frac{gr^2(\rho_p - \rho_s)}{\eta} \quad (1.11)$$

with g [m s^{-2}] as the gravitational acceleration. For PS₅₀₀ and PS₂₀₀₀ in aqueous buffer at room temperature a v_{sed} of $\sim 0.5 \mu\text{m min}^{-1}$ and $\sim 7.7 \mu\text{m min}^{-1}$ respectively is expected. This leads to the assumption, that the PS₅₀₀ in the lower $15 \mu\text{m}$ and the PS₂₀₀₀ in the lower $230 \mu\text{m}$ of suspension in the cylindrical well will have sedimented onto the cell layer after incubation for 30 min. Considering the cylindrical form of the microplate well with a base of 33 mm^2 and a uniform distribution of the particles, this amounts to deposition of 0.5 % of the added PS₅₀₀ and 7.6 % of the added PS₂₀₀₀. Consequently, an about 15 times higher deposition of PS₂₀₀₀ can be expected. For the highest concentration of $\sim 16 \mu\text{g}/100\mu\text{L}/\text{well}$ this corresponds to deposition of 0.08 and $1.2 \mu\text{g}$ of PS₅₀₀ and PS₂₀₀₀ respectively.

These rough estimates indicate that only a small fraction of the colloids actually deposits on the cell monolayer within 30 min. As illustrated by the almost linear binding curves for all particle types on Caco-2 and HUVEC monolayers, no saturation of the cell layer occurs during the experiment. In the case of PS₂₀₀₀ the theoretical deposition rates seem realistic if compared with the experimentally observed values for positively ($1.46 \pm 0.30 \mu\text{g}$) and negatively charged particles ($1.07 \pm 0.15 \mu\text{g}$) on HUVECs. In case of PS₅₀₀ however, the calculated deposition rates seem to be rather inaccurate. All positively charged PS₅₀₀ bind in higher quantities as expected on HUVEC and Caco-2 monolayers. A reason for this might be the formation of aggregates which sediment at a higher v_{sed} than single particles. However, aggregates were never observed with negatively charged PS₅₀₀ and nevertheless $0.67 \pm 0.07 \mu\text{g}$ of particles were detected as cell-bound at a concentration of $\sim 14.8 \mu\text{g}$ added to HUVEC monolayers (Figure 21). This is clearly higher than the calculated value of $<0.1 \mu\text{g}$. Thus, aggregation is not solely responsible for the discrepancies between theoretical and experimentally observed deposition rates in case of PS₅₀₀. Transport of particles to the cell layer by diffusion is likely to lead to additional deposition, however this is not accounted for in the calculation above.

Larger particles are expected to expose a higher surface area per particle to the cell monolayer. This should entail a higher probability of interaction between oppositely charged groups and thus a higher likelihood of cell-binding. A clear bias of the experimentally observed cell-bound particle mass according to these considerations however was not observed. Although PS₂₀₀₀ are generally characterized by higher binding, it is at maximum only twice as high as that of the corresponding PS₅₀₀. This is in clear contrast to the theoretically predicted 15 times higher deposition of PS₂₀₀₀. The reasons for this are not entirely clear. However, it is plausible that the increased surface area available for binding does not necessarily lead to improved anchoring of the particles. Possibly, this can be explained by the difference in radius between the particles which affects their susceptibility to hydrodynamic stress. In the experiments presented, the washing steps to remove non-bound particles might impose sufficient shear stress to dissociate the interaction between PS₂₀₀₀ and the cells. At the same time, PS₅₀₀ could remain cell-bound since smaller colloids are relatively unaffected by shear stress due to their smaller radius and thus exposed surface area.[381] Consequently, efficient cell-binding could be attained by working with particles at an optimal ratio of particle size to adhesion area. Studies with parallel plate flow chambers (PPFC) [287, 381, 382] or microfluidic devices [383, 384, 296] could help to precisely investigate

the effect of hydrodynamic drag forces on the binding of positively and negatively charged particles to cell monolayers. This would not only improve the present understanding of particle binding studies *in vitro*, but also might allow to deduce an optimal particle size for the targeting of biological barriers with bioadhesive colloids.

1.2.3.4 Conclusions

As illustrated by the results presented, positively charged particles are not generally characterized by higher cytoadhesion than negatively charged particles. While binding studies with an intestinal epithelial cell model indicated a preferential binding of cationic particles, no such tendencies were observed on primary endothelial cells. In the future, it would be highly interesting to perform the same studies with primary intestinal epithelial cells. This could clarify if Caco-2 cells, despite originating from a tumour, are representative of intestinal epithelium in terms of cell membrane charges.

In the present study, the experiments were performed under stationary conditions. To investigate if the adhesive force of positively and negatively charged nano- and microparticles is sufficient to mediate binding under physiological conditions, experiments with dynamic assays should be performed. In combination with experiments in the presence of serum, it might be possible to elucidate if charged micro- and nanoparticles could serve as bioadhesive and potentially targeted drug carriers *in vivo*.

As indicated by the data presented, nanoparticles are characterized by a higher binding efficiency as microparticles. This becomes clear when the experimentally observed deposited particle mass is compared with the theoretical deposition rates. Although microparticles can carry a larger amount of drug due to their volume, nanoparticles might be more efficient for drug delivery because they spread in the tissue evenly and are less prone to removal by shear forces.

SURFACE ACOUSTIC WAVE (SAW) CHIPS: INTEGRATING FLOW INTO MINIATURIZED BIOPHARMACEUTICAL TEST SYSTEMS

2.1 BACKGROUND

2.1.1 *Relevance of flow to drug delivery with particles*

Micro- and nanoparticles have been extensively investigated as to their potential utility as drug delivery systems. The interaction of drug-loaded particulates in the nano- and micrometer range with the organism, however, is expected to clearly differ from that of dissolved drug molecules. A parameter that might be of considerable importance in this regard is the flow of materials under physiological conditions.[7]

Regardless of whether particles are administered perorally or parenterally, hydrodynamic forces will act on them. The peristaltic motion in the gastrointestinal tract leads to streaming velocities of $\sim 90 \mu\text{m s}^{-1}$ in the jejunum and $\sim 60 \mu\text{m s}^{-1}$ in the ileum respectively.[385] As compared to these values the flow velocities in the circulatory system are considerably higher (Table 8). Characteristically, blood flow velocity correlates with the vessel diameter. While the velocities are clearly lowest in the capillary system they concurrently increase with increasing vessel size in the arterial and venous system.[386] Interestingly, in tumors this correlation is lost due to the morphologically aberrant vasculature.[388] Colloidal drug carriers in a certain size range are preferentially retained in tumor tissue due to the EPR effect.[389] However, it has to be highlighted that this is not a static and general but rather than that inter- and intratumorally varying characteristic.[390] While vessel permeability changes over time, tumor growth also leads to compression of the intratumoral vasculature which consequently reduces blood supply.[391] Thus, tumor targeting rationales might not be efficient in a multitude of cases if they are exclusively based on abnormalities in microvascular flow and vessel permeability.[392]

A direct comparison of the physiological flow rates in the circulatory system with the gastrointestinal tract is not entirely meaningful due to the different size scales of the systems. In order to be able to better compare the flow rates despite the different diameters of blood vessels and the intestine, the shear rate γ can be employed. For a Newtonian fluid flowing in a pipe, γ can be calculated according to 2.1

$$\gamma = \frac{8v}{d} \quad (2.1)$$

with v as the fluid velocity and d as the inside diameter of the pipe. Accordingly, the effective shear rate under normal conditions in the small intestine is about 0.01 s^{-1} and thus clearly lower when compared with the circulatory system (Table 8). These calculations are estimates since mucus [393] and chyme behave non-Newtonian and blood is not Newtonian either until shear rates higher than 100 s^{-1} are applied. Based on the shear rate γ the shear stress τ can be calculated which is

Table 8: Diameter, flow velocity and total cross sectional area of blood vessels of the human body

VESSEL TYPE	DIAMETER ^a [mm]	FLOW VELOCITY [mm s ⁻¹]	TOTAL CROSS SECTIONAL AREA ^b [mm ²]	SHEAR RATE [s ⁻¹]
elastic arteries	>10	300 ^b	530 ^c	~ 250
muscular arteries	0.1 - 10		2000	
arterioles	0.01 - 0.1	≥30 - 5 ^d	50000 - 70000	~ 2000 - 4000
capillaries	0.004 - 0.01	0.2 - 1 ^b	350000	~ 400 - 800
venules	0.01 - 0.1	≤1 - ≥10 ^d	260000	~ 800
veins	0.1 - ≥1	40 - 60 ^b	4000 ^e	~ 500 - 3000

^a according to [386]

^b according to [387]

^c of the aorta

^d according to [388]

^e of large veins

a measure for the hydrodynamic force acting in the system. According to 2.2 τ depends on the shear rate and viscosity of the medium (η).

$$\tau = \gamma \eta \quad (2.2)$$

While the shear rates in the gastrointestinal tract seem negligible when compared with the circulatory system, the differences in shear stress are considerably lower. This is due to the fact that the different viscosities of mucus¹ or chyme and blood² respectively are accounted for. As mentioned previously, these considerations should only serve as approximations. Viscosity highly depends on shear rate.[393] Blood viscosity is dependent on hematocrit and has been shown to vary along the crosssection of vessels especially in tubes with diameters smaller than 500 μm . [395] Pertaining to colloidal drug carriers, shear rate and shear stress might be highly relevant parameters. In order for nano- and microparticles to release their payload in the body the colloids have to be retained for a sufficient period of time. In case of peroral delivery, particles will have to localize to cells lining the gastrointestinal tract. Subsequently, firm adhesion has to be established in the presence of peristalsis which mixes the luminal contents. If particles can not reach or bind to the lining cells, they will be removed by mucus shed. Similarly, upon parenteral administration particles will be affected by blood or lymph flow. Most likely the hydrodynamic forces occurring in either system will affect adhesion of the particulate drug carriers to vessel-lining tissue. This is underlined by theoretical and experimental particle binding studies on healthy and inflamed endothelium. Seminal contributions dealing with the effect of shear force on adhesion have been published by Goetz et al., [382, 396, 381] Lauffenburger et al., [397, 398] Hammer et al., [203, 287] and others. [399, 400]

Under stationary conditions which normally occur *in vitro* the deposition rate of particles onto cells primarily will be governed by sedimentation and diffusion. However, this will not occur in a similar fashion *in vivo* where extracellular material is in constant flux. As a consequence flow might not generally decrease the binding of particles to cells but also could enhance mass transport to the cell membrane in certain shear regimes. [401]

The circulatory system consists of an immense system of vessels with varying diameters. Collectively, the length of the blood vessels amounts to about 95000 km in children and about 160000 km in adults. An interesting fact in the face of current demographic developments is that with every additional kilogram of fat on top of the normal body weight, 650 km of vasculature are developed. [386] At large, this provides an immense inner surface area for adsorption of injected drug carriers which is further increased by the presence of blood cells. Similarly, diversification of the surface of cells lining the intestinal lumen and folding of the tissue generates a considerable adsorptive surface in the gastrointestinal tract. In the small intestine this amounts to an inner surface area of about 200 m^2 . It is unclear whether the flow in tissues with high cellular surface area will aid particle adsorption or antagonize it.

In addition to potential non-specific adsorption highly efficient filtration mechanisms remove colloids from the bloodstream. The primary

¹ up to 2000 mPa s [394], highly dependent on shear rate

² at hematocrit of 40: 2.7 mPa s at 37°C; plasma viscosity: 1.5 mPa s at 20°C; alternative reference: normal hematocrit at shear rate 100 s^{-1} : 4 mPa s [395]

organs for particle sequestration are the liver and spleen. Uptake of particles in these organs is largely accomplished by cells of the RES which recognize colloids via adsorbed complement proteins, antibodies as well as other serum proteins ³.^[261, 262] While particle sequestration mainly relies on phagocytosis, a complementary mechanism based on hydrodynamic filtration in the liver has been discussed.^[256] According to this hypothesis, white blood cells serve as plungers which cause the filtration of material through fenestrations of liver capillaries into the space of Disse. This might further contribute to the liver functioning as a “sponge” which effectively removes colloids from the bloodstream.

Fluid flow in small tubes furthermore leads to counterintuitive phenomena. As a consequence of the Fahraeus effect, erythrocytes are not uniformly distributed over the vessel cross section. Rather, they accumulate in the center thus creating a cell-depleted layer of plasma at the vessel wall.^[395] In vessels larger than 30 μm , white blood cells are forced into this wall layer by collisions with erythrocytes. Thereby, the interaction of leukocytes with endothelial cells, especially in post-capillary venules, is enhanced.^[402] This leads to leukocyte rolling which is the first step in a cascade of events which finally enable the recruitment of immune cells to inflamed tissue areas. This intrinsic separation of cells by flow could certainly also affect the distribution of particles in the bloodstream. While a margination into the cell-depleted plasma layer could favour adhesion to endothelial cells, accumulation in the center might lead to interaction with erythrocytes.

Hydrodynamic forces acting on particles might result in an overcoming of colloidal repulsive forces.^[403] This could ultimately increase the likelihood of aggregate formation of injected particulate drug carriers, which might lead to vessel obstruction. Moreover, theoretical considerations indicate that shear forces acting on polymer particles or liposomes could result in deformation of the drug carriers and extrusion of the encapsulated payload.^[404] Similarly, carrier elasticity will influence passage of the particles through capillaries or fenestrations of the endothelium.

As illustrated by this certainly incomplete list, a variety of factors relating to flow will influence the performance of particulate drug carriers upon administration *in vivo*. However, the majority of *in vitro* studies dealing with the interaction between particles and cells are conducted under stationary conditions. Thereby, the complexity encountered in the human body is underestimated.^[7]

To be able to investigate the effects of flow in preclinical biopharmaceutical test systems *in vitro* and to integrate the obtained knowledge into the design of potential drug carrier systems, easy to handle and versatily adaptable techniques for flow generation have to be available. The main body of data on hydrodynamic shear effects has been generated in parallel plate flow chambers. Similar systems have more recently been made available in a simplified form for higher throughput⁴. Vessel-like models such as non-transparent hollow-fibers ^[405] and non-ionic surfactant microtubules also have been proposed for flow-related studies.^[406] Finally, recently developed microfluidic setups and alternative pumping techniques bear high potential for preclinical biopharmaceutical flow test systems.

³ see 1.1.2.4, section “Prolonged circulation time” for more details

⁴ <http://www.ibidi.de/>

2.1.2 Acoustically-driven microfluidics

Waves on the surface of a solid already have been described theoretically by Lord Rayleigh in 1885 as to their relation to earthquakes.[407] In the meanwhile it has become possible to generate SAW on the nanometer scale by use of chip technology. In a very effective and controlled manner, these “nanoquakes” can be induced on piezoelectric materials. At this, interdigital electrode structures (Figure 27) deposited on a piezoelectric substrate serve as effective transducers. When an electrical signal of proper frequency is applied to the transducer, a periodic deformation of the underlying crystal surface is induced via the inverse piezoelectric effect.[9] As illustrated in Figure 23 the resulting SAW

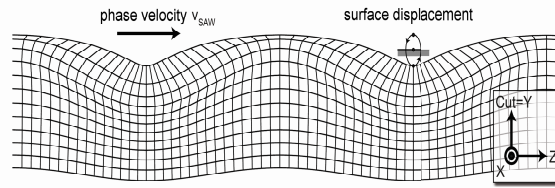


Figure 23: Surface deformation associated with surface acoustic wave (SAW). Image by courtesy of T. Franke, University of Augsburg

is characterized by subsequent regions of compressed and expanded material. All matter in the path of the SAW will be exposed to its energy propagating which is largely of mechanical nature. If a liquid is in contact with the substrate surface, the pressure difference exerted by the SAW will excite a longitudinal sound wave in the fluid.[8] Due to the differences in sound velocity between solid and liquid, the SAW couples into the liquid under a diffraction angle Θ_r according to 2.3

$$\Theta_r = \arcsin \frac{v_s}{v_f} \quad (2.3)$$

where v_s and v_f are the sound velocities in the solid and fluid respectively. [8] The acoustic radiation pressure associated with the SAW leads to the generation of pressure jets in the fluid (Figure 24) which



Figure 24: Dye at the interface between a piezoelectric substrate and a fluid is ejected by pressure jets of a surface acoustic wave (SAW). Image by courtesy of T. Franke, University of Augsburg

can be made use of for directional streaming. These jets constitute the force-generating mechanism of SAW-pumps for liquid streaming. The average force density exerted by the surface acoustic wave $\langle f_{SAW} \rangle$ can be calculated from the nonlinear term of the Navier-Stokes equation as

$$\langle f_{SAW} \rangle \approx \frac{-\rho(1 + \alpha_e^2)A^2\omega^2}{l} \quad (2.4)$$

where ρ is the density of the piezoelectric material, α_e a constant, l a characteristic decay length, ω the frequency, and A the amplitude of the wave. The amplitude A can be controlled by applying a voltage with sub-Angström precision to the interdigital transducers (IDTs). From 2.4 the corresponding force generated near the chip surface can be calculated using $\alpha_e \approx 2.46$, $l = 1$ mm, $\omega = 150 - 375$ MHz, and $\rho = 5 \times 10^3$ kg m⁻³. This leads to an average force $\langle F \rangle$ that can be calculated according to 2.5

$$\langle F \rangle \approx 0.9f^2A^2 \quad (2.5)$$

where f is the excitation frequency ($\omega = 2\pi f$) of the SAW on the substrate.

While SAW chips have been extensively used for RF signal processing and filtering purposes in the telecommunication industry as well as sensors,[408] several fields of application in fluid actuating have been reported recently. One of the main advantages of the chip-based technique is its high degree of miniaturization. This makes acoustic streaming well suited for processes involving small liquid volumes which are not easily handled by conventional pumping techniques. Successful implementation of SAW-pumps for droplet mixing,[9] microarray hybridization,[409] PCR in nL-volumes on a chip⁵,[410] and particle separation has been shown.[411, 412] If the chip surface is chemically patterned a SAW can be employed to actuate droplets on predefined tracks in a contact-free manner.[8] Furthermore, recently developed techniques for the production of microfluidic devices have allowed to channelize the flow generated by SAW-pumps.[413, 414] A combination of the latter with cell culturing would represent an advantageous approach for the mimicking of blood vessels, gastrointestinal as well as urinary tract and thus more generally speaking: physiological flow conditions *in vitro*. This application will be discussed further in the specific topics.

⁵ the interested reader is referred to <http://www.advalytix.com> for more information on already commercialized SAW-devices for biotechnology

2.2 SPECIFIC TOPICS

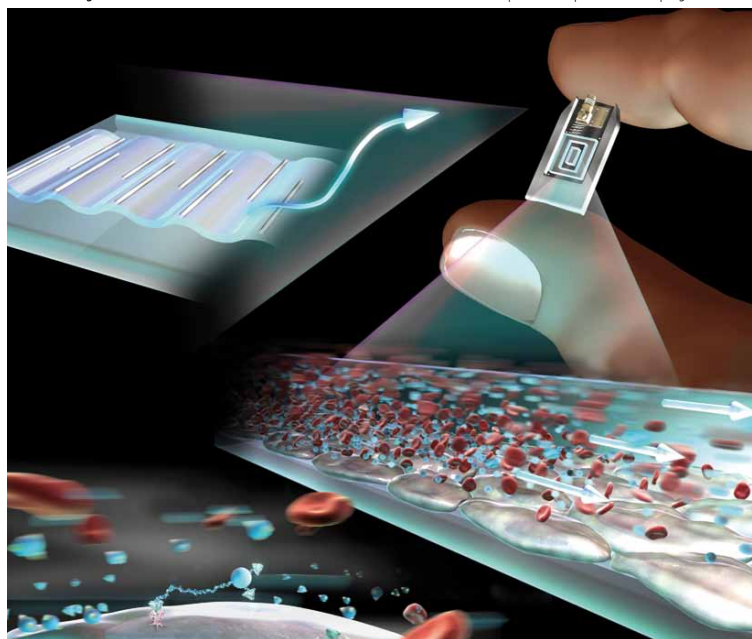
2.2.1 *An acoustically-driven biochip – impact of flow on the cell-association of targeted drug carriers*

Lab on a Chip

Miniaturisation for chemistry, physics, biology, & bioengineering

www.rsc.org/loc

Volume 9 | Number 19 | 7 October 2009 | Pages 2745–2860



ISSN 1473-0197

RSCPublishing

Gabor
Acoustic biochip

Whitesides
Multi-color microdroplet dye laser

Bashir
Heating on silicon FETs

Franke
Manipulation/mixing in vesicles

An acoustically-driven biochip – impact of flow on the cell-association of targeted drug carriers†

Christian Fillafer,^a Gerda Ratzinger,^a Jürgen Neumann,^b Zeno Guttenberg,^c Silke Dissauer,^a Irene K. Lichtscheidl,^d Michael Wirth,^a Franz Gabor^{*,a} and Matthias F. Schneider^b

Received 25th March 2009, Accepted 15th June 2009

First published as an Advance Article on the web 6th July 2009

DOI: 10.1039/b906006e

The interaction of targeted drug carriers with epithelial and endothelial barriers *in vivo* is largely determined by the dynamics of the body fluids. To simulate these conditions in binding assays, a fully biocompatible *in vitro* model was developed which can accurately mimic a wide range of physiological flow conditions on a thumbnail-format cell-chip. This acoustically-driven microfluidic system was used to study the interaction characteristics of protein-coated particles with cells. Poly(D,L-lactide-co-glycolide) (PLGA) microparticles ($2.9 \pm 1 \mu\text{m}$) were conjugated with wheat germ agglutinin (WGA-MP, cytoadhesive protein) or bovine serum albumin (BSA-MP, non-specific protein) and their binding to epithelial cell monolayers was investigated under stationary and flow conditions. While mean numbers of $1500 \pm 307 \text{ mm}^{-2}$ WGA-MP and $94 \pm 64 \text{ mm}^{-2}$ BSA-MP respectively were detected to be cell-bound in the stationary setup, incubation at increasing flow velocities increasingly antagonized the attachment of both types of surface-modified particles. However, while binding of BSA-MP was totally inhibited by flow, grafting with WGA resulted in a pronounced anchoring effect. This was indicated by a mean number of $747 \pm 241 \text{ mm}^{-2}$ and $104 \pm 44 \text{ mm}^{-2}$ attached particles at shear rates of 0.2 s^{-1} and 1 s^{-1} respectively. Due to the compactness of the fluidic chip which favours parallelization, this setup represents a highly promising approach towards a screening platform for the performance of drug delivery vehicles under physiological flow conditions. In this regard, the flow-chip is expected to provide substantial information for the successful design and development of targeted micro- and nanoparticulate drug carrier systems.

Introduction

Physiological and pathological processes such as the site-specific adhesion of platelets, leukocytes or metastasizing cancer cells are based on sophisticated mechanisms in order to efficiently function in the presence of hydrodynamic flow. Substantial knowledge about these processes has been generated by simulating physiological shear conditions with *in vitro* fluidic systems such as the parallel plate flow chamber (PPFC) and the radial flow detachment assay (RFDA).^{1–4} Although primarily aimed at understanding physiology, these fundamental studies also bear essential implications for the development of targeted colloidal drug carriers.^{1,5,6} Presently, the target effect of site-specific drug delivery systems is by default determined with *in vitro* cell binding assays under stationary conditions. However, regarding the extent and specificity of particle binding, recent reports have identified clear discrepancies between

the results obtained from stationary and more realistic, dynamic models of the *in vivo* environment.^{6–8} Particularly, the presence of substantial hydrodynamic drag forces upon application *in vivo* is expected to explicitly affect the deposition characteristics of ligand-coated particles.^{9,10} The most pronounced variations of flow conditions in the human organism are expected in the circulatory system. This is illustrated by effective shear rates ranging from 1 s^{-1} in wide vessels to 10^5 s^{-1} in small arteries.¹¹ Temporally high shear rates of about 400 s^{-1} also have to be expected in the urethra upon emission.¹² To attain preferential binding of the carrier to the diseased tissue in these environments, the size and ligand coating density of the colloids has to be adjusted according to the flow conditions as well as the expected receptor density and affinity at the target tissue.^{1,2,3} In order to be able to practically optimize these parameters of potential drug delivery vehicles, parallelizable *in vitro* bioassays have to be developed which offer the possibility of controllable flow generation. At this, increased experimental throughput is highly necessary in order to cope with the extensive amount of samples which have to be processed to generate sufficient data sets. Although well suited for specific questions, the PPFC and RFDA are of limited use for such applications. When multiple experiments are demanded at high reproducibility, the complexity of these methods' tubing and chambers becomes cumbersome to handle. Microfluidic pumping techniques might allow for approaching these shortcomings successfully. The most common methods to generate flow in miniaturized systems are thermophoresis (*via* Marangoni forces), electrochemical reactions,

^aDepartment of Pharmaceutical Technology and Biopharmaceutics, Faculty of Life Sciences, University of Vienna, A-1090 Vienna, Austria. E-mail: franz.gabor@univie.ac.at; Fax: (+43)-1-4277-9554; Tel: (+43)-1-4277-55406

^bUniversity of Augsburg Experimentalphysik I – Biological Physics Group, 86135 Augsburg, Germany. E-mail: matthias.schneider@physik.uni-augsburg.de; Fax: (+49)-821-598-3225; Tel: (+49)-821-598-3311

^cOlympus Life Science Research Europa GmbH, 81377 Munich, Germany

^dCell Imaging and Ultrastructure Research, Faculty of Life Sciences, University of Vienna, A-1090 Vienna, Austria

† Electronic supplementary information (ESI) available: Video S1, video S2, Fig. S3, Fig. S4 and Calculation S5. See DOI: 10.1039/b906006e

Christian Fillafer, Gerda Ratzinger, Jürgen Neumann, Zeno Guttenberg, Silke Dissauer, Irene K. Lichtscheidl, Michael Wirth, Franz Gabor, Matthias F. Schneider. An acoustically-driven biochip - impact of flow on the cell-association of targeted drug carriers. *Lab on a Chip*, 9:2782-2788, 2009.

2.2.1.1 Abstract

The interaction of targeted drug carriers with epithelial and endothelial barriers *in vivo* is largely determined by the dynamics of the body fluids. To simulate these conditions in binding assays, a fully biocompatible *in vitro* model was developed which can accurately mimic a wide range of physiological flow conditions on a thumbnail-format cell-chip. This acoustically-driven microfluidic system was used to study the interaction characteristics of protein-coated particles with cells. PLGA microparticles ($2.9 \pm 1 \mu\text{m}$) were conjugated with wheat germ agglutinin (WGA-MP, cytoadhesive protein) or bovine serum albumin (BSA-MP, non-specific protein) and their binding to epithelial cell monolayers was investigated under stationary and flow conditions. While mean numbers of $1500 \pm 307 \text{ mm}^{-2}$ WGA-MP and $94 \pm 64 \text{ mm}^{-2}$ BSA-MP respectively were detected to be cell-bound in the stationary setup, incubation at increasing flow velocities increasingly antagonized the attachment of both types of surface-modified particles. However, while binding of BSA-MP was totally inhibited by flow, grafting with WGA resulted in a pronounced anchoring effect. This was indicated by a mean number of $747 \pm 241 \text{ mm}^{-2}$ and $104 \pm 44 \text{ mm}^{-2}$ attached particles at shear rates of 0.2 s^{-1} and 1 s^{-1} respectively. Due to the compactness of the fluidic chip which favours parallelization, this setup represents a highly promising approach towards a screening platform for the performance of drug delivery vehicles under physiological flow conditions. In this regard, the flow-chip is expected to provide substantial information for the successful design and development of targeted micro- and nanoparticulate drug carrier systems.

2.2.1.2 Introduction

Physiological and pathological processes such as the site-specific adhesion of platelets, leukocytes or metastasizing cancer cells are based on sophisticated mechanisms in order to efficiently function in the presence of hydrodynamic flow. Substantial knowledge about these processes has been generated by simulating physiological shear conditions with *in vitro* fluidic systems such as the PPFC and the radial flow detachment assay (RFDA).[\[381, 415, 382, 416\]](#) Although primarily aimed at understanding physiology, these fundamental studies also bear essential implications for the development of targeted colloidal drug carriers.[\[381, 382, 287\]](#) Presently, the target effect of site-specific drug delivery systems is by default determined with *in vitro* cell binding assays under stationary conditions. However, regarding the extent and specificity of particle binding, recent reports have identified clear discrepancies between the results obtained from stationary and more realistic, dynamic models of the *in vivo* environment.[\[363, 384, 417\]](#) Particularly, the presence of substantial hydrodynamic drag forces upon application *in vivo* is expected to explicitly affect the deposition characteristics of ligand-coated particles. The most pronounced variations of flow conditions in the human organism are expected in the circulatory system. This is illustrated by effective shear rates ranging from 1 s^{-1} in wide vessels to 10^5 s^{-1} in small arteries.[\[418\]](#) Temporally high shear rates of about 400 s^{-1} also have to be expected in the urethra upon emission.[\[419\]](#) To attain preferential binding of the carrier to the diseased tissue in these environments, the size and ligand coating density of the colloids has to be adjusted according to the flow condi-

tions as well as the expected receptor density and affinity at the target tissue.[381, 415, 287] In order to be able to practically optimize these parameters of potential drug delivery vehicles, parallelizable *in vitro* bioassays have to be developed which offer the possibility of controllable flow generation. At this, increased experimental throughput is highly necessary in order to cope with the extensive amount of samples which have to be processed to generate sufficient data sets. Although well suited for specific questions, the PPFC and RFDA[384, 7, 400] are of limited use for such applications. When multiple experiments are demanded at high reproducibility, the complexity of these methods' tubing and chambers becomes cumbersome to handle. Microfluidic pumping techniques might allow for approaching these shortcomings successfully. The most common methods to generate flow in miniaturized systems are thermophoresis (via Marangoni forces), electrochemical reactions, surface patterning methods, electro-osmosis, induced charge electro-osmosis as well as several mechanical pumping strategies.[420, 421] However, these techniques' suitability is limited for systems which are required to comply with cell growth and cell viability. For such applications a micropumping technology based on acoustic streaming might represent a highly promising alternative.[8, 422, 423, 424] This technique generates locally defined SAWs which, when coupled into liquid, result in a defined pressure gradient that can be utilized for streaming (Figure 25 A). In the work presented, the applicability of

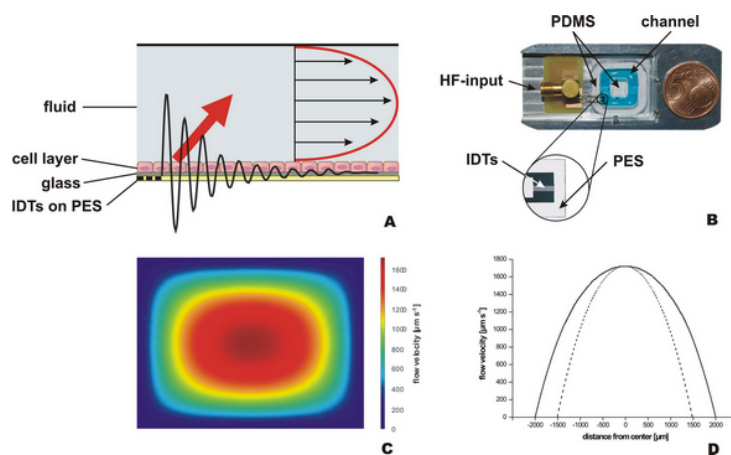


Figure 25: Interdigital transducers (IDTs) on a piezoelectric substrate (PES) generating SAWs which lead to the streaming of fluid over a cell monolayer in a liquid-filled channel (A). SAW-pump consisting of the high frequency connector (HF-input) and the IDTs on a PES which are annulated in the bottom left corner of the 3D-microchannel. A PDMS-cast attached to a glass coverslip confines a channel structure for the cultivation of cells (B, for disassembled view see Figure 26, for close-up view of IDTs see Figure 27). Cross section of the flow velocity profile generated in the channel shown in (B) by acoustic streaming (C). Horizontal (D, solid line) and vertical cut (D, dashed line) through (C).

this technology to controllably produce fluid flow in a miniaturized pharmaceutically relevant *in vitro* bioassay was tested. At this, the effect of shearing on the cell-association of protein-decorated particles was investigated using monolayer forming Caco-2 cells as a frequently used *in vitro* tissue model. Biocompatible PLGA microparticles conjugated with

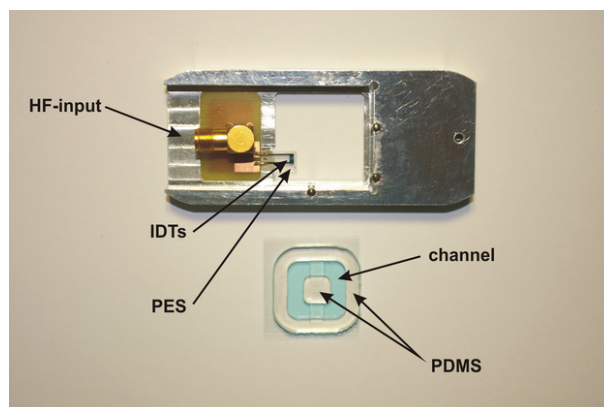


Figure 26: Acoustically-driven biochip and 3D-microchannel. Surface acoustic wave (SAW) pump consisting of the high frequency connector (HF-input) and piezoelectric substrate (PES) with interdigital transducers (IDTs).

fluorescence-labeled wheat germ agglutinin (F-WGA) and bovine serum albumin (F-BSA) served as representative targeted and non-targeted model drug carrier systems. The combination of human epithelial cells and surface-modified particles was chosen, since several studies have shown that decoration with WGA mediates binding to the pharmaceutically relevant Caco-2 cell line under stationary conditions.[285, 425] The extent of a targeting effect in the presence of low to moderate shear rates between 0.2 s^{-1} and 1 s^{-1} was investigated using the micropumping SAW-chip (Figure 25 B) to simulate flow conditions.



Figure 27: Interdigital transducers (IDTs). Bar represents 100 μm .

2.2.1.3 Results and discussion

THE ACOUSTICALLY-DRIVEN MICROFLUIDIC SYSTEM Similar to conventional flow assays such as the PPFC and RFDA, the biochip is based on a fluidic channel which is directly accessible during the experiment via microscopy. However, in contrast to the previously mentioned assays that are driven by external mechanical pumps, the developed microfluidic chip makes use of planar, non-invasive SAW-pumping for flow generation. IDTs structured on a piezoelectric substrate (Figure 25 B and 27) are excited when a high frequency signal is applied. This leads to deformation of the substrate and results in a surface acoustic wave. When the acoustic radiation pressure exerted by the SAW couples into a fluid, a pressure gradient is generated which leads to directional

streaming.[8, 422, 423, 424] Thereby, contamination-free pumping of liquid volumes as small as a few microliters can be realized at shear rates between 0.01 s^{-1} and 1000 s^{-1} depending on the system's geometry. As a consequence of the high frequency signal based generation of the SAW, the pumping performance is continuously actuated and varied via the parameters of a conventional signal generator (see video S1).[413] By channelizing the streamed liquid into 3D-microchannels, which are readily fabricated in almost arbitrary geometries by elastomeric molding, a flow chamber can be created. In this study, a rather simple $44 \text{ mm} \times 4 \text{ mm} \times 3 \text{ mm}$ (length \times width \times height) racetrack-format poly(dimethylsiloxane) (PDMS)-cast was used (Figure 25 B). The channel was dimensioned in such a manner that sufficient medium could be included for uncomplicated cell culturing of epithelial Caco-2 monolayers. Thus, the usually necessary transfer of a cell-covered substrate to the flow chamber or alignment of an elastomeric cast on the cultured cells can be avoided. However, the pumping technique is not limited to rectangular casts of this size, but can be easily adapted to drive flow in smaller structures with constrictions or bifurcations. Channels including the latter geometries could be exceptionally insightful tools for a realistic simulation of the complex vessel flow in the circulatory system.[7] At this, it is additionally helpful, that not only continuous flow modes can be accurately mimicked on the SAW-chip, but also precisely defined pulsed pumping is possible. While being hardly achievable with mechanical pumps, this streaming mode is controllably induced by amplitude modulation of the high frequency signal (see video S2). Thereby, the effects of pulsating flow combined with defined shear rates could be collectively investigated regarding their impact on distribution and adhesion processes in the branched circulatory system.[7] Besides its compliance with microfluidic channels, which allows for reducing the necessary amount of reagents to a minimum, the chip-based setup additionally bears the advantage of omitting tubing and connectors which are otherwise necessary to pipeline liquid within the system. Consequently, the dead volume associated with mechanical pumps is avoidable and the entire device can be downsized notably (Figure 25 B). This feature is essential, as it permits parallelization of several SAW-chips in one platform thus increasing the amount of samples which can be processed simultaneously. Even a setup with multiple SAW-pumps and channels in a microplate format is realizable, entailing the possibility of using microplate readers for analysis. Such an extension to more sensitive analytical methods could be a powerful tool to gain information on adhesion phenomena involving nanoparticles or proteins, since analyses based on microscopic imaging hit on their limits in this size regime.

CELL-BINDING OF SURFACE-MODIFIED MICROPARTICLES UNDER STATIONARY CONDITIONS To establish reference values for the experiments involving fluid flow, the extent of binding of BSA- and WGA-MP to Caco-2 monolayers was primarily determined in a stationary setup (flow velocity_{max} = $0 \text{ } \mu\text{m s}^{-1}$). For the used microparticles with a mean size of $2.9 \pm 1 \text{ } \mu\text{m}$ and a density of 1.28 g cm^{-3} a sedimentation controlled particle deposition is expected.[376] In the equilibrium state between frictional force and gravitation, settling of the colloids occurs with a constant z-velocity of $1.4 \text{ } \mu\text{m s}^{-1}$. Consequently, 83% of the ho-

mogenously distributed particles are assumed to deposit on the surface within 30 min leading to a maximum coverage of 3500 mm^{-2} . In practice, however, only $94 \pm 64 \text{ mm}^{-2}$ BSA-MP were detected after stationary loading (30 min), washing and stationary chase-incubation (30 min) (Figure 28, stars). The rather low number of cell-associated particles,

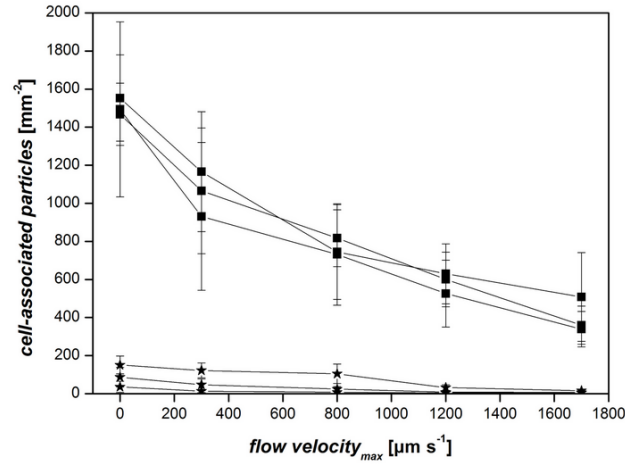


Figure 28: Mean number of WGA- (squares) and BSA-MP (stars) associated with Caco-2 monolayers after loading for 30 min at stationary conditions, washing and chase-incubation under stationary or flow conditions. Each set of data points was obtained from independent experimental series.

which corresponds to 3% of the theoretical load, can be explained by the reportedly low affinity of albumin-coated PLGA-particles to Caco-2 cells.[363, 285] Due to the lack of interactive strength the washing steps resulted in the detachment of all except a few non-specifically bound particles. In contrast, conjugation with WGA led to a clearly enhanced adhesion of colloids to the monolayer. This is in line with previous studies which have identified WGA as an agent for enhancing adhesion to Caco-2 cells. Following[426, 285] incubation under stationary conditions a mean number of $1500 \pm 307 \text{ mm}^{-2}$ cell-associated particles, which corresponds to 43% of the maximum load, were detected. This 16-fold increased interaction as compared to BSA-MP is explicitly illustrated in Figure 29 and can be attributed to specific binding of the lectin to membrane-associated N-acetyl-D-glucosamine and N-acetylneuraminic-acid residues.[427, 373] WGA-MP which had not bound to the cell membrane were removed in course of the washing steps.

IMPACT OF FLOW ON CELL-BOUND PARTICLES To investigate the effect of different shear rates on cell-associated BSA- and WGA-MP, stationary particle-loaded Caco-2 monolayers were chase-incubated under flow conditions. At this, acoustic streaming induces laminar fluid flow in the channel and thereby generates hydrodynamic forces acting on the attached microparticles. If the adhesive bonds break and do not re-establish elsewhere, the fluid flow transports the colloids to the coupling region of the SAW, where the considerable lift forces redisperse them in the channel cross-section. Consequently, most of these parti-

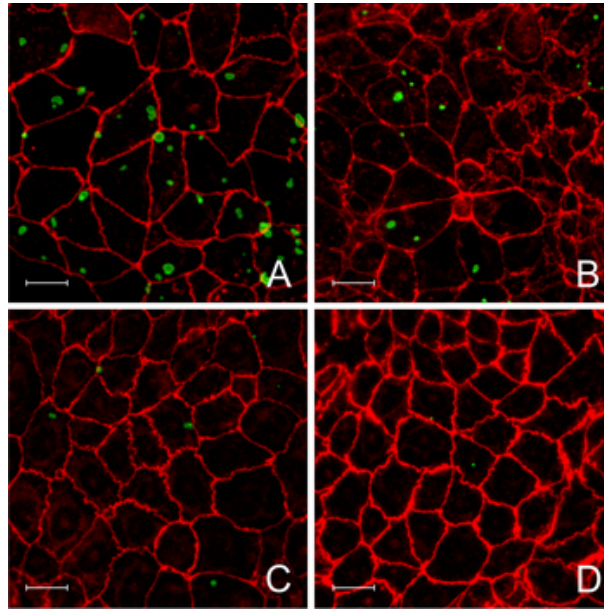


Figure 29: Cell-associated microparticles (green) after stationary loading, washing and chase-incubation under stationary conditions (flow velocity_{max} = 0 $\mu\text{m s}^{-1}$; WGA-MP (A); BSA-MP (C)). Same loading procedure but chase-incubation under flow conditions (flow velocity_{max} = 1700 $\mu\text{m s}^{-1}$; WGA-MP (B); BSA-MP (D)). Tight junction associated protein ZO-1 (red). Bar represents 20 μm .

cles are not available for reattachment to the cells. Using this setup, a shear rate dependent reduction of the number of cell-bound particles was monitored for both types of surface-modified colloids (Figure 28). While low shear rates (flow velocity_{max} = 300 $\mu\text{m s}^{-1}$ and 800 $\mu\text{m s}^{-1}$) led to the detachment of 30% and 50% respectively of the initially cell-associated BSA-MP, incubation at higher shear rates (flow velocity_{max} = 1200 $\mu\text{m s}^{-1}$ and 1700 $\mu\text{m s}^{-1}$) almost completely removed the albumin-conjugated colloids from the cell-surface (Figure 29 D). Obviously, the few BSA-MP, which were associated with the Caco-2 monolayer after stationary loading and washing, are characterized by low adhesivity which is not sufficient to anchor the particles in the presence of shear forces. In contrast, conjugation of microparticles with carbohydrate-binding protein not only led to higher cell binding under stationary conditions but also enhanced retention on the Caco-2 monolayer in the presence of flow (Figure 28, squares). This is illustrated by a mean number of $1057 \pm 351 \text{ mm}^{-2}$ and $400 \pm 168 \text{ mm}^{-2}$ monolayer-associated colloids at the lowest and highest flow velocity studied. Consequently, as compared with BSA-MP, WGA-MP were characterized by at least 17-fold increased retention over the whole range of flow velocities investigated. Interestingly, in the case of the highest shear rates, the effect of the lectin corona was even more pronounced as exemplified by 39-fold and 44-fold improved adhesion over albumin-conjugated colloids (Figure 29 C). Regarding reproducibility of the binding assays on the SAW-chip, it should be highlighted that the three data series for each particle type plotted in Figure 28 were obtained from separate experiments. The low deviation between the curves underlines the SAW-pump's ability to controllably and reproducibly generate flow in the 3D-microchannels, which is a crucial prerequisite that determines

the practical usability of the system. The standard deviation of each data point is comparable with those in similar studies and very likely a result of the image-based quantification combined with the cellular substrate inherent characteristics.[384] To minimize this, homogenous receptor-coated surfaces could be used, albeit at the cost of setting aside the complexly constituted cell membrane. Hence, when probing the interaction of targeted drug carriers with biological barriers, a substitution of the cell monolayer by an artificial substrate is not expedient since it reduces the relevance for comparisons with the *in vivo* conditions.[382, 384, 417] When studying isolated adhesion phenomena, however, the incorporation of precisely surface-engineered substrates is certainly realizable as well as preferable in terms of analytical accuracy.[287, 418, 383]

CELL-BINDING OF SURFACE-MODIFIED MICROPARTICLES UNDER FLOW CONDITIONS

Impact of flow on particle sedimentation in the channel. To estimate whether flow affects the calculated sedimentation rate of particles in the 3D-microchannels, the stationary condition was compared with streaming (Calculation S5). The experimental microfluidic setup is characterized by Reynolds numbers of $Re = 1$ and $Re = 6$ for the lowest and highest velocity respectively which indicates laminar flow. As determined by computational fluid dynamics simulations the flow profile in the channel is parabolic (Figure 25 C, D). Considering these conditions and that the images used for quantification of the adherent particles were taken in a small central region of the channel, the lateral y-component of the velocity was assumed to be widely independent from the vertical z-component. Therefore, a particle's trajectory in the flowing fluid contains components in the direction of flow (x) as well as in the vertical direction (z) with the former one depending on the latter. At the start of the experiment, the 3D-microchannels are filled with buffer containing 7.5×10^5 homogeneously distributed microparticles which sediment with a constant z-velocity. Upon engaging the flow, these particles are travelling for one channel length until again reaching the coupling zone of the SAW-pump where they are homogeneously redistributed over the cross-section of the channel. On each of these rotations, only particles below a critical height (z_{crit}) settle out on the cell monolayer. For a flow velocity_{max} (v_{max}) of $1700 \mu\text{m s}^{-1}$ the critical height z_{crit} is determined to be $224 \mu\text{m}$. Taking into account that the particle density in the channel decreases with duration of the experiment, 56% of the microparticles are expected to have deposited on the cell monolayer after 30 min. This corresponds to a theoretical surface coverage of 2400mm^{-2} which is clearly lower than that of 3500mm^{-2} under stationary conditions. Calculations also showed that the increased critical heights z_{crit} in the case of lower flow velocities (v_{max} from $300 \mu\text{m s}^{-1}$ to $1200 \mu\text{m s}^{-1}$) do not lead to higher deposition rates since their effect is widely levelled out by the proportionally lowered particle flux densities. Consequently, almost equal particle deposition rates on the cell monolayer would be expected under all investigated flow conditions if flow only had an effect on particle sedimentation. Any further deviations between the numbers of cell-associated particles at the different flow

conditions, however, would indicate an additional effect of flow on the particle–cell interaction.

Binding of BSA- and WGA-MP to epithelial monolayers under flow conditions. In order to investigate the binding of BSA- and WGA-MP from a streaming medium to epithelial model monolayers, the particle suspension was transferred to the 3D-microchannels and fluid flow was instantly engaged. As illustrated in Figure 30 (open symbols), incu-

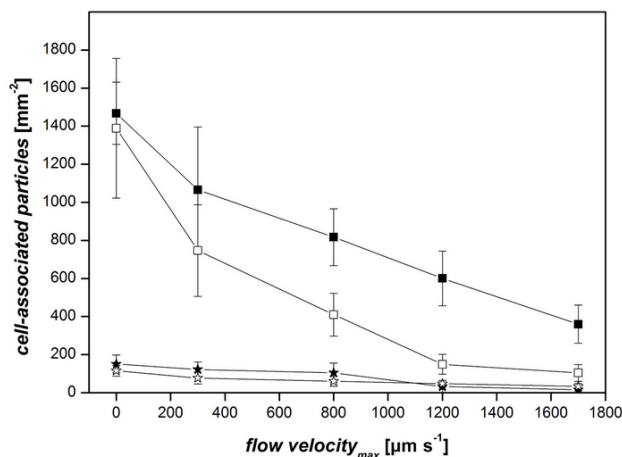


Figure 30: Mean number of WGA-MP (squares) and BSA-MP (stars) associated with Caco-2 monolayers upon incubation under stationary and flow conditions. Monolayers pre-loaded with microparticles for 30 min under stationary conditions (filled symbols). Direct incubation of microparticles with monolayers under stationary and flow conditions (open symbols).

bation under flow conditions led to clearly decreased cell binding of the ligand-conjugated colloids. Partially, this effect is inherent to the system and can be attributed to the previously discussed reduction of particle sedimentation due to the parabolic flow in the channel. Taking this into account and considering the binding potential of 3% and 43% as determined in the absence of hydrodynamic forces, a maximal surface coverage of 70 mm^{-2} and 1000 mm^{-2} is expected for BSA- and WGA-MP respectively under flow conditions. In case of the lowest shear force studied, this estimate seems quite realistic as illustrated by $77 \pm 31 \text{ mm}^{-2}$ and $747 \pm 241 \text{ mm}^{-2}$ respectively bound particles. However, aside from the generally lowered base deposition, the number of cell-bound colloids was additionally diminished by the antagonizing effect of flow on particle-surface bonds.[416, 287] For BSA-MP, increased hydrodynamic drag resulted in a nearly complete inhibition of the association with the Caco-2 monolayer. This is explicated by a marginal surface coverage of $34 \pm 16 \text{ mm}^{-2}$ cell-associated particles at the highest shear rate. Apparently, albumin-modified particles which are deposited on the monolayer under flow conditions do not notably interact with the cell membrane. Similar effects have been described in a recent study where a gas lift driven Ussing chamber setup was used to simulate the impact of flow on particle binding.[363] WGA-MP

exhibited higher binding in comparison to albumin-conjugated colloids at all investigated flow-conditions. The advantage of lectin-conjugation was clearest at low shear rates. However, even at the highest flow velocities studied at least threefold more particles associated with the cell monolayer as compared with BSA-MP. These observations lead to the conclusion that colloids lacking appropriate surface chemistry do not notably attach to the cell layer at relatively moderate shear rates ranging from 0.2 s^{-1} to 1 s^{-1} . When considering this combined with the very low cytoadhesion under stationary conditions, the use of BSA-MP as drug carriers is limited. The use of plain colloids for most pharmaceutically relevant applications has to be relativized even more due to the reportedly marginal cytoadhesion of unconjugated PLGA particles.[285] To efficiently compliment the advantageous biocompatibility and biodegradability of particles made from PLGA and similar polymers, surface modification with targeting ligands is essential. In this regard, however based on stationary studies, wheat germ agglutinin is a promising candidate to serve this purpose for peroral applications. Due to its carbohydrate binding properties, which mediate adhesion to enterocytes as well as mucus, a prolonged gastrointestinal residence time of sustained release drug carriers might be achieved.[363, 427, 5] Using the SAW-driven microfluidic device, it was possible to show that the interaction between WGA and the Caco-2 cell's glycocalyx is indeed sufficient to mediate the binding of $3 \text{ }\mu\text{m}$ -sized particles in the presence of low hydrodynamic drag. This observation further underlines the potential of wheat germ agglutinin for peroral delivery, where the peristaltic motion in the small intestine only generates rather low shear forces. However, the physiology and motility of the gastrointestinal tract is complex and not yet fully resolved, so this conclusion is only based on current estimates indicating shear rates of about 0.01 s^{-1} . [385] In the presence of higher flow velocities, the studied WGA-MP exhibit a propensity to detach from the cell monolayer, possibly limiting their applicability for delivery to the endothelium or urinary tract epithelium. This could be counteracted by using smaller particles in the nanometer size range, since the effective hydrodynamic drag forces decrease with particle diameter.[381] Moreover, conjugation of particles with alternative targeting moieties could lead to enhanced cytoadhesion in the presence of higher shear rates. In this regard, the underlying mechanisms of shear-activated proteinic ligands like the FimH subunit of Type-1 fimbriae of *E. coli* or von Willebrand factor might lead the way for the engineering of site-specific drug carriers that efficiently adhere under flow conditions.[419, 428]

2.2.1.4 Experimental

MATERIALS Sylgard® 184 Silicone Elastomer Kit was purchased from Baltres (Baden, Austria). Resomer® RG502H (PLGA, lactide/glycolide ratio 50:50, inherent viscosity 0.22 dL g^{-1} , acid number 9 mg KOH g^{-1}) was obtained from Boehringer Ingelheim (Ingelheim, Germany). F-WGA (molar ratio fluorescein/protein (F/P) = 2.9) from *Triticum vulgare* was bought from Vector laboratories (Burlingame, USA). F-BSA (F/P = 12), EDAC, NHS, and Pluronic® F-68 were purchased from Sigma Aldrich (Vienna, Austria). All other chemicals used were of analytical purity.

PREPARATION OF FUNCTIONALIZED MICROPARTICLES PLGA microparticles with a mean diameter of $2.9 \pm 1 \mu\text{m}$ were prepared by spray drying of a 6.5% (w/v) solution of PLGA in dichloromethane with a Buechi Mini Spray Dryer B-191 (Buechi, Flawil, Switzerland) as previously described.[426] For surface modification, 100 mg of the PLGA microparticles were suspended in 20 mM HEPES/NaOH buffer pH 7.0 (10 mL) and activated with solutions of EDAC (360 mg in 1.5 mL) and NHS (15 mg in 1 mL) in the same buffer for 2 h under end-over-end rotation at room temperature. In order to remove excess coupling reagent, the suspension was diluted threefold with HEPES and centrifuged (10 min, 2500 rpm, 4°C). The resulting pellet was resuspended in HEPES (10 mL). Upon addition of F-WGA (1.00 mg) and F-BSA (1.83 mg) respectively, end-over-end incubation was performed overnight at room temperature. The remaining active ester intermediates were saturated by addition of glycine (450 mg) in HEPES (6 mL) and further incubation for 30 min. Subsequently, the microparticles were washed three times by centrifugation (3200 rpm/10 min/4°C) and resuspension in HEPES (30 mL). After the last centrifugation step, the particles were suspended in a solution of 0.1% Pluronic® F-68 in isoHEPES (10 mL).

FABRICATION OF STERILE 3D-MICROCHANNELS Base (10 g) and curing agent (1 g) of the silicone elastomer kit were mixed in a test tube, vigorously stirred and evacuated for 30 min to remove gas bubbles. After pouring the liquid prepolymer into pre-structured aluminium molds and hardening over night at 70°C, the PDMS replicas were peeled from the master and placed on 24 x 24 mm (length x width) glass coverslips. Following assembly, the 3D-microchannels dimensioned 44 x 4 x 3 mm (length x width x height; see Figure 25 B) were transferred to glass Petri dishes and autoclaved for 50 min at 121°C (1 bar).

CELL CULTURE IN 3D-MICROCHANNELS The Caco-2 cell line was purchased from DSMZ (Braunschweig, Germany). Tissue culture reagents were obtained from Sigma (St. Louis, USA) and Gibco Life Technologies Ltd. (Invitrogen Corp., Carlsbad, USA). Cells were cultivated in RPMI 1640 cellculture medium containing 10% fetal bovine serum, 4 mM L-glutamine and 150 mg mL⁻¹ gentamycine in a humidified 5% CO₂/95% air atmosphere at 37°C and subcultured with Tryple Select from Gibco (Lofer, Austria). For the microfluidic experiments, each sterile 3D-microchannel was filled with 500 μL of Caco-2 single cell suspension (1.36×10^5 cells mL⁻¹) and cultivated under standard cell culture conditions until a confluent cell monolayer had formed.

PREPARATION OF SAW-CHIP LiNbO₃ slides (128°-cut-propagation) dimensioned 15 x 15 x 0.4 mm (length x width x height) were used as piezoelectric substrates. IDTs were structured on these slides by standard lithographic processes in order to predominantly generate (Rayleigh-mode) SAWs.[429] The used IDTs had 45 fingerpairs, an aperture of 400 μm and a periodicity of 25 μm, resulting in a resonance frequency of about 152 MHz (Figure 27). To enhance the resistance

against mechanical cleaning procedures, the fingers were additionally coated with a radio frequency (RF)-sputtered SiO₂ protective coating.

MICROPARTICLE–CELL INTERACTION STUDIES AT STATIONARY AND FLOW CONDITIONS For the interaction studies the BSA-MP and WGA-MP were suspended in isoHEPES at a concentration of 7.5×10^5 particles per 500 μL . Shortly before the experiment, the cell culture medium was removed from the 3D-microchannels and the monolayers were washed once with isoHEPES (500 μL). Subsequently, the microparticle suspension was added and the channels were covered with a glass coverslip. In order to grant efficient transmission of the SAWs, 50 μL of water were pipetted onto the piezoelectric chip as a coupling fluid before the 3D-microchannel was placed on top of it. This setup was mounted on a fluorescence microscope and connected to the high frequency generator, which had been configured to supply preset energy inputs corresponding to flow velocities of $0 \mu\text{m s}^{-1}$, $300 \mu\text{m s}^{-1}$, $800 \mu\text{m s}^{-1}$, $1200 \mu\text{m s}^{-1}$, and $1700 \mu\text{m s}^{-1}$ respectively. This corresponds to shear rates of 0.2 s^{-1} , 0.5 s^{-1} , 0.7 s^{-1} , and 1 s^{-1} respectively. Following incubation at either stationary or flow conditions for 30 min, the monolayers were washed three times with isoHEPES (500 μL) and embedded as described below. For an alternative set of experiments, monolayers loaded for 30 min under stationary conditions were washed and subsequently subjected to stationary or flow chase-incubation. After two additional washing steps with isoHEPES (500 μL) the PDMS-structure was peeled off. The glass coverslips with the adherent monolayers were embedded in a drop of FluorSave (Calbiochem, USA and Canada) and were stored at 4°C for 12 hours until further analyzed.

QUANTIFICATION OF CELL-ASSOCIATED MICROPARTICLES The embedded Caco-2 monolayers were analyzed on a Nikon Eclipse 50i microscope (Nikon Corp., Japan) equipped with an EXFO X-Cite 120 fluorescence illumination system. A random series of non-overlapping fluorescence microscopic images ($n = 6$) was acquired over the channel area. At this, care was taken to analyze monolayer parts located in the centre of the 3D-microchannels, in order to allow for comparison of the experimental and theoretically calculated deposition rates. To grant comparability, the settings of the fluorescence lamp and exposure time were left constant during the data acquisition process. Finally, the number of cell-associated microparticles in every image was determined with the threshold-dependent automated particle analysis of ImageJ (NIH, USA). The number of cell-associated particles represents the mean value which was calculated from the images acquired in independent channels ($n = 2$).

ANTIBODY STAINING After incubation at stationary and flow conditions respectively, the monolayers were fixed with a 2% solution of paraformaldehyde for 15 min at room temperature and were washed with PBS (500 μL). Upon treatment with a 50 mM solution of NH₄Cl for 15 min and with a 0.1% solution of Triton X-100 for 10 min, the cells were washed again with PBS (500 μL). The tight junction associated protein ZO-1 was stained for 1 h at 37°C with a primary antibody (BD

Biosciences, San Jose, USA) diluted 1 : 100 in a 1% solution of BSA in PBS. Upon washing thrice with a 1% solution of BSA in PBS, the monolayers were incubated with a 1 : 100 dilution of a secondary Anti-Mouse Immunoglobulin-RPE antibody (Dako Denmark A/S, Glostrup, Denmark) for 30 min at 37°C. Finally, the cell layer was washed three times with a 1% solution of BSA in PBS and mounted in a drop of FluorSave.

2.2.1.5 Conclusion

Stationary binding assays have become the current standard in pre-clinical biopharmaceutical testing due to the rather simple handling and lack of alternative *in vitro* models. To approach this shortcoming, an acoustically-driven thumbnail-sized microfluidic chip was developed that can controllably and reproducibly generate flow in 3D-microchannels which are compatible with cell culture. This SAW-chip was used to investigate the binding properties of albumin- and wheat germ agglutinin-conjugated microparticles to an epithelial cell layer under flow conditions. As illustrated in the present work, the results obtained from binding assays under stationary conditions notably differ from those obtained in systems simulating the dynamic *in vivo* environment. It was found that non-targeted microparticles possess a very low propensity to bind and are detached in the presence of flow, while conjugation with WGA led to a distinctly improved adhesion of particles to the cell-layer at shear rates ranging from 0.2 s^{-1} to 1 s^{-1} . In conclusion, these results clearly underline the importance of surface functionalization for the design of nano- and microparticulate drug delivery vehicles. Elaborate models of the *in vivo* conditions are necessary in order to realistically predict and optimize the performance of such systems prior to animal studies. In this context, the developed microfluidic SAW-chip is expected to provide a highly versatile platform for an investigation of flow-associated effects on particle–cell adhesion processes. Fundamental information distilled from studies using this technology will deeply benefit the engineering of artificial drug carrier systems which perform with high efficiency in the dynamically complex physiological environment.

Acknowledgements

The authors thank U. Länger and Y. X. Wang for help with preparation of the microspheres, Rohde&Schwarz GmbH for assistance with the high frequency generator and K. Sritharan, S. Nuschele for helpful discussions. Financial support by the Deutsche Forschungsgemeinschaft DFG (SFB 486, SPP 1313 and SCHN 1077), Elite Netzwerk Bayern (IDK-NBT and CompInt), and the German Excellence Initiative via the Nanosystems Initiative Munich (NIM) is acknowledged. MFS was supported by the Bayerische Forschungstiftung and JN by the German government (BMBF). Parts of this work were supported by the CellPROM project, funded by the European Community as contract No. NMP4-CT-2004-500039 under the 6th Framework Programme for Research and Technological Development in the thematic area of “Nanotechnologies and nanosciences, knowledge-based multifunctional materials and new production processes and devices”. The contribution reflects the author’s views and the community is not liable for any use that may be made of the information contained therein.

Electronic supplementary information

Calculation 5. Calculation of sedimentation rate

The calculation of the critical height for particle sedimentation (z_{crit}) is based on a parabolic flow velocity profile $v_x(z)$ (2.6) which is justified by numerical simulation.

$$v_x(z) = a \cdot z^2 + b \cdot z + c \quad (2.6)$$

The sedimentation of a microparticle is primarily affected by gravity. Stoke's law leads to a constant sedimentation velocity (v_z) which leads to a linear diminution of the particles' z -position in the 3D-microchannel (2.7).

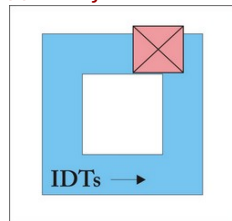
$$z(t) = z_0 - v_{\text{sed}} \cdot t \quad (2.7)$$

Upon substitution of z in (2.6) with $z(t)$, an expression $v_x(z_0; t)$ is obtained. Time integration from zero to τ leads to (2.8) with $\alpha = av_{\text{sed}}^2$, $\beta = 2az_0v_{\text{sed}} + bv_{\text{sed}}$, $\gamma = bz_0 + c + az_0^2$.

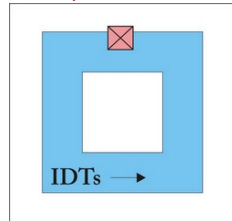
$$x(\tau) = \frac{\alpha}{3}\tau^3 + \frac{\beta}{2}\tau^2 + \gamma\tau \quad (2.8)$$

When a particle is deposited on the surface at time τ , $z(\tau)$ (2.7) will be zero. Shifting round, we can substitute τ with $\frac{z_0}{v_{\text{sed}}}$. Since it is assumed that the SAW leads to a homogeneous redistribution of the microparticles near the IDTs, sedimentation has to occur within one cycle corresponding to the length of the channel L . Therefore, a third order equation for z_0 has to be solved which leads to the critical height z_{crit} . It turns out that the number of deposited particles should be independent from the maximum value of v_x . This estimation is only valid, as long as z_{crit} is below half the height of the channel.

Video 1. Variation of the fluid flow velocity in a 3D-microchannel by controlling the input power of the SAW-pump. Fluorescence labelled polystyrene beads (3 μm , Polysciences Inc., Germany) were used as indicators of flow. Observation with a Nikon Labophot microscope (magnification 2x) equipped with a low light sensitive video camera (Photonic Science); recording on digital video tape (Sony). <http://www.youtube.com/watch?v=hmM98T3Nqkk>



- Video 2. Generation of constant and pulsating fluid flow in a 3D-microchannel by amplitude modulation of the high frequency signal. No modulation (“no pulse”), modulation of the signal amplitude with 0.5 Hz (“pulse frequency: 30 min⁻¹), 1 Hz (“pulse frequency: 60 min⁻¹) and 2 Hz (“pulse frequency: 120 min⁻¹). Fluorescence labelled polystyrene beads (3 μm, Polysciences Inc., Germany) were used as indicators of flow. Observation with a Nikon Labophot microscope (magnification 4x) equipped with a low light sensitive video camera (Photonic Science); recording on digital video tape (Sony). <http://www.youtube.com/watch?v=kBzdqh4GkRM>



2.2.2 A SAW-platform for parallelized microfluidic applications

2.2.2.1 Setup of the chip and system

In order to integrate flow as a standard parameter into preclinical biopharmaceutical test systems, flow models have to be available which grant reproducibility, versatile applicability and acceptable throughput. Classical flow systems widely depend on tubing for transport of the medium between a reservoir and the flow channel. In order to achieve parallelization, additional tubing or pumps have to be introduced which notably increases the complexity of the setup. This can be circumvented with SAW-modules. As a consequence of the different operation principle, which enables direct pumping of liquid in the channel, no tubing is needed. Moreover, the parallelization of SAW-pumps will be facilitated due to the fact that transducer structures and electrode connections on a chip require very little space. To make use of these advantages and to illustrate feasibility of the concept, a SAW-platform was developed which can be used to pump liquid in four microfluidic channels in parallel (Figure 31). At this, four IDTs were glued into a prestructured



Figure 31: Platform with four integrated SAW-pumps for flow studies in microchannels.

aluminium block and were connected with ports for cabling. Holes in the aluminium block allow microscopic observation with inverted or upright microscopes during flow experiments. The system is operated via a radio frequency generator (SMB100A, Rohde&Schwarz GmbH, Austria) connected in series to a coaxial amplifier (LZY-1, Mini Circuits, Brooklyn, USA) and a fixed attenuator (VAT-3W2+, Mini Circuits, Brooklyn, USA). Finally, the RF signal is distributed to the four IDTs by a 4-way divider (D1572-102, Werlatone, Brewster, USA).

The setup of the microchannels used for the flow experiments can be based on the work described in 2.2.1. However, instead of attaching the PDMS microchannels on glass coverslips with a size of 24 x 24 x 0.1 mm (length x width x height, Figure 26), four channels are placed on a glass plate dimensioned 127 x 85 x 1.1 mm (length x width x height). This allows for a high degree of versatility with channel structures since the size of the glass support does not limit the channel size. Moreover, the dimensions of the glass plate match the dimensions of standard microplates. This allows for compatibility with microplate readers. Thereby the detection of channel-associated luminescence, absorbance or fluorescence is possible. This will represent a clear improvement over currently used detection techniques. Typically, quantification of

cell-bound analytes in flow chambers is achieved by counting from fluorescence microscopic images 2.2.1.4.[384] While being reliable, this method is time consuming and thus mainly applicable if the number of samples is small. Due to the compatibility with automated read-out the SAW platform is expected to fully harvest the advantages of parallelization. The geometry of the microchannels can be digitized and programmed into a microplate reader's software. Thereby, precise readout from predefined regions in the channels can be achieved within a minimum of time. Preliminary experiments with aqueous solutions of sodium fluorescein have shown that parallelized quantitative readout from different positions in the microchannels via fluorimetry is indeed possible. Since the glass plates used are fully transparent and optically high grade, it is to be expected that similar detection limits as with conventional microplate assays can be attained.

2.2.2.2 Flow velocity measurements

In order to characterize if the four IDTs on the SAW-platform indeed operate constantly and comparably, the flow velocities generated in the different microchannels were monitored. This was accomplished by using fluorescence-labelled polystyrene microparticles (3 μ m, FluoresbriteTM, Polysciences Inc., Warrington, USA) as tracers of fluid flow. The flow velocity was determined in the center of the channel by measuring the translational velocity of the particles via fluorescence microscopy on a Zeiss Observer.Z1 microscope. As illustrated in Figure 32 a clear relation exists between the input power delivered to the SAW-pumps and the resulting flow velocities in the channels. The input power is given in [dBm] since this scale is preferable for adding up the power contributions of multiple components in the RF generation chain. Conversion to the commonly used [mW]-scale can be attained by substituting in 2.9

$$P = P_{ref} 10^{\frac{x}{10}} \quad (2.9)$$

where P is the power in [mW] P_{ref} is the reference power (1 mW) and x is the power in [dBm]. For the setup used in these experiments a range of total power inputs from 25 mW (14 dBm) to 1400 mW (31.5 dBm) was investigated. Every transducer is operated with a fourth of the total input power. This results in the generation of flow velocities between 0.3 mm s⁻¹ and 10 mm s⁻¹. As illustrated by the similar slopes of the curves for the individual IDTs, almost identical velocities were observed in the four 3D-microchannels after 15 min of operation (Figure 32, top graph). Upon continued streaming for 15 min, the velocities had not changed as illustrated in Figure 32 (bottom graph). This underlines that temporally constant flow velocities can be generated in parallel channels by integrating several SAW-pumps in a platform. Although higher input powers and thus higher streaming velocities are possible in principle, experimental problems occur at powers above 30 dBm. Due to the generation of radiative energy by the SAW the system heats considerably leading to evaporation of the water film which is used as a coupling medium between the chip surface and the glass plate. This drastically reduces the coupling efficiency of the SAW into the 3D-microchannels and can ultimately lead to the cessation of flow. Thus, the platform should primarily be operated up to a maximal input power of about 30 dBm. Input powers lower than 14 dBm can certainly be applied and will lead to flow velocities below 0.3 mm s⁻¹.

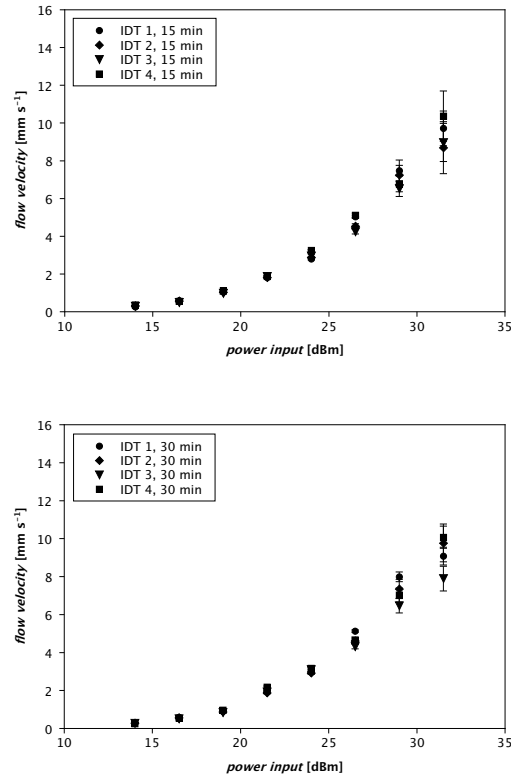


Figure 32: Flow velocities generated by four IDTs in microchannels on a SAW-platform for parallelized microfluidics. Channels 1-4 represent the respective microchannels arranged on top of the four IDTs of the chip (Figure 31). Flow velocities of $n=10$ particles per channel were determined after 15 min (top graph) and 30 min of operation (bottom graph).

In order to be able to routinely use the SAW-platform for flow experiments, reproducible generation of streaming has to be granted. A decisive parameter that might affect the reproducibility of flow generation by the SAW-pumps is the localization of the IDTs underneath the 3D-microchannels. This potential issue was accounted for in the chip architecture. Two framing bars were structured on the aluminium block which allow fixation of the glass plate which in turn ensures that the SAW-pumps are reproducibly positioned underneath the microchannels. As illustrated in Figure 33 this setup is indeed characterized by minimal variations of the generated flow velocities between experiments performed on different days.

Aside from the generation of flow in plain channels, the SAW-platform can certainly also be used for the generation of constant⁶ and pulsatile flow⁷ in cell-lined 3D-microchannels as described in 2.2.1.

2.2.2.3 Culturing of endothelial cells in 3D-microchannels

HUVECs represent an established *in vitro* cell model for endothelial cells which has been used for studies in flow chambers.[399] Since

6 constant flow of 6 μm sized fluorescent microparticles (orange) over a pre-confluent Caco-2 monolayer (green); <http://www.youtube.com/watch?v=VivswokWaGo>

7 pulsatile flow of 6 μm sized fluorescent microparticles (orange) over a pre-confluent Caco-2 monolayer (green); <http://www.youtube.com/watch?v=gggPiSwJY4I>

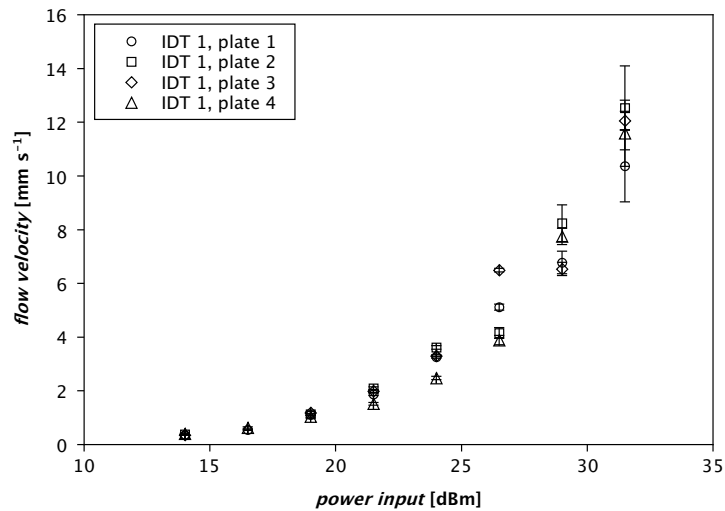


Figure 33: Flow velocities generated by one of the four IDTs of the SAW-platform in a microchannel on four different glass plates on consecutive days. Flow velocities of $n=10$ particles were determined after 15 min of operation.

HUVECs do not attach and proliferate on plain glass, standard coating techniques with gelatine (10 mg mL^{-1} in PBS), collagen (0.14 mg mL^{-1} in PBS), FBS and fibronectin (0.1 mg mL^{-1} in PBS) were investigated. Among the different proteins tested, fibronectin proved to be superior for mediating the binding of HUVECs to the glass substrate and for providing a suitable growth substrate for the cell monolayer (Figure 34).

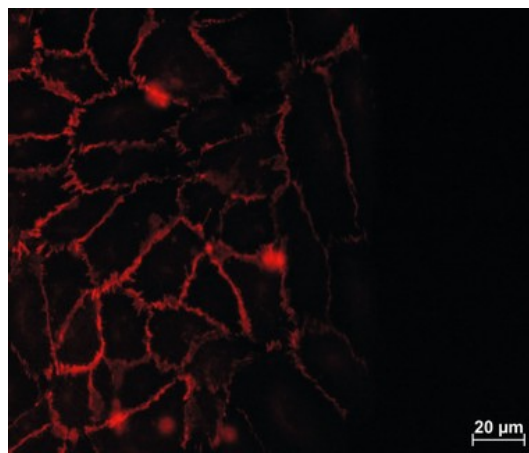


Figure 34: HUVEC monolayer grown in 3D-microchannels. VE-cadherin immunostained according to the procedure described in 1.2.3.2 (red). Note the border of the cell monolayer at the right as structured by the wall of the PDMS channel.

2.2.3 Transport studies under flow: metal grids as growth supports for cell monolayers

2.2.3.1 Potential improvements of currently used systems for permeation studies

Transport studies across cell monolayers *in vitro* are not only of interest for studying the processing of novel drug carrier systems by cells. Moreover, they are standard tools for determining permeation of drugs and prodrugs in the framework of the BCS. Typically, *in vitro* models for transport systems consist of an apical compartment which is separated from a basolateral compartment by a filter membrane. At this, the filter membrane serves as a growth support for cells which simulate the intestinal epithelial barrier *in vitro*. The entire cup-like device fits into a microplate well and thus is optimally suited for parallelization and high throughput. Transport experiments in microplates are frequently performed under stationary conditions. Regardless of the route of transport by which the drug permeates through the cell monolayer, its delivery from the apical medium to the cells will widely be controlled by diffusion. Systems for permeation studies which simulate peristaltic motion in the apical compartment might be beneficial. Thereby, the transport rate of drug molecules to the cell monolayer could be improved. As underlined by drug permeation studies with Caco-2 monolayers performed under stationary and dynamic conditions, higher permeabilities are attained indeed under dynamic conditions.[356]

Since SAW-modules can induce constant as well as at pulsatile flow (2.2.2.2, 2.2.1.3), they might be well suited for the generation of peristalsis-like motions in transport systems. Due to the chip-based nature of the pump a dynamic transport system could certainly be developed in similar if not smaller dimensions as those of currently available devices.

Another parameter which deserves consideration concerning the currently used systems for transport studies is the filter membrane. The essential function of the filter membrane is to provide a growth support for the cell monolayer. Several filter materials with a wide range of pore sizes are available. For transport studies with low molecular weight drugs filter membranes with pore diameters of 0.4 μm are mostly used. At this, different materials are characterized according to the filter membrane thicknesses (h_{pore}) and pore densities (β) (Table 9). In combination with the pore radius r_{pore} , these specific parameters determine the area available for filtration according to 2.10.

$$A_{\text{filtration}} = \beta(r_{\text{pore}}^2 \pi) \quad (2.10)$$

As can be deduced from Table 9 the filtration areas for 0.4 μm filters are in the range of 0.003 - 0.126 mm^2 per 1 mm^2 of filter membrane. This consequently amounts to a maximum filtration area of about 12.6 %. Similar orders of magnitude are calculated for filter membranes with pore radii of 1 and 3 μm respectively. In turn this means that more than 87% of filter material can not contribute to transport of drug molecules which pass across the cell monolayer. The situation is schematically illustrated in Figure 35. Moreover, it can be assumed that a gradient of transported drug molecules will build up inside the filter pores which leads to decelerated diffusion of analyte into the basolateral compartment.

Table 9: Comparison of commercially available filter materials for transport studies with metal grid

Pore size	Material	Membrane thickness (t_{pore}) [μm]	Pore density ^a (β)	Filtration area ($A_{\text{filtration}}$) ^a [mm ²]	Total surface area (A_{total}) ^a [mm ²]	Filter quotient (δ)
Transwell® System ^b						
0.4 μm transparent	PE	10	4×10^4	0.005	2.5	0.002
0.4 μm translucent	PC	10	1×10^6	0.126	14.3	0.009
3 μm transparent	PE	10	2×10^4	0.141	3.6	0.040
3 μm translucent	PC	10	2×10^4	0.141	3.6	0.040
ThinCert™ System ^c						
0.4 μm transparent	PET	22.6	2×10^4	0.003	2.6	0.001
0.4 μm translucent	PET	22.6	1×10^6	0.126	30.2	0.004
1 μm transparent	PET	22	2×10^4	0.016	3.4	0.005
3 μm transparent	PET	20	6×10^3	0.042	3.1	0.014
3 μm translucent	PET	20	2×10^4	0.141	5.5	0.026
metal grid						
25 μm mesh width	stainless steel	25 - 50	4×10^2	0.25	3.14	0.080

^a per 1 mm² of filter material

^b <http://www.corning.com/Index.aspx>

^c <http://www.greinerbioone.com/>

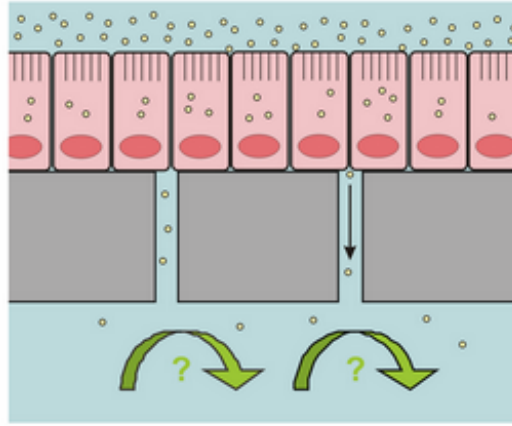


Figure 35: Transport of drug molecules from an apical compartment through a polarized cell monolayer grown on a filter membrane into a basolateral compartment. Insufficient filtration area due to low pore densities will result in the buildup of a concentration gradient inside the filter.

Adsorption of drug molecules to the polystyrene components of transport systems has been shown to bias results of permeability assays.[430] It is not clear from the literature to which extent substances are adsorbed by the filter material itself. However, it seems possible that upon transport across the cell monolayer a substantial amount of drug might be sequestered before it reaches the basolateral compartment. The surface area of the filter membrane available for adsorption A_{total} can be calculated from 2.11

$$A_{\text{total}} = A_{\text{out}} + A_{\text{pores}} \quad (2.11)$$

with A_{out} as the area of the apical and basolateral sides of the filter excluding $A_{\text{filtration}}$ according to 2.12

$$A_{\text{out}} = 2[r_{\text{filter}}^2 \pi - A_{\text{filtration}}] \quad (2.12)$$

and A_{pores} as the total surface area of the cylindrical pores that can be calculated from 2.13.

$$A_{\text{pores}} = \beta(2r_{\text{pore}} \pi h_{\text{pore}}) \quad (2.13)$$

r_{filter} and r_{pore} are the radii of the filter membrane and pore respectively. β is the number of pores per filter area and h_{pore} is the height of the pore which is equivalent to the membrane thickness. As illustrated in Table 9, appreciable A_{total} are obtained for several of the commercially available filter materials. In case of filters with 0.4 μm pore size and high pore densities, which are most frequently used for drug permeation studies, A_{total} amounts to about 14 and 30 mm^2 per 1 mm^2 of growth area. According to these rough estimates, a 24-well microplate insert with a growth area of about 33 mm^2 actually is characterized by a surface area of 4.5 and 10 cm^2 of filter material.

In order to facilitate comparison of $A_{\text{filtration}}$ and A_{total} between different types of filters, the filter quotient δ is introduced 2.14.

$$\delta = \frac{A_{\text{filtration}}}{A_{\text{total}}} \quad (2.14)$$

If adsorption of analyte to the filter material indeed poses a problem, suitable alternatives could be identified by choosing a filter with higher δ .

Individually or in combination the above discussed issues indicate that in addition to the cell layer the filter membrane used as growth support might constitute a barrier to drug permeation in transport studies.

2.2.3.2 Metal grids as high porosity growth supports for cell monolayers

Considering the above it is expedient to investigate potential alternatives to conventional filter membranes which could be integrated into a dynamic transport system. A high pore density metal grid with 25 μm mesh width (Bückmann GmbH, Mönchengladbach, Germany) might represent a suitable alternative. The metal grid is a comparably unexpensive woven stainless steel fabric which can be obtained in reproducible and large quantities. In terms of $A_{\text{filtration}}$ this material is superior to commercially available filter membranes (see Table 9).

To be able to compare the grid with filter membranes regarding the total surface area available for adsorption of drug, A_{grid} is calculated (2.16). A_{grid} can be obtained by treating each pore as an elementary cell which is lined by four half cylinders. At this, A_{cell} is the total surface area of the wire forming an elementary cell where r_{wire} is the radius of the wire and l is the height of one cylinder 2.15.

$$A_{\text{cell}} = 4 r_{\text{wire}} \pi l \quad (2.15)$$

$$A_{\text{grid}} = \beta A_{\text{cell}} \quad (2.16)$$

A_{grid} can be substituted for A_{total} in 2.14 to yield δ . δ of the grid can be directly compared with that of commercially available filters. From Table 9 it is deduced that the grid provides notable advantages over filters as illustrated by an at least 2-fold and 8-fold higher δ respectively as that of 3 μm and 0.4 μm pore size membranes.

To study if growth of a cell layer with characteristic transepithelial electrical resistance (TEER) can also be attained on a highly porous substrate, Caco-2 cell monolayers were cultivated on metal grids. To enable direct comparison with commercially available systems, the filter membrane was excised from a polystyrene cup of ThinCertTM 24-well inserts. Subsequently, a similar sized piece of metal grid was attached to the cup with Microset 101FF glue (Microset Products Ltd., Nuneaton, UK). Normally, Caco-2 cells with a diameter of 17 - 20 μm would pass through the pores of the grid upon seeding. To accumulate the cells on the wires, Caco-2 cells in RPMI-1640 medium (1.25×10^4 cells/120 μL) were pipetted into the apical compartment and importantly no basolateral medium was added for the first 24 hours of incubation. Thus, the Caco-2 cells sedimented towards the grid where a liquid-gas interface was formed due to the high surface tension. This led to complete deposition of the cells at or close to the wires where they had the possibility to attach to the stainless steel surface. Upon addition of 600 μL of medium to the basolateral compartment on the next day the cells were incubated for 14 days with exchange of the medium at regular intervals.

To assess if a confluent and potentially polarized cell monolayer with appropriate resistance had formed, the TEER and localization of tight-junction associated protein ZO-1 was investigated. At this, the TEER

was determined with chopstick electrodes of an EVOMX voltmeter (World Precision Instruments, Sarasota, USA). In the absence of cells the metal grid itself had a resistance of $75 \Omega \text{ cm}^2$ in plain medium. This is similar to $64 \Omega \text{ cm}^2$ of $3 \mu\text{m}$ transparent filter membranes (ThinCert™, Greiner Bio One, Kremsmünster, Austria). Upon incubation of Caco-2 cells for 14 days on the commercially available filter membrane a resistance of $533 \Omega \text{ cm}^2$ was observed. This indicates formation of a confluent monolayer with a TEER that is typically observed on filter membranes. Interestingly, comparable resistances of about $480 \Omega \text{ cm}^2$ were observed for Caco-2 cells grown on metal grids which indicates that a cell layer had formed. These results were underlined by immunostaining of ZO-1 which was consistently localized at the cell

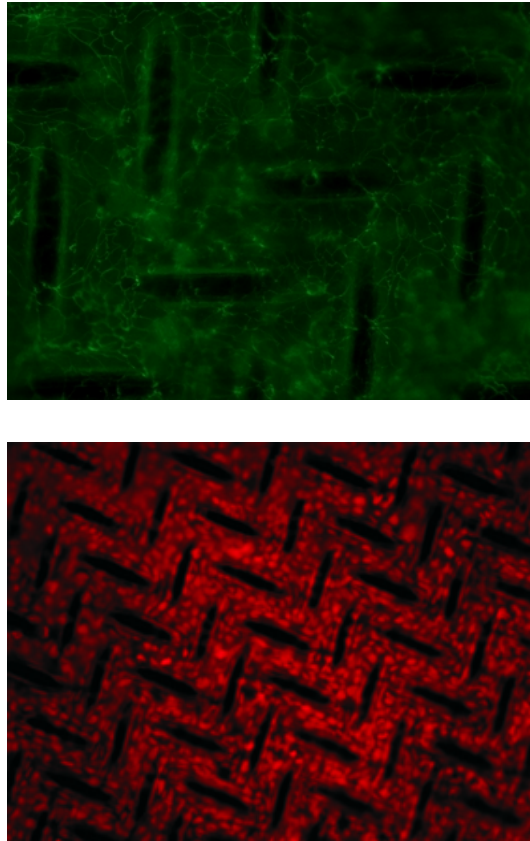


Figure 36: Caco-2 layer grown on metal grid with mesh width of $25 \mu\text{m}$. Tight-junction associated protein ZO-1 (green, top image) and cell nuclei stained with propidium iodide (red, bottom image). The steel wires appear as dark structures in the background.

borders (Figure 36, top image). This is characteristic for confluent Caco-2 monolayers (see Figures 19 and 29). Moreover, staining of the cell nuclei with propidium iodide illustrated that the Caco-2 cells indeed proliferate and form a confluent monolayer on metal grids (Figure 36, bottom image).

As illustrated by the presented experiments, cell growth can be attained on materials with high pore density and pore size. Future work will have to resolve if the Caco-2 layer on the metal grids is indeed a morphologically and functionally polarized tissue that can be used for permeation studies. Ultimately, the grid or similar materials

might represent highly beneficial alternatives as growth supports for transport studies in academic and industrial research.

CONCLUSIONS

Micro- and nanoparticles differ from small molecules in size by orders of magnitude. While this brings with it potential benefits, it at the same time represents the central challenge for their use in drug delivery.

Owing to their physical dimensions and surface properties, colloids are characterized by peculiar interactions with structures at the cellular, tissue as well as systemic level. These properties can be masked or intensified by appropriate engineering of the particle structure and particle surface functionality. One of the fundamental aims of drug delivery research is to harvest this potential in order to achieve specific or nonspecific bioadhesion of micro- and nanoparticles.

A variety of strategies have been employed to modify the interaction properties of particles with cells.[4, 360] The rationales involved and techniques employed for this purpose were reviewed in the present thesis for particles made from the biodegradable and biocompatible polymer PLGA. Generally, to achieve cytoadhesion the chemical properties of the cell membrane can be exploited. All eukaryotic cells are negatively charged on their surface.[6] Moreover, in regenerating tissue and upon malignant transformation the density of charged moieties in the plasma membrane is altered.[379, 378] This ubiquitary existence of anionic groups suggests that the introduction of opposite charges at the surface of particles will increase their binding potential for the cell membrane. Since cell surfaces are negatively charged, particles coated with cationic polyelectrolytes are expected to exhibit increased interactions. However, as illustrated by the experimental data in the present thesis, this rationale is not generally applicable. In contrast to literature reports, it was found that the specificity and quantity of binding do not generally correlate with particle surface charge. Positively charged micro- and nanoparticles were characterized by a 3-fold and 5-fold higher binding to artificial intestinal epithelium as compared to their negative counterparts. In contrast, no differences between the interaction properties of positively and negatively charged colloids were observed on primary endothelial cells. Accordingly, the approach of improving bioadhesion by introduction of positive surface charges has to be relativized. This only seems to be possible for certain cell types.

In terms of specificity, bioadhesion mediated by biorecognition is superior over ionic interactions. In principle, any molecules in or associated with the cell membrane which are sterically accessible can serve as potential targets. Membrane-associated carbohydrates, which at large make up the cellular glycocalyx, can be addressed with lectins.[5] WGA, which is a representative of this class of proteins, specifically binds to N-Acetyl-D-glucosamine and N-acetylneuraminic acid. As illustrated by histological ultrastructure studies in the present thesis, WGA is characterized by advantageous interaction properties with epithelial monolayers. Once bound to the apical membrane, WGA is quickly internalized via endosomes which subsequently fuse with multivesicular bodies. Interestingly, a considerable amount of the internalized lectin is transported to the lateral and basolateral side of the cell membrane within relatively short timescales. In combination

with previous reports in the literature this indicates that conjugation of drugs or prodrugs with WGA represents a potent approach for shuttling poorly bioavailable molecules across the intestinal epithelial barrier. In addition, at least the cytoadhesive properties of WGA could be transferred to particulate drug carriers. Since WGA is a dimeric protein with two high affinity and two low affinity binding sites for the complementary carbohydrates, it is well suited for the conjugation with micro- and nanoparticles. Independent of the orientation of the immobilized molecule on the particle surface it is likely that at least one binding pocket will be available for interaction with sugar residues of the glycocalyx. These considerations were experimentally corroborated in the present thesis. By using nanoparticles that had been labelled with the fluorophore BOD, the bioadhesive effect resulting from surface modification with ligands can be detected at a highly sensitive level. When conjugated with WGA, these particles are characterized by 73-fold increased binding to epithelial cells as compared to plain colloids. Moreover, inhibition experiments with the complementary carbohydrate N,N',N''-triacetylchitotriose demonstrated that at least 90 % of the particles are bound via specific lectin-sugar interactions. These findings underline that lectins in general and WGA in particular can serve as mediators of bioadhesion when immobilized on the surface of particles.[5, 431] This potential could be further exploited for targeted delivery of drug carriers, since the quantitative and qualitative composition of the glycocalyx differs between cell types and is altered upon malignant transformation.[351]

Generally, the total affinity of the particles for a tissue is the essential factor which determines if binding will occur and be sustained. The affinity required for firm attachment of a particle to a specific tissue will widely depend on the local microenvironment. In this regard, shear forces might play a decisive role.

In the gastrointestinal lumen, a viscous mass of chyme and mucus is transported by directional flow due to peristalsis. Upon peroral administration, particulate drug carriers will have to firmly bind to cells lining the intestinal tract in order to resist premature removal from the body by this mechanism. Similar considerations apply to parenterally administered drug carriers. Particularly in case of i.m., s.c. and i.p. injection particles have to bind to cells at or close to the site of injection. Otherwise, the colloids will be distributed in the body by lymph- and bloodstream. While this might allow translocalization to distant tissue sites, it also increases the probability of sequestration of the particles by the liver, spleen or other parts of the RES.[262, 254] The mechanisms which will influence the behavior of micro- and nanoparticles during these dynamic processes are not entirely clear. However, it is very probable that hydrodynamic effects take a substantial part.[7] Systematic studies dealing with the effect of flow on particles themselves and on their interaction with cells have to be conducted in order to better understand its impact on drug delivery. A microfluidic flow model for this purpose was developed in the present thesis. The controlled actuation of fluid in this system is achieved by a chip-based planar SAW-pump.[8, 9, 413] In contrast to conventional flow chambers, no tubing is needed due to the contact-free pumping principle. This allows for a high degree of miniaturization of the device. Moreover, it facilitates parallelization as was successfully demonstrated by integration of multiple SAW-pumps in one platform. The system is fully

compatible with tissue culture. This was achieved by use of polymeric microchannels in which tissues can be cultivated. The latter was successfully demonstrated for epithelial and endothelial monolayers. Amongst other potential applications, this chip-tissue hybrid can be used to study the effects of flow on the bioadhesion of drug carrier systems. As indicated by data presented in this thesis, hydrodynamic shear forces indeed reduce the binding of surface-modified microparticles to cell monolayers. WGA-conjugated particles (diameter $\sim 3 \mu\text{m}$) pronouncedly interact with artificial intestinal epithelium under stationary conditions. In the presence of hydrodynamic drag, however, a shear rate dependent reduction of binding was observed. Similar observations were made by others with particles targeted to inflamed endothelium.[399, 382] Collectively, these results underline the influence of shear forces on the adhesion process of particles to cells. In the face of this, the current practice of conducting bioadhesion assays under stationary conditions *in vitro* has to be scrutinized.

It is important to highlight that the physical size of particles will influence their exposure and thus susceptibility to shear forces.[381, 399] Particles in the nanometer range are expected to be considerably less influenced by hydrodynamic drag. It needs to be clarified if this property constitutes one of the major advantages of submicron particles for drug delivery. As discussed herein, when assessing potential benefits of different particle sizes and particle types it will be expedient to account for the different deposition characteristics of colloids onto cells. This applies to *in vivo* as well as *in vitro* assays and includes possible influences of the environment on particle stability. The latter is especially relevant *in vivo* since protein adsorption as well as hydrodynamic effects likely lead to flocculation.[7, 432] Finally, it remains to be resolved if the particle surface properties that have been engineered and optimized *in vitro* are conserved upon administration *in vivo*.[433]

In conclusion, the results presented underline that surface functionalization with proteins and polyelectrolytes can improve the bioadhesion of micro- and nanoparticles. Integration of flow as a parameter in preclinical biopharmaceutical test systems is expected to allow more realistic estimates of the bioadhesive effects resulting from surface modification. This might ultimately facilitate the development of particulate drug carriers for medical conditions which are not efficiently addressable by conventional formulations.

Part III

APPENDIX

BIBLIOGRAPHY

- [1] C. Wischke and S.P. Schwendeman. Principles of encapsulating hydrophobic drugs in pla/plga microparticles. *International Journal of Pharmaceutics*, 364:298–327, 2008.
- [2] C.E. Astete and C.M. Sabliov. Synthesis and characterisation of plga nanoparticles. *Journal of Biomaterials Science Polymer Edition*, 17:247–289, 2006.
- [3] I. Bala, S. Hariharan, and M. N. V. R. Kumar. Plga nanoparticles in drug delivery: The state of the art. *Critical Reviews in Therapeutic Drug Carrier Systems*, 21(5):387–422, 2004. 864XY Times Cited:53 Cited References Count:117.
- [4] G. Ratzinger, C. Fillafer, V. Kerleta, M. Wirth, and F. Gabor. The role of surface functionalization in the design of plga micro- and nanoparticles. *Critical Reviews in Therapeutic Drug Carrier Systems*, 27(1):1–83, 2010.
- [5] F. Gabor, E. Bogner, A. Weissenboeck, and M. Wirth. The lectin-cell interaction and its implications to intestinal lectin-mediated drug delivery. *Advanced Drug Delivery Reviews*, 56(4):459–480, 2004.
- [6] J. N. Mehrishi and J. Bauer. Electrophoresis of cells and the biological relevance of surface charge. *Electrophoresis*, 23(13):1984–1994, 2002.
- [7] A. T. Florence. Nanoparticle flow: Implications for drug delivery. In V. P. Torchilin, editor, *Nanoparticles as drug carriers*, pages 9–27. Imperial College Press, London, 2006.
- [8] A. Wixforth. Acoustically driven planar microfluidics. *Superlattices and Microstructures*, 33(5-6):389–396, 2003.
- [9] T.A. Franke and A. Wixforth. Microfluidics for miniaturized laboratories on a chip. *ChemPhysChem*, 9(15):2140–2156, 2008.
- [10] F. Chen and D. Gerion. Fluorescent cdse/zns nanocrystal-peptide conjugates for long-term, nontoxic imaging and nuclear targeting in living cells. *Nano Letters*, 4(10):1827–1832, 2004.
- [11] X. Gao, Y. Cui, R.M. Levenson, L.W.K. Chung, and S. Nie. In vivo cancer targeting and imaging with semiconductor quantum dots. *Nature Biotechnology*, 22(8):969–976, 2004.
- [12] L. Brannon-Peppas and J.O. Blanchette. Nanoparticle and targeted systems for cancer therapy. *Advanced Drug Delivery Reviews*, 56(11):1649–1659, 2004.
- [13] G. Oberdörster, E. Oberdörster, and J. Oberdörster. Nanotoxicology: An emerging discipline evolving from studies of ultrafine particles. *Environmental Health Perspectives*, 113(7):823–839, 2005.

- [14] B.D. Chithrani, A.A. Ghazani, and W.C.W. Chan. Determining the size and shape dependence of gold nanoparticle uptake into mammalian cells. *Nano Letters*, 6(4):662–668, 2006.
- [15] M. P. Desai, V. Labhasetwar, E. Walter, R. J. Levy, and G. L. Amidon. The mechanism of uptake of biodegradable microparticles in caco-2 cells is size dependent. *Pharmaceutical Research*, 14(11):1568–1573, 1997.
- [16] M. P. Desai, V. Labhasetwar, G. L. Amidon, and R. J. Levy. Gastrointestinal uptake of biodegradable microparticles: Effect of particle size. *Pharmaceutical Research*, 13(12):1838–1845, 1996.
- [17] M.P. Desai, V. Labhasetwar, G.L. Amidon, and R.J. Levy. Gastrointestinal uptake of biodegradable microparticles: Effect of particle size. *Pharmaceutical Research*, 13(12):1838–1845, 1996.
- [18] P. Jani, G. W. Halbert, J. Langridge, and A. T. Florence. Nanoparticle uptake by the rat gastrointestinal mucosa: Quantitation and particle size dependency. *Journal of Pharmacy and Pharmacology*, 42(12):821–826, 1990.
- [19] J. Rejman, V. Oberle, I. S. Zuhorn, and D. Hoekstra. Size-dependent internalization of particles via the pathways of clathrin- and caveolae-mediated endocytosis. *Biochemical Journal*, 377:159–169, 2004.
- [20] S.K. Lai, K. Hida, S.T. Man, C. Chen, C. Machamer, T.A. Schroer, and J. Hanes. Privileged delivery of polymer nanoparticles to the perinuclear region of live cells via a non-clathrin, non-degradative pathway. *Biomaterials*, 28(18):2876–2884, 2007.
- [21] C. Passirani and J.P. Benoît. *Biomaterials for Delivery and Targeting of Proteins and Nucleic Acids*. CRC Press, Boca Raton, 2005.
- [22] S.M. Moghimi. Modulation of lymphatic distribution of subcutaneously injected poloxamer 407-coated nanospheres: The effect of the ethylene oxide chain configuration. *FEBS Letters*, 540(1-3):241–244, 2003.
- [23] J.C. Neal, S. Stolnik, E. Schacht, E.R. Kenawy, M.C. Garnett, S.S. Davis, and L. Illum. In vitro displacement by rat serum of adsorbed radiolabeled poloxamer and poloxamine copolymers from model and biodegradable nanospheres. *Journal of Pharmaceutical Sciences*, 87(10):1242–1248, 1998.
- [24] J. A. Baker and J. C. Berg. Investigation of the adsorption configuration of poly(ethylene oxide) and its copolymers with poly(propylene oxide) on model polystyrene latex dispersion. *Langmuir*, 4:1055–1061, 1988.
- [25] T. Trimaille, C. Pichot, A. Elaissari, H. Fessi, S. Briancon, and T. Delair. Poly(d,l-lactic acid) nanoparticle preparation and colloidal characterization. *Colloid and Polymer Science*, 281(12):1184–1190, 2003.
- [26] G. Reich. In vitro stability of poly(d,l-lactide) and poly(d,l-lactide)/poloxamer nanoparticles in gastrointestinal fluids. *Drug Development and Industrial Pharmacy*, 23(12):1191–1200, 1997.

- [27] A. Bozkir and O.M. Saka. Formulation and investigation of 5-fu nanoparticles with factorial design-based studies. *Farmaco*, 60(10):840–846, 2005.
- [28] N. Csaba, A. Sánchez, and M.J. Alonso. Plga: Poloxamer and plga: Poloxamine blend nanostructures as carriers for nasal gene delivery. *Journal of Controlled Release*, 113(2):164–172, 2006.
- [29] P.D. Scholes, A.G.A. Coombes, L. Illum, S.S. Davis, J.F. Watts, C. Ustariz, M. Vert, and M.C. Davies. Detection and determination of surface levels of poloxamer and pva surfactant on biodegradable nanospheres using ssims and xps. *Journal of Controlled Release*, 59(3):261–278, 1999.
- [30] M.J. Santander-Ortega, A.B. Jódar-Reyes, N. Csaba, D. Bastos-González, and J.L. Ortega-Vinuesa. Colloidal stability of pluronic f68-coated plga nanoparticles: A variety of stabilisation mechanisms. *Journal of Colloid and Interface Science*, 302(2):522–529, 2006.
- [31] S.E. Dunn, A.G.A. Coombes, M.C. Garnett, S.S. Davis, M.C. Davies, and L. Illum. In vitro cell interaction and in vivo biodistribution of poly(lactide-co-glycolide) nanospheres surface modified by poloxamer and poloxamine copolymers. *Journal of Controlled Release*, 44(1):65–76, 1997.
- [32] S. Stolnik, M.C. Davies, L. Illum, S.S. Davis, M. Boustta, and M. Vert. The preparation of sub-200 nm biodegradable colloidal particles from poly (beta-malic acid-co-benzyl malate) copolymers and their surface modification with poloxamer and poloxamine surfactants. *Journal of Controlled Release*, 30(1):57–67, 1994.
- [33] M.H. El-Shabouri. Positively charged nanoparticles for improving the oral bioavailability of cyclosporin-a. *International Journal of Pharmaceutics*, 249(1-2):101–108, 2002.
- [34] T. M. Göppert and R. H. Müller. Plasma protein adsorption of tween 80- and poloxamer 188-stabilized solid lipid nanoparticles. *Journal of Drug Targeting*, 11(4):225–231, 2003.
- [35] A. Weissenbock, M. Wirth, and F. Gabor. Wga-grafted plga-nanospheres: preparation and association with caco-2 single cells. *Journal of Controlled Release*, 99(3):383–392, 2004.
- [36] H. Ghebeh, A. Handa-Corrigan, and M. Butler. Development of an assay for the measurement of the surfactant pluronic f-68 in mammalian cell culture medium. *Analytical Biochemistry*, 262(1):39–44, 1998.
- [37] J.A. Baker and J.C. Berg. Investigation of the adsorption configuration of poly(ethylene oxide) and its copolymers with poly(propylene oxide) on model polystyrene latex dispersions. *Langmuir*, 4(4):1055–1061, 1988.
- [38] J.M. Anderson and M.S. Shive. Biodegradation and biocompatibility of pla and plga microspheres. *Advanced Drug Delivery Reviews*, 28(1):5–24, 1997.

- [39] J. Vandervoort, K. Yoncheva, and A. Ludwig. Influence of the homogenisation procedure on the physicochemical properties of plga nanoparticles. *Chemical and Pharmaceutical Bulletin*, 52(11):1273–1279, 2004.
- [40] S. Prabha and V. Labhasetwar. Critical determinants in plga/pla nanoparticle-mediated gene expression. *Pharmaceutical Research*, 21(2):354–364, 2004.
- [41] Amsterdam Elsevier B.V. Scopus.com [database on the internet; cited 2009 aug 4].
- [42] H. Okada and Toguchi H. Biodegradable microspheres in drug delivery. *Critical Reviews in Therapeutic Drug Carrier Systems*, 12(1):1–99, 1995.
- [43] D.K. Gilding and Reed A.M. Biodegradable polymers for use in surgery: polyglycolic/poly(lactic acid) homo- and copolymers. *Polymer*, 20:137–143, 1979.
- [44] M.J. Dorta, O. Manguia, and M. Llabres. Effects of polymerization variables on plga properties: molecular weight, composition and chain structure. *International Journal of Pharmaceutics*, 100:9–14, 1993.
- [45] N.P. Huang, R. Michel, J. Voros, M. Textor, R. Hofer, A. Rossi, D.L. Elbert, J.A. Hubbell, and N.D. Spencer. Poly(l-lysine)-g-poly(ethylene glycol) layers on metal oxide surfaces: Surface-analytical characterization and resistance to serum and fibrinogen adsorption. *Langmuir*, 17(2):489–498, 2001.
- [46] S. Faraasen, J. Voros, G. Csucs, M. Textor, H.P. Merkle, and E. Walter. Ligand-specific targeting of microspheres to phagocytes by surface modification with poly(l-lysine)-grafted poly(ethylene glycol) conjugate. *Pharmaceutical Research*, 20(2):237–246, 2003.
- [47] J. Hermann and Bodmeier R. Biodegradable somatostatin acetate containing microspheres prepared by various aqueous and non-aqueous solvent evaporation methods. *European Journal of Pharmaceutics and Biopharmaceutics*, 45:72–85, 1998.
- [48] G. Rafler and M. Jobmann. Microparticle preparation by a salting out process. *PharmInd*, 59:620–627, 1997.
- [49] F. Pavanetto, I. Genta, P. Giunchedi, and P. Conti. Evaluation of spray-drying as a method for polylactide and polylactide-co-glycolide microsphere preparation. *Journal of Microencapsulation*, 10:487–497, 1993.
- [50] P. Johansen, H.P. Merkle, and B. Gander. Technological considerations related to up-scaling of protein microencapsulation by spray-drying. *European Journal of Pharmaceutics and Biopharmaceutics*, 50:413–417, 2000.
- [51] P. Herbert, K. Murphy, O. Johnson, N. Dong, W. Jaworowicz, M.A. Tracy, J.L. Cleland, and S.D. Putney. A large-scale process to produce microencapsulated proteins. *Pharmaceutical Research*, 15:357–362, 1998.

- [52] C. Lecaroz, C. Gamazo, M.J. Renedo, and M.J. Blanco-Prieto. Biodegradable micro- and nanoparticles as long-term delivery vehicles for gentamycin. *Journal of Microencapsulation*, 23:782–792, 2006.
- [53] O.I. Corrigan and X. Li. Quantifying drug release from plga nanoparticulates. *European Journal of Pharmaceutical Sciences*, 37:477–485, 2009.
- [54] T. Govender, S. Stolnik, M.C. Garnett, L. Illum, and S.S. Davis. Plga nanoparticles prepared by nanoprecipitation: drug loading and release studies of a water soluble drug. *Journal of Controlled Release*, 57:171–185, 1999.
- [55] U. Bilati, E. Allemann, and E. Doelker. Development of a nanoprecipitation method intended for the entrapment of hydrophilic drugs into nanoparticles. *European Journal of Pharmaceutical Sciences*, 24:67–75, 2005.
- [56] A.K. Mehta, K.S. Yadav, and K.K. Sawant. Nimodipine loaded plga nanoparticles: Formulation optimization using factorial design, characterization and in vitro evaluation. *Current Drug Delivery*, 4:185–193, 2007.
- [57] S. Freitas, H.P. Merkle, and B. Gander. Microencapsulation by solvent extraction/evaporation: reviewing the state of the art of microsphere preparation process technology. *Journal of Controlled Release*, 102:313–332, 2005.
- [58] R.C. Mundargi, V.R. Babu, V. Rangaswamy, P. Patel, and T.M. Aminabhavi. Nano/micro technologies for delivering macromolecular therapeutics using poly(d,l-lactide-co-glycolide) and its derivatives. *Journal of Controlled Release*, 125(3):193–209, 2008.
- [59] L. Brannon-Peppas and M. Vert. *Handbook of pharmaceutical controlled release technology*, chapter Polylactic and polyglycolic acid as drug delivery carriers. Marcel Dekker, New York, 2000.
- [60] D.A. Perrin and J.P. English. *Handbook of biodegradable polymers*, chapter Polyglycolide and polylactide. Harwood Academic Publishers, Amsterdam, 1997.
- [61] G. Spenlehauer, M. Vert, J.P. Benoit, and A. Boddaert. In vitro and in vivo degradation of poly(d,l-lactide/glycolide) type microspheres made by solvent evaporation method. *Biomaterials*, 10:557–563, 1989.
- [62] J. Kang and S.P. Schwendeman. Pore closing and opening in biodegradable polymers and their effect on the controlled release of proteins. *Molecular Pharmaceutics*, 4:104–118, 2007.
- [63] K. Makino, T. Mogi, N. Ohtake, M. Yoshida, S. Ando, T. Nakajima, and H. Ohshima. Pulsatile drug release from poly(lactide-co-glycolide) microspheres: How does the composition of the polymer matrices affect the time interval between the initial burst and the pulsatile release of drugs? *Colloids and Surfaces B: Biointerfaces*, 19:173–179, 2000.

- [64] Q. Cai, G.X. Shi, J.Z. Bei, and S.G. Wang. Enzymatic degradation behaviour and mechanism of poly(lactide-co-glycolide) foams by trypsin. *Biomaterials*, 24:629–638, 2003.
- [65] K. Avgoustakis and J.R. Nixon. Biodegradable controlled release tablets: Iii. effect of polymer characteristics on drug release from heterogenous poly(lactide-co-glycolide) matrices. *International Journal of Pharmaceutics*, 99:247–252, 1993.
- [66] N. Hua and J. Sun. Body distribution of poly(d,l-lactide-co-glycolide) copolymer degradation products in rats. *Journal of Materials Science: Materials in Medicine*, 19:3243–3248, 2008.
- [67] D.S. Kohane, J.Y. Tse, Y. Yeo, R. Padera, M. Shubina, and R. Langer. Biodegradable polymeric microspheres and nanospheres for drug delivery in the peritoneum. *Journal of Biomedical Materials Research*, 77:351–361, 2006.
- [68] E. Cenni, D. Granchi, S. Avnet, C. Fotia, M. Salerno, D. Micieli, M.G. Sarpietro, R. Pignatello, F. Castelli, and N. Baldini. Biocompatibility of poly(d,l-lactide-co-glycolide) nanoparticles conjugated with alendronate. *Biomaterials*, 29:1400–1411, 2008.
- [69] D. Kim, H. El-Shall, D. Dennis, and T. Morey. Interaction of plga nanoparticles with human blood constituents. *Colloids and Surfaces B: Biointerfaces*, 40:83–91, 2005.
- [70] A.A. Ignatius and L.E. Claes. In vitro biocompatibility of bioresorbable polymers: poly(l,dl-lactide) and poly(l-lactide-co-glycolide). *Biomaterials*, 17:831–839, 1996.
- [71] P. Malyala, D.T. O'Hagan, and M. Singh. Enhancing the therapeutic efficacy of cpg oligonucleotides using biodegradable particles. *Advanced Drug Delivery Reviews*, 61:218–225, 2009.
- [72] J. Wendorf, M. Singh, J. Chesko, J. Kazzaz, E. Soewanan, M. Ugozoli, and D. O'Hagan. A practical approach to the use of nanoparticles for vaccine delivery. *Journal of Pharmaceutical Sciences*, 95:2738–2750, 2006.
- [73] G.T. Hermanson. *Bioconjugate techniques*. Academic Press, San Diego, 1996.
- [74] P.S. Kasturi, H. Qin, K.S. Thomson, S. El-Bereir, S.C. Cha, S. Neelapu, L.W. Kwak, and K. Roy. Prophylactic anti-tumor effects in a b cell lymphoma model with dna vaccines delivered on polyethylenimine (pei) functionalized plga microparticles. *Journal of Controlled Release*, 113(3):261–270, 2006.
- [75] F. Gabor, K. Trimmel, G. Ratzinger, V. Kerleta, C. Fillafer, and M. Wirth. Characterization of binding and uptake of biomimetic nanoparticles by flow cytometry. *Journal of Drug Delivery Science and Technology*, 18(1):51–57, 2008.
- [76] H. Chen, J. Gao, Y. Lu, G. Kou, H. Zhang, L. Fan, Z. Sun, Y. Guo, and Y. Zhong. Preparation and characterization of pe38kdel-loaded anti-her2 nanoparticles for targeted cancer therapy. *Journal of Controlled Release*, 128:209–216, 2008.

- [77] N. Brandhonneur, F. Chevanne, V. Vie, B. Frisch, Primault R., M.F. Le Poitier, and P. Le Corre. Specific and non-specific phagocytosis of ligand-grafted plga microspheres by macrophages. *European Journal of Pharmaceutical Sciences*, 36:474–485, 2009.
- [78] J.L. Sharon and D.A. Puleo. The use of n-terminal immobilization of pth(1-34) on plga to enhance bioactivity. *Biomaterials*, 29:3137–3142, 2008.
- [79] P.A. McCarron, W.M. Marouf, D.J. Quinn, F. Fay, R.E. Burden, S.A. Olwill, and C.J. Scott. Antibody targeting of camptothecin-loaded plga nanoparticles to tumor cells. *Bioconjugate Chemistry*, 19(8):1561–1569, 2008.
- [80] G. Ratzinger, U. Länger, L. Neutsch, F. Pittner, M. Wirth, and F. Gabor. Surface modification of plga particles: The interplay between stabilizer, ligand size, and hydrophobic interactions. *Langmuir*, 26(3):1855–1859, 2010.
- [81] M.A.G. Dahlgren. Effect of counterion valency and ionic strength on polyelectrolyte adsorption. *Langmuir*, 10(5):1580–1583, 1994.
- [82] T. Trimaille, C. Pichot, and T. Delair. Surface functionalization of poly(d,l-lactic acid) nanoparticles with poly(ethylenimine) and plasmid dna by the layer-by-layer approach. *Colloids and Surfaces A: Physicochemical and Engineering Aspects*, 221(1-3):39–48, 2003.
- [83] I. Messai and T. Delair. Adsorption of chitosan onto poly(d,l-lactic acid) particles: A physico-chemical investigation. *Macromolecular Chemistry and Physics*, 206(16):1665–1674, 2005.
- [84] A. Vila, A. Sánchez, M. Tobío, P. Calvo, and M. J. Alonso. Design of biodegradable particles for protein delivery. *Journal of Controlled Release*, 78(1-3):15–24, 2002.
- [85] K. Dillen, J. Vandervoort, G. Van den Mooter, and A. Ludwig. Evaluation of ciprofloxacin-loaded eudragit® rs100 or rl100/plga nanoparticles. *International Journal of Pharmaceutics*, 314(1):72–82, 2006.
- [86] L. Thiele, B. Rothen-Rutishauser, S. Jilek, H. Wunderli-Allenspach, H.P. Merkle, and E. Walter. Evaluation of particle uptake in human blood monocyte-derived cells in vitro. does phagocytosis activity of dendritic cells measure up with macrophages? *Journal of Controlled Release*, 76(1-2):59–71, 2001.
- [87] J.K. Vasir and V. Labhasetwar. Quantification of the force of nanoparticle-cell membrane interactions and its influence on intracellular trafficking of nanoparticles. *Biomaterials*, 29(31):4244–4252, 2008.
- [88] B.S. Kim, C.S. Kim, and K.M. Lee. The intracellular uptake ability of chitosan-coated poly (d,l-lactide-co-glycolide) nanoparticles. *Archives of Pharmacal Research*, 31(8):1050–1054, 2008.
- [89] J.M. Martínez Gómez, N. Csaba, S. Fischer, A. Sichelstiel, T.M. Kündig, B. Gander, and P. Johansen. Surface coating of plga microparticles with protamine enhances their immunological performance through facilitated phagocytosis. *Journal of Controlled Release*, 130(2):161–167, 2008.

- [90] L. Thiele, H.P. Merkle, and E. Walter. Phagocytosis and phagosomal fate of surface-modified microparticles in dendritic cells and macrophages. *Pharmaceutical Research*, 20(2):221–228, 2003.
- [91] M.N.V.R. Kumar, S.S. Mohapatra, X. Kong, P.K. Jena, U. Bakowsky, and C.M. Lehr. Cationic poly(lactide-co-glycolide) nanoparticles as efficient in vivo gene transfection agents. *Journal of Nanoscience and Nanotechnology*, 4(8):990–994, 2004.
- [92] M.N.V. Ravi Kumar, U. Bakowsky, and C.M. Lehr. Preparation and characterization of cationic plga nanospheres as dna carriers. *Biomaterials*, 25(10):1771–1777, 2004.
- [93] H. Yamamoto, Y. Kuno, S. Sugimoto, H. Takeuchi, and Y. Kawashima. Surface-modified plga nanosphere with chitosan improved pulmonary delivery of calcitonin by mucoadhesion and opening of the intercellular tight junctions. *Journal of Controlled Release*, 102(2):373–381, 2005.
- [94] S. Fischer, C. Foerg, S. Ellenberger, H.P. Merkle, and B. Gander. One-step preparation of polyelectrolyte-coated plga microparticles and their functionalization with model ligands. *Journal of Controlled Release*, 111(1-2):135–144, 2006.
- [95] N. Nafee, S. Taetz, M. Schneider, U. F. Schaefer, and C. M. Lehr. Chitosan-coated plga nanoparticles for dna/rna delivery: effect of the formulation parameters on complexation and transfection of antisense oligonucleotides. *Nanomedicine: Nanotechnology, Biology, and Medicine*, 3(3):173–183, 2007.
- [96] C. Guo and R.A. Gemeinhart. Understanding the adsorption mechanism of chitosan onto poly(lactide-co-glycolide) particles. *European Journal of Pharmaceutics and Biopharmaceutics*, 70(2):597–604, 2008.
- [97] M.L. Manca, S. Mourtas, V. Dracopoulos, A.M. Fadda, and S.G. Antimisiaris. Plga, chitosan or chitosan-coated plga microparticles for alveolar delivery?: A comparative study of particle stability during nebulization. *Colloids and Surfaces B: Biointerfaces*, 62(2):220–231, 2008.
- [98] R. Yang, W.S. Shim, F.D. Cui, G. Cheng, X. Han, Q.R. Jin, D.D. Kim, S.J. Chung, and C.K. Shim. Enhanced electrostatic interaction between chitosan-modified plga nanoparticle and tumor. *International Journal of Pharmaceutics*, 371(1-2):142–147, 2009.
- [99] R. Yang, S. G. Yang, W. S. Shim, F. Cui, G. Cheng, I. W. Kim, D. D. Kim, S. J. Chung, and C. K. Shim. Lung-specific delivery of paclitaxel by chitosan-modified plga nanoparticles via transient formation of microaggregates. *Journal of Pharmaceutical Sciences*, 98(3):970–984, 2009.
- [100] M.J. Tsung and D.J. Burgess. Preparation and characterization of gelatin surface modified plga microspheres. *AAPS Pharmaceutical Sciences*, 3(2):E11, 2001.
- [101] C. Wischke, J. Zimmermann, B. Wessinger, A. Schendler, H. H. Borchert, J. H. Peters, T. Nesselhut, and D. R. Lorenzen. Poly(i:c) coated plga microparticles induce dendritic cell maturation. *International Journal of Pharmaceutics*, 365(1-2):61–68, 2009.

- [102] M. Bivas-Benita, S. Romeijn, H. E. Junginger, and G. Borchard. Plga-pei nanoparticles for gene delivery to pulmonary epithelium. *European Journal of Pharmaceutics and Biopharmaceutics*, 58(1):1–6, 2004.
- [103] B. Mandal, M. Kempf, H.P. Merkle, and E. Walter. Immobilisation of gm-csf onto particulate vaccine carrier systems. *International Journal of Pharmaceutics*, 269(1):259–265, 2004.
- [104] C.G. Oster, N. Kim, L. Grode, L. Barbu-Tudoran, A. K. Schaper, S. H. E. Kaufmann, and T. Kissel. Cationic microparticles consisting of poly(lactide-co-glycolide) and polyethylenimine as carriers systems for parental dna vaccination. *Journal of Controlled Release*, 104(2):359–377, 2005.
- [105] S.P. Kasturi, K. Sachaphibulkij, and K. Roy. Covalent conjugation of polyethyleneimine on biodegradable microparticles for delivery of plasmid dna vaccines. *Biomaterials*, 26(32):6375–6385, 2005.
- [106] Y.W. Yang and P.Y.J. Hsu. The effect of poly(d,l-lactide-co-glycolide) microparticles with polyelectrolyte self-assembled multilayer surfaces on the cross-presentation of exogenous antigens. *Biomaterials*, 29(16):2516–2526, 2008.
- [107] C. Cui and S.P. Schwendeman. Surface entrapment of polylysine in biodegradable poly(dl-lactide-co-glycolide) microparticles. *Macromolecules*, 34(24):8426–8433, 2001.
- [108] M. Müller, J. Voros, G. Csucs, E. Walter, G. Danuser, H. P. Merkle, N. D. Spencer, and M. Textor. Surface modification of plga microspheres. *Journal of Biomedical Materials Research - Part A*, 66(1):55–61, 2003.
- [109] S.H. Kim, J.H. Jeong, K.W. Chun, and T.G. Park. Target-specific cellular uptake of plga nanoparticles coated with poly(l-lysine)-poly(ethylene glycol)-folate conjugate. *Langmuir*, 21(19):8852–8857, 2005.
- [110] F. Reynolds, R. Weissleder, and L. Josephson. Protamine as an efficient membrane-translocating peptide. *Bioconjugate Chemistry*, 16(5):1240–1245, 2005.
- [111] O. Boussif, F. Lezoualc’h, M.A. Zanta, M.D. Mergny, D. Scherman, B. Demeneix, and J.P. Behr. A versatile vector for gene and oligonucleotide transfer into cells in culture and in vivo: polyethylenimine. *Proceedings of the National Academy of Sciences of the United States of America*, 92(16):7297–7301, 1995.
- [112] R. Kircheis, L. Wightman, and E. Wagner. Design and gene delivery activity of modified polyethylenimines. *Advanced Drug Delivery Reviews*, 53(3):341–358, 2001.
- [113] M. Neu, D. Fischer, and T. Kissel. Recent advances in rational gene transfer vector design based on poly(ethylene imine) and its derivatives. *Journal of Gene Medicine*, 7(8):992–1009, 2005.

- [114] M. Shakweh, M. Besnard, V. Nicolas, and E. Fattal. Poly (lactide-co-glycolide) particles of different physicochemical properties and their uptake by peyer's patches in mice. *European Journal of Pharmaceutics and Biopharmaceutics*, 61(1-2):1-13, 2005.
- [115] I.S. Kim, S.K. Lee, Y.M. Park, Y.B. Lee, S.C. Shin, K.C. Lee, and I.J. Oh. Physicochemical characterization of poly(l-lactic acid) and poly(d,l-lactide-co-glycolide) nanoparticles with polyethylenimine as gene delivery carrier. *International Journal of Pharmaceutics*, 298(1):255-262, 2005.
- [116] L.J. Arnold, A. Dagan, J. Gutheil, and N.O. Kaplan. Antineoplastic activity of poly(l-lysine) with some ascites tumor cells. *Proceedings of the National Academy of Sciences of the United States of America*, 76(7):3246-3250, 1979.
- [117] G. Kou, J. Gao, H. Wang, H. Chen, B. Li, D. Zhang, S. Wang, S. Hou, W. Qian, J. Dai, Y. Zhong, and Y. Guo. Preparation and characterization of paclitaxel-loaded plga nanoparticles coated with cationic sm5-1 single-chain antibody. *Journal of Biochemistry and Molecular Biology*, 40(5):731-739, 2007.
- [118] S.K. Sahoo, J. Panyam, S. Prabha, and V. Labhasetwar. Residual polyvinyl alcohol associated with poly (d,l-lactide-co-glycolide) nanoparticles affects their physical properties and cellular uptake. *Journal of Controlled Release*, 82(1):105-14, 2002.
- [119] O.J. Rojas, M. Ernstsson, R.D. Neuman, and P.M. Claesson. Effect of polyelectrolyte charge density on the adsorption and desorption behavior on mica. *Langmuir*, 18(5):1604-1612, 2002.
- [120] C.J. Kim. *Advanced pharmaceutics: physicochemical principles*. CRC Press, Boca Raton, 2004.
- [121] J. Israelachvili. *Intramolecular and surface forces*. Academic Press, London, 1991.
- [122] D.F. Evans and H. Wennerström. *The colloidal domain: where physics, chemistry, biology, and technology meet*. Wiley-VCH, New York, 1999.
- [123] F.X. Lacasse, M.C. Fillion, N.C. Phillips, E. Escher, J.N. McMullen, and P. Hildgen. Influence of surface properties at biodegradable microsphere surfaces: Effects on plasma proteins adsorption and phagocytosis. *Pharmaceutical Research*, 15:312-317, 1998.
- [124] C.C. DeMerlis and D.R. Schoneker. Review of the oral toxicity of polyvinyl alcohol (pva). *Food Chemistry and Toxicology*, 41:319-326, 2003.
- [125] A.R. Patel, S. Kulkarni, T.D. Nandekar, and P.R. Vavia. Evaluation of alkyl polyglucoside as an alternative surfactant in the preparation of peptide-loaded nanoparticles. *Journal of Microencapsulation*, 25(8):531-540, 2008.
- [126] International Agency for Research on Cancer World Health Organization. Agents reviewed by the iarc monographs.
- [127] Silver Spring: US Food and Drug Administration. Inactive ingredient search for approved drug products.

- [128] A. Besheer, J. Vogel, D. Glanz, J. Kressler, T. Groth, and K. Mäder. Characterization of plga nanospheres stabilized with amphiphilic polymers: Hydrophobically modified hydroxyethyl starch vs pluronics. *Molecular Pharmaceutics*, 6(2):407–415, 2009.
- [129] J. Chang, Y. Jallouli, M. Kroubi, X.B. Yuan, W. Feng, C.S. Kang, P.Y. Pu, and D. Betbeder. Characterization of endocytosis of transferrin-coated plga nanoparticle by the blood-brain barrier. *International Journal of Pharmaceutics*, 379(2):285–292, 2009.
- [130] M. Singh, M. Briones, G. Ott, and D. O'Hagan. Cationic microparticles: A potent delivery system for dna vaccines. *Proceedings of the National Academy of Sciences of the United States of America*, 97(2):811–816, 2000.
- [131] G.R. Otten, M. Schaefer, B. Doe, H. Liu, I. Srivastava, J. Megede, J. Kazzaz, Y. Lian, M. Singh, M. Ugozzoli, D. Montefiori, M. Lewis, D.A. Driver, T. Dubensky, J.M. Polo, J. Donnelly, D.T. O'Hagan, S. Barnett, and J.B. Ulmer. Enhanced potency of plasmid dna microparticle human immunodeficiency virus vaccines in rhesus macaques by using a priming-boosting regimen with recombinant proteins. *Journal of Virology*, 79(13):8189–8200, 2005.
- [132] J. Kazzaz, J. Neidleman, M. Singh, G. Ott, and D. T. O'Hagan. Novel anionic microparticles are a potent adjuvant for the induction of cytotoxic t lymphocytes against recombinant p55 gag from hiv-1. *Journal of Controlled Release*, 67(2-3):347–356, 2000.
- [133] M. Singh, J. Kazzaz, J. Chesko, E. Soenawan, M. Ugozzoli, M. Giuliani, M. Pizza, R. Rappouli, and D. T. O'Hagan. Anionic microparticles are a potent delivery system for recombinant antigens from neisseria meningitidis serotype b. *Journal of Pharmaceutical Sciences*, 93(2):273–282, 2004.
- [134] S.S. Feng and G.F. Huang. Effects of emulsifiers on the controlled release of paclitaxel (taxol (r)) from nanospheres of biodegradable polymers. *Journal of Controlled Release*, 71(1):53–69, 2001.
- [135] S. Sengupta, D. Eavarone, I. Capila, G.L. Zhao, N. Watson, T. Kiziltepe, and R. Sasisekharan. Temporal targeting of tumour cells and neovasculature with a nanoscale delivery system. *Nature*, 436(7050):568–572, 2005.
- [136] A. Besheer, G. Hause, J. Kressler, and K. Mäder. Hydrophobically modified hydroxyethyl starch: Synthesis, characterization, and aqueous self-assembly into nano-sized polymeric micelles and vesicles. *Biomacromolecules*, 8:359–367, 2007.
- [137] L. Mu and S.S. Feng. Vitamin e tpgs used as emulsifier in the solvent evaporation/extraction technique for fabrication of polymeric nanospheres for controlled release of paclitaxel (taxol(r)). *Journal of Controlled Release*, 80:129–144, 2002.
- [138] K.Y. Win and S.S. Feng. Effects of particle size and surface coating on cellular uptake of polymeric nanoparticles for oral delivery of anticancer drugs. *Biomaterials*, 26:2713–2722, 2005.

- [139] H.Z. Zhao, E.C. Tan, and L.Y.L. Yung. Potential use of cholecalciferol polyethylene glycol succinate as a novel pharmaceutical additive. *Journal of Biomedical Materials Research - Part A*, 84:954–964, 2008.
- [140] H. Laroui, L. Grossin, M. Leonard, J.F. Stoltz, P. Gillet, P. Netter, and E. Delacherie. Hyaluronate-covered nanoparticles for the therapeutic targeting of cartilage. *Biomacromolecules*, 8:3879–3885, 2007.
- [141] T.M. Fahmy, R.M. Samstein, C.C. Harness, and W.M. Saltzman. Surface modification of biodegradable polyesters with fatty acid conjugates for improved drug targeting. *Biomaterials*, 26:5727–5736, 2005.
- [142] S.L. Demento, S.C. Eisenbarth, H.G. Foellmer, C. Platt, M.J. Caplan, W.M. Saltzman, I. Mellman, M. Ledizet, E. Fikrig, R.A. Flavell, and T.M. Fahmy. Inflammasome-activating nanoparticles as a modular system for optimizing vaccine efficacy. *Vaccine*, 27:3013–3021, 2009.
- [143] C. Cui and S.P. Schwendeman. One-step surface modification of poly(lactide-co-glycolide) microparticles with heparin. *Pharmaceutical Research*, 24(12):2381–2393, 2007.
- [144] L. Mu and S.S. Feng. A novel controlled release formulation for the anticancer drug paclitaxel (taxol(r)): PLGA nanoparticles containing vitamin E TPGS. *Journal of Controlled Release*, 86:33–48, 2003.
- [145] M.J. Montisci, G. Giovannucci, D. Duchene, and G. Ponchel. Covalent coupling of asparagus pea and tomato lectins to poly(lactide) microspheres. *International Journal of Pharmaceutics*, 215:153–161, 2001.
- [146] S.K. Sahoo and V. Labhasetwar. Enhanced antiproliferative activity of transferrin-conjugated paclitaxel-loaded nanoparticles is mediated via sustained intracellular drug retention. *Molecular Pharmaceutics*, 2(5):373–383, 2005.
- [147] K.S. Rao, M.K. Reddy, J.L. Horning, and V. Labhasetwar. Tat-conjugated nanoparticles for the CNS delivery of anti-HIV drugs. *Biomaterials*, 29:4429–4438, 2008.
- [148] J. Lu, J.K. Jackson, M.E. Gleave, and H.M. Burt. The preparation and characterization of anti-VEGF2 conjugated, paclitaxel-loaded PLGA or PLGA microspheres for the systematic targeting of human prostate tumors. *Cancer Chemotherapy and Pharmacology*, 61(6):997–1005, 2008.
- [149] M.E. Keegan, J.L. Falcone, T.C. Leung, and W.M. Saltzman. Biodegradable microspheres with enhanced capacity for covalently bound surface ligands. *Macromolecules*, 37:9779–9784, 2004.
- [150] C. Chittasupho, S.X. Xie, A. Baoum, T. Yakovleva, T.J. Siahaan, and C.J. Berkland. ICAM-1 targeting of doxorubicin-loaded PLGA nanoparticles to lung epithelial cells. *European Journal of Pharmaceutical Sciences*, 37(2):141–150, 2009.

- [151] C. Cui, V.C. Stevens, and S.P. Schwendeman. Injectable polymer microspheres enhance immunogenicity of a contraceptive peptide vaccine. *Vaccine*, 25(3):500–509, 2007.
- [152] J. Chesko, J. Kazzaz, M. Ugozzoli, D. T. O'Hagan, and M. Singh. An investigation of the factors controlling the adsorption of protein antigens to anionic plg microparticles. *Journal of Pharmaceutical Sciences*, 94(11):2510–2519, 2005.
- [153] C. Cai, U. Bakowsky, E. Rytting, A.K. Schaper, and T. Kissel. Charged nanoparticles as protein delivery systems: A feasibility study using lysozyme as a model protein. *European Journal of Pharmaceutics and Biopharmaceutics*, 69:31–42, 2008.
- [154] G. Crotts, H. Sah, and T.G. Park. Adsorption determines in-vitro protein release rate from biodegradable microspheres: quantitative analysis of surface area during degradation. *Journal of Controlled Release*, 47:101–111, 1997.
- [155] G. Crotts and T.G. Park. Stability and release of bovine serum albumin encapsulated within poly(d,l-lactide-co-glycolide) microparticles. *Journal of Controlled Release*, 44:123–134, 1997.
- [156] P. Kocbek, N. Obermajer, M. Gegnar, J. Kos, and J. Kristl. Targeting cancer cells using plga nanoparticles surface modified with monoclonal antibody. *Journal of Controlled Release*, 120:18–26, 2007.
- [157] V. Villari and N. Micali. Light scattering as spectroscopic tool for the study of disperse systems useful in pharmaceutical sciences. *Journal of Pharmaceutical Sciences*, 97:1703–1730, 2008.
- [158] R.H. Muller, C. Jacobs, and O. Kayser. Nanosuspensions as particulate drug formulations in therapy: Rationale for development and what we can expect for the future. *Advanced Drug Delivery Reviews*, 47(1):4–12, 2001.
- [159] C. Augsten, M.A. Kiselev, R. Gehrke, G. Hause, and K. Mäder. A detailed analysis of biodegradable nanospheres by different techniques—a combined approach to detect particle sizes and size distributions. *Journal of Pharmaceutical and Biomedical Analysis*, 47(1):95–102, 2008.
- [160] W. Fraunhofer and G. Winter. The use of asymmetrical flow field-flow fractionation in pharmaceutics and biopharmaceutics. *European Journal of Pharmaceutics and Biopharmaceutics*, 58:369–383, 2004.
- [161] M. Schimpf, K. Caldwell, and J.C. Giddings. *Field-flow fractionation handbook*. Wiley-Interscience, Hoboken, 2000.
- [162] A. Musyanovych, J. Schmitz-Wienke, V. Mailänder, P. Walther, and K. Landsfester. Preparation of biodegradable polymer nanoparticles by miniemulsion technique and their cell interactions. *Macromolecular Bioscience*, 8:127–139, 2008.
- [163] M. Gaumet, A. Vargas, R. Gurny, and F. Delie. Nanoparticles for drug delivery: The need for precision in reporting particle size parameters. *European Journal of Pharmaceutics and Biopharmaceutics*, 69:1–9, 2008.

- [164] S. Giovagnoli, P. Blasi, M. Ricci, A. Schoubben, L. Perioli, and C. Rossi. Physicochemical characterization and release mechanism of a novel prednisone biodegradable microsphere formulation. *Journal of Pharmaceutical Sciences*, 97:303–317, 2008.
- [165] M. Gaumet, R. Gurny, and F. Delie. Fluorescent biodegradable plga particles with narrow size distributions: Preparation by means of selective centrifugation. *International Journal of Pharmaceutics*, 342(1-2):222–230, 2007.
- [166] X.P. Guan, D.P. Quan, K.R. Liao, T. Wang, P. Xiang, and K.C. Mai. Preparation and characterization of cationic chitosan-modified poly(d,l-lactide-co-glycolide) copolymer nanospheres as dna carriers. *Journal of Biomaterial Applications*, 22:353–371, 2008.
- [167] K. Gvili, O. Benny, D. Danino, and M. Machluf. Poly(d,l-lactide-co-glycolide acid) nanoparticles for dna delivery: Waiving preparation complexity and increasing efficiency. *Biopolymers*, 85:379–391, 2007.
- [168] R. Dorati, M. Patrini, P. Perugini, F. Pavanetto, A. Stella, T. Modena, I. Genta, and B. Cont. Surface characterization by atomic force microscopy of sterilized plga microspheres. *Journal of Microencapsulation*, 23:123–133, 2006.
- [169] H. Bunjes and T. Unruh. Characterization of lipid nanoparticles by differential scanning calorimetry, x-ray and neutron scattering. *Advanced Drug Delivery Reviews*, 59:379–402, 2007.
- [170] S.M. Agnihotri, H. Ohshima, H. Terada, K. Tomoda, and K. Makino. Electrophoretic mobility of colloidal gold particles in electrolyte solutions. *Langmuir*, 25:4804–4807, 2009.
- [171] F. Kesisoglou, S. Panmai, and Y. Wu. Nanosizing - oral formulation development and biopharmaceutical evaluation. *Advanced Drug Delivery Reviews*, 59(7):631–644, 2007.
- [172] M. Shinkai, M. Yanase, H. Honda, T. Wakabayashi, J. Yoshida, and Kobayashi T. Intracellular hyperthermia for cancer using cationic liposomes: in vitro study. *Japanese Journal of Cancer Research*, 87:1179–1183, 1996.
- [173] A. Ito, M. Shinkai, H. Honda, and T. Kobayashi. Medical application of functionalized magnetic nanoparticles. *Journal of Bioscience and Bioengineering*, 100:1–11, 2005.
- [174] S. Stolnik, S.E. Dunn, M.C. Garnett, M.C. Davies, A.G. Coombes, D.C. Taylor, M.P. Irving, S.C. Purkiss, T.F. Tadros, S.S. Davis, and L. Illum. Surface modification of poly(lactide-co-glycolide) nanospheres by biodegradable poly(lactide)-poly(ethylene glycol) copolymers. *Pharmaceutical Research*, 11(12):1800–1808, 1994.
- [175] M. Lück, K.F. Pistel, Y.X. Li, T. Blunk, R.H. Müller, and T. Kissel. Plasma protein adsorption on biodegradable microspheres consisting of poly(d,l-lactide-co-glycolide), poly(l-lactide) or aba triblock copolymers containing poly(oxyethylene). influence of production method and polymer composition. *Journal of Controlled Release*, 55(2-3):107–20, 1998.

- [176] K.M. Shakesheff, C. Evora, I. Soriano, and R. Langer. The adsorption of poly(vinyl alcohol) to biodegradable microparticles studied by x-ray photoelectron spectroscopy (xps). *Journal of Colloid and Interface Science*, 185:538–547, 1996.
- [177] M. Gaumet, R. Gurny, and F. Delie. Localization and quantification of biodegradable particles in an intestinal cell model: The influence of particle size. *European Journal of Pharmaceutical Sciences*, 36:465–473, 2009.
- [178] B. Weiss, M. Schneider, L. Muys, S. Taetz, D. Neumann, U.F. Schaefer, and C.M. Lehr. Coupling of biotin-(poly(ethylene glycol))amine to poly(d,l-lactide-co-glycolide) nanoparticles for versatile surface modification. *Bioconjugate Chemistry*, 18:1087–1094, 2007.
- [179] R. Gref, M. Luck, P. Quellec, M. Marchand, E. Dellacherie, S. Harnisch, T. Blunk, and R. H. Muller. 'stealth' corona-core nanoparticles surface modified by polyethylene glycol (peg): influences of the corona (peg chain length and surface density) and of the core composition on phagocytic uptake and plasma protein adsorption. *Colloids and Surfaces B: Biointerfaces*, 18(3-4):301–313, 2000.
- [180] C.S. Ha and J.A. Gardella. Surface chemistry of biodegradable polymers for drug delivery systems. *Chemical Reviews*, 105:4205–4232, 2005.
- [181] J. Chesko, J. Kazzaz, M. Ugozzoli, M. Singh, D.T. O'Hagan, C. Madden, M. Perkins, and N. Patel. Characterization of antigens adsorbed to anionic plg microparticles by xps and tof-sims. *Journal of Pharmaceutical Sciences*, 97:1443–1453, 2008.
- [182] J. Wang, B.M. Wang, and S.P. Schwendeman. Mechanistic evaluation of the glucose-induced reduction in initial burst release of octreotide acetate from poly(d,l-lactide-co-glycolide) microspheres. *Biomaterials*, 25:1919–1927, 2004.
- [183] Q. Xu, A. Crossley, and J. Czernuszka. Preparation and characterization of negatively charged poly(lactic-co-glycolic acid) microspheres. *Journal of Pharmaceutical Sciences*, 98:2377–2389, 2009.
- [184] L. Thiele, J.E. Diederichs, R. Reszka, H.P. Merkle, and E. Walter. Competitive adsorption of serum proteins at microparticles affects phagocytosis by dendritic cells. *Biomaterials*, 24(8):1409–1418, 2003.
- [185] D.N. Nguyen, J.J. Green, J.M. Chan, R. Langer, and D. G. Anderson. Polymeric materials for gene delivery and dna vaccination. *Advanced Materials*, 21(8):847–867, 2009.
- [186] V. Labhasetwar, C. Song, W. Humphrey, R. Shebuski, and R. J. Levy. Arterial uptake of biodegradable nanoparticles: Effect of surface modifications. *Journal of Pharmaceutical Sciences*, 87(10):1229–1234, 1998.

- [187] S. Ran, A. Downes, and P.E. Thorpe. Increased exposure of anionic phospholipids on the surface of tumor blood vessels. *Cancer Research*, 62(21):6132–6140, 2002.
- [188] M. Roser, D. Fischer, and T. Kissel. Surface-modified biodegradable albumin nano- and microspheres. ii: effect of surface charges on in vitro phagocytosis and biodistribution in rats. *European Journal of Pharmaceutics and Biopharmaceutics*, 46(3):255–263, 1998.
- [189] S.K. Lai, Y.Y. Wang, and J. Hanes. Mucus-penetrating nanoparticles for drug and gene delivery to mucosal tissues. *Advanced Drug Delivery Reviews*, 61(2):158–171, 2009.
- [190] G.P. Andrews, T.P. Lavery, and D.S. Jones. Mucoadhesive polymeric platforms for controlled drug delivery. *European Journal of Pharmaceutics and Biopharmaceutics*, 71(3):505–518, 2009.
- [191] G. Ponchel and J.M. Irache. Specific and non-specific bioadhesive particulate systems for oral delivery to the gastrointestinal tract. *Advanced Drug Delivery Reviews*, 34(2-3):191–219, 1998.
- [192] Y. Kawashima, H. Yamamoto, H. Takeuchi, and Y. Kuno. Mucoadhesive dl-lactide/glycolide copolymer nanospheres coated with chitosan to improve oral delivery of elcatonin. *Pharmaceutical Development and Technology*, 5(1):77–85, 2000.
- [193] V. Grabovac and A. Bernkop-Schnürch. Development and in vitro evaluation of surface modified poly(lactide-co-glycolide) nanoparticles with chitosan-4-thiobutylamidine. *Drug Development and Industrial Pharmacy*, 33(7):767–774, 2007.
- [194] Y. Cu and W.M. Saltzman. Drug delivery: Stealth particles give mucus the slip. *Nature Materials*, 8(1):11–13, 2009.
- [195] S.S. Olmsted, J.L. Padgett, A.I. Yudin, K.J. Whaley, T.R. Moench, and R.A. Cone. Diffusion of macromolecules and virus-like particles in human cervical mucus. *Biophysical Journal*, 81(4):1930–1937, 2001.
- [196] Y.Y. Wang, S.K. Lai, J.S. Suk, A. Pace, R. Cone, and J. Hanes. Addressing the peg mucoadhesivity paradox to engineer nanoparticles that "slip" through the human mucus barrier. *Angewandte Chemie - International Edition*, 47(50):9726–9729, 2008.
- [197] S.K. Lai, D.E. O'Hanlon, S. Harrold, S.T. Man, Y.Y. Wang, R. Cone, and J. Hanes. Rapid transport of large polymeric nanoparticles in fresh undiluted human mucus. *Proceedings of the National Academy of Sciences of the United States of America*, 104(5):1482–1487, 2007.
- [198] Y. Cu and W.M. Saltzman. Controlled surface modification with poly(ethylene)glycol enhances diffusion of plga nanoparticles in human cervical mucus. *Molecular Pharmaceutics*, 6(1):173–181, 2008.
- [199] M. Dawson, E. Krauland, D. Wirtz, and J. Hanes. Transport of polymeric nanoparticle gene carriers in gastric mucus. *Biotechnology Progress*, 20(3):851–857, 2004.

- [200] B. Sun, B. Ranganathan, and S.S. Feng. Multifunctional poly(d,l-lactide-co-glycolide)/montmorillonite (plga/mmt) nanoparticles decorated by trastuzumab for targeted chemotherapy of breast cancer. *Biomaterials*, 29(4):475–486, 2008.
- [201] S. Acharya, F. Dilnawaz, and S.K. Sahoo. Targeted epidermal growth factor receptor nanoparticle bioconjugates for breast cancer therapy. *Biomaterials*, 30:5737–5350, 2009.
- [202] C.J. Scott, W.M. Marouf, D.J. Quinn, R.J. Buick, S.J. Orr, R.F. Donnelly, and P.A. McCarron. Immunocolloidal targeting of the endocytic siglec-7 receptor using peripheral attachment of siglec-7 antibodies to poly(lactide-co-glycolide) nanoparticles. *Pharmaceutical Research*, 25(1):135–146, 2008.
- [203] A.O. Eniola and D.A. Hammer. In vitro characterization of leukocyte mimetic for targeting therapeutics to the endothelium using two receptors. *Biomaterials*, 26(34):7136–7144, 2005.
- [204] N. Sharon and H. Lis. History of lectins: from hemagglutinins to biological recognition molecules. *Glycobiology*, 14(11):53–62, 2004.
- [205] S. Diez, G. Navarro, and C.T. de Illarduya. In vivo targeted gene delivery by cationic nanoparticles for treatment of hepatocellular carcinoma. *Journal of Gene Medicine*, 11(1):38–45, 2009.
- [206] F. Gabor and M. Wirth. Lectin-mediated drug delivery: fundamentals and perspectives. *STP Pharma Sciences*, 13(1):3–16, 2003.
- [207] F. Gabor, U. Klausegger, and M. Wirth. The interaction between wheat germ agglutinin and other plant lectins with prostate cancer cells du-145. *International Journal of Pharmaceutics*, 221:35–47, 2001.
- [208] F. Gabor, M. Stangl, and M. Wirth. Lectin-mediated bioadhesion: Binding characteristics of plant lectins on the enterocyte-like cell lines caco-2, ht-29 and hct-8. *Journal of Controlled Release*, 55(2-3):131–142, 1998.
- [209] S. Toegel, N. Harrer, V.E. Plattner, F.M. Unger, H. Viernstein, M.B. Goldring, F. Gabor, and M. Wirth. Lectin binding studies on c-28/i2 and t/c-28a2 chondrocytes provide a basis for new tissue engineering and drug delivery perspectives in cartilage research. *Journal of Controlled Release*, 117(1):121–129, 2007.
- [210] V.E. Plattner, M. Wagner, G. Ratzinger, F. Gabor, and M. Wirth. Targeted drug delivery: Binding and uptake of plant lectins using human 5637 bladder cancer cells. *European Journal of Pharmaceutics and Biopharmaceutics*, 70(2):572–576, 2008.
- [211] V.E. Plattner, G. Ratzinger, E.T. Engleder, S. Gallauner, F. Gabor, and M. Wirth. Alteration of the glycosylation pattern of monocytic thp-1 cells and its impact on lectin-mediated drug delivery. *European Journal of Pharmaceutics and Biopharmaceutics*, 73(3):324–330, 2009.
- [212] F. Gabor, M. Wirth, B. Jurkovich, I. Haberl, G. Theyer, G. Walcher, and G. Hamilton. Lectin-mediated bioadhesion: Proteolytic stability and binding-characteristics of wheat germ agglutinin and

- solanum tuberosum lectin on caco-2, ht-29 and human colonocytes. *Journal of Controlled Release*, 49(1):27–37, 1997.
- [213] N. Lochner, F. Pittner, M. Wirth, and F. Gabor. Wheat germ agglutinin binds to the epidermal growth factor receptor of artificial caco-2 membranes as detected by silver nanoparticle enhanced fluorescence. *Pharmaceutical Research*, 20(5):833–839, 2003.
- [214] F. Roth-Walter, I. Scholl, E. Untersmayr, A. Ellinger, G. Boltz-Nitulescu, O. Scheiner, F. Gabor, and E. Jensen-Jarolim. Mucosal targeting of allergen-loaded microspheres by aleuria aurantia lectin. *Vaccine*, 23(21):2703–2710, 2005.
- [215] M.A. Jepson, M.A. Clark, and B.H. Hirst. M cell targeting by lectins: A strategy for mucosal vaccination and drug delivery. *Advanced Drug Delivery Reviews*, 56:511–525, 2004.
- [216] R.N. Palumbo and C. Wang. Bacterial invasin: Structure, function, and implication for targeted oral gene delivery. *Current Drug Delivery*, 3(1):47–53, 2006.
- [217] A. des Rieux, V. Fievez, M. Garinot, Y.J. Schneider, and V. Préat. Nanoparticles as potential oral delivery systems of proteins and vaccines: A mechanistic approach. *Journal of Controlled Release*, 116(1):1–27, 2006.
- [218] G.F. Dawson and G.W. Halbert. The in vitro cell association of invasin coated polylactide-co-glycolide nanoparticles. *Pharmaceutical Research*, 17(11):1420–5, 2000.
- [219] S.A. Townsend, G.D. Evrony, F.X. Gu, M.P. Schulz, R.H. Brown, and R. Langer. Tetanus toxing c fragment-conjugated nanoparticles for targeted drug delivery to neurons. *Biomaterials*, 28:5176–5184, 2007.
- [220] D.A. Rothenfluh, H. Bermudez, C.P. O’Neil, and J.A. Hubbell. Biofunctional polymer nanoparticles for intra-articular targeting and retention in cartilage. *Nature Materials*, 7:248–254, 2008.
- [221] U. Hersel, C. Dahmen, and H. Kessler. Rgd modified polymers: biomaterials for stimulated cell adhesion and beyond. *Biomaterials*, 24:4385–4415, 2003.
- [222] Z. Wang, W.K. Chui, and P.C. Ho. Design of a multifunctional plga nanoparticulate drug delivery system: Evaluation of its physicochemical properties and anticancer activity to malignant cancer cells. *Pharmaceutical Research*, 26(5):1162–1171, 2009.
- [223] M. Garinot, V. Fievez, V. Pourcelle, F. Stoffelbach, A. des Rieux, L. Plapied, I. Theate, H. Freichels, C. Jerome, J. Marchand-Brynaert, Y.J. Schneider, and V. Preat. Pegylated plga-based nanoparticles targeting m cells for oral vaccination. *Journal of Controlled Release*, 120:195–204, 2007.
- [224] V. Fievez, L. Plapied, A. des Rieux, V. Pourcelle, H. Freichels, V. Wascotte, M.L. Vanderhaeghen, C. Jerome, A. Vanderplasschen, J. Marchand-Brynaert, Y.J. Schneider, and V. Preat. Targeting nanoparticles to m cells with non-peptidic ligands for oral vaccination. *European Journal of Pharmaceutics and Biopharmaceutics*, 73:16–24, 2009.

- [225] N. Zhang, C. Chittasupho, C. Duangrat, T.J. Siahaan, and C. Berklund. Plga nanoparticle-peptide conjugate effectively targets intercellular cell-adhesion molecule-1. *Bioconjugate Chemistry*, 19(1):145–152, 2008.
- [226] L. Costantino, F. Gandolfi, G. Tosi, F. Rivasi, M. A. Vandelli, and F. Forni. Peptide-derivatized biodegradable nanoparticles able to cross the blood-brain barrier. *Journal of Controlled Release*, 108(1):84–96, 2005.
- [227] G. Tosi, L. Costantino, F. Rivasi, B. Ruozi, E. Leo, A. V. Vergoni, R. Tacchi, A. Bertolini, M. A. Vandelli, and F. Forni. Targeting the central nervous system: in vivo experiments with peptide-derivatized nanoparticles loaded with loperamide and rhodamine-123. *Journal of Controlled Release*, 122(1):1–9, 2007.
- [228] O.C. Farokhzad, J. Cheng, B.A. Teply, I. Sherifi, S. Jon, P.W. Kantoff, J.P. Richie, and R. Langer. Targeted nanoparticle-aptamer bioconjugates for cancer chemotherapy in vivo. *Proceedings of the National Academy of Sciences of the United States of America*, 103(16):6315–6320, 2006.
- [229] A.R. Hilgenbrink and P.S. Low. Folate receptor-mediated drug targeting: from therapeutics to diagnostics. *Journal of Pharmaceutical Sciences*, 94(10):2135–2146, 2005.
- [230] H.S. Yoo and T.G. Park. Folate receptor targeted biodegradable polymeric doxorubicin micelles. *Journal of Controlled Release*, 96(2):273–283, 2004.
- [231] Z. Zhang, S.H. Lee, and S.S. Feng. Folate-decorated poly(lactide-co-glycolide)-vitamin e tpgs nanoparticles for targeted drug delivery. *Biomaterials*, 28:1889–1899, 2007.
- [232] P.R. Lockman, M.O. Oyewumi, J.M. Koziara, K.E. Roder, R.J. Mumper, and D.D. Allen. Brain uptake of thiamine-coated nanoparticles. *Journal of Controlled Release*, 93:271–282, 2003.
- [233] H.H. Salman, C. Gamazo, P.C. de Smidt, G. Russell-Jones, and J.M. Irache. Evaluation of bioadhesive capacity and immunoadjuvant properties of vitamin b(12)-gantrez nanoparticles. *Pharmaceutical Research*, 25(12):2859–2868, 2008.
- [234] S.W. Choi and J.H. Kim. Design of surface-modified poly(d,l-lactide-co-glycolide) nanoparticles for targeted drug delivery to the bone. *Journal of Controlled Release*, 122:24–30, 2007.
- [235] J.K. Vasir and V. Labhasetwar. Biodegradable nanoparticles for cytosolic delivery of therapeutics. *Advanced Drug Delivery Reviews*, 59:718–728, 2007.
- [236] M. Breunig, S. Bauer, and A. Goepferich. Polymers and nanoparticles: intelligent tools for intracellular targeting? *European Journal of Pharmaceutics and Biopharmaceutics*, 68:112–128, 2008.
- [237] J.P. Behr. The proton sponge: A trick to enter cells the viruses didn't exploit. *Chimia*, 51:34–36, 1997.

- [238] D.W. Pack, A.S. Hoffmann, S. Pun, and P.S. Stayton. Design and development of polymers for gene delivery. *Nature Reviews Drug Discovery*, 4:581–593, 2005.
- [239] M. Bivas-Benita, M.Y. Lin, S.M. Bal, K.E. van Meijgaarden, K.L.M.C. Franken, A.H. Friggen, H.E. Junginger, G. Borchard, M.R. Klein, and T.H.M. Ottenhoff. Pulmonary delivery of dna encoding mycobacterium tuberculosis latency antigen rv1733c associated to plga-pei nanoparticles enhances t cell responses in a dna prime/protein boost vaccination regimen in mice. *Vaccine*, 27(30):4010–4017, 2009.
- [240] J. Panyam, W.Z. Zhou, S. Prabha, S.K. Sahoo, and V. Labhasetwar. Rapid endo-lysosomal escape of poly(dl-lactide-co-glycolide) nanoparticles: implications for drug and gene delivery. *FASEB Journal*, 16(10):1217–1226, 2002.
- [241] B. Gupta, T.S. Levchenko, and V.P. Torchilin. Intracellular delivery of large molecules and small particles by cell-penetrating proteins and peptides. *Advanced Drug Delivery Reviews*, 57:637–651, 2005.
- [242] C. Foerg and H.P. Merkle. On the biomedical promise of cell penetrating peptides: Limits versus prospects. *Journal of Pharmaceutical Sciences*, 97(1):144–162, 2008.
- [243] J.S. Wadia, R.V. Stan, and S.F. Dowdy. Transducible tat-ha fusogenic peptide enhances escape of tat-fusion proteins after lipid raft micropinocytosis. *Nature Medicine*, 10(3):310–315, 2004.
- [244] Y.S. Nam, J.Y. Park, S.H. Han, and I.S. Chang. Intracellular drug delivery using poly(d,l-lactide-co-glycolide) nanoparticles derivatized with a peptide from a transcriptional activator protein of hiv-1. *Biotechnology Letters*, 24:2093–2098, 2002.
- [245] S.J. Lee, J.R. Jeong, S.C. Shin, Y.M. Huh, H.T. Song, J.S. Suh, Y.H. Chang, B.S. Jeon, and J.D. Kim. Intracellular translocation of superparamagnetic iron oxide nanoparticles with peptide-conjugated poly(d,l-lactide-co-glycolide). *Journal of Applied Physics*, 97(10):1–3, 2005.
- [246] C.W. Pouton, K.M. Wagstaff, D.M. Roth, G.W. Moseley, and D.A. Jans. Targeted delivery to the nucleus. *Advanced Drug Delivery Reviews*, 59:698–717, 2007.
- [247] J. Suh, M. Dawson, and J. Hanes. Real-time multiple-particle tracking: applications to drug and gene delivery. *Advanced Drug Delivery Reviews*, 57:63–78, 2005.
- [248] C.P. Ng, T.T. Goodman, I.K. Park, and S.H. Pun. Bio-mimetic surface engineering of plasmid-loaded nanoparticles for active intracellular trafficking by actin comet-tail motility. *Biomaterials*, 30(5):951–958, 2009.
- [249] F.Y. Cheng, S.P.H. Wang, C.H. Su, T.L. Tsai, P.C. Wu, D.B. Shieh, J.H. Chen, P.C.H. Hsieh, and C.S. Yeh. Stabilizer-free poly(lactide-co-glycolide) nanoparticles for multimodal biomedical probes. *Biomaterials*, 29(13):2104–2112, 2008.

- [250] P. Xu, E. Gullotti, L. Tong, C.B. Highley, D.R. Errabelli, T. Hasan, J.X. Cheng, D.S. Kohane, and Y. Yeo. Intracellular drug delivery by poly(lactic-co-glycolic acid) nanoparticles, revisited. *Molecular Pharmaceutics*, 6(1):190–201, 2008.
- [251] J. Gruenberg and F.G. Van der Goot. Mechanisms of pathogen entry through the endosomal compartments. *Nature Reviews Molecular Cell Biology*, 7:495–504, 2006.
- [252] L.K. Medina-Kauwe. "alternative" endocytic mechanisms exploited by pathogens: new avenues for therapeutic delivery? *Advanced Drug Delivery Reviews*, 59:798–809, 2007.
- [253] A.E. Wright and S.R. Douglas. An experimental investigation of the role of the blood fluids in connection with phagocytosis. *Proceedings of the Royal Society of London*, 72:357–370, 1903.
- [254] H.M. Patel. Serum opsonins and liposomes: Their interaction and opsonophagocytosis. *Critical Reviews in Therapeutic Drug Carrier Systems*, 9(1):39–90, 1992.
- [255] S. M. Moghimi, I. S. Muir, L. Illum, S. S. Davis, and V. Kolb-Bachofen. Coating particles with a block co-polymer (poloxamine-908) suppresses opsonization but permits the activity of dysopsonins in the serum. *Biochimica et Biophysica Acta - Molecular Cell Research*, 1179(2):157–165, 1993.
- [256] H. Harashima, H. Matsuo, and H. Kiwada. Identification of proteins mediating clearance of liposomes using a liver perfusion system. *Advanced Drug Delivery Reviews*, 32(1-2):61–79, 1998.
- [257] R. Gref, A. Domb, P. Quellec, T. Blunk, R. H. Müller, J. M. Verbaatz, and R. Langer. The controlled intravenous delivery of drugs using peg-coated sterically stabilized nanospheres. *Advanced Drug Delivery Reviews*, 16(2-3):215–233, 1995.
- [258] K. I. Ogawara, K. Higaki, and T. Kimura. Major determinants in hepatic disposition of polystyrene nanospheres: Implication for rational design of particulate drug carriers. *Critical Reviews in Therapeutic Drug Carrier Systems*, 19(4-5):277–306, 2002.
- [259] S.M. Moghimi and J. Szebeni. Stealth liposomes and long circulating nanoparticles: critical issues in pharmacokinetics, opsonization and protein-binding properties. *Progress in Lipid Research*, 42(6):463–478, 2003.
- [260] D.E. Owens and N.A. Peppas. Opsonization, biodistribution, and pharmacokinetics of polymeric nanoparticles. *International Journal of Pharmaceutics*, 307(1):93–102, 2006.
- [261] A. Vonarbourg, C. Passirani, P. Saulnier, and J.P. Benoit. Parameters influencing the stealthiness of colloidal drug delivery systems. *Biomaterials*, 27(24):4356–4373, 2006.
- [262] S.M. Moghimi, A.C. Hunter, and J.C. Murray. Long-circulating and target-specific nanoparticles: Theory to practice. *Pharmacological Reviews*, 53(2):283–318, 2001.

- [263] J.K. Gbadamosi, A.C. Hunter, and S.M. Moghimi. Pegylation of microspheres generates a heterogeneous population of particles with differential surface characteristics and biological performance. *FEBS Letters*, 532(3):338–344, 2002.
- [264] F. Meng, G.H.M. Engbers, A. Gessner, R.H. Müller, and J. Feijen. Pegylated polystyrene particles as a model system for artificial cells. *Journal of Biomedical Materials Research - Part A*, 70(1):97–106, 2004.
- [265] P.M. Claesson, E. Blomberg, J.C. Fröberg, T. Nylander, and T. Arnebrant. Protein interactions at solid surfaces. *Advances in Colloid and Interface Science*, 57:161–227, 1995.
- [266] C. Lemarchand, R. Gref, and P. Couvreur. Polysaccharide-decorated nanoparticles. *European Journal of Pharmaceutics and Biopharmaceutics*, 58(2):327–341, 2004.
- [267] S.I. Jeon, J.H. Lee, J.D. Andrade, and P.G. De Gennes. Protein-surface interactions in the presence of polyethylene oxide: I. simplified theory. *Journal of Colloid and Interface Science*, 142(1):149–158, 1991.
- [268] S.I. Jeon and J.D. Andrade. Protein-surface interactions in the presence of polyethylene oxide: II. effect of protein size. *Journal of Colloid and Interface Science*, 142(1):159–166, 1991.
- [269] M. Vittaz, D. Bazile, G. Spenlehauer, T. Verrecchia, M. Veillard, F. Puisieux, and D. Labarre. Effect of pco surface density on long-circulating pla-pco nanoparticles which are very low complement activators. *Biomaterials*, 17(16):1575–1581, 1996.
- [270] Y. Li, Y. Pei, X. Zhang, Z. Gu, Z. Zhou, W. Yuan, J. Zhou, J. Zhu, and X. Gao. Pegylated plga nanoparticles as protein carriers: synthesis, preparation and biodistribution in rats. *Journal of Controlled Release*, 71(2):203–211, 2001.
- [271] Z. Panagi, A. Beletsi, G. Evangelatos, E. Livaniou, D. S. Ithakissios, and K. Avgoustakis. Effect of dose on the biodistribution and pharmacokinetics of plga and plga-mpeg nanoparticles. *International Journal of Pharmaceutics*, 221(1-2):143–152, 2001.
- [272] T. Ameller, R. Marsaud, P. Legrand, R. Gref, G. Barratt, and J. M. Renoir. Polyester-poly(ethylene glycol) nanoparticles loaded with the pure antiestrogen ru 58668: Physicochemical and opsonization properties. *Pharmaceutical Research*, 20(7):1063–1070, 2003.
- [273] K. Avgoustakis, A. Beletsi, Z. Panagi, P. Klepetsanis, E. Livaniou, G. Evangelatos, and D. S. Ithakissios. Effect of copolymer composition on the physicochemical characteristics, in vitro stability, and biodistribution of plga-mpeg nanoparticles. *International Journal of Pharmaceutics*, 259(1-2):115–127, 2003.
- [274] A. Beletsi, Z. Panagi, and K. Avgoustakis. Biodistribution properties of nanoparticles based on mixtures of plga with plga-peg diblock copolymers. *International Journal of Pharmaceutics*, 298(1):233–241, 2005.

- [275] Y. Duan, X. Sun, T. Gong, Q. Wang, and Z. Zhang. Preparation of dhaq-loaded mpeg-plga-mpeg nanoparticles and evaluation of drug release behaviors in vitro/in vivo. *Journal of Materials Science: Materials in Medicine*, 17(6):509–16, 2006.
- [276] K.J. Taek, M.O. Yu, and B.C. Shin. Preparation of poly(dl-lactide-co-glycolide) nanoparticles by peg-ppg diblock copolymer. *Polymer (Korea)*, 27(4):370–376, 2003.
- [277] J.C. Neal, S. Stolnik, E. Schacht, E.R. Kenawy, M.C. Garnett, S.S. Davis, and L. Illum. In vitro displacement by rat serum of adsorbed radiolabeled poloxamer and poloxamine copolymers from model and biodegradable nanospheres. *Journal of Pharmaceutical Sciences*, 87(10):1242–1248, 1998.
- [278] H.M. Redhead, S.S. Davis, and L. Illum. Drug delivery in poly(lactide-co-glycolide) nanoparticles surface modified with poloxamer 407 and poloxamine 908: in vitro characterisation and in vivo evaluation. *Journal of Controlled Release*, 70(3):353–363, 2001.
- [279] J.C. Olivier. Drug transport to brain with targeted nanoparticles. *NeuroRX*, 2(1):108–119, 2005.
- [280] F. von Burkersroda, R. Gref, and A. Göpferich. Erosion of biodegradable block copolymers made of poly(-lactic acid) and poly(ethylene glycol). *Biomaterials*, 18(24):1599–1607, 1997.
- [281] K. Avgoustakis. Pegylated poly(lactide) and poly(lactide-co-glycolide) nanoparticles: preparation, properties and possible applications in drug delivery. *Current Drug Delivery*, 1(4):321–333, 2004.
- [282] R. Karnik, F. Gu, P. Basto, C. Cannizzaro, L. Dean, W. Kyei-Manu, R. Langer, and O. C. Farokhzad. Microfluidic platform for controlled synthesis of polymeric nanoparticles. *Nano Letters*, 8(9):2906–2912, 2008.
- [283] S.M. Moghimi. Prolonging the circulation time and modifying the body distribution of intravenously injected polystyrene nanospheres by prior intravenous administration of poloxamine-908. a 'hepatic-blockade' event or manipulation of nanosphere surface in vivo? *Biochimica et Biophysica Acta - General Subjects*, 1336(1):1–6, 1997.
- [284] K.S. Denis-Mize, M. Dupuis, M. Singh, C. Woo, M. Ugozzoli, D.T. O'Hagan, J.J. Donnelly, G. Ott, and D.M. McDonald. Mechanisms of increased immunogenicity for dna-based vaccines adsorbed onto cationic microparticles. *Cellular Immunology*, 225(1):12–20, 2003.
- [285] C. Fillafer, D.S. Friedl, M. Wirth, and F. Gabor. Fluorescent bio-nanoprobes to characterize cytoadhesion and cytoinvasion. *Small*, 4(5):627–633, 2008.
- [286] J. Kang and S.P. Schwendeman. Determination of diffusion coefficient of a small hydrophobic probe in poly(lactide-co-glycolide) microparticles by laser scanning confocal microscopy. *Macromolecules*, 36(4):1324–1330, 2003.

- [287] A.O. Eniola and D.A. Hammer. Artificial polymeric cells for targeted drug delivery. *Journal of Controlled Release*, 87(1-3):15–22, 2003.
- [288] E.G. de Jalón, M.J. Blanco-Prieto, P. Ygartua, and S. Santoyo. Plga microparticles: possible vehicles for topical drug delivery. *International Journal of Pharmaceutics*, 226(1-2):181–184, 2001.
- [289] V. Saxena, M. Sadoqi, and J. Shao. Indocyanine green-loaded biodegradable nanoparticles: preparation, physicochemical characterization and in vitro release. *International Journal of Pharmaceutics*, 278(2):293–301, 2004.
- [290] B.J. Nehilla, P.G. Allen, and T.A. Desai. Surfactant-free, drug-quantum-dot coloaded poly(lactide-co-glycolide) nanoparticles: Towards multifunctional nanoparticles. *ACS Nano*, 2(3):538–544, 2008.
- [291] J. Panyam, S.K. Sahoo, S. Prabha, T. Bargar, and V. Labhasetwar. Fluorescence and electron microscopy probes for cellular and tissue uptake of poly(,-lactide-co-glycolide) nanoparticles. *International Journal of Pharmaceutics*, 262(1-2):1–11, 2003.
- [292] B. Weiss, U. F. Schaefer, J. Zapp, A. Lamprecht, A. Stallmach, and C. M. Lehr. Nanoparticles made of fluorescence-labelled poly(l-lactide-co-glycolide): preparation, stability, and biocompatibility. *Journal of Nanoscience and Nanotechnology*, 6(9-10):3048–3056, 2006.
- [293] G. Tosi, F. Rivasi, F. Gandolfi, L. Costantino, M. A. Vandelli, and F. Forni. Conjugated poly(d,l-lactide-co-glycolide) for the preparation of in vivo detectable nanoparticles. *Biomaterials*, 26(19):4189–4195, 2005.
- [294] H.J. Chung, H.K. Kim, J.J. Yoon, and T.G. Park. Heparin immobilized porous plga microspheres for angiogenic growth factor delivery. *Pharmaceutical Research*, 23(8):1835–1841, 2006.
- [295] Y. Mo and L.Y. Lim. Mechanistic study of the uptake of wheat germ agglutinin-conjugated plga nanoparticles by a549 cells. *Journal of Pharmaceutical Sciences*, 93(1):20–28, 2004.
- [296] C. Fillafer, G. Ratzinger, J. Neumann, Z. Guttenberg, S. Dissauer, I.K. Lichtscheidl, M. Wirth, F. Gabor, and M.F. Schneider. An acoustically-driven biochip - impact of flow on the cell-association of targeted drug carriers. *Lab on a Chip*, 9(19):2782–2788, 2009.
- [297] A.E. Hawley, L. Illum, and S.S. Davis. Lymph node localisation of biodegradable nanospheres surface modified with poloxamer and poloxamine block co-polymers. *FEBS Letters*, 400(3):319–323, 1997.
- [298] A. Delgado, I. Soriano, E. Sánchez, M. Oliva, and C. Évora. Radiolabelled biodegradable microspheres for lung imaging. *European Journal of Pharmaceutics and Biopharmaceutics*, 50(2):227–236, 2000.
- [299] Y. J. Park, S. H. Nah, J. Y. Lee, J. M. Jeong, J. K. Chung, M. C. Lee, V. C. Yang, and S. J. Lee. Surface-modified poly(lactide-co-glycolide) nanospheres for targeted bone imaging with enhanced labeling and delivery of radioisotope. *Journal of Biomedical Materials Research - Part A*, 67(3):751–760, 2003.

- [300] K. K. Halder, B. Mandal, M. C. Debnath, H. Bera, L. K. Ghosh, and B. K. Gupta. Chloramphenicol-incorporated poly lactide-co-glycolide (plga) nanoparticles: Formulation, characterization, technetium-99m labeling and biodistribution studies. *Journal of Drug Targeting*, 16(4):311–320, 2008.
- [301] J. Shukla, G.P. Bandopadhyaya, and I.K. Varma. 188rhenium(v)-dimercaptosuccinic acid loaded poly(lactic-co-glycolic)acid microspheres for targeted radiotherapy: Production and effectivity. *Pharmazie*, 60(8):583–587, 2005.
- [302] Y. Mo and L.Y. Lim. Paclitaxel-loaded plga nanoparticles: potentiation of anticancer activity by surface conjugation with wheat germ agglutinin. *Journal of Controlled Release*, 108(2-3):244–262, 2005.
- [303] A.M. Le Ray, M. Vert, J.C. Gautier, and J.P. Benoit. End-chain radiolabeling and in vitro stability studies of radiolabeled poly(hydroxy acid) nanoparticles. *Journal of Pharmaceutical Sciences*, 83(6):845–851, 1994.
- [304] E. Dadachova and S. Mirzadeh. The role of tin in the direct labelling of proteins with rhenium-188. *Nuclear Medicine and Biology*, 24(6):605–608, 1997.
- [305] T. Banerjee, A.K. Singh, R.K. Sharma, and A.N. Maitra. Labeling efficiency and biodistribution of technetium-99m labeled nanoparticles: interference by colloidal tin oxide particles. *International Journal of Pharmaceutics*, 289(1-2):189–195, 2005.
- [306] C. Fillafer, D.S. Friedl, A.K. Ilyes, M. Wirth, and F. Gabor. Bionanoprobes to study particle-cell interactions. *Journal of Nanoscience and Nanotechnology*, 9(5):3239–3245, 2009.
- [307] P. Pietzonka, B. Rothen-Rutishauser, P. Langguth, H. Wunderli-Allenspach, E. Walter, and H. P. Merkle. Transfer of lipophilic markers from plga and polystyrene nanoparticles to caco-2 monolayers mimics particle uptake. *Pharmaceutical Research*, 19(5):595–601, 2002.
- [308] S. Cohen, T. Yoshioka, M. Lucarelli, L.H. Hwang, and R. Langer. Controlled delivery systems for proteins based on poly(lactic/glycolic acid) microspheres. *Pharmaceutical Research*, 8(6):713–720, 1991.
- [309] W. Jiang, R.K. Gupta, M.C. Deshpande, and S.P. Schwendeman. Biodegradable poly(lactic-co-glycolic acid) microparticles for injectable delivery of vaccine antigens. *Advanced Drug Delivery Reviews*, 57(3):391–410, 2005.
- [310] A.O. Abbas, M.D. Donovan, and A.K. Salem. Formulating poly(lactide-co-glycolide) particles for plasmid dna delivery. *Journal of Pharmaceutical Sciences*, 97(7):2448–2461, 2008.
- [311] S. Ando, D. Putnam, D.W. Pack, and R. Langer. Plga microspheres containing plasmid dna: Preservation of supercoiled dna via cryopreparation and carbohydrate stabilization. *Journal of Pharmaceutical Sciences*, 88(1):126–130, 1999.

- [312] M. Wolf, M. Wirth, F. Pittner, and F. Gabor. Stabilisation and determination of the biological activity of l-asparaginase in poly(d,l-lactide-co-glycolide) nanospheres. *International Journal of Pharmaceutics*, 256(1-2):141–152, 2003.
- [313] K. Fu, D.W. Pack, A.M. Klibanov, and R. Langer. Visual evidence of acidic environment within degrading poly(lactic-co-glycolic acid) (plga) microspheres. *Pharmaceutical Research*, 17(1):100–106, 2000.
- [314] A.G. Ding and S.P. Schwendeman. Acidic microclimate ph distribution in plga microspheres monitored by confocal laser scanning microscopy. *Pharmaceutical Research*, 25(9):2041–2052, 2008.
- [315] E. Walter, K. Moelling, J. Pavlovic, and H.P. Merkle. Microencapsulation of dna using poly(-lactide-co-glycolide): stability issues and release characteristics. *Journal of Controlled Release*, 61(3):361–374, 1999.
- [316] S.P. Schwendeman. Recent advances in the stabilization of proteins encapsulated in injectable plga delivery systems. *Critical Reviews in Therapeutic Drug Carrier Systems*, 19(1):73–98, 2002.
- [317] M. Singh, J. Kazzaz, M. Ugozzoli, P. Malyala, J. Chesko, and D. T. O'Hagan. Polylactide-co-glycolide microparticles with surface adsorbed antigens as vaccine delivery systems. *Current Drug Delivery*, 3(1):115–120, 2006.
- [318] Y.I. Chung, G. Tae, and S. Hong Yuk. A facile method to prepare heparin-functionalized nanoparticles for controlled release of growth factors. *Biomaterials*, 27(12):2621–2626, 2006.
- [319] M. Singh, J. Chesko, J. Kazzaz, M. Ugozzoli, E. Kan, I. Srivastava, and D. T. O'Hagan. Adsorption of a novel recombinant glycoprotein from hiv (env gp120dv2 sf162) to anionic plg microparticles retains the structural integrity of the protein, whereas encapsulation in plg microparticles does not. *Pharmaceutical Research*, 21(12):2148–2152, 2004.
- [320] A. Sapin, A. Clavreul, E. Garcion, J. P. Benoit, and P. Menei. Evaluation of particulate systems supporting tumor cell fractions in a preventive vaccination against intracranial rat glioma. *Journal of Neurosurgery*, 105(5):745–752, 2006.
- [321] M. Singh, G. Ott, J. Kazzaz, M. Ugozzoli, M. Briones, J. Donnelly, and D. T. O'Hagan. Cationic microparticles are an effective delivery system for immune stimulatory cpg dna. *Pharmaceutical Research*, 18(10):1476–1479, 2001.
- [322] D. O'Hagan, M. Singh, M. Ugozzoli, C. Wild, S. Barnett, M. Chen, M. Schaefer, B. Doe, G. R. Otten, and J. B. Ulmer. Induction of potent immune responses by cationic microparticles with adsorbed human immunodeficiency virus dna vaccines. *Journal of Virology*, 75(19):9037–9043, 2001.
- [323] M. Singh, M. Ugozzoli, M. Briones, J. Kazzaz, E. Soenawan, and D. T. O'Hagan. The effect of ctab concentration in cationic plg microparticles on dna adsorption and in vivo performance. *Pharmaceutical Research*, 20(2):247–251, 2003.

- [324] X.Q. Zhang, J. Intra, and A.K. Salem. Comparative study of poly (lactic-co-glycolic acid)-poly ethyleneimine-plasmid dna microparticles prepared using double emulsion methods. *Journal of Microencapsulation*, 25(1):1–12, 2008.
- [325] M. Briones, M. Singh, M. Ugozzoli, J. Kazzaz, S. Klakamp, G. Ott, and D. O'Hagan. The preparation, characterization, and evaluation of cationic microparticles for dna vaccine delivery. *Pharmaceutical Research*, 18(5):709–712, 2001.
- [326] X.Q. Zhang, J. Intra, and A.K. Salem. Conjugation of polyamidoamine dendrimers on biodegradable microparticles for nonviral gene delivery. *Bioconjugate Chemistry*, 18(6):2068–2076, 2007.
- [327] N. Stivaktakis, K. Nikou, Z. Panagi, A. Beletsi, L. Leondiadis, and K. Avgoustakis. Immune responses in mice of β -galactosidase adsorbed or encapsulated in poly(lactic acid) and poly(lactic-co-glycolic acid) microspheres. *Journal of Biomedical Materials Research - Part A*, 73(3):332–338, 2005.
- [328] P. Johansen, Y. Men, H.P. Merkle, and B. Gander. Revisiting plga microspheres: An analysis of their potential in parenteral vaccination. *European Journal of Pharmaceutics and Biopharmaceutics*, 50(1):129–146, 2000.
- [329] P. Johansen, J.M. Martínez Gomez, and B. Gander. Development of synthetic biodegradable microparticulate vaccines: A roller coaster story. *Expert Review of Vaccines*, 6(4):471–474, 2007.
- [330] D.T. O'Hagan, M. Singh, and J.B. Ulmer. Microparticle-based technologies for vaccines. *Methods*, 40(1):10–19, 2006.
- [331] Y. Capan, B.H. Woo, S. Gebrekidan, S. Ahmed, and P.P. DeLuca. Preparation and characterization of poly (d,l-lactide-co-glycolide) microspheres for controlled release of poly(l-lysine) complexed plasmid dna. *Pharmaceutical Research*, 16(4):509–513, 1999.
- [332] K.A. Howard and H.O. Alpar. The development of polyplex-based dna vaccines. *Journal of Drug Targeting*, 10(2):143–151, 2002.
- [333] X. Zhou, B. Liu, X. Yu, X. Zha, X. Zhang, X. Wang, Y. Jin, Y. Wu, Y. Chen, Y. Shan, Y. Chen, J. Liu, W. Kong, and J. Shen. Controlled release of pei/dna complexes from plga microspheres as a potent delivery system to enhance immune response to hiv vaccine dna prime/mva boost regime. *European Journal of Pharmaceutics and Biopharmaceutics*, 68(3):589–595, 2008.
- [334] K.A. Howard, X.W. Li, S. Somavarapu, J. Singh, N. Green, K.N. Atuah, Y. Ozsoy, L.W. Seymour, and H.O. Alpar. Formulation of a microparticle carrier for oral polyplex-based dna vaccines. *Biochimica et Biophysica Acta - General Subjects*, 1674(2):149–157, 2004.
- [335] D.T. O'Hagan, M. Singh, C. Dong, M. Ugozzoli, K. Berger, E. Glazer, M. Selby, M. Wininger, P. Ng, K. Crawford, X. Paliard, S. Coates, and M. Houghton. Cationic microparticles are a potent delivery system for a hcv dna vaccine. *Vaccine*, 23(5):672–680, 2004.

- [336] H.J. Mollenkopf, G. Dietrich, J. Fensterle, L. Grode, K. D. Diehl, B. Knapp, M. Singh, D. T. O'Hagan, J. B. Ulmer, and S. H. E. Kaufmann. Enhanced protective efficacy of a tuberculosis dna vaccine by adsorption onto cationic plg microparticles. *Vaccine*, 22(21-22):2690–2695, 2004.
- [337] M. Liman, L. Peiser, G. Zimmer, M. Pröpsting, H. Y. Naim, and S. Rautenschlein. A genetically engineered prime-boost vaccination strategy for oculonasal delivery with poly(d,l-lactic-co-glycolic acid) microparticles against infection of turkeys with avian metapneumovirus. *Vaccine*, 25(46):7914–7926, 2007.
- [338] S. Choudary, P. Ravikumar, C. Ashok Kumar, V. Suryanarayana, and G. Reddy. Enhanced immune response of dna vaccine (vp1-pcdna) adsorbed on cationic plg for foot and mouth disease in guinea pigs. *Virus Genes*, 37(1):81–87, 2008.
- [339] X. He, L. Jiang, F. Wang, Z. Xiao, J. Li, S. L. Liu, D. Li, D. Ren, X. Jin, K. Li, Y. He, K. Shi, Y. Guo, Y. Zhang, and S. Sun. Augmented humoral and cellular immune responses to hepatitis b dna vaccine adsorbed onto cationic microparticles. *Journal of Controlled Release*, 107(2):357–372, 2005.
- [340] C.H. Pan, N. Nair, R.J. Adams, M.C. Zink, E.Y. Lee, F.P. Polack, M. Singh, D.T. O'Hagan, and D.E. Griffin. Dose-dependent protection against or exacerbation of disease by a polylactide glycolide microparticle-adsorbed, alphavirus-based measles virus dna vaccine in rhesus macaques. *Clinical and Vaccine Immunology*, 15(4):697–706, 2008.
- [341] S. Pai Kasturi, H. Qin, K. S. Thomson, S. El-Bereir, S. c Cha, S. Neelapu, L. W. Kwak, and K. Roy. Prophylactic anti-tumor effects in a b cell lymphoma model with dna vaccines delivered on polyethylenimine (pei) functionalized plga microparticles. *Journal of Controlled Release*, 113(3):261–270, 2006.
- [342] R. M. Verdijk, T. Mutis, B. Esendam, J. Kamp, C. J. M. Melief, A. Brand, and E. Goulmy. Polyriboinosinic polyribocytidylic acid (poly(i:c)) induces stable maturation of functionally active human dendritic cells. *Journal of Immunology*, 163(1):57–61, 1999.
- [343] M.S. Cartiera, K.M. Johnson, V. Rajendran, M.J. Caplan, and W.M. Saltzman. The uptake and intracellular fate of plga nanoparticles in epithelial cells. *Biomaterials*, 30:2790–2798, 2009.
- [344] C. Fillafer, M. Wirth, and F. Gabor. Stabilizer-induced viscosity alteration biases nanoparticle sizing via dynamic light scattering. *Langmuir*, 23(17):8699–8702, 2007.
- [345] J.M. Pean, M.C. Venier-Julienne, F. Boury, P. Menei, B. Denizot, and J.P. Benoit. Ngf release from poly(d,l-lactide-co-glycolide) microspheres. effect of some formulation parameters on encapsulated ngf stability. *Journal of Controlled Release*, 56:175–187, 1998.
- [346] G Binnig, C.F. Quate, and C. Gerber. Atomic force microscope. *Physical Review Letters*, 56(9):930–933, 1986.

- [347] D. J. Wilkins and P. A. Myers. Studies on the relationship between the electrophoretic properties of colloids and their blood clearance and organ distribution in the rat. *British Journal of Experimental Pathology*, 47(6):568–576, 1966.
- [348] G. Thurston, J. W. McLean, M. Rizen, P. Baluk, A. Haskell, T. J. Murphy, D. Hanahan, and D. M. McDonald. Cationic liposomes target angiogenic endothelial cells in tumors and chronic inflammation in mice. *Journal of Clinical Investigation*, 101:1401–1413, 1998.
- [349] K.M. Ainslie, R.D. Lowe, T.T. Beaudette, L. Petty, E.M. Bachelder, and T.A. Desai. Microfabricated devices for enhanced bioadhesive drug delivery: attachment to and small-molecule release through a cell monolayer under flow. *Small*, 5(24):2857–2863, 2009.
- [350] M.A. Wheatley, F. Forsberg, K. Oum, R. Ro, and D. El-Sherif. Comparison of in-vitro and in-vivo acoustic response of a novel 50:50 plga contrast agent. *Ultrasonics*, 44:360–367, 2006.
- [351] V.E. Plattner. *Lectin binding pattern of selected human cell lines and its impact on improved drug delivery*. PhD thesis, University of Vienna, 2009.
- [352] N. Sharon and H. Lis. *Lectins*. Kluwer Academic Publishers, 2nd edition edition, 2003.
- [353] V.E. Plattner, B. Germann, W. Neuhaus, C.R. Noe, F. Gabor, and M. Wirth. Characterization of two blood-brain barrier mimicking cell lines: Distribution of lectin-binding sites and perspectives for drug delivery. *International Journal of Pharmaceutics*, 387(1-2):34–41, 2010.
- [354] F. Gabor, M. Stangl, and M. Wirth. Lectin-mediated bioadhesion: binding characteristics of plant lectins on the enterocyte-like cell lines caco-2, ht-29 and hct-8. *Journal of Controlled Release*, 55(2-3):131–142, 1998.
- [355] F. Gabor, A. Schwarzbauer, and M. Wirth. Lectin-mediated drug delivery: binding and uptake of bsa-wga conjugates using the caco-2 model. *International Journal of Pharmaceutics*, 237(1-2):227–239, 2002.
- [356] F. Delie and W. Rubas. A human colonic cell line sharing similarities with enterocytes as a model to examine oral absorption: Advantages and limitations of the caco-2 model. *Critical Reviews in Therapeutic Drug Carrier Systems*, 14(3):221–286, 1997.
- [357] M. Wirth, K. Gerhardt, C. Warm, and F. Gabor. Lectin-mediated drug delivery: influence of mucin on cytoadhesion of plant lectins in vitro. *Journal of Controlled Release*, 79(1-3):183–191, 2002.
- [358] M. Wirth, C. Kneuer, C.M. Lehr, and F. Gabor. Lectin-mediated drug delivery: Discrimination between cytoadhesion and cytoinvasion and evidence for lysosomal accumulation of wheat germ agglutinin in the caco-2 model. *Journal of Drug Targeting*, 10(6):439–448, 2002.

- [359] S. K. Lai, K. Hida, S. T. Man, C. Chen, C. Machamer, T. A. Schroer, and J. Hanes. Privileged delivery of polymer nanoparticles to the perinuclear region of live cells via a non-clathrin, non-degradative pathway. *Biomaterials*, 28(18):2876–2884, 2007.
- [360] O.C. Farokhzad and R. Langer. Nanomedicine: developing smarter therapeutic and diagnostic modalities. *Advanced Drug Delivery Reviews*, 58(14):1456–1459, 2006.
- [361] D. Peer, J. M. Karp, S. Hong, O. C. Farokhzad, R. Margalit, and R. Langer. Nanocarriers as an emerging platform for cancer therapy. *Nature Nanotechnology*, 2(12):751–60, 2007.
- [362] N. S. White and R.J. Errington. Fluorescence techniques for drug delivery research: theory and practice. *Advanced Drug Delivery Reviews*, 57(1):17–42, 2005.
- [363] A. Weissenboeck, E. Bogner, M. Wirth, and F. Gabor. Binding and uptake of wheat germ agglutinin-grafted plga-nanospheres by caco-2 monolayers. *Pharmaceutical Research*, 21(10):1917–1923, 2004.
- [364] H. Suh, B. Jeong, F. Liu, and S. W. Kim. Cellular uptake study of biodegradable nanoparticles in vascular smooth muscle cells. *Pharmaceutical Research*, 15(9):1495–1508, 1998.
- [365] K. Langer, S. Balthasar, V. Vogel, N. Dinauer, H. von Briesen, and D. Schubert. Optimization of the preparation process for human serum albumin (hsa) nanoparticles. *International Journal of Pharmaceutics*, 257(1-2):169–180, 2003.
- [366] R. P. Haugland. *The Handbook-A guide to fluorescent probes and labelling technologies*. Invitrogen Corp., 10th edition, 2005.
- [367] C. Cortez, E. Tomaskovic-Crook, A. P. Johnston, A. M. Scott, E. C. Nice, J. K. Heath, and F. Caruso. Influence of size, surface, cell line, and kinetic properties on the specific binding of a33 antigen-targeted multilayered particles and capsules to colorectal cancer cells. *ACS Nano*, 1(2):93–102, 2007.
- [368] J.J. Green, E. Chiu, E.S. Leshchiner, J. Shi, R. Langer, and D.G. Anderson. Electrostatic ligand coatings of nanoparticles enable ligand-specific gene delivery to human primary cells. *Nano Letters*, 7(4):874–879, 2007.
- [369] O. C. Farokhzad, J. Cheng, B. A. Teply, I. Sherifi, S. Jon, P. W. Kantoff, J. P. Richie, and R. Langer. Targeted nanoparticle-aptamer bioconjugates for cancer chemotherapy in vivo. *Proceedings of the National Academy of Sciences of the United States of America*, 103(16):6315–6320, 2006.
- [370] W.R. Gombotz and D.K. Pettit. Biodegradable polymers for protein and peptide drug delivery. *Bioconjugate Chemistry*, 6(4):332–351, 1995.
- [371] R.A. Jain. The manufacturing techniques of various drug loaded biodegradable poly(lactide-co-glycolide) (plga) devices. *Biomaterials*, 21(23):2475–2490, 2000.

- [372] L. Brannon-Peppas. Recent advances on the use of biodegradable microparticles and nanoparticles in controlled drug delivery. *International Journal of Pharmaceutics*, 116(1):1–9, 1995.
- [373] M. Monsigny, A. C. Roche, C. Sene, R. Magetdana, and F. Delmotte. Sugar-lectin interactions - how does wheat-germ-agglutinin bind sialoglycoconjugates. *European Journal of Biochemistry*, 104(1):147–153, 1980.
- [374] R.H. Müller. *Zetapotential und Partikelladung in der Laborpraxis*. Wissenschaftliche Verlags Gesellschaft, Stuttgart, 1996.
- [375] I.J. Goldstein, S. Hammarstrom, and G. Sundblad. Precipitation and carbohydrate binding specificity studies on wheat germ agglutinin. *Biochimica et Biophysica Acta*, 405(1):53–61, 1975.
- [376] C. Vauthier, C. Schmidt, and P. Couvreur. Measurement of the density of polymeric nanoparticulate drug carriers by isopycnic centrifugation. *Journal of Nanoparticle Research*, 1(3):411–418, 1999.
- [377] G. Adam, P. Läuger, and G. Stark. *Physikalische Chemie und Biophysik*. Springer, Berlin, 2007.
- [378] E. J. Ambrose, A.M. James, and J. H. B. Lowick. Differences between the electrical charge carried by normal and homologous tumour cells. *Nature*, 177:576–577, 1956.
- [379] S. Ben-Or, S. Eisenberg, and F. Doljanski. Electrophoretic mobilities of normal and regenerating liver cells. *Nature*, 188:1200–1201, 1960.
- [380] T. Osaka, T. Nakanishi, S. Shanmugam, S. Takahama, and H. Zhang. Effect of surface charge of magnetite nanoparticles on their internalization into breast cancer and umbilical vein endothelial cells. *Colloids and Surfaces B: Biointerfaces*, 71:325–330, 2009.
- [381] V. R. Shinde Patil, C. J. Campbell, Y. H. Yun, S. M. Slack, and D. J. Goetz. Particle diameter influences adhesion under flow. *Biophysical Journal*, 80(4):1733–1743, 2001.
- [382] H. S. Sakhalkar, M. K. Dalal, A. K. Salem, R. Ansari, J. Fu, M. F. Kiani, D. T. Kurjiaka, J. Hanes, K. M. Shakesheff, and D. J. Goetz. Leukocyte-inspired biodegradable particles that selectively and avidly adhere to inflamed endothelium in vitro and in vivo. *Proceedings of the National Academy of Sciences of the United States of America*, 100(26):15895–15900, 2003.
- [383] B. Prabhakarandian, K. Pant, R. C. Scott, C. B. Patillo, D. Irimia, M. F. Kiani, and S. Sundaram. Synthetic microvascular networks for quantitative analysis of particle adhesion. *Biomedical Microdevices*, 10(4):585–595, 2008.
- [384] O. C. Farokhzad, A. Khademhosseini, S. Jon, A. Hermmann, J. Cheng, C. Chin, A. Kiselyuk, B. Teply, G. Eng, and R. Langer. Microfluidic system for studying the interaction of nanoparticles and microparticles with cells. *Analytical Chemistry*, 77(17):5453–5459, 2005.

- [385] J.B. Dressman, G.L. Amidon, C. Reppas, and V.P. Shah. Dissolution testing as a prognostic tool for oral drug absorption: Immediate release dosage forms. *Pharmaceutical Research*, 15(1):11–22, 1998.
- [386] G.J. Tortora and B. Derrickson. *Principles of anatomy and physiology*. John Wiley and Sons, Inc., 11th edition edition, 2006.
- [387] U. Welsch. *Lehrbuch Histologie*. Elsevier, München, 2nd edition edition, 2006.
- [388] R.K. Jain. Delivery of molecular medicine to solid tumors: lessons from in vivo imaging of gene expression and function. *Journal of Controlled Release*, 74:7–25, 2001.
- [389] F. Yuan, M. Leunig, S.K. Huang, D.A. Berk, D. Papahadjopoulos, and R.K. Jain. Microvascular permeability and interstitial penetration of sterically stabilized (stealth) liposomes in a human tumor xenograft. *Cancer Research*, 54:3352–3356, 1994.
- [390] Susan K. Hobbs, Wayne L. Monsky, Fan Yuan, W. Gregory Roberts, Linda Griffith, Vladimir P. Torchilin, and Rakesh K. Jain. Regulation of transport pathways in tumor vessels: Role of tumor type and microenvironment. *Proceedings of the National Academy of Sciences of the United States of America*, 95(8):4607–4612, 1998.
- [391] T. P. Padera, B. R. Stoll, J. B. Tooredman, D. Capen, E. di Tomaso, and R. K. Jain. Pathology: cancer cells compress intratumour vessels. *Nature*, 427(6976):695, 2004.
- [392] R.K. Jain. personal communication.
- [393] J.R.N. Curt and R. Pringle. Viscosity of gastric mucus in duodenal ulceration. *Gut*, 10:931–934, 1969.
- [394] C. Jacobs. *Nanosuspensions for various applications*. PhD thesis, Free University of Berlin, 2004.
- [395] M. Sugihara-Seki and B.M. Fu. Blood flow and permeability in microvessels. *Fluid Dynamics Research*, 37(1-2 SPEC. ISS.):82–132, 2005.
- [396] J. E. Blackwell, N. M. Dagia, J. B. Dickerson, E. L. Berg, and D. J. Goetz. Ligand coated nanosphere adhesion to e- and p-selectin under static and flow conditions. *Annals of Biomedical Engineering*, 29(6):523–33, 2001.
- [397] M. R. Wattenbarger, D. J. Graves, and D. A. Lauffenburger. Specific adhesion of glycophorin liposomes to a lectin surface in shear flow. *Biophysical Journal*, 57(4):765–77, 1990.
- [398] C. Cozens-Roberts, J. A. Quinn, and D. A. Lauffenburger. Receptor-mediated cell attachment and detachment kinetics. ii. experimental model studies with the radial-flow detachment assay. *Biophysical Journal*, 58(4):857–872, 1990.
- [399] P. Charoenphol, R.B. Huang, and O. Eniola-Adefeso. Potential role of size and hemodynamics in the efficacy of vascular-targeted spherical drug carriers. *Biomaterials*, 31:1392–1402, 2010.

- [400] P. Decuzzi and M. Ferrari. Design maps for nanoparticles targeting the diseased microvasculature. *Biomaterials*, 29(3):377–384, 2008.
- [401] C. Fillafer, R. Nowotny, M. Wirth, and F. Gabor. Influence of microplate mixing on binding assays. In *Scientia Pharmaceutica* 77 (1), page 189, 2009.
- [402] Sergey S. Shevkoplyas, Tatsuro Yoshida, Lance L. Munn, and Mark W. Bitensky. Biomimetic autoseparation of leukocytes from whole blood in a microfluidic device. *Analytical Chemistry*, 77(3):933–937, 2005.
- [403] V.V. Ramachandran, R. Venkatesan, G. Tryggvason, and F.H. Scott. Low reynolds number interactions between colloidal particles near the entrance to a cylindrical pore. *Journal of Colloid and Interface Science*, 229(2):311–322, 2000.
- [404] G.A. Buxton. The fate of a polymer nanoparticle subject to flow-induced shear stresses. *Europhysics Letters*, 84(2), 2008.
- [405] W. Neuhaus, R. Lauer, S. Oelzant, U.P. Fringeli, G.F. Ecker, and C.R. Noe. A novel flow based hollow-fiber blood-brain barrier in vitro model with immortalised cell line pbmec/c1-2. *Journal of Biotechnology*, 125(1):127–141, 2006.
- [406] B. Nasser and A.T. Florence. Microtubules formed by capillary extrusion and fusion of surfactant vesicles. *International Journal of Pharmaceutics*, 266(1-2):91–98, 2003.
- [407] Lord Rayleigh. On waves propagated along the plane surface of an elastic solid. *Proceedings of the London Mathematical Society*, 17:4–11, 1885.
- [408] J. Neumann. *Sensorische und aktorische Anwendungen akustischer Oberflächenwellen*. PhD thesis, University of Augsburg, 2009.
- [409] A. Toegl, R. Kirchner, C. Gauer, and A. Wixforth. Enhancing results of microarray hybridizations through microagitation. *Journal of Biomolecular Techniques*, 14(3):197–204, 2003.
- [410] Z. Guttenberg, H. Müller, H. Habermüller, A. Geisbauer, J. Pipper, J. Felbel, M. Kielpinski, J. Scriba, and A. Wixforth. Planar chip device for pcr and hybridization with surface acoustic wave pump. *Lab on a Chip*, 5(3):308–317, 2005.
- [411] J. Shi, H. Huang, Z. Stratton, Y. Huang, and T.J. Huang. Continuous particle separation in a microfluidic channel via standing surface acoustic waves (ssaw). *Lab on a Chip*, 9:3354–3359, 2009.
- [412] T. Franke, A.R. Abate, D.A. Weitz, and A. Wixforth. Surface acoustic wave (saw) directed droplet flow in microfluidics for pdms devices. *Lab on a Chip*, 9(18):2625–2627, 2009.
- [413] M. F. Schneider, Z. Guttenberg, S. W. Schneider, K. Sritharan, V. M. Myles, U. Pamukci, and A. Wixforth. An acoustically driven microliter flow chamber on a chip (mufcc) for cell-cell and cell-surface interaction studies. *Chemphyschem*, 9(4):641–645, 2008.

- [414] L. Y. Yeo and J. R. Friend. Ultrafast microfluidics using surface acoustic waves. *Biomicrofluidics*, 3(1), 2009.
- [415] J. B. Dickerson, J. E. Blackwell, J. J. Ou, V. R. Shinde Patil, and D. J. Goetz. Limited adhesion of biodegradable microspheres to e- and p-selectin under flow. *Biotechnology and Bioengineering*, 73(6):500–509, 2001.
- [416] C. Cozens-Roberts, J. A. Quinn, and D. A. Lauffenberger. Receptor-mediated adhesion phenomena. model studies with the radical-flow detachment assay. *Biophysical Journal*, 58(1):107–125, 1990.
- [417] E. Mennesson, P. Erbacher, M. Kuzak, C. Kieda, P. Midoux, and C. Pichon. Dna/cationic polymer complex attachment on a human vascular endothelial cell monolayer exposed to a steady laminar flow. *Journal of Controlled Release*, 114(3):389–397, 2006.
- [418] S. W. Schneider, S. Nuschele, A. Wixforth, C. Gorzelanny, A. Alexander-Katz, R. R. Netz, and M. F. Schneider. Shear-induced unfolding triggers adhesion of von willebrand factor fibers. *Proceedings of the National Academy of Sciences of the United States of America*, 104(19):7899–7903, 2007.
- [419] R. J. Albright and J. H. Harris. Diagnosis of urethral flow parameters by ultrasonic backscatter. *IEEE Transactions on Biomedical Engineering*, BME-22(1):1–11, 1975.
- [420] T. M. Squires and S. R. Quake. Microfluidics: Fluid physics at the nanoliter scale. *Reviews of Modern Physics*, 77(3):977 – 1026, 2005.
- [421] N. Lion, T. C. Rohner, L. Dayon, I. L. Arnaud, E. Damoc, N. Youhnovski, Z. Y. Wu, C. Roussel, J. Josserand, H. Jensen, J. S. Rossier, M. Przybylski, and H. H. Girault. Microfluidic systems in proteomics. *Electrophoresis*, 24(21):3533–3562, 2003.
- [422] A. Wixforth, C. Strobl, C. Gauer, A. Toegl, J. Scriba, and Z. V. Guttenberg. Acoustic manipulation of small droplets. *Analytical and Bioanalytical Chemistry*, 379(7-8):982–991, 2004.
- [423] K. Sritharan, C. J. Strobl, M. F. Schneider, A. Wixforth, and Z. Guttenberg. Acoustic mixing at low reynold’s numbers. *Applied Physics Letters*, 88(5):art.no. 054102, 2006.
- [424] H. Li, J. R. Friend, and L. Y. Yeo. Surface acoustic wave concentration of particle and bioparticle suspensions. *Biomedical Microdevices*, 9(5):647–656, 2007.
- [425] Y. Mo and L.Y. Lim. Preparation and in vitro anticancer activity of wheat germ agglutinin (wga)-conjugated plga nanoparticles loaded with paclitaxel and isopropyl myristate. *Journal of Controlled Release*, 107(1):30–42, 2005.
- [426] B. Ertl, F. Heigl, M. Wirth, and F. Gabor. Lectin-mediated bioadhesion: Preparation, stability and caco-2 binding of wheat germ agglutinin-functionalized poly(d,l-lactic-co-glycolic acid)-microspheres. *Journal of Drug Targeting*, 8(3):173–184, 2000.

- [427] A. P. Gunning, S. Chambers, C. Pin, A. L. Man, V. J. Morris, and C. Nicoletti. Mapping specific adhesive interactions on living human intestinal epithelial cells with atomic force microscopy. *FASEB Journal*, 22(7):2331–2339, 2008.
- [428] W. E. Thomas, E. Trintchina, M. Forero, V. Vogel, and E. V. Sokurenko. Bacterial adhesion to target cells enhanced by shear force. *Cell*, 109(7):913–923, 2002.
- [429] T. Frommelt, M. Kostur, M. Wenzel-Schäfer, P. Talkner, P. Hänggi, and A. Wixforth. Microfluidic mixing via acoustically driven chaotic advection. *Physical Review Letters*, 100(3):art. no. 034502, 2008.
- [430] Y.J. Lee, S.J. Chung, and C.K. Shim. The prevention of cyclosporin adsorption to transwell surfaces by human plasma. *International Journal of Pharmaceutics*, 224(1-2):201–204, 2001.
- [431] F. Gabor and M. Wirth. Lectin-mediated bioadhesion: wheat germ agglutinin and solanum tuberosum lectin as targeting moieties in particulate drug delivery systems. *European Journal of Cell Biology*, 74:35–35, 1997.
- [432] P. Aramwit, T. Kerdcharoen, and H. Qi. In vitro compatibility study of a nanosuspension formulation. *PDA Journal of Pharmaceutical Science and Technology*, 60(4):211–217, 2006.
- [433] I. Lynch, A. Salvati, and K.A. Dawson. What does the cell see? *Nature Nanotechnology*, 4:546–547, 2009.

CURRICULUM VITAE

PERSONAL

Name Christian FILLAFER
Born 9th of June 1982 (in Rangersdorf, Austria)
Address Hubergasse 11/8; A-1160 Wien
Email christian.fillafer@univie.ac.at

EDUCATION

since 06 Doctorate Thesis at the Department of Pharmaceutical Technology and Biopharmaceutics, University of Vienna
07 - 09 Stays in the lab of Prof. Schneider and Prof. Wixforth, Experimentalphysik I, University of Augsburg
05 - 06 Diploma Thesis: Covalent immobilisation of PEG as a novel approach towards stealth-PLGA-nanoparticles, supervised by Prof. Franz Gabor, Department of Pharmaceutical Technology and Biopharmaceutics, University of Vienna
01 - 06 Diploma studies in Pharmacy, University of Vienna
00 - 01 Army service - Medical corps training
92 - 00 Grammar school, Lienz, Austria
98 - 99 High school year abroad, High Level, Alberta, Canada
88 - 92 Elementary school, Winklern, Austria

PRACTICAL EXPERIENCE INCLUDING TEACHING

since 06 University assistant-in-training (teaching), Department of Pharmaceutical Technology and Biopharmaceutics, University of Vienna
06 Research assistant, EU-funded project CellProm - Cell Programming by Nanoscaled Devices, Department of Pharmaceutical Technology and Biopharmaceutics, University of Vienna

Tutor for courses at University of Vienna

06 Practical course on galenics
04 - 05 Methods for the identification and characterisation of pharmaceutically relevant organisms
03 - 05 General microbiology and hygiene

Study-related internships

- 05 Applied Theoretical Biochemistry Group, Institute for Theoretical Chemistry, University of Vienna
- 04 Pharmacy, Zum goldenen Elephanten, Vienna
- 03 Aging Group, Institute for Applied Microbiology, University of Natural Resources and Applied Life Sciences

LANGUAGE SKILLS

- German native
- English fluent
- French basic

RESEARCH SCHOLARSHIPS AND AWARD

- 07, 08 Research scholarship of the University of Vienna
- 07 Diploma thesis award of the Austrian Pharmaceutical Society

TALKS AT CONFERENCES

- [5] C. Fillafer, M. Prantl, G. Ratzinger, J. Neumann, M.F. Schneider, W. Neuhaus, R. Hofer-Warbinek, M. Wirth, F. Gabor. Microfluidic system to study the impact of flow on particle-cell interactions. *Doctorate Student Conference of the German Pharmaceutical Society*, November 2009.
- [4] C. Fillafer, R. Nowotny, M. Wirth, F. Gabor. Influence of microplate mixing on binding assays. *21st Scientific Congress of the Austrian Pharmaceutical Society*, April 2009.
- [3] C. Fillafer, G. Ratzinger, J. Neumann, S. Dissauer, M. Wirth, F. Gabor, M.F. Schneider. An acoustically-driven biochip: Particle-cell interactions under physiological flow conditions. *21st Scientific Congress of the Austrian Pharmaceutical Society*, April 2009.
- [2] C. Fillafer, D.S. Friedl, M. Wirth, F. Gabor. Lectin-mediated targeting: Characterisation by fluorescent bio-nanoprobes. *International Graz Workshop for Pharmaceutical Engineering*, May 2008.
- [1] C. Fillafer, M. Wirth, F. Gabor. Dynamic light scattering of nanospheres - Implications of the tenside concentration on particle size. *Pharmaceutical Sciences World Congress, Pre-Satellite Meeting*, April 2007.

PEER-REVIEWED PUBLICATIONS

- [6] G. Ratzinger, C. Fillafer, V. Kerleta, M. Wirth, F. Gabor. The role of surface functionalization in the design of PLGA

micro- and nanoparticles. *Critical Reviews in Therapeutic Drug Carrier Systems* 27 (1) (2010) 1-83.

- [5] C. Fillafer, G. Ratzinger, J. Neumann, Z. Guttenberg, S. Dis-sauer, I.K. Lichtscheidl, M. Wirth, F. Gabor, M.F. Schneider. An acoustically-driven biochip - Impact of flow on the cell-association of targeted drug carriers. *Lab on a Chip* 9 (2009) 2782-2788⁸.
- [4] C. Fillafer, D.S. Friedl, A.K. Ilyes, M. Wirth, F. Gabor. Bio-nanoprobes to study particle-cell interactions. *Journal of Nanoscience and Nanotechnology* 9 (5) (2009) 3239-3245.
- [3] C. Fillafer, D.S. Friedl, M. Wirth, F. Gabor. Fluorescent bio-nanoprobes to characterize cytoadhesion and cytoinvasion. *Small* 4 (5) (2008) 627-633.
- [2] F. Gabor, K. Trimmel, G. Ratzinger, V. Kerleta, C. Fillafer, M. Wirth. Characterisation of binding and uptake of biomimetic nanoparticles by flow cytometry. *Journal of Drug Delivery Science and Technology* 18 (1) (2008) 51-57.
- [1] C. Fillafer, M. Wirth, F. Gabor. Stabilizer-induced viscos-ity alteration biases nanoparticle sizing via dynamic light scattering. *Langmuir* 23 (17) (2007) 8699-8702.

BOOK CHAPTER

- [1] F. Gabor, C. Fillafer, L. Neutsch, G. Ratzinger, M. Wirth. Im-proving oral delivery. in: *Handbook of Experimental Pharmacol-ogy - Drug Delivery* (Ed.: M. Schäfer-Korting) Springer-Verlag Berlin Heidelberg, 346-398.

POSTERS

- [7] H. Wanzenböck, C. Peter, L. Schneider, C. Fillafer, M. Wirth, F. Gabor, E. Bertagnolli. Bioimpedance spectroscopy of ep-ithelial cell culture on a MEA chip. *MEA Meeting 2010*, June 2010.
- [6] C. Fillafer, M. Prantl, G. Ratzinger, J. Neumann, M.F. Schnei-der, W. Neuhaus, R. Hofer-Warbinek, M. Wirth, F. Gabor. Microfluidics on a chip - Impact of flow on the particle-cell interaction. 7th *World Meeting on Pharmaceutics, Biopharma-ceutics and Pharmaceutical Technology*, March 2010.
- [5] C. Meisslitzer-Ruppitsch, C. Fillafer, M. Wirth, F. Gabor, J. Neumüller, M. Pavelka, A. Ellinger. Inter- and transcellular traffic of internalized WGA to be used for drug targeting. 33rd *Annual Meeting of the German Society for Cell Biology*, March 2010.
- [4] L. Neutsch, C. Fillafer, D.S. Friedl, M. Wirth, F. Gabor. Characterisation of a novel fluorescent bioprobe to study

8 Cover article of October Issue, featured in Highlights in Chemical Biology 4 (2009) B67

nanoparticle-cell interactions. 6th *World Meeting on Pharmaceutics, Biopharmaceutics and Pharmaceutical Technology*, April, 2008.

- [3] V. Kerleta, C. Fillafer, M. Wirth, F. Gabor. Dynamic light scattering of nanoparticles: Influence of the surfactant viscosity on particle size. 6th *World Meeting on Pharmaceutics, Biopharmaceutics and Pharmaceutical Technology*, April, 2008.
- [2] C. Fillafer, D.S. Friedl, A. Ertl, M. Wirth, F. Gabor. Colloidal platform to investigate the cytoadhesive and cytoinvasive potential of ligand-conjugated nanoparticles. 6th *World Meeting on Pharmaceutics, Biopharmaceutics and Pharmaceutical Technology*, April, 2008.
- [1] C. Fillafer, G. Ratzinger, M. Wirth, F. Gabor. Covalent immobilisation of PEG as a novel approach towards stealth-PLGA-nanospheres. *INNANO - Advances in Nanobiotechnology*, October 2006.